

Green Energy and Technology

Bernardo Ruggeri  
Tonia Tommasi  
Sara Sanfilippo



# BioH<sub>2</sub> & BioCH<sub>4</sub> Through Anaerobic Digestion

From Research to Full-scale Applications

 Springer

# **Green Energy and Technology**

More information about this series at <http://www.springer.com/series/8059>

Bernardo Ruggeri · Tonia Tommasi  
Sara Sanfilippo

# BioH<sub>2</sub> & BioCH<sub>4</sub> Through Anaerobic Digestion

From Research to Full-scale Applications

 Springer

Bernardo Ruggeri  
Department of Applied Science  
and Technology  
Politecnico di Torino  
Turin  
Italy

Sara Sanfilippo  
Department of Applied Science  
and Technology  
Politecnico di Torino  
Turin  
Italy

Tonia Tommasi  
Center for Space Human Robotics  
Istituto Italiano di Tecnologia  
Turin  
Italy

ISSN 1865-3529

ISSN 1865-3537 (electronic)

Green Energy and Technology

ISBN 978-1-4471-6430-2

ISBN 978-1-4471-6431-9 (eBook)

DOI 10.1007/978-1-4471-6431-9

Library of Congress Control Number: 2014956902

Springer London Heidelberg New York Dordrecht

© Springer-Verlag London 2015

This work is subject to copyright. All rights are reserved by the Publisher, whether the whole or part of the material is concerned, specifically the rights of translation, reprinting, reuse of illustrations, recitation, broadcasting, reproduction on microfilms or in any other physical way, and transmission or information storage and retrieval, electronic adaptation, computer software, or by similar or dissimilar methodology now known or hereafter developed.

The use of general descriptive names, registered names, trademarks, service marks, etc. in this publication does not imply, even in the absence of a specific statement, that such names are exempt from the relevant protective laws and regulations and therefore free for general use.

The publisher, the authors and the editors are safe to assume that the advice and information in this book are believed to be true and accurate at the date of publication. Neither the publisher nor the authors or the editors give a warranty, express or implied, with respect to the material contained herein or for any errors or omissions that may have been made.

Printed on acid-free paper

Springer-Verlag London Ltd. is part of Springer Science+Business Media ([www.springer.com](http://www.springer.com))

*Non basta guardare, occorre guardare con occhi  
che vogliono vedere, che credono in quello che vedono.*

*Watching is not enough, you need to look  
with eyes that want to see, that believe in what they see.*

Galileo Galilei  
Pisa, 1564—Arcetri, 1642

*To my son Diego and my daughter Alice  
in the hope that the information contained  
herein will contribute to  
improve a little bit their world,  
and to Mina, who gives my life meaning.*

Bernardo Ruggeri

*To my husband Miguel and to my family  
in Salento (Italy) and Chile, for their  
love and support.*

Tonia Tommasi

*To Amma, who teaches love to humanity;  
to my dear partner Alessandro  
and to my family, for being part  
of my life.*

Sara Sanfilippo

# Acknowledgments

We are glad to express our gratitude to all the people and institutions involved in the project of this book, which made this experience possible for us, giving their support and enabled the results obtained. We would like to thank the Regione Piemonte for financial support under the grant C 16, offering us the opportunity to work on this project; Didacta Italia for the continuous support in arranging the pilot plant used to carry out the experimental tests. Very special thanks go to Giuseppe Aghem and Michele Dichiaro of technical area of DISAT (Politecnico di Torino) for their invaluable support during the run of experiments. We also want to express sincere gratitude to all the master and PhD students for their help in carrying out the tests and to Milena Bernardi to perform the experimental determinations; her continuous collaboration makes our work more reliable and stronger. Finally, we want to give a sincere thank to Prof. Giuseppe Genon for the work spent to read all the Chapters of the book; his own remarks and suggestions have paved the road to the final version of the book.

Lastly, we sincerely thank to the Springer personnel, for their patience and support in correcting the final version of the manuscript.

Bernardo Ruggeri  
Tonia Tommasi  
Sara Sanfilippo



# Contents

<b>1</b>	<b>Ecological Mechanisms of Dark H<sub>2</sub> Production by a Mixed Microbial Community</b>	<b>1</b>
1.1	The Energy Metabolism of Microorganisms	1
1.1.1	The Tower of Electrons	2
1.1.2	Electron Carriers	4
1.1.3	The Energy Released in Biological Systems	5
1.1.4	The Role of Ferredoxin (Fd) and Hydrogenase	8
1.2	General Information on the Dark H <sub>2</sub> Production Process	11
1.2.1	Differences Between Producers and Consumers of Hydrogen Bacteria	12
1.3	Parameters Affecting HPB Activity	16
1.3.1	Temperature	16
1.3.2	pH	16
1.3.3	Redox Potential	19
1.3.4	Substrate	19
1.3.5	Nutrients	19
1.3.6	H <sub>2</sub> Partial Pressure	20
1.3.7	Mixing	21
1.4	Conclusion	22
	References	22
<b>2</b>	<b>Pretreatment to Increase Hydrogen Producing Bacteria (HPB)</b>	<b>25</b>
2.1	Physiological Differences Between HPB and HCB	25
2.2	Methods of Obtaining HPB	26
2.3	Experimental Evaluation of Acid Pretreatment of Anaerobic Microflora to Produce Bio-H <sub>2</sub>	29
2.3.1	Applied Methodology	29
2.3.2	Results and Discussion	31
2.4	Conclusion	35
	References	35

**3 Kinetics, Dynamics and Yield of H<sub>2</sub> Production by HPB. . . . . 37**

3.1 Kinetic Models. . . . . 37

    3.1.1 Microorganism Growth Model . . . . . 37

    3.1.2 Kinetic Models of Anaerobic Processes . . . . . 39

    3.1.3 Some Kinetic Models for H<sub>2</sub> Production . . . . . 41

3.2 Experimental Section. . . . . 42

    3.2.1 HPB Sewage Sludge Enrichment . . . . . 42

    3.2.2 Fermentation Tests . . . . . 42

    3.2.3 Analytical Methods . . . . . 43

    3.2.4 Kinetics Study . . . . . 43

3.3 Results and Comments . . . . . 44

    3.3.1 Lag Phase . . . . . 46

    3.3.2 Exponential Phase. . . . . 49

    3.3.3 Kinetics Evaluation . . . . . 50

    3.3.4 Dynamics of bioH<sub>2</sub> Evolution. . . . . 51

    3.3.5 Test in Bioreactor . . . . . 54

    3.3.6 Yield. . . . . 55

3.4 Conclusion. . . . . 57

Appendix . . . . . 58

    Macro-approach and Relaxation Time . . . . . 58

    Application to First-Order Kinetics . . . . . 60

References. . . . . 62

**4 Effect of Temperature on Fermentative H<sub>2</sub> Production by HPB . . . . . 65**

4.1 Temperature: A Key Factor in Anaerobic Digestion . . . . . 65

4.2 Material and Test Procedure. . . . . 66

    4.2.1 Apparatus and Operative Conditions . . . . . 66

    4.2.2 Test with Bioreactor . . . . . 67

    4.2.3 Monitored Parameters . . . . . 69

4.3 Results of the Test at Ambient Temperature. . . . . 69

    4.3.1 Dynamics of Parameters Monitored. . . . . 69

    4.3.2 Evolution of H<sub>2</sub> Production . . . . . 71

    4.3.3 The Significance of Tests at Uncontrolled Temperature. . . . . 71

4.4 Results of Tests at Different Temperatures . . . . . 72

    4.4.1 Comparison Between Tests at Different Temperatures . . . . . 72

    4.4.2 Liquid Products from H<sub>2</sub> Fermentation . . . . . 77

    4.4.3 Yield of Tests According to Temperatures and Metabolic Products . . . . . 81

4.5 Conclusion. . . . . 82

References. . . . . 83

<b>5</b>	<b>Net Energy Production of H<sub>2</sub> in Anaerobic Digestion</b> . . . . .	85
5.1	Introduction . . . . .	85
5.2	Maximum Obtainable Energy . . . . .	86
5.3	Energy Conversion Parameters . . . . .	88
5.4	Net Energy Balance . . . . .	90
5.4.1	Energy Production . . . . .	91
5.4.2	Heating Heat . . . . .	92
5.4.3	Heat Loss . . . . .	93
5.4.4	Electrical Energy . . . . .	96
5.5	Results and Comments . . . . .	97
5.5.1	Energy Production . . . . .	97
5.5.2	Net Energy Production . . . . .	98
5.6	Uncertainty Evaluation . . . . .	102
5.7	Conclusion. . . . .	103
	References. . . . .	104
<b>6</b>	<b>Hydrogen Production from Biowaste</b> . . . . .	107
6.1	Biomass as Food for Microorganisms . . . . .	107
6.2	Lignocelluloses in Organic Waste Materials . . . . .	109
6.3	Biomass Pretreatments . . . . .	113
6.3.1	Physical and Physical–Chemical Pretreatments . . . . .	114
6.3.2	Chemical Pretreatment . . . . .	116
6.3.3	Biological Pretreatment . . . . .	118
6.4	Biomass Feedstock for bioH <sub>2</sub> Production: An Overview . . . . .	119
6.5	Experimental Tests from Renewable Agro-Waste . . . . .	121
6.5.1	Investigation on Pretreatments and H <sub>2</sub> Production . . . . .	121
6.5.2	H <sub>2</sub> Production from Vegetable Wastes in a Laboratory-Scale Bioreactor. . . . .	128
6.6	Conclusion. . . . .	132
	References. . . . .	133
<b>7</b>	<b>Valorization of Liquid End-Residues of H<sub>2</sub> Production by Microbial Fuel Cell</b> . . . . .	137
7.1	Overview of Bioroutes for Recovery of Additional Energy. . . . .	137
7.1.1	Photofermentation . . . . .	137
7.1.2	Biogas Production. . . . .	139
7.1.3	Microbial Fuel Cells . . . . .	140
7.1.4	Microbial Electrolysis Cells . . . . .	140
7.1.5	Metabolic Engineering. . . . .	141
7.1.6	Mitochondria-Based Fuel Cells. . . . .	141
7.1.7	Enzyme-Based Fuel Cells . . . . .	142

7.2	MFCs: Principles and Applications . . . . .	142
7.2.1	Anode Microbiology . . . . .	144
7.2.2	Electrical Parameters . . . . .	147
7.3	Application of MFCs. . . . .	149
7.4	Integrated Bioenergy Production System . . . . .	150
7.5	Experimental Study. . . . .	151
7.5.1	Production of H <sub>2</sub> from Acetate by MEC . . . . .	152
7.5.2	Production of Electricity from Acetate by MFCs. . . . .	154
7.6	Conclusion. . . . .	158
	References. . . . .	158
<b>8</b>	<b>Two-Step Anaerobic Digestion Process. . . . .</b>	<b>161</b>
8.1	Introduction . . . . .	161
8.2	Scientific Rationale of TSAD . . . . .	164
8.3	Energy Efficiency . . . . .	171
8.4	Modeling of TSAD. . . . .	172
8.5	Experimental Tests for H <sub>2</sub> and CH <sub>4</sub> Production . . . . .	172
8.5.1	Preparation and Pretreatment of the Feedstock . . . . .	173
8.5.2	Seed Microflora for H <sub>2</sub> and CH <sub>4</sub> Production . . . . .	173
8.5.3	Experimental Procedure. . . . .	174
8.6	Results . . . . .	179
8.6.1	Batch Tests . . . . .	179
8.6.2	Continuous Tests TSAD from OWM. . . . .	186
8.7	Conclusion. . . . .	188
	References. . . . .	189
<b>9</b>	<b>Energy Sustainability Evaluation of Anaerobic Digestion . . . . .</b>	<b>193</b>
9.1	Introduction to Energy Sustainability. . . . .	193
9.2	Tools and Definition of Operative Conditions. . . . .	194
9.3	Energy Sustainability Index (ESI) . . . . .	196
9.3.1	Theoretical Definition of ESI . . . . .	196
9.3.2	ESI Application to AD Technology. . . . .	197
9.4	Analogical Model . . . . .	198
9.4.1	Analogical Model Description . . . . .	198
9.4.2	Analogical Model Application to AD Technology. . . . .	203
9.5	EROI and EPT. . . . .	207
9.5.1	EROI and EPT Description . . . . .	207
9.5.2	Use of EROI and EPT in TSAD. . . . .	208
9.5.3	Use of EROI and EPT in AD. . . . .	209
9.6	Conclusion. . . . .	211
	References. . . . .	212
	<b>Conclusion . . . . .</b>	<b>213</b>

## About the Authors



**Bernardo Ruggeri** is Associate Professor of Sustainable Engineering at Politecnico di Torino, 2000–2008; CEO of the Environment Park S.p.A. of Torino, a Science and Technology Park dedicated to the research on sustainable production and development of energy from renewable sources. 1995–2000; President of the Municipal Waste Management Company (AMIAT) of Torino City. His scientific interest and ongoing research activities include modelling bioreactors and scale-up criteria for large-scale cultivation plants; evaluation of human activities impacts using LCA approach; assessment of process sustainability by ESI and EROI approaches; fuzzy modelling of new bioreactor configurations including landfill bioreactor; development of microbial fuel cell devices for scale-up purpose; advanced development of new bioreactors for hydrogen and methane production in anaerobic conditions using organic refuse. He co-funds and is the secretary of a charity “Comitato RUDI onlus” aimed at soliciting and supporting the scientific research to find a cure for Friederich’ Ataxia disease.



**Tonia Tommasi** MSc in Environmental Engineering and PhD in Chemical Engineering both obtained at the Politecnico di Torino. Actually she is a senior Postdoc at the Center for Space Human Robotics of the Istituto Italiano di Tecnologia, located in Torino (Italy). Currently, she works on electricity generation by microbial fuel cells. She has a great passion about the fascinating world of microorganisms, and in particular their strategies to naturally solve environmental and today’s energy problems. Her research interests focus

on energy production from biowaste, sustainability analysis of bioprocesses, biological hydrogen production and wastewater treatments. Moreover, she pays specific attention to the spread of the scientific knowledge proposing research-communication activities, both through divulgation laboratories and interviews on national mass media scientific programs.



**Sara Sanfilippo** MSc and PhD in Chemical Engineering at Politecnico di Torino. Currently she is a researcher in Energy and Environmental Sustainability and expert in Life Cycle Assessment (LCA). She is involved in evaluating many technologies of research projects on both industrial and laboratory scale, identifying the best promising ones and their best operating conditions to ensure the energy and environmental sustainability. She is moreover interested in revamping the actual plants toward the sustainability. Besides, she applies LCA to diet and transport, from a local and a global perspective,

demonstrating that little personal choices can also make the difference in reducing the energy demand and environmental pollution.

# Introduction

Nowadays, some of the most important problems in our society concern environment pollution and energy supply: the increasingly negative conditions of the environment, linked to the use of fossil fuel, and the real need to guarantee a greater safety of energy supply, have made the use of energy sources that respect the world in which we live of primary importance. Fossil fuels have ruled the world for more than a century and their intensive use has not only polluted the environment, but also exhausted our limited fuel reserves. The quest for a clean alternative energy should be independent from the availability of oil reserves, which could be used for other worthwhile purposes, such as in the chemical and pharmaceutical industries.

Biological hydrogen production is becoming important from the point of view of renewable fuel: it is becoming the most promising in the succession of fuels, with several technical and socio-economic benefits. This is why research on hydrogen has been increasing more and more in recent years. The use of hydrogen could satisfy three main requirements:

- it can be produced and utilized with a low impact on the environment ( $\text{H}_2\text{O}$  as a by-product);
- it can be obtained from renewable energy resources (water, organic refuse and solar energy);
- the surplus can be stored and used over time (e.g. when the demand for electricity is very high).

At present, hydrogen is produced mainly from natural gas through steam reforming (40 %), 30 % from heavy oils and naphtha, 18 % from coal, 4 % from electrolysis and about 1 % from biomass. Fossil fuel processing and water electrolysis require the input of energy, both directly and indirectly, but these methods of hydrogen production do not solve environmental issues, unlike the biological production of hydrogen, which can be carried out from renewable sources.

Anaerobic digestion (AD) of organic matter is a well-known process that is already utilized in the production of biogas. It represents a promising and environmental-friendly method that offers the possibility of obtaining  $\text{H}_2$  using a wide variety of low-price renewable feedstock and leads to a suitable improvement

in organic waste refuse treatments. The use of biomass is therefore potentially interesting as a component of a sustainable energy market for many reasons:

- various organic wastes, such as agriculture residues and municipal and industrial wastewaters, which should have a negative value since they lead to disposal and treatment problems, can instead increase in value if used to produce a high-quality fuel;
- the contribution of greenhouse gases to the atmosphere is minimal, due to the lack of fossil fuel input in both the  $H_2$  production step and the following utilization:  $H_2$  is the only carbon-free fuel;
- there are no external costs due to environmental pollutants, as occur when conventional fuels are used.

External costs are heavy costs that societies have to pay, and they are very often hidden in the case of an apparently low-cost technology. They arise from environmental damage, due to the almost total dependence on petroleum, and they rebound on the environment and therefore on humans. The externalities are, for example welfare spending because of human diseases, air and soil contamination and agriculture underproduction. If in the total costs of conventional fuel we include external ones,  $bioH_2$  production could become a cost-competitive process.

Although AD for biogas production is a widely diffused full-scale process in different countries around the world, including Europe and China, very little information is available on the geographical distribution of full-scale plants for biological hydrogen production. In fact it is an emerging technology that still needs careful study to understand the best and most economic conditions for setting up the plants.

Hydrogen is an important intermediate in the microbe-dominated degradation of organic material in anaerobic environments and it is utilized by methanogens to produce methane in conventional biogas plants. Two stages can be used, which involve separating the acidogenesis from the methanogenesis processes, leading to  $bioH_2$  and  $bioCH_4$  production, respectively, to enhance the energy and treatment benefits of AD.

The aim of the book is to find a good design via a scale-up procedure, and good anaerobic reactor operating conditions in order to produce  $H_2$  from residual biomass and then use the volatile fatty acid, residues of the  $H_2$  production, to produce methane obtaining higher energy recovery from the organic refuse. To reach these goals, it is necessary to consider many different aspects, connected to the biological and energetic features of the process, by analysing the reference literatures and by experimenting at a laboratory scale and at a pilot-plant scale; moreover less obvious aims are to promote environmental safety and to improve the value of organic refuse as a resource.

The book basically deals with an experimental approach, but the theoretical introduction is not neglected, especially concerning novel aspects connected to the sustainability of the process. Experimental tests to produce biological hydrogen from AD using organic wastes, mainly produced at several points in the food chain,



were conducted in flasks at a bench-scale bioreactors. They were conducted for optimizing the  $\text{bioH}_2$  production on the basis of several parameters: temperature, pH, redox potential, substrate concentration and rheological behaviour. An energy study was conducted in order to discover the best design conditions and working temperatures of the bioreactor, using a net energy balance tool. The working temperature in fact plays a key role in the total energy balance of the process, and therefore in the global sustainability of the process.

The analysis of the energy process sustainability is carefully addressed from both a theoretical point of view and through practical applications; sustainable energy parameters, such as Energy Sustainability Index (ESI), Energy Return On Investment (EROI) and Energy Payback Time (EPT), are introduced and analysed to evaluate the sustainability of AD technology. They are moreover used as tools for selecting the most appropriate one among many technologies that are available to produce useful energy, i.e. the energy available to society. Theoretical models and applications are presented and fully described by analysing the two-step anaerobic fermentation of  $\text{bioH}_2$  plus  $\text{bioCH}_4$ .

The book provides a substantial body of useful information extracted from the literature and experimental tests oriented towards the main objective of highlighting the two-step anaerobic fermentation process. To accomplish this, several research studies are carefully reviewed in detail and to have a better understanding of the key steps of the biological, biotechnological and engineering nature of anaerobic  $\text{H}_2$  production.

**Chapter 1** is an overview of  $\text{bioH}_2$  which is mainly dedicated to explaining the microbial processes that govern  $\text{H}_2$  production, the microorganisms and their enzymes and electron shuttles involved in the electron chain towards  $\text{H}_2$  generation. **Chapter 2** summarizes the pre-treatments reported in the literature to inhibit methanogens. Among these methods, particular attention is given to the acid treatment, which was selected as the method for obtaining hydrogen-forming bacteria in all the tests reported in the book. The experimental results of the investigation are reported in detail. **Chapter 3** is dedicated to a kinetic study of  $\text{H}_2$  production from glucose by means of a mixed consortium of microorganisms, taking into account structural information on the enzymes involved in hydrogen production, such as ferredoxin and hydrogenase. Through the kinetics obtained, the dynamics of  $\text{bioH}_2$  production is well explained, according to the pH and redox variations, as a direct consequence of bacterial activity. In **Chap. 4**, after looking at the working temperatures tested by other researchers, the effect of temperature on  $\text{H}_2$  production and on liquid end-metabolites in the mesophilic range is analysed. **Chapter 5** looks at the energy balances at various temperatures, with the aim of optimizing the net energy production in a single stage of  $\text{H}_2$  production. The diameter of the reactor was chosen as a key parameter in a scale-up procedure because it affects both the energy produced and the energy lost as heat. In **Chap. 6** attention is focused on waste organic residues for using them as electron donors for  $\text{H}_2$  production. This chapter highlights suitable vegetable residues with the aim of understanding the easiest and most efficient pre-treatment for producing hydrogen. Several available pre-treatment approaches are reviewed and analysed with particular attention to their

combinations. **Chapter 7** is devoted to explore the potential of microbial fuel cell (MFC) technology in order to add value to the metabolic products of acetogenesis fermentation after  $H_2$  production. Nevertheless, the aim of this book is to focus on anaerobic technology and its energy sustainability; the conversion of  $H_2$  production residues, such as volatile fatty acids into additional  $H_2$  or  $CH_4$  or electricity needs to be investigated. Even though MFC is in a state of infancy, it deserves close attention because of the possibility of generating electrical energy or additional  $H_2$  taking into account synergic effects among the  $bioH_2$ ,  $bioCH_4$  and electricity that are able to increase the recovery of energy present in the organic wastes. **Chapter 8** is dedicated to the methanogenic step, which is able to increase the value of the liquid end metabolites of the acetogenesis stage when  $bioH_2$  shuts down. Experimental results are highlighted, considering that two-step AD is ready to move from laboratory scale to full plant application. In **Chap. 9** a theoretical energy sustainability approach is conducted in order to produce useful energy to provide an energy service to society. A detailed analysis of the sustainability of the whole process is presented using ESI, EROI and EPT approaches in a framework of life cycle assessment thinking.

The book ends with the **Conclusion** in which a general discussion is given about the two-step technology and its future trends and the role of AD in a sustainable future society.

# Chapter 1

## Ecological Mechanisms of Dark H<sub>2</sub> Production by a Mixed Microbial Community

In this chapter the energy metabolism of *hydrogen-producing bacteria* (HPB) microorganisms is described. This method of hydrogen production depends principally on the activity of some essential enzymes such as hydrogenase and ferredoxin, and therefore a description of the mechanisms involved in dark H<sub>2</sub> production is given. The principles of dark fermentation are illustrated, focusing on the physiological functions of the enzymes involved and on the main bacteria responsible for H<sub>2</sub> production by anaerobic digestion (AD). The chapter then describes the ecological factors that influence HPB, like temperature, pH and partial pressure of hydrogen.

### 1.1 The Energy Metabolism of Microorganisms

The study of the metabolism concerns insight into the biochemical reactions which take place in the cell. The metabolism involves two types of biochemical transformations: biosynthesis (*anabolism*), i.e. the construction processes of the cells, and degradation processes (*catabolism*), which generally release energy. During metabolism, the cells absorb nutrients, convert them into cellular compounds, get energy from them and excrete waste products into the extracellular environment. Two types of energy resources can be used by cells: light and chemicals. Organisms that use light as an energy source are called *phototrophic*, while those that use organic compounds are called *chemotrophic* [1].

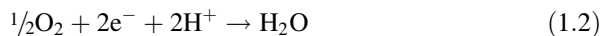
Chemical energy is the energy released when organic or inorganic compounds are oxidized. Every chemical reaction takes place in the cell with energy transformations: a chemical reaction can occur with the release of free energy (*exergonic reaction*), or conversely with the consumption of chemical energy (*endoergonic reaction*). Most of the reactions in living organisms do not occur at the appropriate speed without a catalyst. Biological reaction catalysts are proteins called enzymes, which are highly specific for the reactions that they catalyze: each type of enzyme catalyzes a single type of biochemical reaction. This specificity is related to the characteristic three-dimensional structures of the enzyme molecules. Enzymes,

being proteins, are subject to the effects of physical and chemical variables, especially temperature and pH. The use of the chemical energy in living organisms involves redox reactions. Oxidation is chemically defined as the removal of one or more electrons from a substance, while reduction is defined as the addition of one or more electrons. In biochemistry, oxidations and reductions often involve the transfer not only of electrons but of whole atoms of hydrogen; the transfer of hydrogen atoms H (or electrons e<sup>-</sup>) is important in redox reactions where molecular oxygen (O<sub>2</sub>) is not involved. For example, hydrogen gas (H<sub>2</sub>) can release electrons and hydrogen ions (protons H<sup>+</sup>) and becomes oxidized:



The electrons cannot be isolated in solution, but they must be part of atoms or molecules.

The above reaction (1.1) is only half a reaction, because for every oxidation a following reduction must also occur. For example, the oxidation of H<sub>2</sub> could be coupled to the reduction of several different substances, including oxygen, in a reduction reaction:



This semi-reaction of reduction, when coupled to the H<sub>2</sub> oxidation, leads to the balanced overall reaction:



In the 2H<sup>+</sup>/H<sub>2</sub> redox couple, which has a reduction potential  $E_0$  of -0.421 V, H<sub>2</sub> has a strong tendency to donate electrons, in contrast to the redox couple  $\frac{1}{2}\text{O}_2/\text{H}_2\text{O}$ , which has a potential of 0.82 V, where O<sub>2</sub> has a low tendency to donate electrons and hence has a high tendency to acquire electrons.

### 1.1.1 The Tower of Electrons

A convenient way to visualize electron transfer in biological systems is to imagine a vertical tower, as shown in Fig. 1.1. The tower represents the range of reduction potential for redox couples, from the most negative at the top to the most positive at the bottom. When electrons fall from electron donors in the tower, they can be captured by acceptors at various levels. The difference in electrical potential between two substances is expressed as  $\Delta E'_0$ . The further the electrons fall before being caught, the greater the amount of released energy; this means that  $\Delta E'_0$  is proportional to the free energy of the coupled reactions  $\Delta G'_0$ . Oxygen at the bottom of the tower is the final acceptor, so it is one of the most powerful oxidizing agents. The redox couple in the middle of the tower can act either as an e<sup>-</sup> acceptor or an e<sup>-</sup> donor.

**Fig. 1.1** The tower of electrons

Tower of electrons	$E_0'$ (Volt)
$\text{Co}(\text{H}_2\text{O})_6^{+2}/[\text{Co}(\text{H}_2\text{O})_6]^{+3}$	-1.84
$[\text{Co}(\text{EDTA})_3]^{-2}/[\text{Co}(\text{EDTA})_3]^{-}$	-0.6
$\text{CO}_2/\text{glucose}$	-0.43
$2\text{H}^+/\text{H}_2$	-0.42
Fd ox/ Fd red	
<i>Clostridium thermoaceticum</i>	-0.39
<i>Clostridium pasteurianum</i>	-0.40
<i>Clostridium thermocellum</i>	-0.43
$\text{CO}_2/\text{methanol}$	-0.38
$\text{NAD}^+/\text{NADH}$	-0.32
$\text{CO}_2/\text{acetate}$	-0.28
$\text{SO}_4^{2-}/\text{H}_2\text{S}$	
$\text{S}^0/\text{H}_2\text{S } 2\text{e}^-$	-0.28
Pyruvate/lactate	-0.19
$\text{S}_4\text{O}_6^{2-}/\text{S}_2\text{O}_3^{2-}$	+0.024
Fumarate/succinate	+0.03
$\text{Fe}^{3+}/\text{Fe}^{2+}$ at pH=7	+0.20
$[\text{Co}(\text{NH}_3)_6]^{+2}/[\text{Co}(\text{NH}_3)_6]^{+3}$	-0.10
Cytochrome $c_{\text{ox/red}}$	+0.25
$[\text{Co}(\text{en})_3]^{+2}/[\text{Co}(\text{en})_3]^{+3}$	+0.26
Cytochrome $c_{\text{ox/red}}$	+0.39
$\text{NO}_3^-/\text{NO}_2^-$	+0.42
$\text{NO}_3^-/\text{N}_2$	+0.74
$\frac{1}{2}\text{O}_2/\text{H}_2\text{O}$	+0.82
$[\text{Co}(\text{CN})_5]^{-3}+\text{CN}^-/[\text{Co}(\text{CN})_6]^{-3}$	+0.83

In conditions of absence of oxygen, e.g. anaerobic conditions, other compounds can act as final electron acceptors, such as succinic and fumaric acids.

In reactions of this type, the oxidized substance, in this case H<sub>2</sub>, is the electron donor and the reduced substance, oxygen, is the electron acceptor. Chemical compounds have different tendencies to release electrons, becoming oxidized, or vice versa to accept electrons, becoming reduced. This trend is expressed as the reduction potential ( $E_0$ ) of substances. This potential is electrically measured with reference to a standard hydrogen electrode (SHE). As often happens in biological reactions, protons are involved in the reaction and hence influence the concentration of H<sup>+</sup> and the pH. By convention, the potential for reduction is thus neutral (pH 7) because the cell cytoplasm is approximately neutral. In microorganism metabolism, metal organic compounds as well as genotype have a strong influence on the same redox system, as shown in Fig. 1.1.

### 1.1.2 Electron Carriers

Electron transfer from the donors to the acceptors in a cellular redox reaction involves the participation of one or more electron carriers associated with the membrane. These systems have two basic functions: (1) to accept electrons from an electron donor transferred to an electron acceptor and (2) to store the energy released during the electron transfer by adenosine triphosphate (ATP) synthesis [1]. Some carriers are set in the cytoplasmic membrane while others are free to diffuse, transferring electrons from one cell to another. The electron transporters are coenzymes, including NAD<sup>+</sup> (nicotinamide adenine dinucleotide) and NADP<sup>+</sup> (NAD phosphate). NAD<sup>+</sup> and NADP<sup>+</sup> are carriers of hydrogen atoms; this transfer of hydrogen atoms is called dehydrogenation. The reduction potential of the couple NAD<sup>+</sup>/NADH is  $-0.32$  V, which puts it high up in the tower of electrons; this means that NADH is a good donor of electrons. Although the couples NAD<sup>+</sup> and NADP<sup>+</sup> have the same reduction potential, generally they have different functions in the cell. NAD<sup>+</sup> is directly involved in energy-producing reactions (catabolism), whereas NADP<sup>+</sup> is involved in biosynthetic reactions (anabolism).

Several types of redox enzymes are involved in electron transport:

- NADH dehydrogenases are proteins that bind to the inner surface of the cell membrane. They accept electrons from NADH, generated in the various cellular reactions, and transfer two hydrogen atoms to flavoproteins;
- Flavoproteins are proteins that contain a riboflavin derivative; they accept hydrogen atoms and donate electrons;
- Cytochromes are proteins that undergo oxidation–reduction reactions through the loss or gain of a single electron by an atom of iron bound to heme in the middle of the cytochrome:  $\text{Cytochrome-Fe}^{2+} \rightarrow \text{Fe}^{3+} + e^{-}$

- Non-heme iron–sulfur proteins, such as  $\text{Fe}_2\text{S}_2$ ,  $\text{Fe}_4\text{S}_4$  and  $\text{Fe}_8\text{S}_8$ ; the iron atoms are linked to free sulfur and proteins via the sulfur atoms of cysteine. Ferredoxin (Fd), a common iron–sulfur protein, has the configuration  $\text{Fe}_2\text{S}_2$ . The potential for reducing iron–sulfur proteins varies greatly, and is dependent on the number of hydrogen and sulfur atoms present and the type of bond by which the iron centers are attached to the protein, as shown in Fig. 1.1. Like the cytochromes, the iron-sulfur proteins donate only electrons, not hydrogen atoms;
- Quinones are soluble in lipids and are involved in electron transport. Similarly to the flavoproteins, quinones act as hydrogen atom acceptors and electron donors.

### 1.1.3 The Energy Released in Biological Systems

The mode of electron transfer during energy generation depends on the microorganisms and the redox couple of the electron donor and acceptor present in the surrounding environment. If bacteria gain reducing equivalents from glucose in the form of NADH, and subsequently shuttle electrons from NADH to oxygen (not considering the potential decrease between NADH and the final bacterial electron shuttle), the potential difference is  $\Delta E = (+0.840 \text{ V}) - (-0.320 \text{ V}) = 1.16 \text{ V}$ , and the energy to be gained (two electrons per molecule of NADH) is  $\Delta G = -223 \text{ kJ/mol}$ . If the electron acceptor is sulfate, the potential difference decreases to approximately 100 mV, yielding a  $\Delta G$  of only  $-19 \text{ kJ/mol}$  [2].

The redox reactions proceed in three stages, each one catalyzed by different enzymes: the removal of electrons from the primary donor, the transfer of electrons through one or more electron processors, and the transfer of electrons to the terminal acceptor. The energy released in the oxidation and reduction reactions is not lost but is preserved for cellular functions in the formation of certain biochemical compounds that contain high-energy phosphate bonds. One of the most common high-energy phosphate compound is ATP, which serves as the primary carrier of energy in the cell.

The ability of microorganisms to maximize their energy gain during the conversion of substrate determines their chances to survive, to grow and to become dominant within a microbial community. In this context, the availability of substrate and nutrients is a necessity, and so is the presence of an appropriate electron acceptor. There are two main modes of microbial energy conservation: respiration, in which molecular oxygen and other oxidants serve as terminal electron acceptors, and fermentation, in which the redox process occurs in the absence of any added terminal acceptor electron [3]. The two mechanisms are shown schematically in Figs. 1.2 and 1.3, respectively.

**Fig. 1.2** Flow of carbon and electrons in aerobic respiration

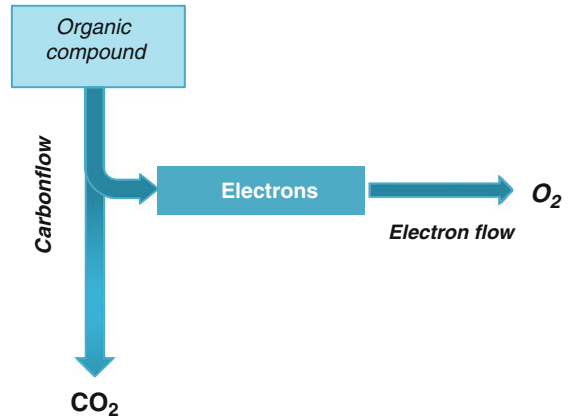
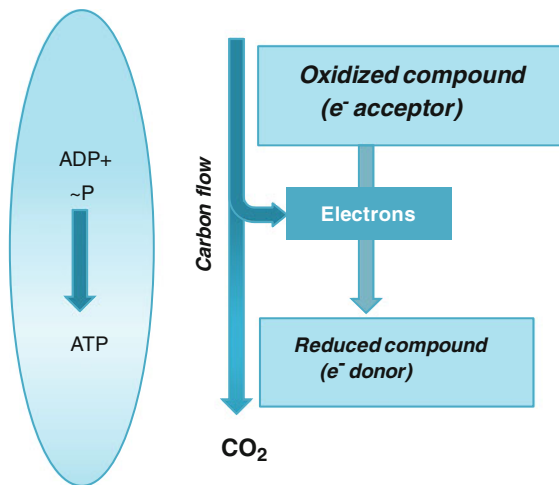


**Fig. 1.3** Flow of carbon atoms and electrons in fermentation



### 1.1.3.1 Respiring Bacteria Gain Energy by Electron Transfer to External Acceptors

Microorganisms survive and grow due to the energy that has been generated by transferring electrons. During respiration, microorganisms liberate electrons from an electron-rich substrate at a low redox potential and transfer these electrons through many electron transport complexes through the cell membrane, where a final electron acceptor is reduced. Electrons and concomitantly protons can be transported by NADH dehydrogenase, ubiquinone, coenzyme Q or cytochrome [4]. Microorganisms do not use the energy produced by the electron flow in a direct way; instead, the electron flow is used to create a proton gradient across the cell membrane, as described in [5]. The energy released by the inward flux of the



protons through a membrane complex (ATP synthase) is used to regenerate energy carrier molecules, such as ATP. Every subsequent component in this chain has a potential higher than the electron donating component. The energy released during the electron transport enables bacteria to pump protons outwards to the periplasm. Thus a proton force is generated, enabling ATP synthase activity and hence the formation of ATP. All electrons not captured for growth within the bacterium can theoretically be transported to the electron acceptor, with concomitant conversion of carbonaceous substrate to  $\text{CO}_2$ . In particular, electrons resulting from intracellular substrate oxidation are transported from the cytoplasm to outer membrane cytochromes associated with the microbe. Once in the extracellular environment, electrons are transferred between cytochromes, either on outer cell membranes, aligned along pili, or in extracellular polymeric substances, until they reach the final electron acceptor; at the same time protons are generated and diffuse toward the medium, creating a proton concentration gradient. If the environment shifts towards a lower redox potential, the normal final electron transferring component can no longer be used, causing the bacteria to either divert electron flows over more reduced compounds or convert from a respiratory to a fermentative metabolism [2].

By creating the proton gradient, the potential difference between the electron donor (i.e. the substrate at low potential) and the electron acceptor is translated into a process for energy generation. The higher the potential difference between electron donor and electron acceptor, the higher the proton-driven potential difference and the higher the potential amount of ATP which can be refuelled [3]. Respiring microorganisms can use a wide variety of different electron acceptors, ranging from oxygen, nitrate, and iron and manganese oxides to sulfate, and their ability to use the acceptor with the highest redox potential will increase their ability to grow [1].

### 1.1.3.2 Fermentative Bacteria Generate Energy by the Internal Recirculation of Electrons

In many environments, the availability of electron acceptors is limited, hindering microorganisms from using the respiratory pathway. In these cases, which are abundant, fermenting organisms are likely to become established. Fermentation is an ATP-regenerating metabolic process in which degradation products or organic substrates serve either as electron donors or electron acceptors [6]. The advantage of this pathway is that fermenting organisms are able to grow in numerous environments which are not able to support organisms that only use the respiratory pathway, because suitable electron acceptors are lacking [3]. During fermentation, bacteria will deposit a portion of the liberated electrons on the oxidized substrate and hence they will form reduced metabolites such as ethanol and acetate [7]. Fermenting organisms are important within the overall microbial processes in nature for their ability to degrade polymeric compounds into readily biodegradable monomers. Part of the electrons and protons in such HPB (e.g. *Clostridium* spp.) will be diverted through ferredoxin (Fd) over hydrogenases, which form hydrogen gas, in order to liberate the reducing equivalents coming from the oxidation of

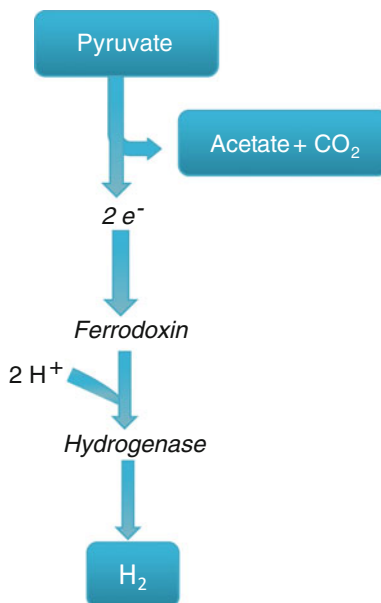
pyruvate to acetyl-CoA, and to render pyruvate available for metabolism. Approximately two thirds of the electrons remain in the fermentation products such as acetate [8], while at most one third of the electrons can theoretically be converted into H<sub>2</sub> gas by hydrogenases which are often situated at locations accessible from outside by mobile electron shuttles in the periplasm.

However, fermentation is energetically far less efficient than respiration, as only 1–4 mol of ATP are formed during the fermentation of glucose, whereas 26–38 mol of ATP are formed during the aerobic degradation of glucose [6]. This is also reflected in the Gibbs free energy value, which is seven times lower in the fermentation of glucose than in aerobic respiration. The remainder of the Gibbs free energy is not lost but is conserved within the excreted fermentation products such as volatile fatty acids, hydrogen, alcohols and many others. The trade-off between their low energetic yield and their ability to colonize niches devoid of readily available electron donors and acceptors determines the success of fermenting organisms in many ecosystems.

#### 1.1.4 The Role of Ferredoxin (Fd) and Hydrogenase

The production of H<sub>2</sub> is associated with the presence of an iron–sulfur protein, ferredoxin (Fd), which is a carrier of electrons at low redox potential. The transfer of electrons from Fd to H<sup>+</sup> is catalyzed by the enzyme hydrogenases, as shown in Fig. 1.4.

**Fig. 1.4** Production of molecular hydrogen from pyruvate



In many anaerobic microorganisms, pyruvate ferredoxin oxidoreductase (PFOR) catalyzes the oxidative decarboxylation of pyruvate to  $\text{CO}_2$  and acetyl-CoA. In anaerobic acetogenic bacteria, 2 mol of  $\text{CO}_2$  are generated from decarboxylation of 2 mol of pyruvate. The two electrons generated by the oxidative decarboxylation of pyruvate are transferred to an eight iron Fd (or other electron carriers). The reverse reaction, carboxylation of acetyl-CoA, is an important reaction for anaerobes like methanogens and acetogens that fix  $\text{CO}_2$ . Uyeda and Rabinowitz [9] isolated and characterized PFOR, demonstrating that low potential electron donors, like reduced ferredoxin, can drive the reductive carboxylation of acetyl-CoA. Combined studies also show that PFOR serves as pyruvate synthetase, and works by linking to Fd, which is the most efficient electron acceptor for pyruvate oxidation from PFOR as well as the electron donor for pyruvate synthesis [10]. The spatial configuration of both Fd and hydrogenase are pH-dependent:

- Free Fd acts increasingly as electron acceptor ( $\text{Fe}^{3+} + 1e^- \rightarrow \text{Fe}^{2+}$ ) when pH decreases and the redox potential moves towards a reductive environment;
- Fd acts as an electron donor ( $\text{Fe}^{2+} \rightarrow \text{Fe}^{3+} + 1e^-$ ) when pH increases and the environment becomes oxidative.

These theoretical considerations are experimentally validated by the dynamics of  $\text{H}_2$  production described in Chap. 3.

Figure 1.5 shows an image of the ferredoxin reductase–NADH complex. The redox reaction and the electron transport occur at the level of aromatic rings, as shown on the right of the figure; the red rings of the terminal NADH–FAD complex indicates that such a terminal complex is in the oxidized state ( $\text{NAD}^+$ –FAD) and is therefore able to participate in the electron transport chain, accepting electrons and then reducing NADH and FADH.

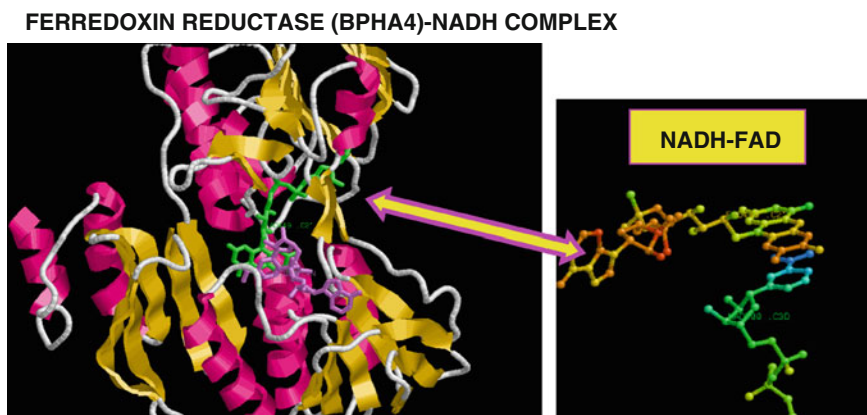


**Fig. 1.5** Image of ferredoxin reductase–NADH complex: redox reaction and electron transport occur at the level of aromatic rings, as shown on the *right*

Iron–sulfur proteins [Fe–S] are omnipresent in nature, with approximately 120 different types identified, having functions ranging from essential electron transfer reactions to regulation of gene expression [11]. Fd can control the reactivity of specific [Fe–S] clusters: the modification of reduction potential ( $E_0'$ ). Thus, even without modifying the cluster type, proteins can modulate the  $E_0'$  of a specific centre by varying its environment [12]. The way in which proteins control reduction potentials of [Fe–S] clusters is a fundamental problem in biochemistry, with implications for understanding the energetic mechanism of electron transfer. Chen et al. [13] have conducted experimental studies regarding the variation of reduction potential with pH and the temperature dependence of crystal structures, and they lead to the conclusion that the largest increase in  $E_0'$  is due to the introduction of positive charge for the protonation of the group.

The hydrogen production serves to maintain redox balance. For example, if the production of hydrogen is prevented, the redox balance of other fermentation products will be transferred towards the formation of more reduced compounds. Most of the HPB also produce ethanol and acetate. Considering that ethanol is easily reduced with respect to acetate, its formation will be favored when the formation of hydrogen is inhibited [12].

#### 1.1.4.1 Hydrogen-Producing Enzymes

Each biohydrogen production method is dependent on the hydrogen-producing enzymes found inside the individual microorganism. These enzymes catalyze a very simple redox reaction:  $2\text{H}^+ + 2\text{e}^- \rightarrow \text{H}_2$ . In order to perform this reaction, most hydrogen-evolving enzymes have complex metalloclusters as active sites and require special maturation proteins [14]. The three main hydrogen-evolving enzymes used by most biohydrogen-producing systems are nitrogenases, [NiFe]-hydrogenases, and [FeFe]-hydrogenases. Here only a brief description of each enzyme is given; for a more detailed one please refer to reviews by Vignais et al. [15]. Nitrogenases catalyze a reaction that fixes nitrogen into ammonia, and it is accompanied by the obligatory reduction of protons ( $\text{H}^+$ ) to hydrogen. The nitrogenase complex consists of two proteins encoded by three structural *nif* genes; the first protein is the dinitrogenase or MoFe-protein, encoded by *nifD* and *nifK*, and the second one is the dinitrogenase reductase or Fe-protein, encoded by *nifH*. The reduction of nitrogen to ammonia with the accompanying production of hydrogen requires ATP and proceeds at a slow turnover rate of about  $6.4 \text{ s}^{-1}$ . In contrast, [NiFe]-hydrogenases work about 15 times better than nitrogenases to produce hydrogen and do not require ATP [14]. [NiFe]-hydrogenases can produce hydrogen and moreover can work as uptake hydrogenases, utilizing the electrons from hydrogen and using them to reduce NADP [16]. The catalytic core of the [NiFe]-hydrogenases is composed of a heterodimeric protein [15]. The large subunit contains the Ni–Fe active site and the small subunit usually contains Fe–S clusters, which serve as electron transfer points to the electron acceptor or donor. The most efficient hydrogen-producing enzymes are [FeFe]-hydrogenases, which can have an

activity 1,000 times higher than nitrogenases and about 10–100 times higher than [NiFe]-hydrogenases [15]. These hydrogenases consist of one protein containing a Fe–Fe catalytic core and can have a variety of electron donors and acceptors. [FeFe]-hydrogenases can either produce or consume hydrogen depending on their environment. All of these three enzymes are generally sensitive to oxygen and must be either spatially or temporally separated from it in order to produce hydrogen at optimal rates.

## 1.2 General Information on the Dark H<sub>2</sub> Production Process

During the natural process of anaerobic digestion, some bacteria convert the organic material present in the digester into hydrogen, carbon dioxide and water-soluble metabolites such as acetic acid, butyric acid, propionic acid and ethanol. Typically, these bacteria live in close proximity to other bacteria that consume the metabolites, including hydrogen, producing their final products such as methane and CO<sub>2</sub>, according to the pathway outlined in Fig. 1.6.

The theoretical yields of hydrogen from dark fermentation depend largely on the type and the combination of anaerobic organisms that are used in the process. Although glucose can theoretically provide 12 mol of hydrogen per mol of glucose (Eq. 1.4), there are no metabolic pathways existing in nature that would allow this, since cell growth would not be possible and the reaction is not thermodynamically possible ( $\Delta G'_0 = 3.2$  kJ/mol).

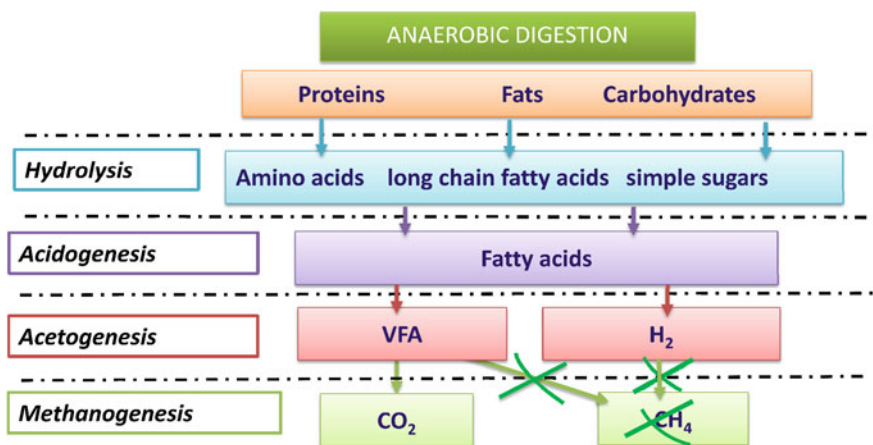
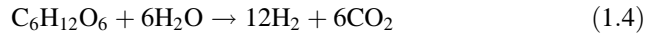


**Fig. 1.6** Overview of the metabolic pathway leading to the formation of hydrogen in the anaerobic digestion process



Facultative anaerobes evolve a maximum of 2 mol of hydrogen from each mole of consumed glucose, whereas strict anaerobes evolve at the most 4 mol [17]. However, these theoretical yields are based on known metabolism and often they are lower in practice for both strict and facultative bacteria, but they can be increased by engineering the metabolic pathways that convert glucose into hydrogen. Dark fermentation seems to hold the best promise for biohydrogen processes due to its low cost, to a relatively high production efficiency, and to stable hydrogen-evolving enzymes. [NiFe]-hydrogenases and [FeFe]-hydrogenases can be utilized in dark fermentations by using pure cultures or a consortium of anaerobic microorganisms [11]. Since no oxygen is produced or consumed in these reactions, both types of hydrogenases are less likely to be inactivated by oxygen. Organic wastes from agriculture or sewage can be fed into large anaerobic bioreactors, achieving the dual goal of waste management and hydrogen production. Dark fermentations also solve the problem of expensive photo-bioreactors, which are necessary for direct biophotolysis and photofermentations. Dark fermentation bioreactors can be kept simple and the production cost can be reduced by lowering the demands of maintenance and operating area [14]. However, several reviews have identified obstacles that limit the viable macro-scale production of hydrogen by dark fermentation: for example, hydrogen consumption by uptake hydrogenases, substrate utilization, and overall low production yields due to inefficient metabolic pathways [18].

### ***1.2.1 Differences Between Producers and Consumers of Hydrogen Bacteria***

The digester design and process need to reach the most favorable conditions, taking into account the differences between the vital conditions of hydrogen-consuming bacteria (HCB) and hydrogen-producing bacteria (HPB). The best operating conditions permit the inhibition of HCB and thus allow HPB to become the dominant population. The differences currently known between HCB and HPB concern their resistance to temperature, the extreme environmental conditions and the different growth rate of each species. These physiological differences are described in more detail in the following chapter, dedicated to explaining the different methods for obtaining a FPB culture.

#### **1.2.1.1 Strict Anaerobic Bacteria Involved in H<sub>2</sub> Production**

Studies carried out by various researchers have shown that bacteria of the genus *Clostridium* are the best candidates in the production of a H<sub>2</sub>-rich biogas. Strict anaerobes utilize dark fermentation to break down glucose into pyruvate and

NADH [14]. Pyruvate is then converted to acetyl-CoA and CO<sub>2</sub> by way of PFOR. The acetyl-CoA is then transformed to acetyl phosphate with the formation of ATP and the excretion of acetate. The oxidation of pyruvate into acetyl-CoA requires the reduction of Fd by PFOR, which is then oxidized by a hydrogenase that regenerates oxidized Fd and hydrogen gas [19]. Additional hydrogen can be produced from the NADH that is generated during glycolysis. The NADH is oxidized by Fd reduction and an NADH-Fd reductase, but only at very low partial pressures of hydrogen (<60 Pa) [20]. Then, the highest theoretical yields of hydrogen, 4 mol hydrogen per mole of glucose, are produced when acetate is the only fermentation end-product. Butyrate formation yields 2 mol of hydrogen per mole of glucose and even lower yields are associated with propionate and reduced end-products such as alcohols and lactic acid. The obligate anaerobe, *C. acetobutylicum*, has long been of great interest due to its ability to ferment various substrates into valuable end-products such as acetone, butanol and ethanol [21]. Fermentation by this organism has two distinct phases. The first phase is characterized by rapid growth and high hydrogen production along with acetic and butyric acid production. The second phase is characterized by slower growth, low hydrogen production, and solvent production [22]. These phases are known as the acidogenic and the solventogenic phases, respectively [21]. Determination of whether *Clostridium* utilizes a solvent- or acidic-producing pathway is dependent on ATP and NADH levels [22]. Recently, *C. acetobutylicum* has been completely sequenced, and both [FeFe]-hydrogenase and a [NiFe]-hydrogenase have been found in its genome. However, the [FeFe]-hydrogenase is ten times more active, suggesting that it is the major producer of hydrogen gas [23]. The mechanism of the [FeFe]-hydrogenase is closely linked to Fd and the enzyme NADH-ferredoxin reductase; during acidogenic metabolism, reduced Fd is oxidized by the [FeFe]-hydrogenase to produce hydrogen gas, while the resulting oxidized Fd is recycled back to the reduced form by an NADH-ferredoxin reductase that oxidizes NADH into NAD<sup>+</sup> in the process. This ferredoxin-redox system is one of the ways in which *C. acetobutylicum* is able to regenerate the NAD<sup>+</sup> needed to drive glycolysis. The *hydA* gene from *C. acetobutylicum* encodes for the [FeFe]-hydrogenase. However, this enzyme needs accessory proteins in order to express for an active hydrogenase. The *hydE*, *hydF* and *hydG* genes from *C. acetobutylicum* encoding the necessary accessory proteins and their heterologous expression along with *hydA* have been shown to produce an active [FeFe]-hydrogenase in *E. coli* [23]. Although active, the expressed [FeFe]-hydrogenase in *E. coli* still requires its native ferredoxin counterpart for in vivo activity. There may be two enzymes with two modes of regulation that serve as an NADH-Fd reductase and Fd-NAD reductase, but they have never been identified in the *C. acetobutylicum* annotated sequence. Recently, the native Fd counterpart for *HydA* was identified as CAC0303 and it was cloned and expressed in *E. coli* [24]. *C. acetobutylicum* has also been shown to be the fastest microorganism for hydrogen production from hexose, with a rate of 2.4 L<sub>H<sub>2</sub></sub> L<sup>-1</sup> h<sup>-1</sup>. However, a recent study showed that *C. beijerinckii* L9 attained the highest hydrogen yield from glucose (2.81 mol/mol glucose) when compared to *C. acetobutylicum* [25].

### 1.2.1.2 Facultative Anaerobic Bacteria Involved in H<sub>2</sub> Production

*E. coli* is an excellent example of a facultative anaerobe, which means that it is able to grow in anaerobic and aerobic conditions. When growing in aerobic conditions, pyruvate generated from the breakdown of sugars is mainly used by pyruvate dehydrogenase (PDH) and then further converted through the tricarboxylic acid (TCA) cycle or into acetate [26]. In contrast, most pyruvate generated during anaerobic conditions is converted by pyruvate formate lyase (PFL) and it produces formate and acetyl coenzyme A (AcCoA). The AcCoA is further broken down into acetate or ethanol and a portion of the pyruvate is converted into lactate depending on conditions. In addition, the cell produces succinate. This anaerobic production of organic acids is referred to as a mixed acid fermentation. Absence of exogenous electron acceptors, such as oxygen and nitrate, requires an alternative way to regenerate NAD<sup>+</sup> in *E. coli* cells. In anaerobic conditions, the excreted products from the fermentation are in reduced form and help cells to maintain a constant supply of NAD<sup>+</sup> for glycolysis. The formation of lactate, ethanol and succinate generates NAD<sup>+</sup>, while the production of acetate yields ATP from substrate phosphorylation. The resulting ATP is essential because an incomplete TCA cycle under anaerobic conditions does not generate ATP [26]. Formate is produced in anaerobic conditions in order to get rid of extra reducing equivalents that would have been lost through the reduction of NAD<sup>+</sup> under aerobic conditions. In addition, formate can be further broken down into hydrogen gas and carbon dioxide during acid conditions to maintain pH of the fermentation broth and to lower the concentration of formate in the cell [27]. *E. coli* utilizes two types of hydrogen metabolism. The first one involves respiratory hydrogen oxidation (uptake) that is combined with quinone reduction. The second one is hydrogen evolution during mixed acid fermentation. Four hydrogenase isoenzymes have been identified in the *E. coli* genome. Two hydrogenases (hydrogenase 1 and 2) are involved in periplasmic hydrogen uptake, while the others (hydrogenases 3 and 4) are part of cytoplasmically oriented formate hydrogenase complexes [28]. The uptake hydrogenases 1 and 2 are multi-subunit, membrane-bound, nickel-containing Fe-S proteins encoded by the *hya* and *hyb* operons, respectively [15]. Hydrogenase 3, located on the *hyc* operon, produces hydrogen from formate as a part of the formate hydrogen lyase complex (FHL-1), which is active during mixed-acid fermentation at slightly acidic pH. Hydrogenase 4, located on the *hyf* operon, has been shown to produce hydrogen as part of the FHL-2 complex at slightly alkaline pH. However expression of hydrogenase 4 is not significant in the wild-type strain [28]. The FHL complex of *E. coli* is a multi-enzyme complex that catalyzes the reversible formation of equimolar amounts of hydrogen and carbon dioxide from the oxidation of formate as a response to the acidic conditions under anaerobic fermentations [29]. Formate dehydrogenase (FDH-H), which is encoded by *fdhF*, is the only protein in the FHL complex that is not encoded by the *hyc* operon. This gene is regulated by the presence of hydrogenase 3 (Hyd-3) and four polypeptides which are all encoded



on the *hyc* operon. Hyd-3 is composed of a cytoplasmically oriented large subunit encoded by *hycE* and a small subunit encoded by *hycG*. The remaining four polypeptides along with the product of *hycG* are membrane integral electron transfer components. Transcription of the FHL complex is activated by the gene product of *fhlA*, called the FHL activator protein (FHLA). The FHL repressor protein (*HycA*) is encoded by *hycA*, which is found on the same operon as Hyd-3. This repressor binds to FHLA and stops FHL transcription [27].

In fermentation by a mixed anaerobic and facultative bacterial population, various metabolic pathways can be simultaneously present during H<sub>2</sub> production. Figure 1.7 shows a number of alternative metabolic pathways. It will be reviewed again in Chap. 3 as part of a detailed study on the kinetics and dynamics of hydrogen production.

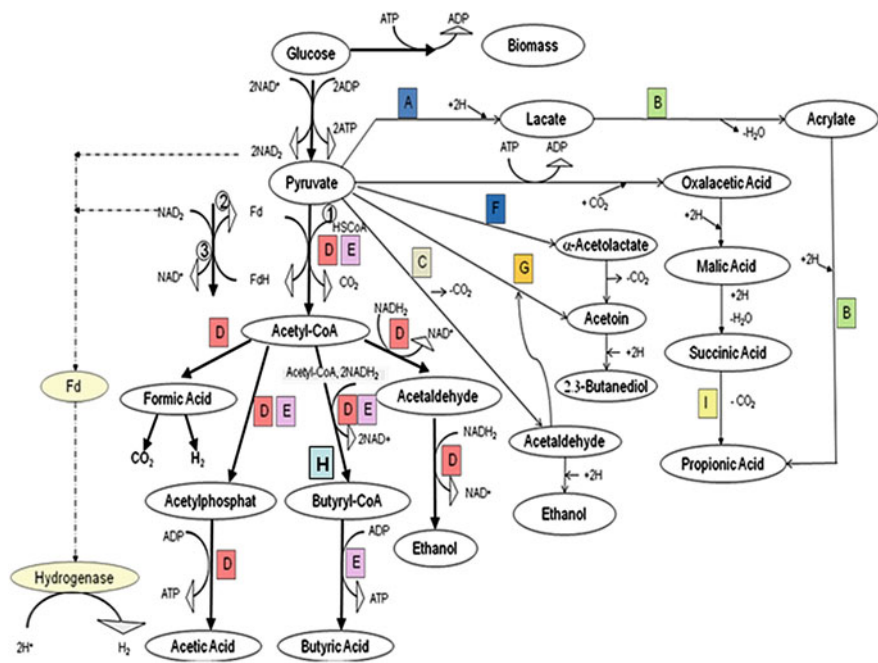


**Fig. 1.7** Metabolic pathway of glucose by HPB under anaerobic conditions. ① Pyruvate ferredoxin oxidoreductase (PFOR); ② Hydrogenase; ③ NADH ferredoxin oxidoreductase. Letters indicate organisms which conduct these reactions as follows: A Lactic acid bacteria (*Streptococcus*, *Lactobacillus*); B *Clostridium propionicum*; C Yeast, *Acetobacter*, *Zymomonas*, *Sarcina ventriculi*, *Erwinia amylovora*; D *Enterobacteriaceae* (coli-aerogens); E, *Clostridia*; F *Aerobacter*; G Yeast; H *Clostridia* (butyric, butylic organisms); I Propionic acid bacteria (adapted from [13, 14])

### 1.3 Parameters Affecting HPB Activity

The microorganisms of the genus *Clostridium* are very sensitive to the environmental conditions in which they live. Depending on environmental conditions it is possible to have acid production associated with hydrogen (*acidogenesis*) or a concentration of alcohol and solvents with low hydrogen production (*solventogenesis*). To date, exactly what determines the transition from an acidogenic to an alcohol metabolism is unknown, but studies have highlighted some parameters that influence hydrogen production.

#### 1.3.1 Temperature

Temperature is one of the most important ecological factors; it greatly influences all kinds of physiological activities of microorganisms, including the production of metabolic products [30]. In Chap. 4 the influence of temperature on metabolic microorganism pathways will be shown to confirm this. By varying the temperature, the distribution of concentrations of volatile fatty acids varies; such variation in soluble metabolites indicates a shift in the metabolic pathway of microorganisms. In many studies presented in the literature, the authors work in the mesophilic or thermophilic range: this results in an advantage in respect of an increment in hydrogen production, but it brings a redundant energy cost, which has a considerable effect on the overall energy balance. Chen et al. [31] analyzed the production of hydrogen from glucose by a mixed anaerobic culture under mesophilic temperatures in the range 33–41 °C. The results show that the rates of glucose degradation, hydrogen production and cell growth increase with temperature. The specific rate of hydrogen production increases when the temperature rises from 33 to 39 °C, and decreases when the temperature is above 41 °C. There is a linear relationship between the production of H<sub>2</sub>, the cell growth of HPB and the temperature. The production of H<sub>2</sub> increases from 0.97 to 1.87 mol H<sub>2</sub>/mol glucose when the temperature increases from 33 to 39 °C. The maximum hydrogen production occurs at 35 °C, while 25 °C gives the minimum, and at 45 °C the activity of HPB is inhibited.

#### 1.3.2 pH

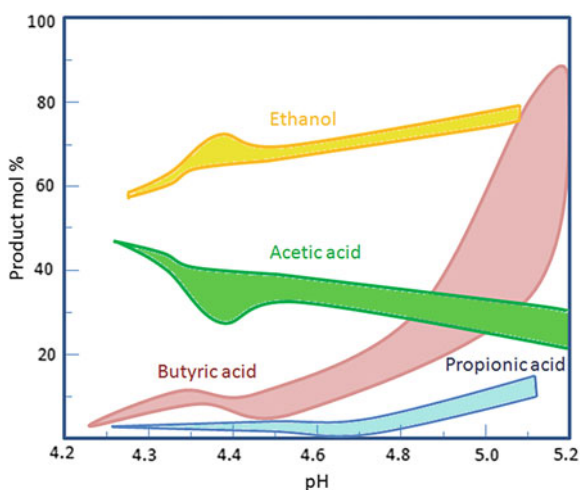
The acidity of the fermentation medium has a great effect on the vital activities of microorganisms, such as growth rate and fermentation dynamics. pH changes provoke a metabolic shift, which means that the microorganisms can switch from one metabolic pathway to another. Many microorganisms can produce several different enzyme complexes to carry more than one type of fermentation; the type of

fermentation that takes place depends on the actual environmental parameters of the fermentation broth and mainly on the pH. The pH changes mean a variation in  $H^+$  ions in the broth, and, since they are charged particles, ultimately also a variation in discharges detected by the redox potential. Consequently pH changes also mean disruption of the energy balance in the electrical term, and can therefore result in different conformations of the enzyme, which thus reduces (or loses) its catalytic activity. All enzymatic and metabolic reactions are strongly affected by the activity of enzymes, so the faster reactions prevail among several metabolic pathways, or particular enzymes with greater turnover. By varying the pH, the enzyme activity changes, and thus some metabolic pathways may become favored and replace the initial one. Often more than two simultaneous products are present in the medium, so the difficulty in comprehension of the metabolic pathway grows considerably. In Chap. 3 a macroscopic approach is used to find the dynamics of such HPB consortia.

Research shows that pH has a great effect on fermentation products and it is an important ecological factor influencing HPB [30]. The effect of pH on fermentation product composition during molasses fermentation is shown in Fig. 1.8. When the pH is below a given value, butyric acid-type fermentation is converted to ethanol-type fermentation, showing that pH plays an important role in the physiological state of microorganisms.

Mizuno et al. [32], analyzing *Clostridium butyricum* CGS5, observed that the pH decreases the production of hydrogen and, in addition, the formation of soluble metabolites and ethanol (Eth). The maximum hydrogen production occurs at pH 5.5; at pH 4.5 production is inhibited. The soluble metabolites include butyric acid (Bu), acetic acid (Ac), propionic acid (Pro) and ethanol (Eth). The most abundant product was Bu, which accounted for 36–60 % of total soluble microbial products. The Eth/total metabolites ratio was essentially less than 13 %. Hence,

**Fig. 1.8** pH effects on molasses fermentation product composition. Areas represent the range of uncertainty



hydrogen fermentation was a favorable event in the *C. butyricum* strain because the production of electron-consuming solvents (e.g. ethanol) was relatively small. The comparison between hydrogen production and soluble metabolite production shows that better hydrogen production was accompanied by a higher volatile fatty acid (VFA) content and a higher Bu/VFA ratio. This suggests that hydrogen production with *C. butyricum* CGS5 was directed by acidogenic pathways and was essentially a butyrate-type fermentation. Higher productivity of H<sub>2</sub> is accompanied by a high VFA content and a high Bu/VFA ratio. This shows that hydrogen produced by *C. butyricum* CGS5 is produced during the acidogenic phase and is essentially the product of butyrate fermentation.

Lay [33] examined the influence of pH on hydrogen production in batch conditions. The highest specific production of hydrogen, 1.47 mol H<sub>2</sub>/mol hexose, occurred at pH 5.2; at pH lower than 4 no activity was observed, while at pH 6 the hydrogen production decreased. The composition of fermentation products was influenced by pH: butyrate was the main component of VFAs and it decreased with increasing pH. These results, which include butyrate as the major metabolites present, are in agreement with our experimental study. Yokoi et al. [34], working with a reactor at 17 h of hydraulic retention time (HRT) and fed with starch (6 g L<sup>-1</sup> d<sup>-1</sup>), obtained hydrogen production at pH values in the range 4.7–5.7; in contrast at pH lower than 4.3 or greater than 6.1 the production of alcohol was predominant, indicating that the transition occurred from the acid to alcohol metabolic pathway. There are many literature data for other pH values, but they broadly confirm all the ranges of production–inhibition above. However, there is still no certainty on the optimal pH for the fermentation of hydrogen generation, since it is a function of all the environmental factors and the chemical nature of the substrate; the majority of studies in this field were performed by varying one or at most two parameters at a time, without considering that the environmental variables, particularly pH, HRT and temperature, have a combined influence on the process.

The control of pH by base-reagent addition considerably increases the cost, and it is a very high cost factor for a large-scale plant. However, this operation is vital to ensure a suitable environment for microorganisms of the genus *Clostridium*, to ensure an adequate H<sub>2</sub> production by preventing the pH falling below 4.5.

A big advantage of the dark H<sub>2</sub> technology could be the utilization of work from microorganisms less sensitive to pH. Lin and Lay [35] have studied the yield of *Enterobacter aerogenes*, a optional bacterium insensitive to pH and dissolved oxygen. They reported hydrogen production for pH between 4 and 7, although the maximum output occurred at pH values between 6 and 7. In batch conditions at pH 6.5 and 37 °C, they obtained 1 mol H<sub>2</sub>/mol glucose. Using *E. aerogenes* it is therefore possible to operate at lower pH, up to 4.5, considerably reducing process costs. Moreover, *E. aerogenes*, being a facultative bacterium, rapidly consumes the oxygen present at the beginning of the fermentation and creates anaerobic conditions in the reactor. Obviously it is more difficult at the industrial scale to use only strict anaerobes such as *Clostridium* spp., due to their extreme sensitivity to the presence of oxygen.

### ***1.3.3 Redox Potential***

Lay et al. [36], during batch tests, noticed that the redox potential fluctuated between  $-340$  and  $-150$  mV, with an average of  $-253$  mV under nitrogen sparging and  $-150$  mV without nitrogen sparging. For redox potentials higher than  $-130$  mV there was deactivation of the HPB activity. They concluded that an increase in redox potential beyond the range above was a clear indication of the deterioration of HPB. These ranges were experimentally verified with several tests.

### ***1.3.4 Substrate***

A large quantity of organic waste is produced by agriculture, industry and domestic processes. Lin and Lay [37] have studied hydrogen production in batch mode using organic solids waste, including rice and potatoes (high in carbohydrates), eggs and lean meat (rich in proteins), fat meat and chicken skin (high fat). They concluded that the chemical nature of the substrate greatly influences the production of hydrogen and the pH optimal for acidogenesis. Carbohydrates are the best substrate for this process. Many organic refuses consist not only of carbohydrates, but also of complex colloidal particles such as proteins and lipids; agricultural crops often have a high content of water and sugar, and are well suited as substrates for fermentation. For example, the liquid fraction extracted from sugar cane has a sugar content of about 170 g/kg liquid. The dry mass of the pulp after extraction is rich in cellulose, hemicelluloses and pectin, with a small and variable nutrient content of lignin. Lay et al. [36] studied the influence of the ratio of carbon to nitrogen (C/N) on bioH<sub>2</sub> production from glucose over a wide range (from 40 to 130 g/L). In fact, an appropriate C/N ratio is fundamentally important in a biological process; a C/N ratio around 47 permits a good quantity of hydrogen production (52–55 % of H<sub>2</sub> in the gas output), due to the ability of microflora to convert sugar to hydrogen in these nutrient conditions. During the saccharification of organic wastes such as wood, paper and agricultural products, glucose and xylose are produced in percentages ranging from 35–45 to 55–65 %.

### ***1.3.5 Nutrients***

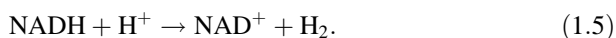
Hussy et al. [38] performed a detailed analysis of the effectiveness of trace elements (such as Mg, Na, Zn, K, I, Mn, NH<sub>4</sub> Ni, Ca, Cu and Mo) for microorganism life processes. Magnesium is the most important nutrient, followed by sodium, zinc and iron. The presence of iron in certain concentrations is an essential element for the reproduction and activity of bacteria, considering that most of the enzymes involved

in hydrogen production contain iron–sulfur clusters, as previously described; the increase in sulfate at 3,000 mg SO<sub>4</sub><sup>2-</sup> L<sup>-1</sup> inhibits the production of hydrogen, due to a change in the metabolic pathway towards butyrate and ethanol.

### 1.3.6 H<sub>2</sub> Partial Pressure

Theory predicts that reducing the partial pressure of hydrogen ( $P_{H_2}$ ), mainly by using inert gas sparging, should increase the hydrogen yields of *Clostridium*-type fermentations. In fact, it seems that the production of hydrogen is kinetically and thermodynamically less favored when  $P_{H_2} > 60\text{--}100$  Pa ( $\sim 0.5\text{--}0.8$   $\mu\text{M}$ ) [39]. Several studies lead to the conclusion that a decrease in partial pressure is one of the best approaches towards improvement of hydrogen productivity, although the degree of improvement is highly variable among studies, ranging from relatively small changes to a remarkable doubling of hydrogen yield to 3.9 mol H<sub>2</sub>/mol glucose, approaching a theoretical 4 mol H<sub>2</sub>/mol glucose when acetic pathways is followed. The lag period as well as the total duration of H<sub>2</sub> production from batch tests decreased at low-hydrogen partial pressure. This approach is considered to be a significant advance towards commercialization of the process since yields close to the theoretical one have been achieved.

Surprisingly, one study which examined dissolved hydrogen concentrations of cultures under moderate N<sub>2</sub> sparging found that dissolved hydrogen concentrations were quite high, due to gas–liquid mass transfer limitations, appreciably above the threshold predicted to be necessary to favor hydrogen production from NADH. It was suggested that the sparging effect could be due to the reduction in substrate availability for acetogens, but of course this would apply only to mixed cultures [38]. In anaerobic digestion,  $P_{H_2}$  is kept low thanks to the activity of methanogens that consume hydrogen to produce methane. In order to produce hydrogen rather than methane, all hydrogen-consuming microorganisms need to be removed from the bacterial microflora and thus the hydrogen accumulates as the reaction proceeds; as seen in the previous paragraph, during the first stage of glucose fermentation, the formation of pyruvate occurs due to the reduction of NAD to NADH. The pyruvate is then oxidized to acetic, butyric, formic, fumaric, lactic and succinic acids, acetone butanediol, butanol and ethanol. The production of hydrogen is also related to the role of NADH to NAD by the following reaction:



As with all chemical reactions, it can happen only if  $\Delta G$  is negative.

Knowing that  $\Delta G = \Delta G_0 + RT \ln \frac{([\text{H}_2][\text{NAD}^+])}{([\text{NADH}][\text{H}^+] )}$ , it is clear that the  $\Delta G$  of the reaction that produces hydrogen depends on the concentration of hydrogen in the liquid phase, which is linked to the partial pressure of the gas phase in equilibrium, as stated by Henry's law. There are various ways to control the partial pressure of hydrogen:

**Table 1.1** Reactions involved in pyruvate fermentation

Glycolysis
$C_6H_{12}O_6 + 2NAD^+ \rightarrow 2CH_3COCOOH + 2NADH + 2H^+$ (pyruvate)
Reactions involving pyruvate fermentation ( $CH_3COCOOH$ )
$CH_3COCOOH + NADH + H^+ \rightarrow CH_3CHOHCOOH + NAD^+$ (lactic acid)
$2CH_3COCOOH \rightarrow CH_3(CH_2)_2COOH + 2CO_2$ (butyric acid)
$CH_3COCOOH + CO_2 + NADH + H^+ \rightarrow (CHCOOH)_2 + H_2O + NAD^+$ (fumaric acid)
$CH_3COCOOH + H_2O \rightarrow CH_3COOH + HCOOH$ (acetic and formic acid)
$2CH_3COCOOH + NADH + H^+ \rightarrow CH_3(CHOH)_2CH_3 + 2CO_2 + NAD^+$ (butanediol)
$CH_3COCOOH + 2NADH + 2H^+ \rightarrow CH_3CH_2OH + HCOOH + 2NAD^+$ (ethanol)
$2CH_3COCOOH + H_2O + 2NAD^+ \rightarrow CH_3COCH_3 + 3CO_2 + 2NADH + 2H^+$ (acetone)
$2CH_3COCOOH + 2NADH + 2H^+ \rightarrow CH_3(CH_2)_2CH_2OH + 2CO_2 + H_2O + 2NAD^+$ (butanol)
$HCOOH \rightarrow H_2 + CO_2$ (formic acid decomposition)
$CH_3COCOOH + CO_2 + 2NADH + 2H^+ \rightarrow (CH_2COOH)_2 + H_2O + 2NAD^+$ (succinic acid)

- $H_2$  decrease by sparging argon or nitrogen;
- $H_2$  stripping by nitrogen sparging;
- operation under vacuum (0.1 atm).

According to Eq. 1.5, increasing the residual NADH can increase the production of hydrogen. Observing the reactions of fermentation of pyruvate (Table 1.1), it is noted that in some reactions the reduction of NAD to NADH occurs, while in others the consumption of NADH and then reoxidation to NAD occurs. The production of NADH favors the formation of lactic acid, fumaric acid, butanediol, ethanol, butanol and succinic acid. The reactions of fumaric and succinic acid formation require that the  $CO_2$  arrives from other metabolic processes. If the  $CO_2$  is removed from the liquid phase, these reactions cannot proceed, thus the residual NADH increases and the production of hydrogen increases too.

Hydrogen has a low solubility in water, and thus it can easily be stripped from the liquid phase. It is possible to forecast a significant increase in hydrogen production with no significant change in fermentation products by sparging nitrogen gas. Hussy et al. [38] have examined the feasibility of continuous production of hydrogen from sugar cane with and without sparging nitrogen in a bench reactor operating at 32 °C, pH 5.2, 15 h hydraulic retention time (HRT), and 10 g d<sup>-1</sup> L<sup>-1</sup> organic loading rate (OLR), as shown in Table 1.2. Using extract of sugar cane, there is an increase of about 2 times with nitrogen sparging.

### 1.3.7 Mixing

Lamed et al. [40] showed that mixing stimulates the production of hydrogen, because mixing promotes the mass transfer of the hydrogen dissolved in the broth from the liquid to gas phase and limits  $H_2$  accumulation in the liquid phase because

**Table 1.2** Yields (mol H<sub>2</sub>/mol glucose) from sugar cane with and without nitrogen sparging

Substrate	Sparging	Yield
Sucrose	Yes	1.9 ± 0.2
Sucrose	Yes	1.7 ± 0.2
Sugarbeet juice	Yes	1.7 ± 0.2
Sucrose	No	1.0 ± 0.1
Sugarbeet juice and pulp	No	0.9 ± 0.2

the enzyme pool involved in hydrogen production can be thermodynamically regulated by the H<sub>2</sub> concentration; concentrations of H<sub>2</sub>  $P_{H_2} > 60\text{--}100$  Pa can inhibit the enzyme activities.

## 1.4 Conclusion

Knowledge of the physiological characteristics of HPB, their metabolisms and the ecological factors which govern dark H<sub>2</sub> production, as described in this chapter, has a key role to play in achieving the goal of increasing H<sub>2</sub> production.

## References

1. T.D. Brock, M.T. Madigan, J.M. Martino, J. Parker, *Biology of Microorganisms*, Prentice-Hal, (New York Press, New York, 1994)
2. K. Rabaey, *Microbial Fuel Cells: Novel Biotechnology for Electricity Generation*. Ph.D. Thesis, Ghent University, Belgium, 2005
3. P. Aelterman, *Microbial Fuel Cells for the Treatment of Waste Streams with Energy Recovery*. Ph.D. Thesis, Gent University Belgium, 2009
4. J.E. Champine, B. Underhill, J.M. Johnston, W.W. Lilly, S. Goodwin, Electron transfer in the dissimilatory iron-reducing bacterium *Geobacter metallireducens*. *Anaerobe* **6**, 187–196 (2000)
5. P. Mitchell, Coupling of phosphorylation to electron and hydrogen transfer by a chemiosmotic type of mechanism. *Nature (London)* **191**, 144–148 (1961)
6. H. Schlegel, *General Microbiology*, 7th edn. (Cambridge University Press, Cambridge, 1992)
7. R.K. Thauer, K. Jungermann, K. Decker, Energy conservation in chemotrophic anaerobic bacteria. *Bacteriol. Rev.* **41**, 100–180 (1977)
8. B.E. Logan, Extracting hydrogen electricity from renewable resources. *Environ. Sci. Technol.* **38**, 160A–167A (2004)
9. K. Uyeda, J.C. Rabinowitz, Pyruvate-ferredoxin oxidoreductase. IV studies on the reaction. *J. Biol. Chem.* **246**, 3120–3125 (1971)
10. C. Furdai, S.W. Ragsdale, The role of pyruvate ferredoxin oxidoreductase in pyruvate synthesis during autotrophic growth by the wood-ljungdahl pathway. *J. Biol. Chem.* **275**(37), 28494–28499 (2000)



11. F.R. Hawkes, R. Dinsdale, D.L. Hawkes, I. Hussy, Sustainable fermentative hydrogen production: challenges for process optimization. *Int. J. Hydrogen Energy* **27**, 1339–1347 (2002)
12. H.J. Beinert, Iron-sulfur proteins: ancient structures, still full of surprises. *J. Biol. Inorg. Chem.* **5**, 2–15 (2000)
13. K. Chen, C.A. Bouagura, G.J. Tilley, J.P. McEvoy, Y.S. Jung, F.A. Armstrong, C.D. Stout, B. K. Burgess, Crystal structure of ferredoxin variant exhibiting large change in [Fe-S] reduction potential. *Nat. Struct. Biol.* **9**, 188–192 (2002)
14. P.C. Hallenbeck, J.R. Benemann, Biological hydrogen production; fundamentals and limiting processes. *Int. J. Hydrogen Energy* **27**, 1185–1193 (2002)
15. P.M. Vignais, B. Billoud, J. Meyer, Classification and phylogeny of hydrogenases. *FEMS Microbiol. Rev.* **25**, 455–501 (2001)
16. A. Dubini, R.L. Pye, R.L. Jack, T. Palmer, F. Sargent, How bacteria get energy from hydrogen: a genetic analysis of periplasmic hydrogen oxidation in *Escherichia coli*. *Int. J. Hydrogen Energy* **27**, 1413–1420 (2002)
17. A. Yoshida, T. Nishimura, H. Kawaguchi, M. Inui, H. Yukawa, Enhanced hydrogen production from glucose using *ldh*- and *frd*-inactivated *Escherichia coli* strains. *Appl. Microbiol. Biotechnol.* **73**, 67–72 (2006)
18. F.A.L. Pinto, O. Troshina, P. Lindblad, A brief look at three decades of research on cyanobacterial hydrogen evolution. *Int. J. Hydrogen Energy* **27**, 1209–1215 (2002)
19. K. Nath, D. Das, Improvement of fermentative hydrogen production: various approaches. *Appl. Microbiol. Biotechnol.* **65**, 520–529 (2004)
20. B. Mandal, K. Nath, D. Das, Improvement of biohydrogen production under decreased partial pressure of H<sub>2</sub> by *Enterobacter cloacae*. *Biotechnol. Lett.* **28**, 831–835 (2006)
21. G. Rao, R. Murtharasan, Altered electron flow in continuous cultures of *Clostridium acetobutylicum* induced by viologen dyes. *Appl. Environ. Microbiol.* **53**, 1232–1235 (1987)
22. L. Girbal, P. Soucaille, Regulation of *Clostridium acetobutylicum* metabolism as revealed by mixed-substrate steady-state continuous cultures: role of NADH/NAD ratio and ATP pool. *J. Bacteriol.* **176**, 6433–6438 (1994)
23. P.W. King, M.C. Posewitz, M.L. Ghirardi, M. Seibert, Functional studies of [FeFe] hydrogenase maturation in an *Escherichia coli* biosynthetic system. *J. Bacteriol.* **188**, 2163–2172 (2006)
24. O. Guerrini, B. Burlat, C. Leger, B. Guigliarelli, P. Soucaille, L. Girbal, Characterization of two 2[4Fe4S] ferredoxins from *Clostridium acetobutylicum*. *Curr. Microbiol.* **56**, 261–267 (2007)
25. P.Y. Lin, L.M. Wang, Y.R. Wu, W.J. Ren, C.J. Hsiao, S.L. Li, J.S. Chang, Biological hydrogen production of the genus *Clostridium*: metabolic study and mathematical model simulation. *Int. J. Hydrogen Energy* **32**, 1728–1735 (2007)
26. A.J. Wolfe, The acetate switch. *Microbiol. Mol. Biol. Rev.* **69**, 12–50 (2005)
27. R.G. Sawers, Formate and its role in hydrogen production in *Escherichia coli*. *Biochem. Soci. Trans.* **33**, 42–46 (2005)
28. W.T. Self, A. Hasona, K.T. Shanmugam, Expression and regulation of a silent operon, *hyf*, coding for hydrogenase 4 isoenzymes in *Escherichia coli*. *J. Bacteriol.* **186**, 580–587 (2004)
29. Y.F. Li, N.Q. Ren, Y. Chen, G.X. Zheng, Ecological mechanisms of fermentative hydrogen production by bacteria. *Int. J. Hydrogen Energy* **32**, 755–760 (2007)
30. Y. Zhang, J. Shen, Effect of temperature and iron concentration on the growth and hydrogen production of mixed bacteria. *Int. J. Hydrogen Energy* **31**, 441–446 (2006)
31. W.M. Chen, Z.J. Tseng, K.S. Lee, J.S. Chang, Fermentative hydrogen production with *Clostridium butyricum* CGS5 isolated from anaerobic sewage sludge. *Int. J. Hydrogen Energy* **30**, 1063–1070 (2005)
32. O. Mizuno, M. Shinia, K. Suzuki, J. Yaguguchi, T. Noike, Effect of pH on hydrogen production from noodle manufacturing wastewater. *Proc. Environ. Eng. Res.* **37**, 97–106 (2000)

33. J.J. Lay, Modeling and optimization of anaerobic digested sludge converting starch to hydrogen. *Biotechnol. Bioeng.* **68**(3), 269–278 (2000)
34. H. Yokoi, T. Ohkawara, J. Hirose, S. Hayashi, Y. Takasaki, Characteristics of Hydrogen production by aciduric *enterobacter aerogenes* Strain HO-39. *J. Ferment. Bioeng.* **80**(6), 571–574 (1995)
35. C.Y. Lin, C.H. Lay, Carbon/nitrogen-ratio effect on fermentative hydrogen production by mixed microflora. *Int. J. Hydrogen Energy* **29**, 41–45 (2004)
36. J.J. Lay, K.S. Fan, J.I. Chang, C.H. Ku, Influence of chemical nature of organic wastes on their conversion to hydrogen by heat-shock digested sludge. *Int. J. Hydrogen Energy* **28**(12), 1361–1367 (2003)
37. C.Y. Lin, C.H. Lay, A nutrient formulation for fermentative hydrogen production using anaerobic sewage sludge microflora. *Int. J. Hydrogen Energy* **30**, 285–292 (2005)
38. I. Hussy, F.R. Hawkes, R. Dinsdale, D.L. Hawkes, Continuous fermentative hydrogen production from sucrose and sugarbeet. *Int. J. Hydrogen Energy* **30**, 471–483 (2005)
39. I. Valdez-Vazquez, H.M. Poggi-Varaldo, Hydrogen production by fermentative consortia. *Renew. Sustain. Energy Rev.* **13**, 1000–1013 (2009)
40. R.J. Lamed, J.H. Lobos, T.M. Su, Effects of stirring and hydrogen on fermentation products of *clostridium thermocellum*. *Appl. Environ. Microbiol.* **54**(5), 1216–1221 (1988)

## Chapter 2

# Pretreatment to Increase Hydrogen Producing Bacteria (HPB)

This Chapter focuses on the investigation of an easy and efficacious method of obtaining a hydrogen-producing bacteria (HPB) culture to the detriment of hydrogen-consuming bacteria (HCB), such as methanogens and homoacetogenic bacteria. Although the use of mixed microflora is more viable from both the practical and biological points of view, important limitations arise from the co-activity of HPB and HCB. In this respect, pretreatment is one of the most important issues in anaerobic hydrogen production, in order to produce suitable inocula of HPB. In particular, we investigated the effectiveness of acid pretreatment applied to mixed microflora in order to stop methanogen activity. We evaluated the content of *Clostridium* bacteria, which are the main ones responsible for H<sub>2</sub> fermentation in two of the most widely used inoculum sources: anaerobic sludge from wastewater treatment plants and rumen microorganisms from cow stomachs.

### 2.1 Physiological Differences Between HPB and HCB

Bacteria belonging to the genus *Clostridium* are the main ones responsible for H<sub>2</sub> production. They are obligate anaerobes, Gram-positive and rod-shaped. *Clostridium* spp. have a substantial characteristic that distinguishes them from other bacteria allowing the production of bioH<sub>2</sub> in anaerobic processes instead of bioCH<sub>4</sub>: they are capable of producing protective end spores by undergoing a process called sporulation. This occurs when bacteria are exposed to harsh environmental conditions for bacterial growth, such as high temperature, ultraviolet radiation, presence of oxygen, extreme acidity and alkalinity, harmful chemicals like antibiotics and disinfectants, drying out, freezing, and many others that would easily kill a normal vegetative cell. To be precise, endospores are metabolically inactive dormant bodies, like seeds, which wait until the environment again becomes favorable to life. These endospore-forming bacteria, mainly Bacilli and Clostridia, have essentially two phases during their life cycle: vegetative cells and endospores. Once environmental conditions change, the endospores germinate back into living

vegetative cells that can grow and thrive. In extremely restrictive conditions, the spores might be very resistant and not easily destroyed, as opposed to HCB that are methanogens without such an ability to resist [1]. It happens in our specific case, in fact, that when the *Clostridium* spores are placed in favorable conditions, with nutrients and anaerobic conditions, the germination and metabolism processes can restart [2], and consequently hydrogen and other metabolic products can be produced. *Enterobacter* spp. are also H<sub>2</sub>-producing microorganisms with the advantage that they are facultative bacteria able to grow in the presence of oxygen. Based on phylogenetic analysis of the rDNA sequences, Fang et al. [3] found that 64.6 % of all the clones were affiliated with three *Clostridium* species, 18.8 % with Enterobacteriaceae and 3.1 % with *Streptococcus bovis* (Streptococcaceae). The remaining 13.5 % belonged to eight operational taxonomic units whose affiliations were not identified. Methanogens play a vital ecological role in anaerobic environments by removing excess hydrogen and fermentation products yielded by acetogenic bacteria, producing methane. Methanogens are usually coccoid rods or rod-shaped bacteria. There are over 50 described species of methanogens, which do not form a monophyletic group, although all of them belong to the Archaea. Methanogens are strict anaerobes and when they are exposed to an aerobic environment, the oxygen lowers their adenylate charge and causes their death [4]. The physiological differences between HPB (also called *acidogenic* bacteria) and HCB (methanogens, Archaea and homoacetogenic bacteria) are the basis of the scientific rationale behind the development of the various methods proposed to prepare hydrogen-producing seeds [5]. The following list summarizes the main differences between HPB and HCB:

- Most methanogens are limited to a relatively narrow pH range (about 7–8) [4], while most HPB can grow over a broader pH range (4.5–7) [5].
- HPB have much faster growth kinetics than HCB.
- HPB are able to resist harsh environmental conditions due to protective spore formation, while HCB are very sensitive and do not have this capacity.

## 2.2 Methods of Obtaining HPB

Various authors have described several pretreatment methods applied to sewage sludge in order to select HPB and to inhibit HCB. All of these methods are based on the physiological differences between HPB and HCB described in the previous paragraph. In particular, most of them are based on the ability of HPB to form endospores in unfavorable growth conditions:

- *Thermal treatment*: heat shock (80–110 °C) for a short time (20–60 min), boiling (several hours), sterilization and freezing/thawing (–20/25 °C for 6 h in two cycles) [6].

Heat shock has been widely used [7–12]. It is advantageous because it can assist in sludge solubilization [7, 12]. Kotay and Das [6] found that, among many pretreatments (acid, alkaline, heat, freeze/thaw, microwave, ultrasonication, chloroform), heat shock best augments  $H_2$  production. Mu et al. [13] comparing three pretreatment methods (acid, base and heat shock) also found that heat shock was the best one. Wang and Wan [14] reached the same conclusion: among acid, base, heat shock, aeration and chloroform, they found that heat shock is the best pretreatment, achieving the highest  $H_2$  yield and substrate degradation efficiency. On the other hand, thermal treatment has the disadvantage of a lower net energy yield of the  $bioH_2$  process due to high energy demand.

- *Wave and radiation stress*: ultrasonication, microwave and ultraviolet radiation. Some authors have tried to use ultrasonication, microwave and ultraviolet radiation pretreatments, among several others [6], but these do not stand out significantly against the others.
- *pH stress*: acid or alkaline pretreatment.

Both acid and alkaline pretreatments are generally carried out by adding a strong acid or base, respectively, until a set pH value is maintained for 24 h in anaerobic conditions. Acid chloride (1 or 2 N) and sodium hydroxide (1 or 2 N) are generally used to reach the desired pH. In particular, Chen et al. [15] conducted pretreatments at different pH values: 3–5 for acid pretreatment, and 10–12 for alkaline pretreatment. They found that HPB enrichment at pH 3 (acid) and pH 10 (alkaline) were the most efficacious. However, treatment at pH 3 gave the best HPB enrichment of all the pH values.

- *Use of chemicals*: chloroform, sodium 2-bromoethansulfonate (BESA) and iodopropane.

These pretreatment methods selectively inhibited methanogenic activity without influencing  $H_2$  production [5, 6]. Zhu and Béland [5] compared six pretreatment methods (acid, base, heat-shock, aeration, 2-bromoethanesulfonic acid and iodopropane) for enriching HPB from digested wastewater sludge. They concluded that the iodopropane pretreatment was the best of the six studied methods. Hu and Chen [16] compared three pretreatment methods (acid, heat-shock and chloroform) and concluded that chloroform was the best. However, the use of these strong chemicals mitigates against the sustainability of the  $bioH_2$  process.

- *Aerobic stress*: Giordano et al. [17] evaluated the use of *aerobic stress* to develop HPB: the result was that 3–4 days are a sufficient time to obtain HPB from anaerobic granular sludge. Furthermore, Zhu and Béland [5] found that the aeration method of completely flushing the sludge with air for 30 min was unsuccessful. In fact the methanogenic activity was not totally suppressed, although the seeds prepared by this method should have a more complex bacterial community than those obtained by heat-shock, acid and base pretreatments [5].

In addition, it is possible to continuously inhibit HCB during dark fermentation metabolism by controlling various parameters, such as the pH and the solid retention time, during acetogenesis, based on so-called *kinetic selection*:

- *Kinetic selection* is based on different growth kinetics of microorganisms by an appropriate loading rate or solid retention time. Kinetic selection needs to work in continuous mode with a hydraulic retention time (HRT) shorter than that utilized in CH<sub>4</sub> production in order to have continuous methanogen washout. Biokinetics studies have showed that the specific growth rate  $\mu$  is greater for HPB than HCB; it is in fact approximately 4–5 times higher than HCB [18]:

$$\mu_{\max \text{ HPB}} = 0.215 \text{ h}^{-1} \quad (2.1)$$

$$\mu_{\max \text{ HCB}} = 0.055 \text{ h}^{-1} \quad (2.2)$$

This means that methanogens need 4–5 times longer residence time in a bioreactor to maintain their vital activity. The fast rate of growth of HPB, higher than that of methanogens, has two consequences: either on the gas production rate or on the HRT as the main process parameter. In terms of productivity, hydrogen production can potentially be obtained much faster than methane, bearing in mind that hydrogen and methane are the metabolites of different populations which grow at different rates. The very marked difference between  $\mu_{\text{HPB}}$  and  $\mu_{\text{HCB}}$  can also be exploited through the management of HRT to slow the process. Methanogenesis needs a much higher HRT than does hydrogen production. The choice of a HRT similar to the characteristic time of the hydrogen-producing reaction means that HCB, on average, are not in contact with the substrate for the necessary time and consequently they are not able to carry out their metabolic functions, with strong inhibition of their activity [19, 20]. Many reviews in the literature report values of the maximum specific growth rate  $\mu_{\max}$  of HPB in the range of 0.08–0.125 h<sup>-1</sup> [13, 21]. Yang and Shen [22] selected the hydrogen producers by holding the HRT at 12 h ( $\mu = 0.083 \text{ h}^{-1}$ ) in a continuous fermentation, so HCB were probably washed out at low HRTs since their growth rates were lower than HPB. Because of the differences in the literature about the  $\mu_{\max \text{ HPB}}$  values, this topic needs a deeper analysis from an experimental point of view because of the presence in both HPB or HCB of many microorganisms with different  $\mu_{\max}$  values.

- *Working at a pH outside the optimal range of HCB*: working at a pH outside the optimal range of methanogens is a good way of avoiding continuous HCB activity during acidogenesis: at pH values lower than 6.3 or higher than 7.8 the methanogenesis rate decreases or shuts down [13].

In some cases, a combination of the aforementioned methods may be more effective. Argun and Kargi [23] found in practice that heat pretreatment (boiled sludge), followed by exposure to chloroform, renders more effective the elimination of HCB present in such anaerobic sludge. Venkata Mohan et al. [24] also showed that integration of pH 3 and chemical pretreatment with BESA gives a higher H<sub>2</sub> production. Among the various parameters, pH is considered to be the most useful one, thanks to its easy application and its low energy cost.

After this short review, it will be noted that there have been several studies comparing various pretreatment methods for enriching HPB bacteria from seed

sludge, but with some conflicting conclusions [14]. Since disagreement on the best pretreatment methods exists, a cost-effective method is required, avoiding some technical and economical difficulties which could be present working at the industrial scale. For this reason, acid pretreatment was chosen for our tests, with a view to scaling up pretreatment for H<sub>2</sub>-anaerobic technology.

## **2.3 Experimental Evaluation of Acid Pretreatment of Anaerobic Microflora to Produce Bio-H<sub>2</sub>**

This study aimed to test the effectiveness and the reproducibility of acid pretreatment of sewage sludge and bovine manure to suppress methanogen activity and to increase HPB activity. Acid pretreatment has several advantages: it could be adapted well in a full-scale plant in which the bioreactor is initially filled with an acid solution and it does not need energy consumption, as occurs with heat treatment, hence no additional devices to generate and transfer heat are necessary. Several experimental tests were performed showing the efficiency of acid conditioning of sewage sludge by using the treated bacteria consortium as inoculum to produce hydrogen by dark fermentation. Both anaerobic wastewater sewage sludge and bovine manure were used, previously treated with 1 N HCl, as inoculum in tests on H<sub>2</sub> production conducted in batch mode by a glucose medium with micro- and macro-nutrients in order to test the effectiveness of acid treatment of both consortia.

### **2.3.1 Applied Methodology**

#### **2.3.1.1 HPB Sewage Sludge Enrichment**

The anaerobic microflora that we used was obtained from a digester of municipal waste water treatment plant and from a cow-breeding farm. The pH, density, volatile suspended solid (VSS) and total solid concentration (TSS) of the sewage sludges used were 7.1–7.4, 1,010–1,200 g/L, 10,875–1,325 mg/L and 14,500–18,500 mg/L, respectively. The sludges, before beginning tests on H<sub>2</sub> production, were pretreated with 1 N HCl until pH 3 for 24 h at 35 °C in anaerobic conditions [13, 15]; the pretreatment test was repeated five times with different portions of sewage sludge for the two sludges.

#### **2.3.1.2 Experimental H<sub>2</sub> Production**

Tests were carried out using 500 ml Erlenmeyer flasks without agitation, flushed at the beginning with nitrogen gas for 5 min in order to reach strictly anaerobic

**Fig. 2.1** Schematic view of batch test conducted in Erlenmeyer flask Gas production was measured by the water-replacement method



conditions. The treated sludges were used as inocula in a ratio of 10 % v/v in five batch anaerobic tests using 50 g/L glucose as carbon source and macro- and micro-nutrient composition as follows (units mg/L):  $\text{NaHCO}_3$  1,250,  $\text{NH}_4\text{Cl}$  2,500;  $\text{KH}_2\text{PO}_4$  250;  $\text{K}_2\text{HPO}_4$  250;  $\text{CaCl}_2$  500;  $\text{NiSO}_4$  32;  $\text{MgSO}_4 \cdot 7\text{H}_2\text{O}$  320;  $\text{FeCl}_3$  20;  $\text{Na}_2\text{BO}_4 \cdot \text{H}_2\text{O}$  7.2;  $\text{Na}_2\text{MoO}_4 \cdot 2\text{H}_2\text{O}$  14.4;  $\text{CoCl}_2 \cdot 6\text{H}_2\text{O}$  21;  $\text{MnCl}_2 \cdot 4\text{H}_2\text{O}$  30; yeast extract 50. The initial pH of the media was set in the range 7–7.5. The experiments were conducted at  $35 \pm 1$  °C in a thermostatically-controlled room. A picture of the simple and effective configuration for the tests is shown in Fig. 2.1.

### 2.3.1.3 Analytical Methods

Before and after acid treatment, *Clostridium* bacteria and total bacteria content were evaluated by the “*Clostridium* spp. plate count protocol” and “total bacteria count method”, respectively [25]. *Clostridium* bacteria were grown in anaerobic conditions for 3 days at 37 °C on “Reinforced Clostridial Agar”, adding Polymyxin B sulfate. Total bacteria were grown on “Plate Count Agar” in aerobic conditions for 48 h at 37 °C. The gas evolution during the fermentation tests was monitored using a water-replacement method. The gas composition was evaluated at the end of each test as average composition. Measurements were performed by gas chromatography (Varian CP, 4900) equipped with a thermal conductivity detector (TCD) and two columns of 10 m, using argon as a carrier gas; pH and redox potential were measured with a pH meter (Infors, AG Switzerland) and Pt4805-DXK-S8/120 electrode (Mettler Toledo, Switzerland), respectively; glucose and ammonia concentrations were evaluated via enzymatic bio-analysis (Biopharm-Roche). Total cell growth was monitored by measuring the optical density (OD) at 620 nm (HP 8452A Diode Array Spectrophotometer).



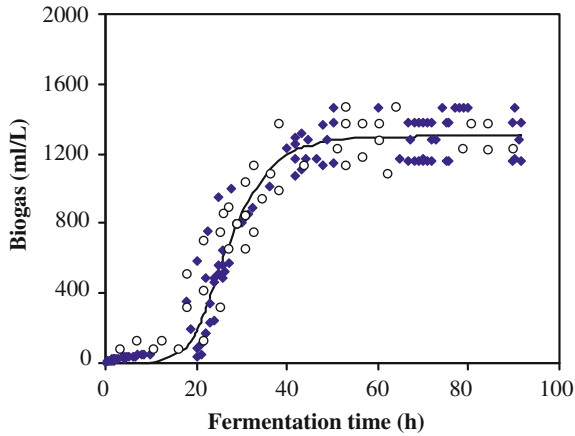


**Fig. 2.2** Best fit of total biogas production ( $H_2$  and  $CO_2$ ) with logistic equation at initial pH (7–7.5), temperature  $\approx 35^\circ C$  and initial glucose 50 g/L.  $\blacklozenge$  Test with anaerobic wastewater sewage sludge and  $\circ$  test with bovine manure, both treated at pH 3 for 24 h at  $31^\circ C$

#### 2.3.1.4 Development of Kinetic Model of Biogas ( $H_2$ and $CO_2$ ) Production

In this study, cumulative biogas production curves versus time were obtained from the hydrogen production experiments (Fig. 2.2). The experimental data were elaborated by a best-fit procedure, following the modified logistic equation (2.3) known as the Gompertz equation [13] to model the biogas production:

$$V_{\text{gas}} = V_{\text{max}} \exp \left\{ - \exp \left[ \frac{R_{\text{max}} * e}{V_{\text{max}}} (\lambda - t) + 1 \right] \right\} \quad (2.3)$$

$V_{\text{gas}}$  ( $\text{mL L}^{-1}$  broth) is the cumulative amount of biogas product ( $CO_2$  and  $H_2$ ) at reaction time  $t$ (h). Equation (2.3) permits evaluation using the potential maximal amount of biogas product  $V_{\text{gas, max}}$ , the maximum biogas production rate  $R_{\text{max}}$  ( $\text{mL L}^{-1} \text{h}^{-1}$ ) and the lag time  $\lambda$ (h).

### 2.3.2 Results and Discussion

#### 2.3.2.1 Clostridium and Total Bacteria Growth

Total bacteria count and *Clostridium* spp. count were performed on the sludge before and after acid pretreatment and during fermentation. Table 2.1 shows that only 25 % of the total bacteria survived the treatment whereas 72 % of *Clostridium* spp. survived the treatment. This implies that the acid treatment is highly selective

**Table 2.1** Effect of acid treatment on *Clostridium* spp. and total bacteria growth

	Before acid treatment (CFU/mL)	After acid treatment (CFU/mL)	Surviving (%)	Fermentation 10 h (CFU/mL)	Fermentation end (CFU/mL)
<i>Clostridium</i> spp.	56,000 ± 1,000	40,400 ± 1,200	72.5 ± 3.5	491,000 ± 1,800	350 × 10 <sup>6</sup> ± 9 × 10 <sup>6</sup>
Total bacteria	371,000 ± 1,500	93,000 ± 950	24.9 ± 0.15	n.d.	n.d.

n.d. not determined

for *Clostridium* with respect to the other bacteria. The protocol utilized for the determination of *Clostridium* spp. is probably not able to detect *Clostridium* spores but only the vegetative form, hence the spores present after acid treatment can germinate when they are placed in favorable conditions. In fact, during the fermentation process, *Clostridium* spp. grew from  $4.91 \times 10^5$  CFU/mL at 10 h from the beginning of the fermentation to  $3.50 \times 10^8$  CFU/mL at the end of the test (mean values), increasing more than 700-fold. Total cell mass, monitored over time by the optical density OD, shows a rapid increase during the exponential phase of hydrogen production, as shown by Fig. 2.3a.

### 2.3.2.2 H<sub>2</sub> Production

In Table 2.2 the results of the whole series of experiments are reported. The biogas produced was composed of hydrogen (range 50–70 %) and carbon dioxide (range 50–38 %). The biogas was free of methane and hydrogen sulfide, indicating the lack of methanogenic activities in the sludge after acid treatment.

In order to obtain a regression curve of the 10 tests (Fig. 2.2), (2.3) (and subsequently) was used to best fit the experimental data. The application of equation (2.3) permits estimation of the potential maximal amount of biogas, maximum biogas production rate and lag time, which results in 1,300 ml/L reactor, 75 mL L<sup>-1</sup> h<sup>-1</sup> and 18 h, respectively. Figure 2.2 shows that biogas developed after 18–20 h (lag phase), the time in which the microorganisms probably reorganized their molecular constituents to adapt to the new environmental conditions when they were transferred from an extremely unfavorable condition to a favorable one. During the exponential phase (20–48 h) there are the major quantities of biogas evolution, while after 48 h biogas evolution was very low and at approximately 60 h biogas shut-down occurred.

### 2.3.2.3 Effect of pH, Redox Potential and Substrate Utilization

In Fig. 2.3, a plot of equation (2.1) is shown in relation to cell growth (a), pH and redox (b) and substrate utilization (c) for test No. 4 of Table 2.2 only.

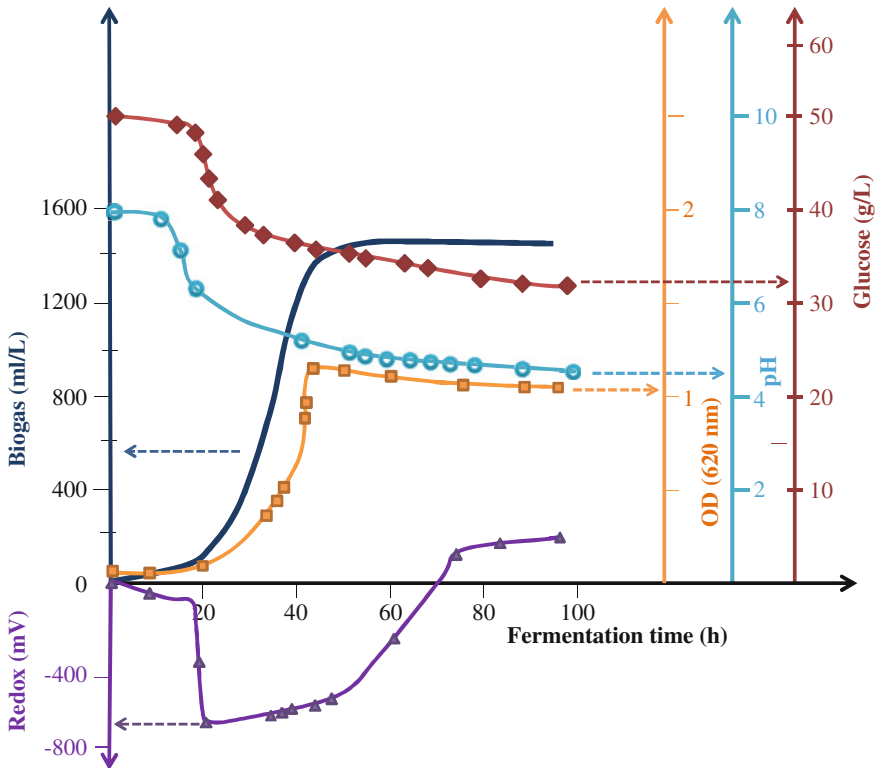


**Fig. 2.3** Cumulative biogas ( $H_2$ ,  $CO_2$ ) production at 35 °C in relation to cell growth, pH, redox and substrate utilization during fermentation time

Figure 2.3a shows that the  $H_2$  production is coupled with microorganism growth. Figure 2.3b shows that, at the begin of the exponential phase, redox suddenly reached a minimum value of  $-518$  mV, but increased thereafter to reach positive values at the end of fermentation, confirming that the substrate was not oxidized in the oxidative environmental conditions, and hence  $H_2$  was not produced [26].

As shown in Table 2.2, the conversion efficiencies (right-hand column) of  $H_2$  from glucose ranged from about 10–15 %, based on the theoretical stoichiometry of 3 mol  $H_2$  from 1 mol glucose, taking into account the average values between the maximum theoretical production of  $H_2$  from acetic acid (4 mol  $H_2$ /mol glucose) and butyric pathways (2 mol  $H_2$ /mol glucose), considering, as a rough approximation, that glucose is equally converted into the two volatile fatty acids. These conversion efficiencies are rather less than that obtained by Mu et al. [13] of 43 % in batch tests with acid pretreatment of sewage sludge (based on the assumption of a maximum 3 mol  $H_2$ /mol glucose). Our low production efficiency of  $H_2$  from glucose probably

**Table 2.2** Summary of total biogas, hydrogen content, glucose utilization, H<sub>2</sub> yield and H<sub>2</sub> conversion efficiency

Run	Gas evolved (ml/L culture)	H <sub>2</sub> content (%)	H <sub>2</sub> content (mmol)	C <sub>6</sub> H <sub>12</sub> O <sub>6</sub> consumed (mmol)	H <sub>2</sub> yield $\frac{\text{molH}_2}{\text{molC}_6\text{H}_{12}\text{O}_6}$	Y <sub>H<sub>2</sub></sub> /Y <sub>th</sub> <sup>a</sup> (%)
<i>Anaerobic wastewater sewage sludge</i>						
1	1463.64	60.40	39.44	93.88	0.42	14.00
2	1373.82	61.82	37.89	101.94	0.37	12.33
3	1154.53	62.85	32.37	105.06	0.31	10.33
4	1274.58	52.18	29.67	102.28	0.29	9.67
5	1176.44	55.53	29.14	99.33	0.29	9.67
Mean	1289 ± 131	59 ± 5	34 ± 5	100 ± 4	0.34 ± 0.06	11.20 ± 1.91
<i>Bovine manure</i>						
1	1560.31	61.32	42.71	91.81	0.46	15.33
2	1480.14	71.84	47.47	100.10	0.47	15.66
3	1250.36	56.70	31.65	95.06	0.33	11.00
4	1110.42	65.72	32.58	103.15	0.32	10.66
5	1325.10	58.32	34.50	98.75	0.35	11.66
Mean	1347 ± 181	63 ± 6	38 ± 7	98 ± 4	0.39 ± 0.07	12.86 ± 2.4

<sup>a</sup> Y yield; Y<sub>th</sub> (theoretical yield) = 3 molH<sub>2</sub>/molC<sub>6</sub>H<sub>12</sub>O<sub>6</sub> taking into account the average values between the maximum theoretical H<sub>2</sub> production from the acetic and butyric pathways of 4 and 2 molH<sub>2</sub>/mol, respectively

depends on the absence of agitation, leading to a high dissolved H<sub>2</sub> concentration that inhibits H<sub>2</sub> and produces enzymes. It is important to point out that acid treatment has the same effect on the different sources of anaerobic microflora (anaerobic wastewater sewage sludge and bovine manure), as confirmed by the conversion efficiency.

In fact, as discussed in Chap. 1, the pool of reduced Fd is generated from two sources: (1) pyruvate oxidation by ferredoxin oxidoreductase (PFOR) and (2) NADH oxidation by NADH, Fd oxidoreductase (NFOR). These enzyme systems can be thermodynamically regulated by the H<sub>2</sub> concentration dissolved in the liquid phase; PFOR can function at the H<sub>2</sub> concentrations observed in fermentative systems so there will always be some H<sub>2</sub> produced, whereas NADH oxidation by NFOR is inhibited at a concentration of H<sub>2</sub> measured as partial pressure in the off-gas  $P_{H_2} > 60\text{--}100$  Pa ( $\sim 0.5\text{--}0.8$  μM).

It is emphasized that the purpose of the present experimental work was not the kinetics set-up of H<sub>2</sub> production from glucose, but only the effectiveness and reproducibility of the acid pretreatment of such anaerobic microorganism consortia, in order to use them as enriched HPB as inoculum in a bioreactor plant to produce hydrogen.

## 2.4 Conclusion

The experimental results obtained in this chapter clearly reveal that acid pretreatment is an effective method of increasing hydrogen-forming bacteria in an anaerobic microorganism consortium and is able to avoid methanogenesis during fermentation. The results of the tests performed on the activity of the treated sludge, repeated five times for each consortium, as bio-hydrogen-producing inoculum in anaerobic fermentation are more than acceptable, indicating that acid pretreatment is a suitable process for preparing the inoculum for a bioreactor producing hydrogen in a full-scale application. The high H<sub>2</sub> gas concentration (50–70 %) and the absence of methane confirm the feasibility of acid treatment. Thus, acid treatment is highly selective for *Clostridium* spp. with respect to other bacteria, including facultative bacteria. Facultative anaerobic bacteria are less sensitive to oxygen than strict anaerobes, i.e. Clostridia, and they are sometimes able to recover hydrogen production activity after accidental oxygen introduction by rapidly depleting oxygen which might be present in the digester. Therefore, it could be feasible to use in a full-scale plant in which the bioreactor is filled with an acid solution in the first phase; this approach does not need high energy expenditure, as occurs in the case of heat treatment. The H<sub>2</sub> production monitored during the evolution of fermentation shows that H<sub>2</sub> is mainly produced by a cellular growth phase in which glucose (except that utilized for cellular reproduction) is converted to volatile fatty acids (VFA), as shown by the decrease in pH.

## References

1. T.D. Brock, M.T. Madigan, J.M. Martino, J. Parker, *Biology of microorganisms* (Prentice-Hall, New York, 1994)
2. R.Y. Stanier, L. John Ingraham, L. Mark, P.D. Wheelis, P.R. Painter, *The Microbial World* (Prentice Hall, Englewood Cliffs, 1986)
3. H.H.P. Fang, T. Zhang, H. Liu, Microbial diversity of a mesophilic hydrogen-producing sludge. *Appl. Microbiol. Biotechnol.* **58**, 112–118 (2002)
4. R.S. Oremland, in *Biology of Anaerobic Microorganisms*, ed. by A.J.B. Zehnder. Biogeochemistry of Methanogenic Bacteria (Wiley Press, New York, 1988), pp. 641–705
5. H. Zhu, M. Béland, Evaluation of alternative methods of preparing hydrogen producing seeds from digested wastewater sludge. *Int. J. Hydrogen Energy* **31**, 1980–1988 (2006)
6. S.M. Kotay, D. Das, Novel dark fermentation involving bioaugmentation with constructed bacterial consortium for enhanced biohydrogen production from pretreated sewage sludge. *Int. J. Hydrogen Energy* **34**, 7489–7496 (2009)
7. M. Yang, H.Q. Yu, G. Wang, Evaluation of three methods for enriching H<sub>2</sub>-producing cultures from anaerobic sludge. *Enzyme Microb. Technol.* **40**, 947–953 (2007)
8. J.J. Lay, Y.J. Lee, T. Noike, Feasibility of biological hydrogen production from organic fraction of municipal solid waste. *Water Resour.* **33**(11), 2579–2786 (1999)
9. S.S. Cheng, M.D. Bai, S.M. Chang, K.L. Wu, W.C. Chen and W.C. Chen, *Studies on the Feasibility of Hydrogen Production Hydrolyzed Sludge by Anaerobic Microorganism*, in The 25th Wastewater Technology Conference, Yunlin, Taiwan, 2000
10. S.M. Kotay, D. Das, *Studies on Maximization of Microbial Production of Hydrogen from Pretreated Sewage Sludge, IChE- CHEMCON 2006* (Ankleshwar, India, 2006)

11. L. Guo, X.M. Li, X. Bo, Q. Yang, G.M. Zeng, D.X. Liao, J.J. Liu, Impacts of sterilization, microwave and ultrasonication pretreatment on hydrogen producing using waste sludge. *Bioresour. Technol.* **99**(9), 3651–3658 (2008)
12. J. Kim, C. Park, T.H. Kim, M. Lee, S. Kim, S.W. Kim, J. Lee, Effects of various pretreatments for enhanced anaerobic digestion with waste activated sludge. *J. Biosci. Bioeng.* **95**(3), 271–275 (2003)
13. Y. Mu, H.Q. Yu, G. Wang, Evaluation of three methods for enriching H<sub>2</sub>-producing cultures from anaerobic sludge. *Enzyme Microb. Technol.* **40**(4), 947–953 (2006)
14. J. Wang, W. Wan, Comparison of different pretreatment methods for enriching hydrogen-producing bacteria from digested sludge. *Int. J. Hydrogen Energy* **33**, 2934–2941 (2008)
15. C.C. Chen, C.Y. Lin, M.C. Lin, Acid-base enrichment enhances anaerobic hydrogen production process. *Appl. Microbiol. Biotechnol.* **58**, 224–228 (2002)
16. B. Hu, S. Chen, Pretreatment of methanogenic granules for immobilized hydrogen fermentation. *Int. J. Hydrogen Energy* **32**(15), 3266–3273 (2007)
17. A. Giordano, R. Farina, M.C. Lavagnolo, A. Spagni, Biological Hydrogen production from mixed cultures using aeration pretreatment, in *Proceedings Second International Symposium on Energy from Biomass and Waste* in Venice, 2008
18. B.E. Ritmann, P.L. McCarty, *Environment Biotechnology: Principle and Application* (McGraw Hill Press, New York, 2001)
19. I. Valdez-Vazquez, H.M. Poggi-Varaldo, Alkalinity and high total solids affecting H<sub>2</sub> production from organic solid waste by anaerobic consortia. *Int. J. Hydrogen Energy* **34**, 3639–3646 (2009)
20. I.C. Clark, R.H. Zhang, S.K. Upadhyaya, The effect of low pressure and mixing on biological hydrogen production via anaerobic fermentation. *Int. J. Hydrogen Energy* **37**, 11504–11513 (2012)
21. W.M. Chen, Z.-J. Tseng, K.-S. Lee, J.-S. Chang, Fermentative hydrogen production with *Clostridium Butyricum* CGS5 isolated from anaerobic sewage sludge. *Int. J. Hydrogen Energy* **30**(10), 1063–1070 (2005)
22. H. Yang, J. Shen, Effect of ferrous iron concentration on anaerobic bio-hydrogen production from soluble starch. *Int. J. Hydrogen Energy* **31**(15), 2137–2146 (2006)
23. H. Argun, F. Kargi, Effect of acid pretreatment method on bio-hydrogen production by dark fermentation of waste ground wheat. *Int. J. Hydrogen Energy* **34**, 8543–8548 (2009)
24. S. Venkata Mohan, V. Lalit Babu, P.N. Sarma, Effect of various pretreatment methods on anaerobic mixed microflora to enhance biohydrogen production utilizing dairy wastewater as substrate. *Bioresour. Technol.* **99**(1), 59–67 (2008)
25. A. Galli, L. Franzetti, *Metodi per l'analisi Microbiologica Degli Alimenti* (DISTAM Università degli Studi di Milano Press, Milano, 2003)
26. A.C. Van Handel, G. Lettinga, *Anaerobic Sewage Treatment- A Practical Guide for Regions with a Hot Climate* (Wiley Press, New York, 1994)

# Chapter 3

## Kinetics, Dynamics and Yield of H<sub>2</sub> Production by HPB

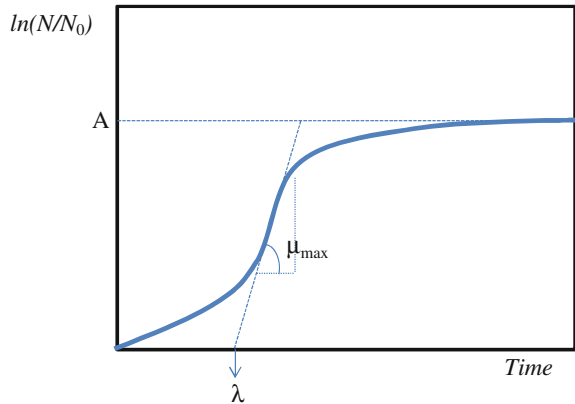
Knowledge of the kinetics of H<sub>2</sub> production is a necessary step towards a thorough understanding of the mechanisms involved in the complex system of microorganisms' metabolic pathways in the substrate, including H<sub>2</sub>-producing bacteria, electron shuttles and hydrogenase enzymes. For this reason, detailed kinetics can shed light on the dynamics of glucose consumption as well as on the evolution of bioH<sub>2</sub> using an enriched HPB biomass. In this chapter, after a general introduction to the kinetics model generally used in anaerobic processes and in particular for H<sub>2</sub> production, we will analyze the kinetics and dynamics of H<sub>2</sub> production utilizing glucose as substrate. The kinetics are studied by applying an experimental approach such as the *modified initial rate method* which experimentally determines the derivatives of substrate consumption as well as the H<sub>2</sub> production.

### 3.1 Kinetic Models

#### 3.1.1 Microorganism Growth Model

Several models are used to describe the behaviour of microorganisms under different physical or chemical conditions such as temperature, pH, and so on. These models allow prediction of microbial activity and metabolic products, and the detection of critical steps of the production and distribution metabolites [1]. In order to build these models, growth has to be measured; bacterial growth (Fig. 3.1) often shows a phase in which the specific growth rate starts at a value of zero time and then accelerates to a maximal value ( $\mu_{\max}$ ) in a certain period of time, resulting in a lag phase time ( $\lambda$ ). In addition, growth curves contain a final phase in which the rate decreases and finally reaches zero, so an asymptote ( $A$ ) is reached. When the growth curve is defined as the logarithm of the number of organisms plotted against time, the changes in growth rate result in a sigmoidal curve, with lag phase just after  $t = 0$  followed by an exponential phase and then by a stationary phase.

**Fig. 3.1** A microorganism growth curve



A number of growth models are found in the literature, such as the models of Gompertz [2], Richards [3], Stannard et al. [4], the logistic model and others [5]. These models use as a variable only the number of organisms and do not include the consumption of substrate as a model based on the Monod equation would do. Besides the lag period and the asymptotic value, another valuable parameter of the growth curve is the maximum specific growth rate ( $\mu_{max}$ ). Since the logarithm of the number is used,  $\mu_{max}$  is given by the slope of the line when the organisms grow exponentially. Usually this parameter is estimated by subjectively deciding which part of the experimental curve is approximately linear and then determining the slope of this curve section, eventually by linear regression. A better method is to describe the entire set of experimental data with a growth model and then estimate  $\mu_{max}$ ,  $\lambda$  and  $A$  by a best-fit procedure. Some authors indeed use growth models as those shown in Table 3.1 to describe their data. These models can describe the number of organisms ( $N$ ) or the logarithm of the number of organisms [ $\log(N)$ ] as a function of time. The motivation for the decision to use a given model is usually not stated. Gibson et al. [7] found better results by a fitting procedure with the Gompertz model than other models.

**Table 3.1** Some growth model used and their modified forms

Model	Equation	Modified equation
Logistic [6]	$y = \frac{a}{1 + e^{(b-cx)}}$	$y = \frac{A}{\left\{1 + e^{\left[\frac{\mu_{max}}{A}(\lambda-t)+2\right]}\right\}}$
Gompertz [2]	$y = a \cdot e^{-e^{(b-cx)}}$	$y = Ae^{-e^{\left[-\frac{\mu_{max}}{A} \cdot e^{(\lambda-t)+1}\right]}}$
Richards [3]	$y = a \left\{1 + v \cdot e^{[k(\tau-x)]}\right\}^{\left(-\frac{1}{v}\right)}$	$y = A \left\{1 + v \cdot e^{(1+v) \cdot e^{\left[\frac{\mu_{max}}{A} \cdot (1+v)\left(1+\frac{1}{v}\right) \cdot (\lambda-t)\right]}}\right\}^{\left(-\frac{1}{v}\right)}$
Stannard et al. [4]	$y = a \left\{1 + e^{\left[-\frac{(t+kv)}{p}\right]}\right\}^{(-p)}$	$y = A \left\{1 + v \cdot e^{(1+v) \cdot e^{\left[\frac{\mu_{max}}{A} \cdot (1+v)\left(1+\frac{1}{v}\right) \cdot (\lambda-t)\right]}}\right\}^{\left(-\frac{1}{v}\right)}$



Since bacteria grow exponentially, it is often useful to plot the logarithm of the relative population size [ $y = \ln(N/N_0)$ ] against time where  $N_0$  is the number of microorganism at time  $t = 0$  (Fig. 3.1). The three phases of the growth curve can be described by three parameters: the maximum specific growth rate  $\mu_{\max}$ , defined as the tangent in the inflection point; the lag time  $\lambda$ , defined as the  $x$ -axis intercept of this tangent; and the asymptote [ $A = \ln(N/N_0)$ ]. Curves may show a decline; this kind of behaviour is called the death phase.

Most of the equations describing a sigmoidal growth curve may contain mathematical parameters (a, b, c ...) rather than parameters with a biological meaning ( $A$ ,  $\mu_{\max}$  and  $\lambda$ ). It is difficult to estimate start values for the parameters if they have no biological meaning.

### 3.1.2 Kinetic Models of Anaerobic Processes

Substrate biodegradation, which occurs in a conventional anaerobic digester under the activity of several microorganism species, depends on the degree of activity of these microorganisms, in which the role of methanogens becomes limiting. The study of the process kinetics can be described by the kinetic models used for a monoculture, such as the model proposed by EI-Mansi [8] (Eq. 3.1), which is a saturation type on carbon source and where the growth is linearly dependent on the microorganism concentration:

$$r_x = \frac{\delta X}{\delta t} = \frac{\mu_{\max} X \cdot S}{K_s + S} \quad (3.1)$$

where

$r_x$  = bacterial growth rate;

$X$  = concentration of biomass;

$t$  = time;

$\mu_{\max}$  = maximum specific growth rate;

$S$  = limiting substrate concentration;

$K_s$  = half saturation coefficient.

This model is applicable to the kinetic study of a bacterial population whose development is limited by only one substrate. Among several equations which relate the specific growth rate coefficient to the concentration of limiting nutrient, the Monod one is the most popular and usually fits actual data quite well. Considering the yield  $Y_{X/S}$  defined as the ratio between the growth rate and the substrate consumption rate [9], it is possible to write that:

$$Y_{X/S} = -\frac{r_x}{r_s} = -\frac{X_0 - X}{S_0 - S} \quad (3.2)$$

where

$X_0$  = initial bacterial concentration;

$S_0$  = initial concentration of the substrate.

The following differential equation is generally used to include microbial growth and maintenance:

$$-\frac{\delta S}{\delta t} = Y_{X/S} \cdot \frac{\delta x}{\delta t} + m_s X \quad (3.3)$$

The first term on the right-hand side refers to substrate consumption for microbial growth, and the second one to microbial activity without growth, where  $m_s$  indicates the maintenance coefficient based on substrates consumed for energy purposes only. Equation (3.3) gives the rate of substrate disappearance in a system, in which the degradation kinetics is controlled only by the concentration of bacteria and the substrate.  $K_s$  is the value of substrate concentration corresponding to half the maximum specific growth rate of biomass. Thus, a low value of this parameter indicates the ability of microorganisms to easily assimilate the substrate. Most of the mathematical models explain the processes of anaerobic digestion by considering completely mixed systems, with or without recirculation of solids. Contois (1959) has proposed a different model based on the following kinetic equation [10]:

$$\mu = \frac{\mu_{\max} S}{(BX + S)} \quad (3.4)$$

where  $B$  is a constant kinetic parameter, and the saturation constant  $K_s$  does not appear. Equation (3.4) describes well the kinetics of systems with microbial growth limited by mass transfer, for example the digestion of animal wastes. Andrews (1968) developed a mathematical model for the processes of anaerobic digestion which considers the metabolism of volatile fatty acids (VFA) (including acetic and propionic acid) [11]. He introduced the concept of substrate inhibition in large concentrations, due to the presence of a fraction of non-ionized VFA whose concentration depends on the pH of the medium. Considering the non-ionized acids as substrate and expressing their limiting effect in the coefficients  $K_s$  and  $K_i$ , the following equation is a so-called inhibition growth kinetics model:

$$\mu = \frac{\mu_{\max} S}{(K_s + S) \left(1 + \frac{S}{K_i}\right)} \quad (3.5)$$

where

$S$  = non-ionized substrate concentration and  $K_i$  = inhibition constant. Heyes and Hall [12] challenged this model by saying that the inhibition is not a function of non-ionized VFA; high concentrations of VFA are the result of substrate utilization and not the cause of the fermentation instability. They found that H<sub>2</sub> concentration could be a useful stability parameter. Instead, Mosey [13] considered the hydrogen

partial pressure as the key regulatory parameter of the anaerobic digestion of glucose, and hence he adopted it as a control variable because it affects the redox potential of the liquid phase. The relative production of VFA is assumed to be dependent on the redox potential or, equivalently, on the ratio  $[\text{NADH}]/[\text{NAD}^+]$  [14]. Lyberatos and Skiadas [14] concluded that the relationship between the reduced form and oxidized form of NADH controls the rate of conversion of propionic acid and butyric acid. Furthermore, they affirmed the existence of a direct relationship between the fraction  $\text{NADH}/\text{NAD}^+$  and the partial pressure of hydrogen in the gas phase, using this relationship in an equation similar to that of Monod.

### 3.1.3 Some Kinetic Models for $\text{H}_2$ Production

To describe the progress of batch fermentative hydrogen production, several authors very often apply the *modified logistic equation* (Eq. 3.6) or *modified Gompertz equation* (Eq. 3.7) to estimate hydrogen production potential ( $V_{\text{gas,max}}$ ), biogas production rate ( $R_{\text{max,gas}}$ ) and lag phase ( $\lambda$ ):

$$V_{\text{gas}} = \frac{V_{\text{gas,max}}}{1 + \exp\left[\left(\frac{R_{\text{max,gas}} \cdot e}{V_{\text{gas,max}}}\right)(\lambda - t) + 1\right]} \quad (3.6)$$

$$V_{\text{gas}} = V_{\text{gas,max}} \exp\left\{-\exp\left[\frac{R_{\text{max,gas}} \cdot e}{V_{\text{gas,max}}}[\lambda - t] + 1\right]\right\} \quad (3.7)$$

where  $V_{\text{gas}}$  is the total amount of  $\text{H}_2$  produced (mL) at reaction time  $t$  (h),  $V_{\text{gas,max}}$  is the potential maximal amount of  $\text{H}_2$  produced,  $R_{\text{max}}$  (mL/h) is the maximum  $\text{H}_2$  production rate,  $\lambda$  (h) is the lag phase to exponential biogas production and  $e$  is  $\exp(1)$ , i.e. 2.71828 [6].

The cumulative experimental data of  $\text{H}_2$  production is described with Eq. 3.7 in order to estimate the three parameters  $V_{\text{gas,max}}$ ,  $R_{\text{max}}$  and  $\lambda$  characterizing the experimental test. The parameters were estimated by employing a non-linear best-fit procedure. In addition, using  $V_{\text{gas,max}}$  values and Eq. 3.7, the half period time (HPT) can be evaluated, which represents the time at which a quantity of  $\text{H}_2$  equal to  $V_{\text{gas,max}}/2$  was produced. HPT is a kinetic parameter, i.e. the time necessary to reach 50 % of the yield; it indicates the time at which the production rate is at its maximal value.

The Monod model is widely used to describe the effects of substrate concentration on the rates of substrate degradation, HPB growth and  $\text{H}_2$  production. The Arrhenius model was used to describe the effect of temperature on fermentative  $\text{H}_2$  production, while the modified Han–Levenspiel model [15] was used to describe the effects of inhibitors on fermentative hydrogen production. The Andrew model was used to describe the effect of  $\text{H}^+$  concentration on the specific  $\text{H}_2$  production rate, while the Luedeking–Piret model and its modified form was widely used to describe the relationship between the HPB growth rate and the product formation

rate [15]. Despite many kinetics studies in the literature, we noticed the lack of models which incorporate important parameters affecting hydrogen production, such as pH and redox, which influence enzymes involved in hydrogen production, such as ferredoxin (Fd) and hydrogenase. Therefore, the aim of the following sections is to suggest a macro-approach methodology to set up a formal kinetics of H<sub>2</sub> evolution. To this end the kinetics of bio-hydrogen production on glucose by HPB culture was set up and described, taking into consideration the structural information on the enzymes involved in hydrogen production.

## 3.2 Experimental Section

### 3.2.1 HPB Sewage Sludge Enrichment

The anaerobic microorganisms used in this study were withdrawn from an anaerobic digester of a municipal wastewater treatment plant. The pH, density, volatile solid (VS) and total solid concentration (TS) of the sewage sludge used were 7.3, 1,010 g/L, 10,875 and 14,500 mg/L respectively. The sludge was pretreated as described in Chap. 2. To avoid differences between the tests, all the seeds came from the same pretreatment batch. At the end of treatment, the sludge was divided in several portions of 50 mL and each of them was frozen. Before inoculation the seed was thawed at ambient temperature and then gently heated to the working temperature.

### 3.2.2 Fermentation Tests

Kinetic studies were carried out in 500 mL (450 mL working volume) Erlenmeyer flasks, agitated daily, and flushed at the beginning with nitrogen gas for 5 min in order to remove air from the system. The treated sludge was used as seed in the ratio of 10 % v/v. Initial glucose concentration values tested in batch condition were 5, 25, 45, 60, 70 and 90 g/L. The composition of the medium was formulated by adding micronutrient solution [16] in order to reach an initial C/N ratio of about 30. The initial pH of the media was set in the range 6.6–7.4 by using 2 N NaOH solution. Tests were conducted at  $35 \pm 1$  °C in a thermostatically controlled room; each measurement is the result of a triplicate test. Tests were stopped when the biogas production shut down.

A single test was conducted in a 2 L bioreactor (Minifors, Infors AG, Switzerland) under the following conditions: 60 g/L of glucose and micronutrients as above, agitation of 100 rpm and ambient temperature of 22–28 °C. The initial pH was 7.3; pH was readjusted to 6 using 2 M NaOH solution when gas production shut down at 60 h of fermentation time and when pH reached 4.4 at 150 and 190 h of fermentation time.

### 3.2.3 Analytical Methods

Gas evolution in the tests conducted in Erlenmeyer flasks was monitored during the fermentation by the water-replacement method, its composition was measured at the end of the lag phase ( $\approx 10$  h) and at the end of fermentation, and an average value was obtained. At the end of fermentation, the concentrations of ethanol and acetic, propionic and butyric acids were also detected. During the tests, liquid samples were withdrawn in order to measure pH and redox potential. Gas composition was measured by gas chromatography (Varian CP, 4900) equipped with a thermal conductivity detector (TCD); pH was measured by a pH meter (Infors AG, Switzerland); redox potential was measured by a Pt4805-DXK-S8/120 electrode (Mettler Toledo, Switzerland). Glucose concentration was measured by enzymatic bio-analysis (Biopharm-Roche). The concentrations of ethanol and acetic, propionic and butyric acids were detected by a gas chromatograph (Model 6580, Agilent Inc., USA) equipped with a flame ionization detector (FID).

### 3.2.4 Kinetics Study

#### 3.2.4.1 Modified “Initial Rate Method”

Gas production rate was evaluated by linear regression of experimental values of the volume of total gas produced per unit reaction volume during the exponential phase; glucose uptake rate was evaluated by linear regression of experimentally determined concentrations during the same exponential phase. This is a type of *initial rate method* usually employed for enzymatic reactions [17], considering as negligible the variation of limiting and inhibiting effects on the measuring range. In the present case the derivative time period starts after a lag phase of about 20 h. The initial rate method involves measuring the rate of reaction at very short times, before any significant change in concentration occurs. During the exponential phase biogas production and glucose uptake rates show a linear behaviour with time until a sharp pH effect (drop to pH 4.3) that shuts down fermentation; this confirms the initial rate method hypotheses. Uncertainty was estimated to be around 20 % as standard deviation on the repeated tests.

#### 3.2.4.2 Data Analysis

Gas production rate and glucose uptake rate were best fitted against average glucose concentration during the exponential phase. Several kinetic models were considered for gas production to fit the experimental data; they are reported in Table 3.2. Instead, linear best fit was used for glucose uptake rate; the  $R^2$  value was taken into account in order to choose the kinetic model. The statistically low number of experimental data limits the  $R^2$  values.

**Table 3.2** Biogas kinetic models used to best fit experimental data

Equation	$R^2$
$r(P) = \frac{r_{\max}S}{K_S+S}$	0.71
$r(P) = \frac{r_{\max}S}{K_S+S+S^2/K_I}$	0.81
$r(P) = \frac{r_{\max}S}{K_S+S} \exp(-S/K_I)$	0.82
$r(P) = aS + bS^2$	0.88
$r(P) = aS + bS^2 + cS^3$	0.94

### 3.3 Results and Comments

The shape of the fermentation line against time is similar for all the glucose concentrations tested and presents four phases, during which different behaviours are observed. Figures 3.2, 3.3 and 3.4 report the values of gas production as volume per unit reaction volume, glucose concentration, measured pH and redox values against fermentation time, for the lowest, the highest and the intermediate glucose concentrations tested, respectively. There are four fermentation phases, as mentioned previously:

1. During the first 18–22 h the gas production rate was very low in all the tests, ranging between 2 and 7 mL/Lh; no hydrogen was measured in the gas produced in this period. Table 3.3 reports the variation of the measured variables at 10 h of fermentation.

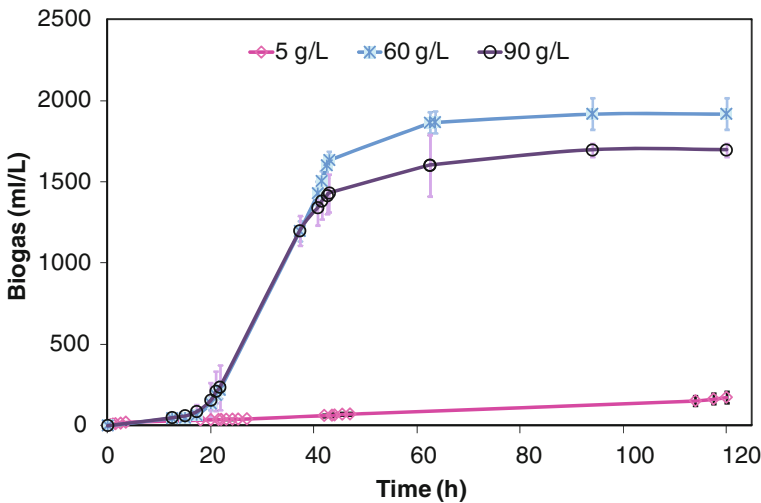


**Fig. 3.2** Biogas production versus time in low (5 g/L), medium (60 g/L) and high (90 g/L) glucose concentration tests

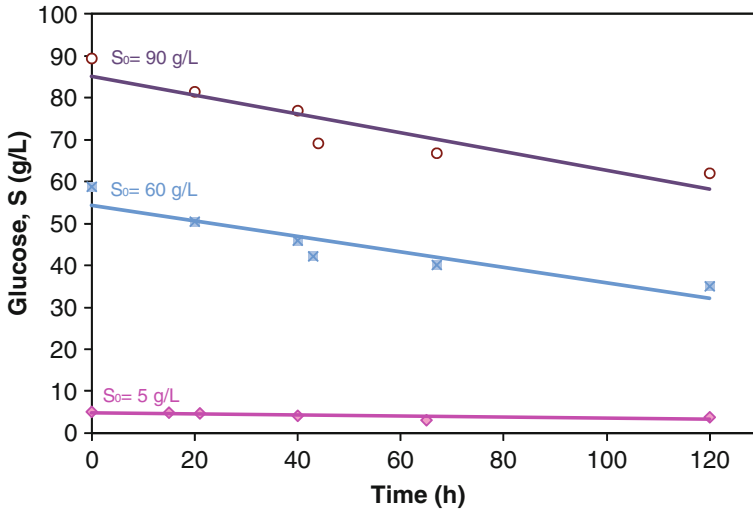


**Fig. 3.3** Glucose concentration variation versus time in low (5 g/L), medium (60 g/L) and high (90 g/L) glucose concentration tests

- At 18 h of fermentation the gas production rate increased sharply to 10–100 mL/Lh depending on initial substrate concentration; the values reached were maintained up to pH values of 4.2–4.4 after around 30–40 h of fermentation.
- When the pH reached 4.2–4.4, the gas production rate decreased sharply in all the tests; biogas shut-down occurred when the pH was in the range 3.2–4.0.
- After the gas production stopped, glucose continued to be consumed at a reduced rate until the complete arrest of fermentation.

The gas production rate has different values in the four phases; during the first two phases it is constant. The measured glucose uptake rate shows similar values in the first three phases and slows down in the fourth one. pH decreases in all the phases, much more rapidly during the first (Fig. 3.4). Redox potential decreases during the first phase, and falls at the end of the first phase to between  $-400$  and  $-500$  mV; it increases very slowly during the exponential phase and increases strongly during the third phase, reaching a value in the range  $-100$  to  $-300$  mV. The redox behaviour in the test at very low glucose concentration (5 g/L) does not show an increase during the exponential phase. During the first phase gas production is in a lag phase, during the second phase gas production is in an exponential phase (i.e. medium composition changes do not affect hydrogen production), during the third phase hydrogen production is inhibited by the low pH values, and during the fourth phase gas production is completely stopped by the low pH values. The main experimental results are reported in Table 3.4.

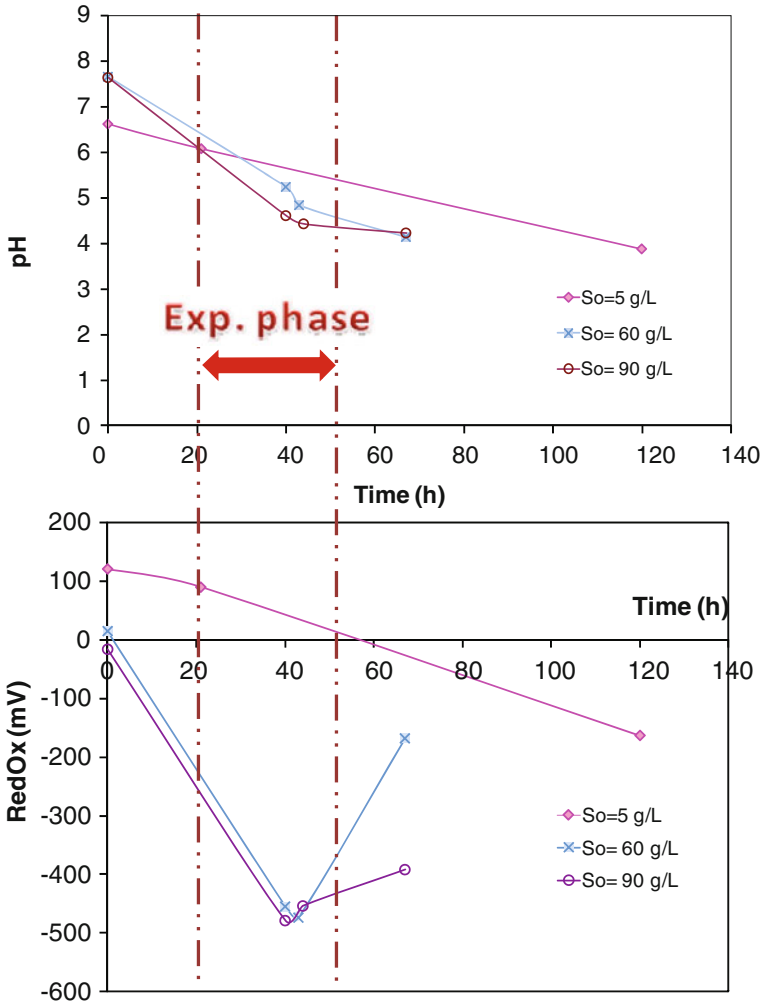


Fig. 3.4 pH and redox versus time

### 3.3.1 Lag Phase

During the first period the microorganisms were active but there were not yet favorable conditions for hydrogen evolution. Although pH and redox are reduced during the lag phase, pH remains in the neutral range (pH > 6.5) and redox remains in the low reductive range (redox > -200 mV). Several phenomena occur during the lag phase owing to the presence of different bacterial species. Facultative bacteria can evolve their metabolism towards the biosynthesis of ethanol, e.g. *Klebsiella pneumoniae*, which is able to produce in anaerobic condition either ethanol from



**Table 3.3** Experimental results at 10 h of fermentation

Parameters	Nominal glucose concentration of tests					
	5 g/L	25 g/L	45 g/L	60 g/L	70 g/L	90 g/L
<i>Glucose (g/L)</i>						
$t = 0$ h	5.05	24.61	45.00	59.76	67.45	89.41
$\Delta S$	0.18	0.79	1.5	2.2	2.80	2.70
<i>Biogas (mL/L)</i>						
$t = 10$ h	54	62	59	59	69	59
H <sub>2</sub> (%)	0	0	0	0	0	0
<i>pH</i>						
$t = 0$ h	6.61	6.64	7.28	7.29	7.07	7.37
$\Delta pH$	-0.32	-0.24	-0.35	-0.48	-0.3	-0.52
<i>Redox potential (mV)</i>						
$t = 0$ h	121	70	80	-47	-10	15
$\Delta redox$	-12	-90	-110	-103	-107	-98

**Table 3.4** Volume and composition of biogas produced and glucose utilization

Runs (g/L)	Biogas produced (mL/L)	H <sub>2</sub> (%)	CO <sub>2</sub> (%)	$\Delta S$ (mmol)	$\Delta S/S$ (%)
5	112 ± 7	60 ± 1	40 ± 1	7.2	25
25	600 ± 150	58 ± 2	42 ± 2	8.2	33
45	630 ± 170	60 ± 1	40 ± 1	49.8	20
60	1,920 ± 100	47 ± 12	53 ± 12	103.7	32
70	1,220 ± 210	58 ± 2	42 ± 2	105.6	28
90	1,700 ± 40	40 ± 12	60 ± 12	125.6	25

glucose or acetic acid from acetyl-CoA [18]. Following the ethanol metabolic pathway, all NADH produced is consumed; in other words the ethanol biosynthesis pathway is in full competition with metabolic products that are coupled with NADH regeneration for biogenesis of H<sub>2</sub>, for example. Acetic acid is produced in low quantities, reducing pH and lowering the redox until *Clostridium* spp. are able to activate the acetic and butyric pathways to produce H<sub>2</sub>. The production of molecular hydrogen maintains the electron balance in which protons act as electron acceptors and the substrate acts as electron donors [19], as shown in Chap 1. This can occur only if an adequate difference in electrical potential exists as the driving force, i.e. redox needs to be at an adequate value. Glucose uptake generates ATP, NADH and NADPH through the glycolysis pathway and oxidative decarboxylation of pyruvate. NADH and NADPH, in anaerobic conditions, need to be oxidized to NAD<sup>+</sup> and NADP<sup>+</sup> for cellular activity. The reoxidation processes are activated by iron–sulfur proteins that act as electron donors in many systems, interacting with flavoproteins, hemoproteins and other more complex iron–sulfur proteins. For *Clostridium* spp. it is well accepted that structural proteins such as Fd are able to transfer electrons to H<sup>+</sup> mediated by the hydrogenase enzyme, whereas the action of

[Fe]-Fd-hydrogenase is to remove excessive reducing equivalents during fermentation by strictly anaerobic bacteria such as Clostridia [20]. [Fe]-Fd-hydrogenase is an active oxidation–reduction group in the chain which transfers electrons from carbohydrates to protons able to generate hydrogen via pyruvate synthesis in anaerobic acetogenic bacteria [17]. The key point to be considered is that the Fd forms a complex such as Fd · Fd NADP<sup>+</sup> reductase, found in *Clostridium acetobutylicum* [21]. The interactions between Fd and the complex are strongly affected by the pH of the medium. At near-neutral pH values (6–7) a proton is taken up when Fd and Fd·NADP<sup>+</sup> reductase form a complex. The complex dissociation constant depends on pH: for pH > 8.5 the Fd is all in the complexed form, while for pH < 8.5 free Fd appears; this suggests that the redox potential of Fd is strongly affected by the pH value. In other words when the pH decreases more the Fd is free and its redox shifts toward its reductive value of –425 mV [21]. Thus the lowering of pH creates a reductive environment (Fd acts as electron donor), while high pH creates an oxidative environment (Fd acts as electron acceptor). Free Fd is predominantly in the oxidized form (Fd<sup>3+</sup>) and presents a lower capacity to act as electron donor to protons via hydrogenase to form hydrogen. In such conditions, electrons produced by the oxidation of pyruvate to acetyl-CoA are used to produce alcohols and lactate instead of hydrogen. The lowered reducing power of Fd·NADP<sup>+</sup> reductase is probably not used to form molecular hydrogen as the terminal electron acceptor; on the contrary, part of the reduced Fd produced is used to generate NADH, which mitigates against hydrogen production. Uyeda and Rabinowitz [22] demonstrated that low-potential electron donors, like reduced Fd, can drive the reductive carboxylation of acetyl-CoA. Moreover it is well known that *Clostridium* spp. do not grow well at pH < 5 [22], as verified also in the present study, and at high glucose concentrations. Other researchers detected the production of ethanol and butanol in experiments using mixed sludge from municipal wastes [23], as occurs in the case of the facultative bacteria *Klebsiella pneumoniae* [18]. Hence one can argue that in the lag phase there is a low activity of the HPB, due to the presence of facultative microorganisms, which take advantage of the presence of micro aeration zones in the broth. Therefore, the metabolic pathways are oriented towards the formation of metabolites other than hydrogen due to the difficulties in Fd and hydrogenase transferring electrons owing to the high value of pH and redox. During the lag phase pH decreases slightly while redox remains at very slightly reductive values (refer to Table 3.3). From this analysis, we suggest that in the lag phase the biomass activity was probably oriented to organize the “environment” to allow *Clostridium* spp. to activate hydrogen production. At the end of the lag phase a metabolic shift occurs and the redox value rapidly decreases to reach values ranging between –400 and –550 mV, enabling reoxidation of NADH and NADPH with hydrogen that acts as an electron acceptor (refer to Fig. 3.4). In order to highlight the experimental evidence, it is important to recall the metabolic pathway of glucose. Owing to the presence of a microorganism consortium it is impossible to refer to such a specific pathway of glucose. Bearing in mind the origin of the biomass used, one can agree that, at least, the following species might be present: *Escherichia*, *Salmonella*, *Shigella*, *Klebsiella*, *Enterobacter* [24] and, obviously,

*Clostridium* spp. All the species present are able to activate acid fermentation with the possibility of an alcoholic fermentation too. Figure 1.7 of Chap. 1 depicts a “virtual” metabolic pathway of glucose which accounts for the main microorganisms present in the HPB culture able to produce metabolites such as acetic, propionic, ethanol and butyric acids, the biomass itself and H<sub>2</sub> and CO<sub>2</sub>.

Chen et al. [25] observed that *C. butyricum* on sucrose started to produce hydrogen at the end of the exponential growth when the microorganisms had entered an early stationary phase. This means that, during the lag phase, glucose is mainly consumed for biomass growth. Thus, one can suppose that during the lag phase electrons mainly flow toward biosynthesis and are not used for hydrogen evolution. The reason for this behaviour remains to be explained.

### 3.3.2 Exponential Phase

The second phase starts at around the 20th hour of fermentation. During this phase the gas production rate and glucose uptake rate are constant (Figs. 3.2 and 3.3). The duration of the exponential phase is different for each test, ranging from 10 to 30 h. It ends when pH goes below a threshold; the comparison of Fig. 3.2 with Fig. 3.4a on the time axis shows that biogas evolution starts when the pH of the medium reaches a value of approximately 6.5 and continues while the pH remains over 4.5. As reported above, the lowering of the pH provokes an increase of free Fd, shifting the redox potential towards reductive values. For the production of H<sub>2</sub> it is necessary that the [Fe] · Fd · hydrogenase complex donates an electron to a proton. Hydrogenase in H<sub>2</sub> production has been studied for several decades [26]; in particular Chen and Blanchard discovered a second hydrogenase (hydrogenase II) in *C. pasteurianum* in addition to hydrogenase I, with the presence of two [8Fe–8S] clusters able to activate the redox reaction. Hydrogenase II as well as hydrogenase I is able to evolve H<sub>2</sub> with Fd as the sole electron carrier. Adams and Mortenson [27] studied the physical and catalytic properties of hydrogenase II compared with hydrogenase I, in particular the pH effect on hydrogenase that catalyzed H<sub>2</sub> evolution. Hydrogenase I has maximal efficiency at pH 6.3, hydrogenase II has maximal efficiency at pH 5.8 and at pH < 5 the activity of both the enzymes decreases rapidly. It is interesting to note that during the exponential phase pH ranges between 4.4 and 6.5 (Figs. 3.1 and 3.3a), while at pH 5 *Clostridium* spp. activity shuts down [25]. The above considerations suggest that the role of pH in the production of H<sub>2</sub> is strongly linked with hydrogenase activity. The positive effect as a consequence of pH decrease is the release of Fd from the complex Fd · NADP<sup>+</sup> reductase, which creates a more reductive environment and the formation of an optimal spatial conformation of hydrogenases I and II with a maximal activity of the enzyme pool, as also reported in Chap. 2. The increase in redox potential during the exponential phase (Fig. 3.4b) indicates that in the medium the availability of electrons decreases because the system moves towards a less reductive range.

All these considerations clearly provide evidence, from an engineering point of view, of the necessity to strictly control the pH in the reactor, in order to prevent the pH going below the 6.2–5.4 range; this can be achieved by addition of NaOH.

### 3.3.3 Kinetics Evaluation

Gas production rate and glucose uptake rate, experimentally evaluated in the exponential phase, were best-fitted against glucose average concentration. As stated previously, several kinetics models were considered for gas production to fit the experimental data reported in Table 3.2. Gas production rate shows a limitation at low substrate concentration and an inhibition at high substrate concentration. No theoretical findings help in choosing one kinetics model among others; hence the best-fit criterion was used to select the regression model. Substrate inhibition is sharper than either the Haldane or exponential models can handle; hence a polynomial of third degree is necessary to reach an acceptable statistical correlation ( $R^2$  value) (Table 3.2). Gas production rate data experimentally evaluated on exponential ranges and the model curve are shown in Fig. 3.5 along with the experimental uncertainty affecting the data. The maximum production rate of over 100 mL/Lh is reached at a glucose concentration below 60 g/L. Experimental data and the regression curve for glucose kinetics are shown in Fig. 3.6. A linear first-order kinetics was set up and a best fit was used for glucose uptake rate; an  $R^2$  value of 0.94 was obtained.

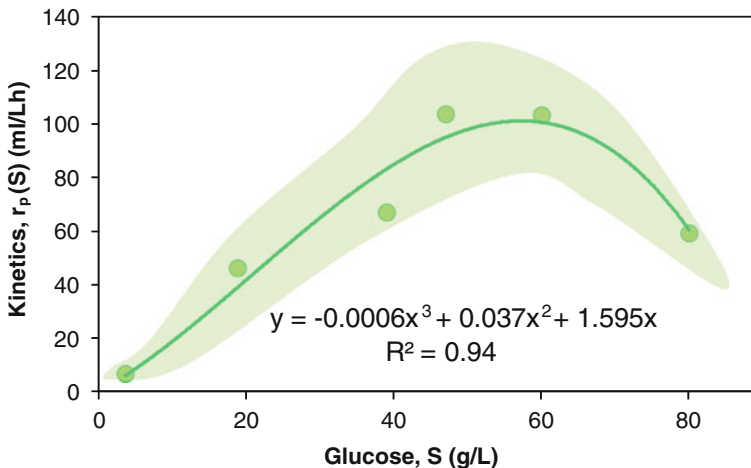
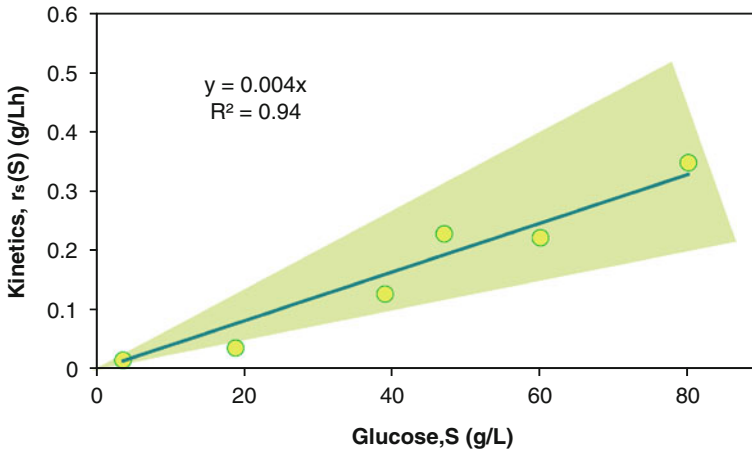


Fig. 3.5 Kinetics of biogas production rate with area of experimental uncertainty



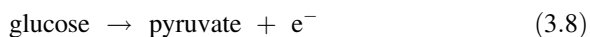
**Fig. 3.6** Kinetics of glucose consumption rate with area of experimental uncertainty

The difference between the kinetics of glucose consumption and biogas evolution is not a surprise, owing to the use of the unstructured modeling approach [28] that allows a good reference model for the design of a reactor and prediction of the system dynamics.

### 3.3.4 Dynamics of $\text{bioH}_2$ Evolution

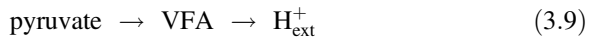
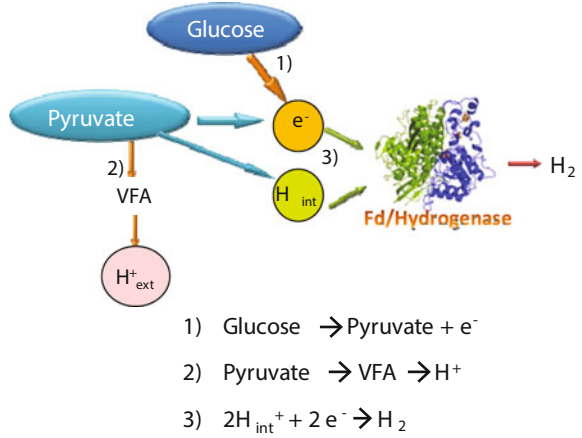
Using the kinetics equations evaluated, this section aims to highlight the system dynamics by a macro-approach [29]. In analyzing such a complex system, as schematized in Fig. 1.7, a reduction of complexity is necessary. The aim of a macro-approach analysis is to find the controlling phenomenon which determines the dynamics of the whole system. To find the controlling step, using the terminology of chemical reaction engineering, it is necessary to put the macro-phenomena, i.e. observable, experimentally detectable phenomena, on the time axis using a relaxation time parameter [30]. A macro-schematization of pathways of Fig. 1.7 is shown in Fig. 3.7, according with the experimentally detected parameters. Three macro-phenomena can be defined and the corresponding *relaxation time* (see Appendix) must be evaluated:

1. Glucose uptake producing electrons by the following macro-reaction:



2. Proton production generating the variation in the pH in the broth by the following macro-reaction:

**Fig. 3.7** Macro-approach to dynamics of H<sub>2</sub> evolution by HPB



3. Hydrogen production experimentally detected by biogas evolution by the following macro-reaction:



The reactions (3.9) and (3.10) proceed in parallel and in series to (3.8). Evidence of this comes from the experimental tests reported in Chap. 4 conducted with continuous pH control with NaOH: during H<sub>2</sub> evolution a concurrent consumption of the base occurs. This suggests that two different locations of proton are present. It is important to remark that serial reactions are controlled by the slowest reaction while parallel reactions are controlled by the most rapid reaction. It is necessary to clarify that the above reactions are only a macro-schema in order to link the experimentally measured macro-parameters with such mechanisms. The protons of reaction (3.9) and (3.10) are topologically different: the first type is external of the cell machinery and is responsible for the pH variation occurring in the broth, while the second type is inside the cell and can be transformed into H<sub>2</sub> gas via hydrogenase activity and hence detected as hydrogen gas.

For each of the above macro-reactions, it is possible to estimate the respective relaxation time. For glucose uptake a first-order kinetics was observed, and thus the relaxation time is a constant:

$$\tau_{Gl} = 1/K \quad (3.11)$$

For bioH<sub>2</sub> production a non-linear kinetics was observed, and hence the relaxation time depends on substrate concentration; it can be estimated using the following equation [30]:

$$\tau_P = [r_P(S)/S]^{-1} \tag{3.12}$$

For  $H^+$  production, the relaxation time  $\tau_{H^+}$  was estimated from the experimental pH values following the definition of relaxation time [30], i.e. the relaxation time is the value of time corresponding to 63 % ( $1 - 1/e$ ) of the observed variation from initial to final  $H^+$  concentration. The relaxation time of the three macro-reactions versus glucose concentration is shown in Fig. 3.8. The range of substrate concentration tested can be divided into two main parts: part A in which the production of electrons is the controlling step, and which occupies almost the whole range of glucose concentration investigated; part B, at very low glucose concentrations ( $<10$  g/L), where the release of  $H^+$  in the medium becomes the slowest phenomenon, i.e. the  $H^+$  formation is the limiting step of the microbial activity. Part A may be divided into two zones: zone  $A_1$  where the production of protons is the faster phenomenon:  $\tau_{H^+} < \tau_P$ , i.e. the dynamics is controlled by the pH decrease and an accumulation of electrons occurs, together with a modification of the environment towards a more reductive electrical potential; and zone  $A_2$  where  $bioH_2$  production becomes the faster phenomenon:  $\tau_{H^+} > \tau_P$ , i.e. the dynamics is governed by the change in the rate of decrease of pH, because the protons generated by reaction (3.9) are partially consumed and a surplus of available electrons occurs. This creates a shift towards a more oxidative potential, because when the hydrogen is produced the redox moves into a more positive range against the  $H_2$  reference electrode. In part B at low glucose concentration in which the controlling step becomes the pH variation ( $\tau_{H^+} > \tau_{Gl} > \tau_P$ ), the overall reaction proceeds very slowly owing to the difficulty of the microorganisms in changing the pH for endogenous phenomena only, i.e. low production of “free” protons.

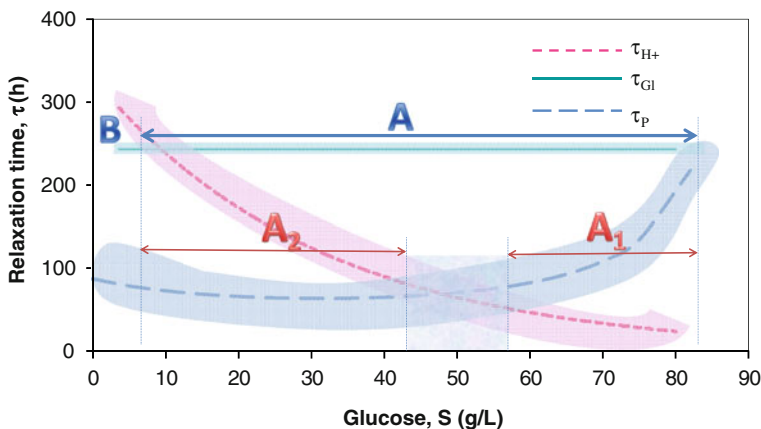


Fig. 3.8 Relaxation time estimation of macro-reactions

The above evaluation of the dynamics of H<sub>2</sub> production deserves some important suggestions for scale-up purposes. In the range A<sub>1</sub>, where the biological system is controlled by the pH variation (towards the acid range) it is most important to have very efficient pH control (probe, controller and actuators). Considering that this occurs at high glucose concentration, which means high viscosity of the fermenting broth, the major role belongs to the mixing system. In the range A<sub>2</sub>, at low glucose concentration, the biological process is governed by H<sub>2</sub> production, which can inhibit the bioreaction (Chap. 1), hence it is important to favor the degassing of the broth in order to lower the amount of H<sub>2</sub> gas dissolved in it. This can be controlled by increasing the mixing of the broth. In conclusion, the mixing of the fermenting broth is a fundamental parameter to consider in the scaling up of such a bioH<sub>2</sub> production bioreactor.

This analysis is valid for the exponential phase because the kinetics is evaluated in this range; nevertheless, in our opinion, in the light of the above dynamic considerations, the apparently strange behaviours of pH and redox reported in Fig. 3.4a, b are elucidated. In fact, in all the tests (initial glucose concentration >10 g/L) the pH presented two rates of variation and the redox shown a decrease toward reductive values; when biogas evolution occurs in the exponential phase, redox quickly moves toward the oxidative range. Recalling the structural considerations about the spatial configuration of Fd and hydrogenase I and II as pH-dependent, one could argue that the dynamic analysis and activities of enzymes are coherent. This is thanks to the macro-approach, even if it presents a low degree of precision but a good degree of exactness in the Zadeh sense [31]. The above dynamics gives an explanation of the different behavior of pH and redox versus time, as a monotonic curve appears for the test using 5 g/L of glucose (Fig. 3.4); the fermentation progress is always under H<sup>+</sup> production, which is the limiting step. Lastly, the above comments on the dynamics of H<sub>2</sub> evolution suggest the necessity to have an external pH control at high glucose concentrations (>5–8 g/L) in order to shift the reoxidation of NADH and NADPH toward H<sub>2</sub> gas formation via Fd and hydrogenase enzymes pools, as experimentally verified.

### 3.3.5 Test in Bioreactor

In order to check the robustness of the dynamical considerations, a fermentation test using a bioreactor with external (no endogenous) pH variation was done. The test was conducted at an initial glucose concentration of 60 g/L and the seed (10 % v/v) was acid-pretreated in the same way as each test presented in this chapter. Figure 3.9 shows the behavior of the fermentation over time: after the “natural” decrease, pH was varied three times by adding NaOH in order to reach the range of optimal enzyme activity (6.8–5.4). In all cases the redox was lowered and biogas evolution restarted, though with a different rate. The test demonstrates, in the authors’ opinion, the validity of the kinetics and dynamics considerations supported by the spatial structural role of Fd and hydrogenase I and II. In particular, from



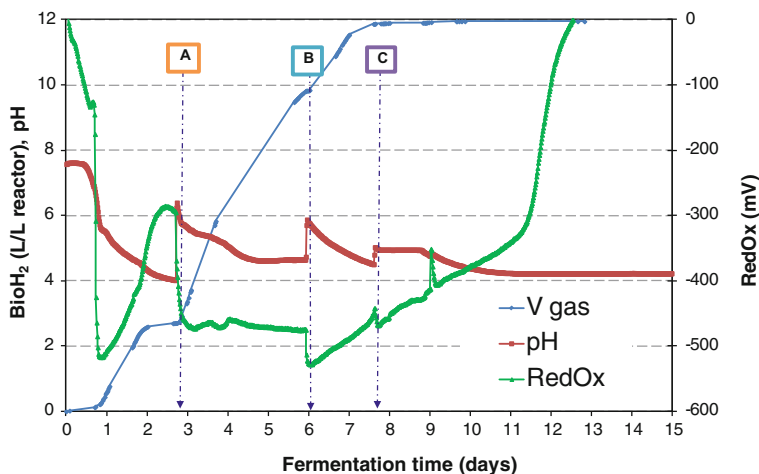


**Fig. 3.9** Test on bioreactor: glucose, bioH<sub>2</sub>, pH and redox versus time. A, B and C are points of pH restoration in the optimal range. Operative conditions are: 60 g/L glucose, (23–28) °C working temperature, 100 rpm mixing rate, 10 % v/v seed HPB

Fig. 3.9, at each pH adjustment the increase in pH provoked a decrease of redox, although this effect was not of the same magnitude. This fact might be due to the incompletely reversible spatial structure of the enzymes. The elucidation of this aspect deserves additional attention and needs more detailing from theoretical as well as experimental point of views.

Regarding bioH<sub>2</sub> production, a comparison between the flask and bioreactor tests can be made almost 3 days before pH adjustment and at the same initial glucose concentration (60 g/L). During this time the only difference is agitation, and an increase in biogas production in the bioreactor test is observable. The quantification of this effect is reported in Sect. 3.3.6. As shown in Fig. 3.9, the pH control increases total biogas production about six-fold. This aspect confirms all the considerations reported in Sect. 3.3.4.

### 3.3.6 Yield

The effectiveness of such a bioreaction is an important parameter for evaluating the process and the operative conditions to be adopted; to this end a theoretical maximum reference yield needs to be defined. In the presence of mixed microorganisms and considering the complex pathways for the production of several VFA, the evaluation of the theoretical H<sub>2</sub> yield is doubtful, due to the fact that some bacteria consume H<sub>2</sub> while others produce alcohols and/or lactic acid, and other bacteria produce H<sub>2</sub> simultaneously with VFA production [32]. Considering the stoichiometry of hydrogen production from glucose, there are three main global reactions:



They account for the acid formation metabolic pathway coupled with hydrogen formation. Bearing in mind that each metabolic product is coupled with different stoichiometric H<sub>2</sub>, the question of how to take into account the differences in moles of hydrogen produced per moles of compound needs to be solved in order to evaluate the yield of H<sub>2</sub> relative to 1 mol of carbon source. To overcome the above question, the authors suggest experimentally evaluating the quantities of the metabolites and consequently correcting the stoichiometric yield for each compound and finally finding a theoretical reference yield value using the following equation:

$$Y^* = \sum_j^m Y_j * w_j \quad (3.16)$$

The reference yield ( $Y^*$ ) means the maximum H<sub>2</sub> production per mole of glucose;  $Y_j$  is the stoichiometric H<sub>2</sub> yield for every  $j$ - $m$  compound and  $w_j$  is the weight determined experimentally in reference to the total quantities of VFA and ethanol, disregarding the weight of other metabolites because of their low concentrations. Equation (3.16) has the advantage of linking  $Y^*$  to the specific fermentation, i.e. the quality of carbon source and the microbial consortium.

Table 3.5 shows the application of the suggested procedure:  $w_j$  is experimentally evaluated as the mean value obtained for all tests at the end of fermentation reported in Sect. 3.2.2. Its variability is about 10 %. The reference H<sub>2</sub> yield ( $Y^*$ ), valid only for the actual fermentation, is equal to 1.66 mol H<sub>2</sub>/mol of glucose. This value represents again a maximum theoretical value because of the difficulty in evaluating the quantity of glucose consumed, either for cellular growth or to produce other metabolites. The cellular growth is difficult to evaluate with precision because the total suspended solids in the feed at the start masks the biomass growth itself. The

**Table 3.5** Experimental evaluation of the theoretical reference yield of H<sub>2</sub> per mole of glucose relative to mixed microorganisms

Compounds	Stoichiometric yield (mol H <sub>2</sub> /mol glucose)	Mean distribution $w_j$ (%)	$Y_j$ (mol H <sub>2</sub> /mol glucose)
EtOH	0	10.37	0.00
Acetic acid	4	3.56	0.14
Butyric acid	2	81.08	1.62
Propionic acid	-2	5.00	-0.10
Reference yield $Y^*$			1.66

**Table 3.6** Effectiveness of H<sub>2</sub> production as ratio of actual yield  $Y_a$  to reference yield  $Y^*$  for all the experimental tests

Tests (g/L)	$Y_a$ (mol H <sub>2</sub> /mol glucose)	$\zeta = Y_a/Y^*$ (%)
5	0.41	0.25
25	0.34	0.20
45	0.34	0.20
60	0.38	0.23
70	0.30	0.18
90	0.24	0.14
<i>Bioreactor 60</i>		
Before pH adjustment	0.49	0.30
At the end of fermentation	1.07	0.64

quantitative measure of the microorganisms involved in the H<sub>2</sub> production in presence of the HPB consortium, in our opinion, remains an open question from the experimental point of view in order to have an acceptable precision of the measure. Lastly, the effectiveness value  $\zeta$ , the ratio between the actual  $Y_a$  determined experimentally and the reference yield  $Y^*$  as a measure of the efficiency of the fermentation, are reported in Table 3.6.

The comparison of the effectiveness of the test carried out in the bioreactor with external pH adjustment and the test with endogenous pH adjustment shows an increase in H<sub>2</sub> production of 2.8 times for the same initial glucose concentration of 60 g/L of Table 3.6. Nevertheless not all this increase can be attributed to pH variation because the test conducted with the bioreactor shows a degassing effect which leads to a higher  $Y_{H_2}$  due to agitation. In fact, the evaluation of the effectiveness at 65 h, i.e. before the first pH adjustment, gives a value of  $\zeta = 0.30$ .

Comparing these results with that of  $\zeta = 0.23$  at an initial glucose concentration of 60 g/L, one can see that the effect of agitation causes an increase in effectiveness of 30 %, while the effect of pH adjustment increases the efficiency more than 100 %. Again, this experimental evidence confirm the dominant role of mixing in the scale-up procedure of bioH<sub>2</sub> production.

### 3.4 Conclusion

In the present Chapter a detailed kinetics was set up for glucose consumption as well as for biogas evolution using an enriched HPB biomass. The glucose consumption was found to be of first-order kinetics while for the biogas evolution an inhibited kinetics appeared over 60 g/L of glucose with a maximum production rate of around 100 mL/Lh. The H<sub>2</sub> content ranged from 40 to 60 %; this suggests that a full-scale application should have a carbohydrate concentration below 60 g/L in the fermenting broth. The positive effect of mixing was highlighted, as this is able to degas the biogas dissolved in the medium, consequently increasing H<sub>2</sub> production.

This effect could be estimated at around 30 %, in other words the present kinetics represents a conservative estimate of H<sub>2</sub> production from a quantitative point of view. The kinetics was used to highlight the dynamics of the biogas evolution using a macro-approach and relaxation time tools, to explain the experimentally detected behavior of pH and redox during the tests. Taking into consideration the behavior of the Fd and hydrogenase enzyme pools in the electron transfer chain, the dynamics appears to be coherent. In particular, pH seems to be the most important parameter in the regulation of the enzyme pool involved in H<sub>2</sub> evolution, suggesting a robust pH control chain in the bioreactors. Lastly, an experimental procedure to evaluate a theoretical reference yield of H<sub>2</sub> using glucose, taking into account the VFA as well as ethanol produced from the HPB microorganisms, was proposed and applied.

## Appendix

### *Macro-approach and Relaxation Time*

A so called *macro-approach* is a description of a complex system using the parameters which can be measured in order to take into account the observable behavior of the system. As the complexity of a system increases, the numbers of differential equations required to describe it grow. The systems encountered in biotechnology as well as in many of the engineering disciplines are of a complex nature and a rigorous description of their behavior leads to large sets of mathematical expressions (the *state equations*) describing the time evolution of a large number of relevant variables (the *state variables*). These equations generally contain a massive number of parameters, which in most cases cannot be readily obtained experimentally. Hence a consistent approach must be developed to simplify the picture of reality to a less complex one which can still describe the aspects of behaviour that are relevant to the desired application with sufficient accuracy. A useful approach to such simplification can be based on an analysis of the internal mechanisms of a system and their so-called *relaxation times*.

When considering a system in contact with an environment and exchanging matter and energy with it, a specific number of intensive quantities at its boundary need to be considered, e.g. concentrations of a number of chemical substances, temperature and pressure. After a sufficiently long time, all the processes of the system will have reached rates which no longer change with time, i.e. the state of the system has become time-independent. This state can be of two different types:

- The system finally reaches a state of *thermodynamic equilibrium*; if this occurs the final rates of the internal processes become zero, i.e. a lack of phenomena.
- The system reaches a so-called *steady-state* in which internal processes with a non-zero rate may still take place. In fact, if this system reaches a different state

from thermodynamic equilibrium, at least one internal process must have a non-zero rate, whether or not a stationary state can exist. Depending on the magnitude of the dynamics of the system, this can be considered a pseudo-steady state or an “evolutionary” system which can move towards stable or unstable conditions.

Following Röels (1983) [30], a time-scale separation approach or *relaxation time* approach is followed, to reduce the description of the dynamics of the system without losing its validity in accordance with the desired applications. In simple words this approach considers, as affecting the dynamics of a phenomenon, only those mechanisms which present a relaxation time of the same order of magnitude independent of whether the phenomenon is internal to the system or belongs to the environment. The relaxation time must not be confused with the intrinsic constant of a different dynamic phenomenon. It represents the dynamics of interaction between the system and its surrounding environment. A brief mathematics is shown to clarify the concept. Considering a first-order system, there is a constant of proportionality between a flux and a driving force:

$$J = k\Delta F \quad (\text{A.1})$$

the relaxation time is

$$\tau_r = 1/k \quad (\text{A.2})$$

but unfortunately first-order systems rarely describe the dynamics of the real world. The kinetics of a biosystem or a more complex system may be described by:

$$r = f(M) \quad (\text{A.3})$$

in which  $f$  is not a first-order relationship, and hence the relaxation time of the observed mechanism cannot be rigorously defined. A way to overcome this difficulty is to define a relaxation time that depends on the actual values of the space parameters. Linearizing Eq. (A.3), it follows that:

$$r = \frac{f(M)}{\prod_{i=1,n} M_i^{1/n}} \prod_{i=1,n} M_i^{1/n} \quad (\text{A.4})$$

and the relaxation time for the  $j$ -th situation is:

$$\tau_{rj} = \frac{\prod_{i=1,n} M_i^{1/n}}{r_j} \quad (\text{A.5})$$

where  $M_i$  is the  $i$ -th state variable and  $r_j$  is the *probe parameter*, i.e. the experimentally valued parameter to follow the dynamics of the phenomena selected in accordance with the purpose of the study and the available experimental

instrumentation. Equation (A.5) means that for a non-linear system it is possible to introduce the concept of *actual relaxation time* in the sense that it gives the time to reach a fraction  $(1 - 1/e)$  of the difference between the actual state (thermodynamic equilibrium or steady-state) and a new one as a consequence of change of matter and/or energy between the environment and the system which determines the dynamics. The rate and magnitude of exchange of matter and energy between system and environment determine the dynamics of the system towards a new stable or unstable state.

### ***Application to First-Order Kinetics***

The following simple example is intended to clarify the approach. Consider a well-stirred reactor in which a first-order chemical reaction takes place. Into the system a substrate solution of concentration  $C_{s0}$  is introduced at a rate  $F$ . The volume of the system  $V$  is considered constant and no volume generation is assumed to take place (note that, in the case of a microorganism population, this is not a valid assumption!). The concentration of the substrate in the flow leaving the system is assumed equal to the substrate concentration in the system (ideal mixing hypothesis). The following kinetic equation is assumed to specify the rate of the first-order process inside the system:

$$r = kC_{si} \quad (\text{A.6})$$

in which  $r$  is the rate of the system evolution per unit of volume,  $k$  is the kinetic constant and  $C_{si}$  is the substrate concentration inside the system. The following balance equation describes the dynamics of the substrate concentration in the system as a CSTR (continuous stirred tank reactor):

$$\frac{dC_{si}}{dt} = F/V(C_{s0} - C_{si}) - KC_{si} \quad (\text{A.7})$$

where  $C_{s0}$  is the inlet concentration. In a stationary state or steady-state the left-hand side vanishes, hence:

$$C_{ssi} = FC_{s0}/(F + kV) \quad (\text{A.8})$$

Thus the following expression describes the rate of reaction in a stationary state:

$$r = kFC_{s0}/(F + kV) \quad (\text{A.9})$$

The rate of reaction is expressed in quantities which can be externally measured (macro-parameters), e.g. the system volume  $V$ , the substrate concentration in the feed

solution  $C_{s0}$ , the flow rate  $F$  and through knowledge of such intensive parameters as the kinetic constant  $k$  of the system. The actual substrate concentration inside the system  $C_{si}$  does not appear. Considering a situation in which at a given moment in time the substrate concentration in the inlet is shifted from  $C_{s0}$  to  $C_{se}$ , the following differential equation describes the system's behaviour during the transient:

$$V \frac{dC'_{si}}{dt} = F(C_{s0} - C'_{si}) - kC'_{si}V \quad (\text{A.10})$$

with the initial condition:

$$C_{ssi} = FC_{s0}/(F + kV) \quad (\text{A.11})$$

Hence the dynamics of the system is the solution of the equation (A.10), in the time domain:

$$C_{si} = \frac{(F/V)}{(F/V) + k} [C_{se} + (C_{s0} - C_{se}) \exp\{-(F/V + k)t\}] \quad (\text{A.12})$$

The concentration  $C_{si}$  increases asymptotically to its new steady-state value. The relaxation time is defined as the time which elapses before the difference between  $C_{si}$  and its initial steady-state value reaches a fraction  $(1 - 1/e)$  of the difference between the old and the new steady-state value, which in this case is given by:

$$\tau_R = 1/(F/V + k) \quad (\text{A.13})$$

The relaxation time contains two contributions: the relaxation time  $V/F$  is the characteristic residence time in the reactor and  $1/k$  is the relaxation time of the chemical reaction taking place. The last equation can be written as:

$$1/\tau_R = 1/\tau_1 + 1/\tau_2 \quad (\text{A.14})$$

From it one can argue that the relative numerical value of the relaxation time determines the behaviour of the system: if the permanence time in the reactor is larger than the relaxation time of the system, the system dynamics is similar of that of a batch reactor (thermodynamic equilibrium will be reached); on the contrary, when the permanence time is less than the relaxation time of the system, the system evolves to reach a concentration equal to that of the feed, i.e. the reaction disappears. Only if the values are of the same order of magnitude there will be such an interaction between the system and the environment (Deborah number equal  $\sim 1$ ). In the second case the evolution of the system is governed only by the permanence time:

$$C_{si} = C_{se} + (C_{s0} - C_{se}) \exp\{-(F/V)t\} \quad (\text{A.15})$$

As one can see, this dynamic equation is a simpler one describing the behaviour of the system than equation (A.12).

Major details can be found in:

J.A. Röels, “*Energetic and kinetics in biotechnology*”, Elsevier Biomedical Press, Amsterdam (1983)

C. Ouwwerker, “*Theory of Macroscopic System*”, Springer Verlag, Berlin (1991).

## References

1. M.H. Zwietering, I. Jongenburger, F.M. Rombouts, K.V. Riet, Modeling of the bacterial growth curve. *Appl. Environ. Microbiol.* **56**(6), 1875–1881 (1990)
2. B. Gombertz, On the nature of the function expressive of the law of human mortality, and on a mode of determining the value of life contingencies. *Philos. Trans. R. Soc. Lond.* **115**, 513–585 (1825)
3. F.J. Richards, A flexible growth function for empirical use. *J. Exp. Bot.* **10**, 290–300 (1959)
4. C.J. Stannard, A.P. Williams, P.A. Gibbs, Temperature/growth relationship for psychotrophic food-spoilage bacteria. *Food Microbiol.* **2**, 115–122 (1985)
5. W.E. Ricker, Growth rates and models. *Fish Physiol.* **8**, 677–743 (1979)
6. Y. Mu, H.Q. Yu, G. Wang, Evaluation of three methods for enriching H<sub>2</sub>-producing cultures from anaerobic sludge. *Enzyme Microb. Technol.* **40**(4), 947–953 (2006)
7. A.M. Gibson, N. Bratchell, T.A. Roberts, The effect of sodium chloride and temperature on the rate and extent of growth of *Clostridium botulinum* type A in pasteurized pork slurry. *J. Appl. Bacteriol.* **62**, 479–490 (1987)
8. E.M.T. El-Mansi, C.F.A. Bryce, *Fermentation Microbiology and Biotechnology* (Taylor & Francis Press, London, 1999)
9. M. Soto, R. Mendez, J.M. Lema, Methanogenic and non-methanogenic activity tests. Theoretical basis and experimental set-up. *Water Res.* **27**(8), 1361–1376 (1993)
10. D.E. Contois, Kinetics of bacterial growth: relationship between population density and specific growth rate of continuous cultures. *J. Gen. Microbiol.* **21**, 40–50 (1959)
11. J.F. Andrews, *A Dynamic Model of the Anaerobic Digestion Process* (Department of Environmental Systems Engineering, Clemson University, Clemson, 1968), p. 52
12. R.H. Heyes, R.J. Hall, Anaerobic digestion modelling—the role of H<sub>2</sub>. *Biotechnol. Lett.* **3**(8), 431–436 (1981)
13. F.E. Mosey, Mathematical modelling of short-chain volatile acids from glucose. *Water Sci. Technol.* **15**, 209–232 (1983)
14. G. Lyberatos, I.V. Skiadas, Modelling of anaerobic digestion—a review. *Global Nest. Int. J.* **1**(2), 63–76 (1999)
15. J. Wang, W. Wan, Kinetic models for fermentative hydrogen production: a review. *Int. J. Hydrogen Energy* **34**, 3313–3323 (2009)
16. H.P.F. Fang, C. Li, T. Zhang, Acidophilic biohydrogen production from rice slurry. *Int. J. Hydrogen Energy* **31**, 683–692 (2006)
17. J.E. Bailey, D.F. Ollis, *Biochemical Engineering Fundamentals*, 2nd edn. (McGraw & Hill Press, New York, 1986)
18. X. Chen, Y. Sun, Z. Xiu, X. Li, D. Zhang, Stoichiometric analysis of biological hydrogen production by fermentative bacteria. *Int. J. Hydrogen Energy* **31**, 539–549 (2006)
19. P.M. Vignais, B. Billond, J. Mayer, Classification and phylogeny of hydrogenase. *FEMS Microbiol. Rev.* **25**, 455–501 (2001)



20. M.W.W. Adams, L.E. Mortenson, J.S. Chen, Hydrogenase. *Biochimica Biophysica Acta* **594**, 105–116 (1981)
21. R. Cammack, K.K. Rao, C.P. Bargeron, K.G. Hutson, P.W. Andrew, L.J. Rogers, Midpoint redox potentials of plant and algal ferredoxins. *Biochem. J.* **168**, 205–209 (1977)
22. K. Uyeda, J.C. Rabinowitz, Pyruvate-ferredoxin oxidoreductase. IV studies on the reaction. *J. Biol. Chem.* **246**, 3120–3125 (1971)
23. C.Y. Lin, C.H. Lay, Carbon/nitrogen-ratio effect on fermentative hydrogen production by mixed microflora. *Int. J. Hydrogen Energy* **29**, 41–45 (2004)
24. A.M.S. Vieira, R. Bergamasco, M.L. Gimenes, C.V. Nakamura, B.P. Diasfilho, Enumeration and isolation of facultative anaerobic bacteria in an upflow anaerobic sludge blanket reactor treating wastewater from gelatine industry. *Acta Scientiarum Biol. Sci.* **25**(2), 257–260 (2003)
25. W.M. Chen, Z.J. Tseng, K.S. Lee, J.S. Chang, Fermentative hydrogen production with *Clostridium butyricum* CGS5 isolated from anaerobic sewage sludge. *Int. J. Hydrogen Energy* **30**, 1063–1070 (2005)
26. J.S. Chen, D.K. Blanchard, Isolation and properties of a unidirectional H<sub>2</sub>-oxidizing hydrogenase from the strictly anaerobic N<sub>2</sub>-fixing bacterium *Clostridium pasterianum* W5. *Biochem. Biophys. Res. Commun.* **84**, 1144–1150 (1978)
27. M.W.W. Adams, L.E. Mortenson, The physical and catalytic properties of hydrogenase II of *Clostridium pasteurianum*. *J. Biol. Chem.* **295**(11), 7045–7055 (1984)
28. B. Ruggeri, G. Sassi, On the modelling approach of biomass behaviour in bioreactor. *Chem. Eng. Commun.* **122**, 1–56 (1993)
29. B. Ruggeri, G. Sassi, V. Specchia, A holistic view of (Bio)kinetics. *Chem. Eng. Sci.* **24**, 4121–4132 (1994)
30. J.A. Röels, *Energetics and Kinetics in Biotechnology* (Elsevier Biomedical Press, Amsterdam, 1982)
31. L. Zadeh, Fuzzy sets. *Inf. Control* **8**, 338–353 (1965)
32. I. Hussy, F.R. Hawkes, R. Dinsdale, D.L. Hawkes, Continuous fermentative hydrogen production from wheat starch co-product by mixed microflora. *Biotechnol. Bioeng.* **84**(6), 619–626 (2003)

## Chapter 4

# Effect of Temperature on Fermentative H<sub>2</sub> Production by HPB

In this chapter the analysis of the temperature effect on bioH<sub>2</sub> production is taken into account. Temperature is a very important factor, because it can affect the activity of HPB by influencing the activity of some essential enzymes such as hydrogenase for fermentative H<sub>2</sub> production [1], but at the same time it determines strongly the overall energy expense, hence the net energy balance. The first section is dedicated to the realization of a test at ambient temperature, which is exposed to natural night and day temperature variations, whereas the second section describes a series of tests at fixed temperatures (ranging from 16 to 50 °C). Each experimental test was conducted in a bench stirred-tank reactor.

### 4.1 Temperature: A Key Factor in Anaerobic Digestion

Among the operational conditions at which to run a bioreactor, the temperature, together with the pH, represents the most important parameter. The intensity of microbial activity on which the production of H<sub>2</sub> occurs depends on temperature. There are three possible ranges of temperature at which the process can be carried out: psychrophilic (15–25 °C), mesophilic (35–40 °C) and thermophilic (50–55 °C). For biogas production, only the mesophilic and thermophilic ranges are used in operational anaerobic digestion (AD) systems [2]. Generally speaking, this means that digesters run at around 35 and 55 °C respectively, though in absolute terms the optimal temperature may depend on the exact type of biowaste material undergoing treatment. Any AD process for biogas production requires a relatively constant temperature to progress at its greatest efficiency [2]. However, nowadays there is no industrial AD plant experience for H<sub>2</sub> production and therefore it is interesting to know the range of H<sub>2</sub> production according to temperature. Acidogenic bacteria seem to have a greater capacity to adapt to environmental variations such as temperature. In any case, the temperature controlling the nature of the microbial consortium is recognized by several authors: at 35 °C *Clostridium* are the dominant species, whereas at 55 °C lactic acid bacteria are more abundant [3]. For this reason, we conducted first of all a test at ambient temperature exposed to night and day

variation under natural decrease of pH in order to determine the flexibility of the microorganisms involved, and, subsequently, a series of tests at controlled temperature and pH in order to evaluate the hydrogen yield according to the working temperature. Very few studies have been conducted on the acetogenesis process at low temperatures. Lee and Chung [4] reported a study on H<sub>2</sub> production at 30 °C showing that there is microbiology activity at low temperature, even if the production rate at 30–34 °C (359 mmol H<sub>2</sub> L<sup>-1</sup> h<sup>-1</sup>) is almost 50 times greater than that at 15–18 °C. Mu et al. [5] conducted tests from 33 to 41 °C, finding that glucose degradation efficiency, H<sub>2</sub> yield and growth rate increased with increasing temperature from 33 to 39 °C, then decreased as the temperature was further increased to 41 °C. The distribution of aqueous products was also greatly influenced by temperature variation. In contrast, Akutzu et al. [6] found that hydrogen was successfully produced under thermophilic conditions and unstable H<sub>2</sub> production was observed in mesophilic conditions. The experimental results of Zhang and Shen [7] show that the hydrogen-producing ability of anaerobic bacteria was strongly affected by either culture temperature or iron concentration. The increase in the culture temperature facilitated hydrogen production when it was in the range of 25–40 °C and high sucrose conversion efficiencies (ca. 98 %) were consistently obtained; when the temperature rose towards 45 °C, however, hydrogen production was strongly inhibited. On the basis of these contrasting results and in order to better understand the influence of temperature, we conducted batch tests in a laboratory-scale reactor using anaerobic wastewater sewage sludge as inoculum, treated with HCl as reported in Chap. 2, in a glucose-rich medium with a concentration of  $58 \pm 2$  g/L, according to the kinetics study described in Chap. 3.

## 4.2 Material and Test Procedure

The following section describes the method used for carrying out the tests. The tests were conducted in the same reactor, with the same medium and initial glucose concentration, monitoring the same parameters. The differences between tests concerning the bioreactor operation were:

- a single test was conducted without temperature and pH control, i.e. at ambient temperature and with the pH adjusted after natural decrease, in order to prove the dynamics evaluated in Chap. 3;
- a series of tests was then conducted under temperature and pH control.

### 4.2.1 Apparatus and Operative Conditions

The sludge was collected from an anaerobic wastewater treatment plant and pre-treated as reported in the previous Sect. 2.3.1. The treated sludge was inoculated in

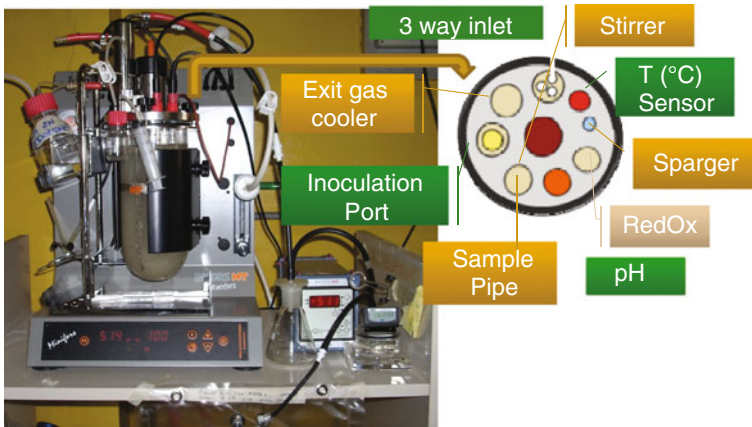


**Fig. 4.1** Schematic view of bioreactor with various components used in the tests

a ratio of 10 % v/v in a stirred-batch reactor STR (Minifors HT, Switzerland), shown in Fig. 4.1, with 2 L as the working volume, running under anaerobic conditions obtained by flushing with nitrogen gas at the beginning of the fermentation, and by mixing the broth at 100 rpm. The reactor is equipped with a mixer, pH and temperature control systems, in order to easily check and change the internal conditions during hydrogen production. The above parameters were monitored continuously, in addition to the redox potential. The initial glucose concentration was  $58 \pm 2$  g/L and the medium had the macro- and micro-nutrient composition described in Methodology in Chap. 2.

## 4.2.2 Test with Bioreactor

### 4.2.2.1 Test at Natural Ambient Temperature

The initial pH of the media was set at 7.5 and the initial C/N ratio was about 30. The experiment was carried out at ambient temperatures, which ranged from  $23 \pm 0.1$  to  $28 \pm 0.1$  °C. At the beginning of the test the fermentation was conducted without any pH regulation. After about 60 h, when the biogas evolution shut down (Fig. 4.2), the pH was adjusted with 2N NaOH at different times during the fermentation to verify if biogas production restarted. To be precise, pH was adjusted at pH 6.3 and pH 5.75 at times  $t = 67$  h and 143 h, respectively, while at time  $t = 183$  h it was set at pH 5.

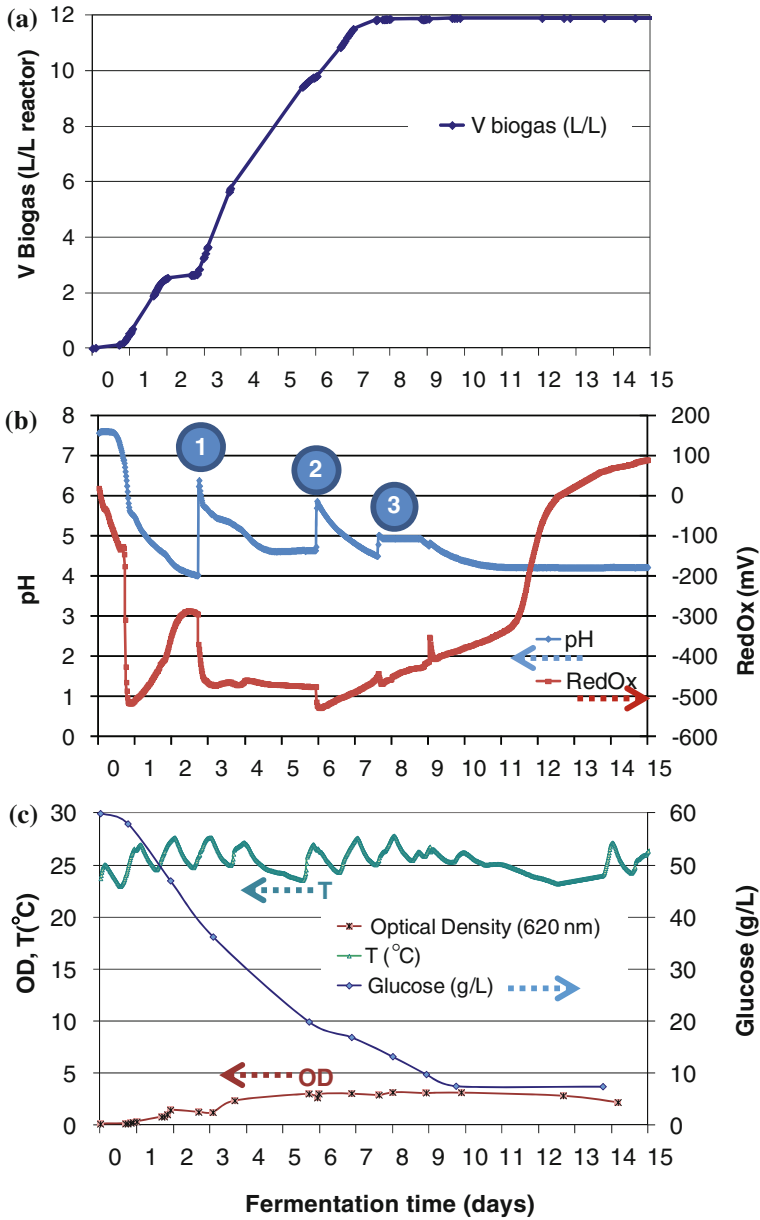


**Fig. 4.2** a Cumulative biogas (H<sub>2</sub> and CO<sub>2</sub>) production, b pH and redox, c optical density, temperature and glucose concentration

### 4.2.2.2 Test at Controlled Temperature

Batch tests for hydrogen production were conducted at different temperatures: 16, 20, 35, 40 and 50 °C ( $\pm 0.1$  °C) with the same glucose concentration as the test reported in Sect. 4.2.2. For each test, the initial pH of the medium was set at  $7.2 \pm 0.1$ . The first hours of fermentation were conducted without any pH regulation; after a natural decrease to 5.2, it was maintained at this value by 2N NaOH dosage by peristaltic pump and pH meter sensor probe. Tests were stopped after the biogas production shut down.

### 4.2.3 Monitored Parameters

Temperature, pH and redox potential were monitored online every minute through a data acquisition system (Iris NT Software; Infors AG, Switzerland). The gas produced during the fermentation was constantly measured with a volumetric gas counter (Milligascounter, Ritter) and then was collected in Tedlar bags (SKC, 231-05 series) and analyzed with a gas chromatograph (Varian, CP 4900). The liquid samples were taken out of the reactor daily at different times during the fermentation for the determination of glucose content, biomass concentration by optical density (OD) and volatile fatty acid (VFA) concentration using a gas chromatographic (GC) method. The GC was equipped with columns (polyethylene glycol ester, 0.5 m  $\times$  0.53 mm as precolumn and Alltech Superax-FABP, 25 m  $\times$  0.53 mm, Banded FSOT), the working temperature was 200 °C at detector, H<sub>2</sub> gas was used as carrier; the sample was filtered (0.45  $\mu$ m) under vacuum, acidified (1 N HCl) and diluted with distilled water before injection.

## 4.3 Results of the Test at Ambient Temperature

### 4.3.1 Dynamics of Parameters Monitored

As a result of acetogenic fermentation, 1 L of glucose medium produced approximately 12 L of gas containing, on average, a hydrogen concentration ranging from 29 to 45 % (v/v) and carbon dioxide from 55 to 71 % (v/v). These values of H<sub>2</sub> content in the biogas under ambient temperature conditions were lower than those obtained in mesophilic conditions. The three graphs (a, b, c) of Fig. 4.2 provide an overview of the parameters monitored during the fermentation time. The first graph (4.2a) shows the amount of biogas (H<sub>2</sub> and CO<sub>2</sub>) developed after 18–20 h (lag phase), the time during which the microorganisms reorganize their molecular constituents to adapt to new environmental conditions, as stated and commented in Chap. 3.

At first glance, from Fig. 4.2b we observe a strict relation between biogas evolution, pH and redox. During the lag phase (without pH control), between  $t = 0$  and  $t \sim 20$  h, pH slightly decreases from 7.5 to 6, while redox remains at very slightly reductive values; just before the beginning of the exponential phase, redox sharply decreases, reaching a minimum value of  $-518$  mV, and subsequently, when the exponential phase of biogas production begins, pH falls and redox gradually starts to rise towards oxidative values. When the pH reaches 4.3, biogas production stops. This observation has been noted in other tests described in Chaps. 2 and 3, and also reported in several studies by other authors [8].

Bearing in mind that biogas production stops at pH 4.3, the pH was adjusted from 4.3 to 6.3 (point 1 in Fig. 4.2b), and then the exponential phase restarted and at the same time redox fell dramatically towards sharply reductive values. The same behaviour was also observed for points 2 and 3. At point 2, the pH was adjusted to 5.75; instead, at point 3, pH was set at 5.2, but only a small quantity of produced gas was detected. During biogas development, the redox moves gradually towards non-reducing environment conditions to oxidize the substrate and consequently also unfavorable conditions for producing H<sub>2</sub>. Chen et al. [8] also found that at pH 4.5 the biogas production shut down in batch tests at 37 °C with HPB obtained by heat pretreatment, but an elevation of pH from 4.5 to 6.5 restored hydrogen production from the culture, suggesting that pH control at an appropriate level can improve the efficiency of hydrogen production, as stated in Chap. 2 from a biological point of view.

Glucose utilization reached a percentage of 77 % w/w, while the maximum rate of glucose consumption was 0.39 g glucose L<sup>-1</sup> h<sup>-1</sup>, detected between 18–46 and 74–137 h, during the exponential phases. The rate of glucose consumption decreased at the same time at which the biogas production rate also dropped, although the pH was set at 5.2 (point 3). Probably microorganisms stressed from pH variations were no longer able to adapt to the new conditions, especially since the pH was adjusted after about 3 h when the bacteria were in unfavorable conditions, i.e. pH < 4.5. This test confirms that the optimal pH for anaerobic H<sub>2</sub> production reported in the literature is essentially within the range 5.2–6.5 [8–10]. This suggests that ensuring a more than satisfactory control loop for pH control in a scaled-up system of biohydrogen production is of utmost importance. HPB demonstrate a great ability to adapt to environmental variations, such as temperature which fluctuates in the range 23–27 °C according to the uncontrolled ambient conditions test (Fig. 4.2c); in addition the pH variation in the range 4.5–6 seems not to suppress HPB activity, even though HPB remaining at low pH values for about 2 h have shown difficulties in reactivating the H<sub>2</sub>-producing pathways. Figure 4.2c shows that there was a cell growth of saturation type. The biomass increased in the first 2 days since the fermentation began, thereafter it remained stable and decreased steadily only during the stationary H<sub>2</sub> production phase, suggesting that the hydrogen production was coupled with the stationary phase of the growth curve of the bacterial population. This consideration is in accordance with the study of Chen et al. [8], where H<sub>2</sub> evolution appeared to start after the middle stage of the exponential phase, with maximal H<sub>2</sub> production when cell growth had entered an

early stationary phase. This seems to imply that  $H_2$  generation was not a preferable event during assimilation of the carbon substrate for gain in biomass; in fact the predominance of metabolic electron flow toward biosynthesis decreases the availability of electrons for hydrogenase to produce  $H_2$ , as seen in the previous Chapters. This aspect suggests that it is necessary to increase the concentration of microorganisms per unit volume in order to increase the volumetric production of hydrogen, for example by using a fixed-bed reactor with immobilized and/or entrapped HPB. Unfortunately this type of bioreactor is only suitable for liquids having very low substrate concentration (total solids less than 2–3 %).

From the above comments, it is possible to conclude that gas production strongly depends on pH and on high reductive redox level. Moreover, an interesting relationship between pH and redox was observed (Fig. 4.2b) throughout the performed tests. This confirms the hypothesis of the two species of  $H^+$  ions present in the medium: one involved in the biological pathway linked to Fd and hydrogenase pool of enzymes, and the other one like protons, acting in the water domain to assure the electrical neutrality of the medium. The pH control of the medium, and hence of the  $H^+$  concentration, determines the redox level, which permits control of the biological activity towards  $H_2$  production.

### ***4.3.2 Evolution of $H_2$ Production***

Thanks to the acid pretreatment, no methane or hydrogen sulfide production was observed during the process. Only small amounts of water vapour were detected in the gas stream. The  $H_2$  productivity was about 0.90 mol  $H_2$ /mol glucose, taking into account the weighted mean of 36 % of  $H_2$  in the total amount of biogas produced (Fig. 4.3). The  $H_2$  productivity obtained in this study, working under uncontrolled ambient temperature and with mixed microflora, is lower than values obtained by many researchers working under mesophilic conditions (35 °C) and with pure fermentative bacteria, such as Clostridia, or with mixed anaerobic culture, such as *C. butyricum* and *Enterobacter aerogenes* [11]. Nevertheless, these results are important in deciding whether the working temperature should be under environmental temperature cycles or not.

### ***4.3.3 The Significance of Tests at Uncontrolled Temperature***

The test at uncontrolled temperature demonstrates that it is also possible to produce  $H_2$  under ambient temperature conditions, even under wide fluctuations ( $24 \pm 3$  °C). This implies that it could be feasible to operate a full-scale plant with a low energy demand, hence maximizing the net energy production, in contrast to the mesophilic (35 °C) or thermophilic (55 °C) regimes. Regarding this aspect, in the next Chapter we will investigate the temperature effect on bio $H_2$  production, in order to analyze,



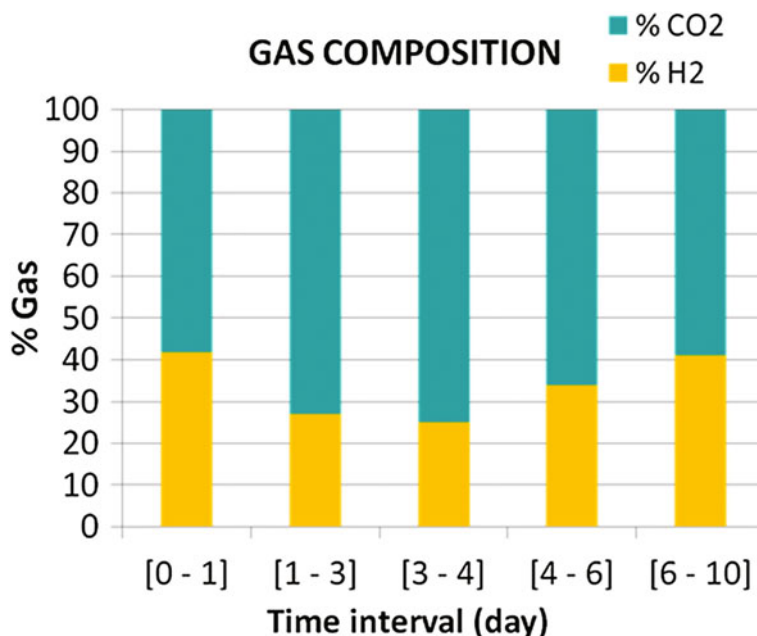


**Fig. 4.3** Composition of biogas (CO<sub>2</sub> and H<sub>2</sub>) at several time intervals during the test

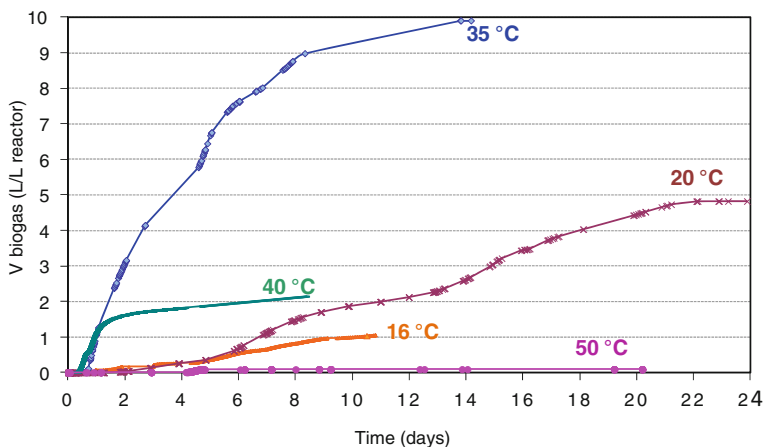
through a net energy analysis, if it is more convenient to produce a smaller quantity of H<sub>2</sub> with low energy consumption, i.e. working at ambient temperature, rather than to produce a larger quantity of H<sub>2</sub> working at higher temperatures. To this end, we designed and performed the tests reported in the following section.

## 4.4 Results of Tests at Different Temperatures

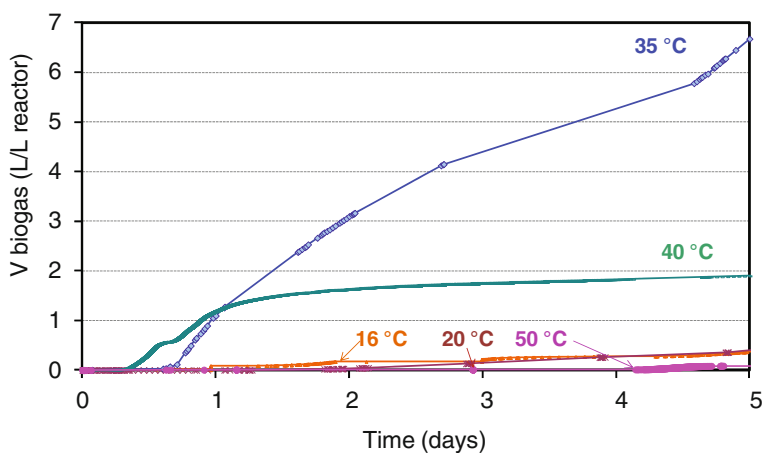
### 4.4.1 Comparison Between Tests at Different Temperatures

Figure 4.4 shows the progress of cumulative hydrogen production in the batch tests at different temperatures. It shows that the duration of H<sub>2</sub> production is very different from one test to another, indicating a strict relationship with the temperature. Figure 4.5 is merely an expansion of Fig. 4.4 on the time axis to better see the lag phase of each temperature tested.

Table 4.1 reports the glucose utilization efficiency, the H<sub>2</sub> yield and the total duration of fermentation; the results show that the greatest glucose utilization efficiencies are obtained at working temperatures of 20 and 35 °C, even though at 35 °C the rate of glucose consumption is almost twice as fast as at 20 °C. The lowest value of glucose utilization occurs at 16 °C. This confirms that at low temperatures the electrons produced by glucose oxidation are mainly utilized for



**Fig. 4.4** Progress of cumulative  $\text{bioH}_2$  production in batch tests at different temperatures



**Fig. 4.5** Expansion of lag phase of cumulative  $\text{H}_2$  production at different temperatures

**Table 4.1** Substrate degradation efficiency and  $\text{H}_2$  yield and duration versus temperatures

$T_w$ ( $^{\circ}\text{C}$ )	Glucose utilization (%)	$\text{H}_2$ yield (mol $\text{H}_2$ /mol glucose)	$\Delta t$ (days)
16	12.0	0.35	10.8
20	99.6	0.65	23.9
35	99.8	1.21	13.8
40	30.0	0.92	8.4
50	73.0	0.005	12.5

metabolic respiration instead of being used via Fd to reduce protons and produce hydrogen. The maximum  $Y_{H_2}$  is at 35 °C, followed by the tests at 40 and 20 °C.

Figure 4.6 shows the course of the fermentation test conducted at 50 °C, including the determination of VFA produced. At 50 °C,  $Y_{H_2}$  is almost zero, but we can suppose that at 50 °C the microorganisms which follow lactic fermentation are dominant in the HPB consortium, considering the large consumption of substrate (73 %) and the great quantity of lactic acid relative to other VFA produced during fermentation, which reach a very high concentration of 23 g/L in about 18 days (Fig. 4.5b).

The strong consumption of sodium hydroxide (2N NaOH) shown in Fig. 4.6 is proportional to glucose consumption; microorganisms oxidize glucose, releasing

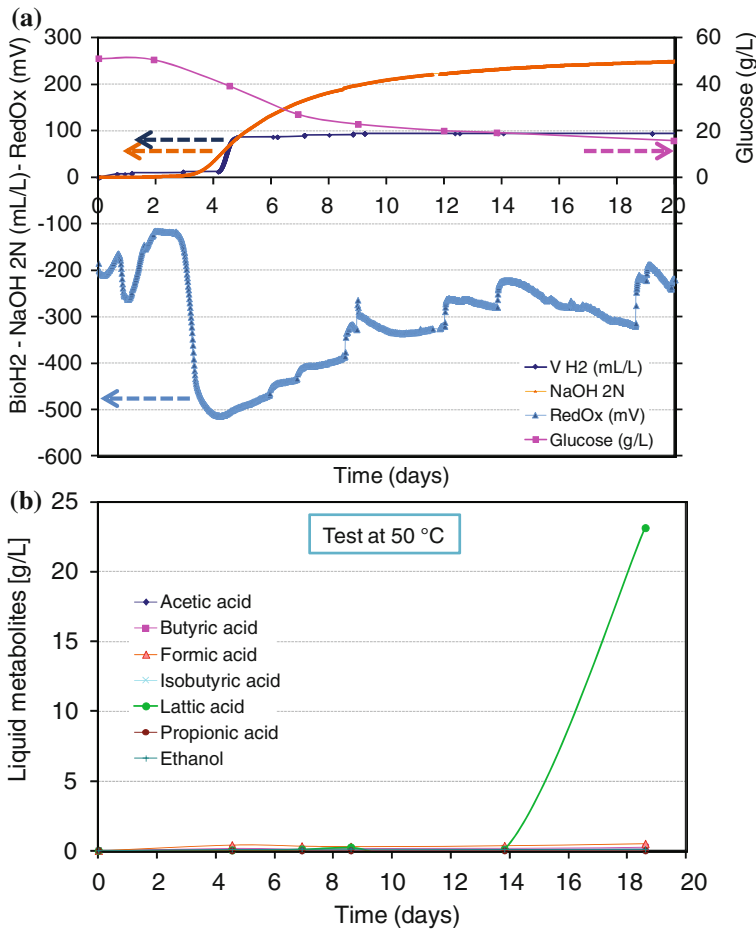


**Fig. 4.6** Test at 50 °C. **a** Production of H<sub>2</sub> in relation to redox, pH, glucose consumption and NaOH consumed during fermentation; **b** development of liquid metabolites during fermentation

electrons and protons that create an acidification of the system, which consequently needs NaOH pump intervention to maintain the pH at 5.2. Furthermore, Fig. 4.6a shows the redox trend of the test: it does not remain stable despite constant pH, but moves towards a less reductive range (-300 to -200 mV) after a rapid drop below -550 mV.

Comparison of the redox behaviour in the tests at 20 and 35 °C (see Figs. 4.7 and 4.8, respectively) shows that, when the pH is constant, the redox potential remains at strongly reductive values (about -500 mV) allowing H<sub>2</sub> production until glucose is completely consumed. This confirms the strong role of pH; it decreases correspondingly with H<sub>2</sub> production and with the formation of acidic metabolites expressed by VFA.

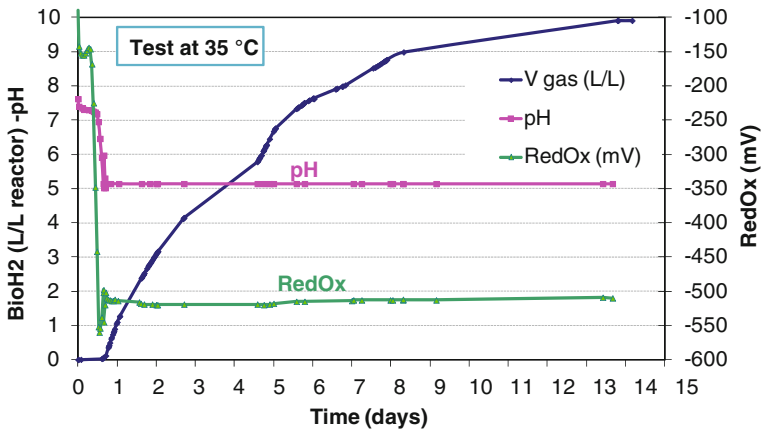


Fig. 4.7 Development of pH, redox and bioH<sub>2</sub> volume in batch test at 35 °C

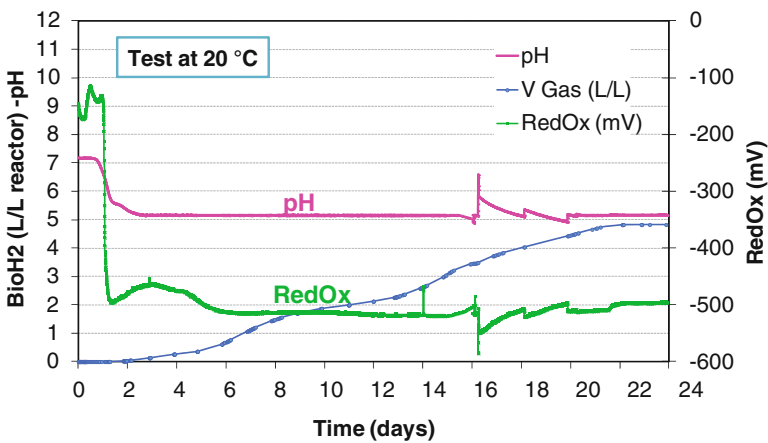
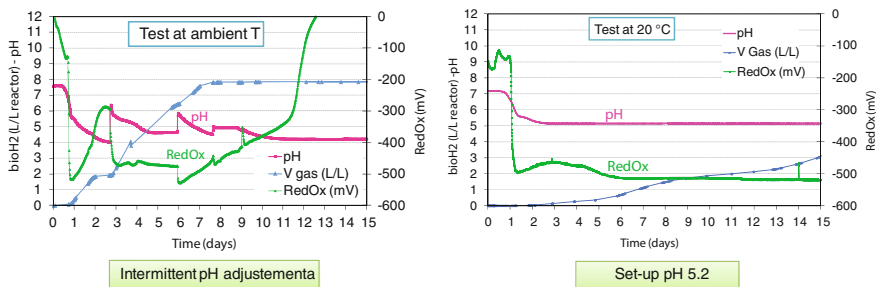


Fig. 4.8 Development of pH, redox and bioH<sub>2</sub> volume in batch test at 20 °C



**Fig. 4.9** Comparison of tests at ambient temperature and at 20 °C to stress the importance of pH set to 5.2

Figure 4.9 shows the comparison between two tests at approximately the same temperature but with different strategies of pH control: one test at ambient temperature with intermittent pH adjustment and the other one at 20 °C with pH set at 5.2, after the natural decrease to this value. The aim of this comparison is not to compare H<sub>2</sub> yields, since the temperatures are slightly different, but to compare the opposite behaviours of redox depending on pH. If pH is constant (graph on the right) redox is constant and gas continues to develop until the glucose is completely consumed; the opposite occurs in the test without pH control. Recalling that when bacteria grow on organic substrates by oxidation of such substrates the oxidation generates electrons which need to be disposed of in order to maintain electrical neutrality, different compounds, i.e. protons, act as electrons acceptors, which are reduced to molecular hydrogen, maintaining in this way the electron balance. These phenomena can occur only if an adequate difference of electrical potential exists as the driving force, i.e. a reducing environment of neighbouring microorganisms (detected by redox) is necessary to produce H<sub>2</sub>.

The increase of redox during the fermentation is due to the production of protons (detected by the rapid drops in pH), in direct correlation to the consumption of substrate. In fact, from the test at ambient temperatures (reported on the left-hand side of Fig. 4.9), we observed that when the pH is very low, the redox is less reduced and biogas shut-down occurs. In contrast, we observe on the right-hand side of Fig. 4.9 that if the pH remains constant during fermentation, i.e. if the medium is well buffered, the protons produced are removed and the redox potential remains constant in a strongly reductive range. As a consequence of constant pH, a greater level of hydrogen production is obtained. From this analysis, we can conclude that it is very important to buffer the pH because it permits a more stable and longer-duration H<sub>2</sub> production, due to the effect of pH on the hydrogenase enzymes that catalyze the reversible reductive formation of hydrogen from protons and electrons:



Adams and Mortenson [12] studied the effect of pH on hydrogenase-catalyzed H<sub>2</sub> evolution. They found that hydrogenases I and II have their maximal efficiency

at pH 6.3 and pH 5.8, respectively, whereas the activity of both enzymes rapidly decreases at pH < 5. The present results confirm the finding of Adams and Mortenson.

#### 4.4.2 Liquid Products from H<sub>2</sub> Fermentation

The soluble metabolites produced by the mixed culture detected in the tests were mainly composed of butyric acid, acetic acid, propionic acid, lactic acid and ethanol.

Table 4.2 shows the percentages present among all soluble metabolites at the end of fermentation: the concentrations of acetic and butyric acid increase from the test at 16 °C to the one at 35 °C, but with a further increase of temperature (40 and 50 °C) they decrease.

In contrast, at 40 and 50 °C high concentrations of lactic acid appear. Considering for both cases the relative small amount of H<sub>2</sub> production, we suppose that a metabolic pathway shift occurred at higher temperatures, induced by different bacteria present in the consortium becoming dominant under less favorable conditions for HPB. The production of H<sub>2</sub> is mainly coupled with acetate and butyrate fermentation pathways, and the anaerobic spore-forming bacteria, Clostridia, form an important part of the acidogenic population performing these fermentation pathways. The production of acetate and butyrate, respectively, from glucose under anaerobic conditions can be explained by the following stoichiometric chemical equations:



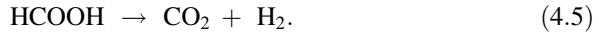
In contrast, the production of propionate requires a consumption of H<sub>2</sub>:



**Table 4.2** Volatile fatty acids and ethanol expressed as percentage of total metabolites at the end of H<sub>2</sub> production versus temperature

T <sub>w</sub> (°C)	H <sub>2</sub> produced (mmol H <sub>2</sub> /L)	Δt (days)	Acetic acid (% w/w)	Butyric acid (% w/w)	Formic acid (% w/w)	Lactic acid (% w/w)	Propionic acid (% w/w)	Ethanol (% w/w)
16	15.4	6.6	1.22	60.22	1.52	17.98	0.42	18.40
20	215.3	23.9	2.91	81.08	2.67	0.04	0	13.30
35	442.0	13.8	7.93	90.81	0.58	0	0.12	0.56
40	96.0	10.4	5.85	61.2	3.42	15.23	0.9	3
50	1.1	12.5	1.66	3.95	3.05	90.44	0.01	0.90

Thus, in practice, high hydrogen yields are associated with a mixture of acetate and butyrate as fermentation products [13]. In addition, formic acid adds to hydrogen production via its decomposition catalyzed by the hydrogenase enzyme:



Facultative bacteria like *Enterobacter* spp., *Escherichia coli*, *Salmonella*, *Shigella* and *Klebsiella* are responsible for mixed acid fermentation, where the products are the three acids (lactate, acetate and formate) as well as ethanol and equal amounts of H<sub>2</sub> and CO<sub>2</sub>; this is also characteristic for members of the Enterobacteriaceae family [14].

In addition, ethanol fermentation leads to H<sub>2</sub> production, as reported by Hwang et al. [15], who conducted ethanol and butyrate–acetate fermentation simultaneously:



The wide range of options for metabolic pathways is due to the mixed bacterial populations present in mixed consortia, which leads the fermentation towards the most appropriate metabolic pathway for the environmental conditions. Figures 4.10 and 4.11 show the production of liquid metabolites during H<sub>2</sub> production in batch tests at 20 and 35 °C, respectively. Furthermore, in the same graphs we inserted a cumulative H<sub>2</sub> production curve in order to see a correlation with metabolite behaviour during acetogenic fermentation. In the test at 20 °C (Fig. 4.6), butyric acid is distinctly dominant over all the other metabolites, reaching a concentration of 27.43 g/L at 20 days.

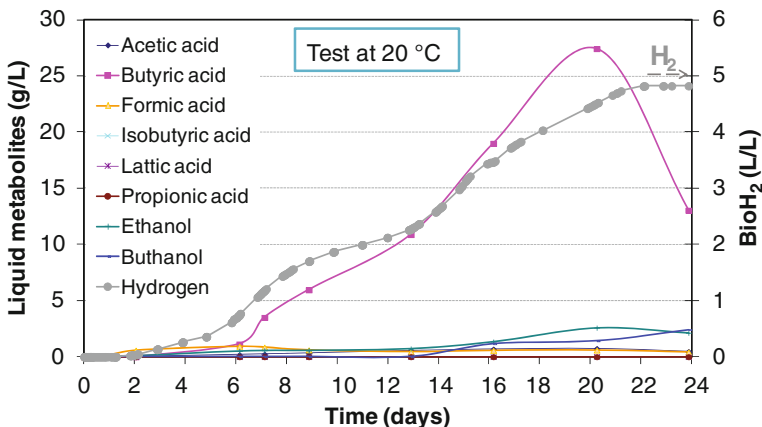
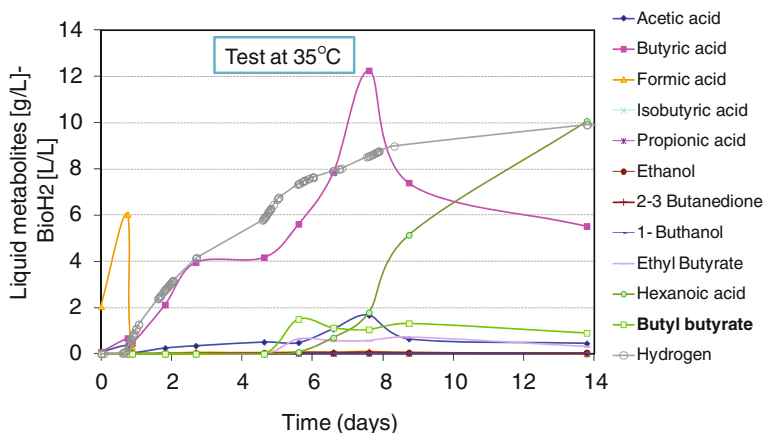


Fig. 4.10 Production of liquid metabolites and hydrogen during batch test at 20 °C



**Fig. 4.11** Production of liquid metabolites and hydrogen during batch test at 35 °C

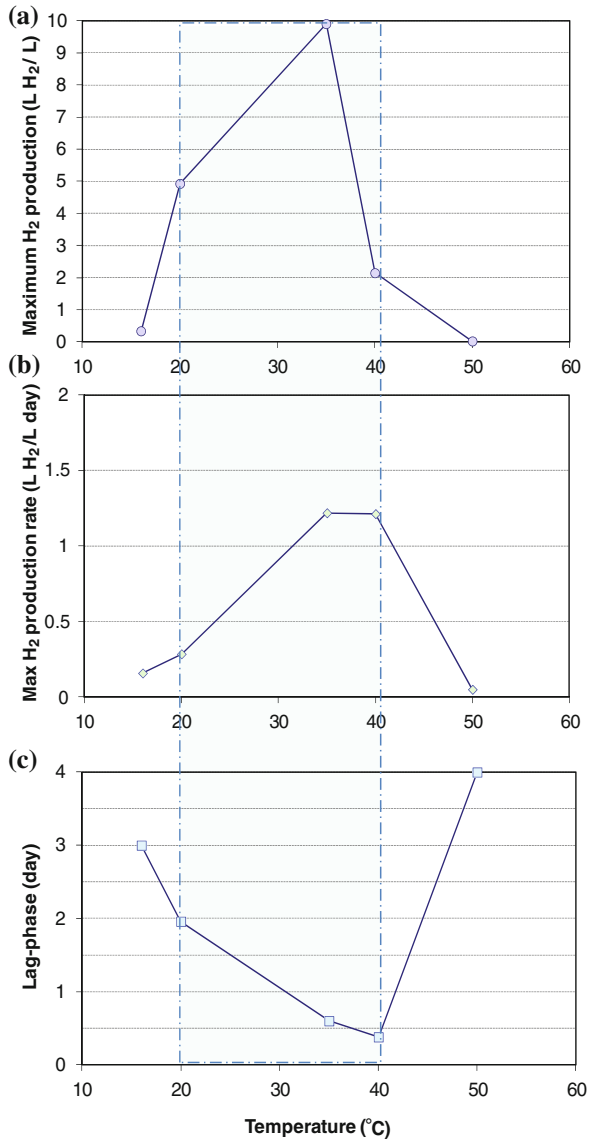
At 35 °C (Fig. 4.11) butyric acid is also dominant (12.42 g/L at 7.6 days), but among all prominent metabolites it is the presence of hexanoic acid ( $C_6H_{12}O_2$ ), also called caproic acid, that becomes more and more evident after about 8 days of fermentation, which coincides with the total consumption of glucose. Probably, microorganisms that follow butyric-type fermentation when glucose is completely consumed utilize butyrate, which in fact decreases, to biosynthesize this saturated acid. At high temperatures (40 and 50 °C) significant amounts of lactate were produced, which becomes the major product at the expense of acetate and butyrate. A marked variation in liquid metabolite production indicates a shift in the metabolic pathways of acid fermentation in the digestion process. Because the metabolic pathway relates to the bioactivity of the dominant microorganisms, the experimental results could be viewed as dependent on the temperature of the different biomass activities.

Figures 4.12a–c show the effect of temperature on  $H_2$  production,  $H_2$  production rate and duration of lag phase, respectively. The results show that the hydrogen production potential in batch tests increased as the temperature increased from 16 to 35 °C, whereas it decreased with further temperature increases from 40 to 50 °C. Among all the tests, the maximum  $H_2$  production and maximum  $H_2$  production rate of almost 10 L  $H_2$ /L<sub>reactor</sub> and 1.5 L  $H_2$  L<sup>-1</sup> day<sup>-1</sup> were obtained at 35 °C. At 40 °C the rate of  $H_2$  production was also high, but the fermentation reached a stationary phase early on, although a large quantity of unused glucose remained.

Figure 4.12c shows that lag phase is shorter at 35 and 40 °C than at other temperatures. The shortest lag phase of 9 h was obtained at 40 °C; the temperatures in the range of 30–40 °C probably facilitate the germination and consequently the acclimatization of *Clostridium* spores. For instance, Gibbs [16] found that, for *C. bifermentans*, the optimal temperature between 12 and 45 °C was 37 °C. At temperatures below 20 °C, little or no germination occurred in 60 min. At 45 °C, germination was markedly decreased. According to similar studies [1, 17],



**Fig. 4.12** Effect of temperature on maximum H<sub>2</sub> production rate (a), maximum H<sub>2</sub> production (b) and duration of lag phase (c)



an appropriate temperature range can enhance the ability of mixed cultures to degrade substrate; with temperatures increasing from 20 to 35–37 °C the H<sub>2</sub> production and the production rate increase, with further increase in the range 40–50 °C. As a holistic consideration, we can argue that in an appropriate range, between 28 and 40 °C, the temperature can raise the hydrogen production and the maximum hydrogen production rate and can shorten the lag phase of acetogenesis fermentation for H<sub>2</sub> production by mixed cultures. Lastly, we can argue that a

bioreactor producing  $H_2$  could work at a temperature in the range 20–40 °C from a microbiological and industrial point of view. From an engineering point of view, the suggestion is to work at the minimum working temperature, for example at 22–23 °C, in order to maximize the net energy production. In the meantime we suggest to adequately insulate the reactor and to have a temperature control loop with a set point (22 °C) able to use the energy provided free by environmental temperatures during the appropriate seasons.

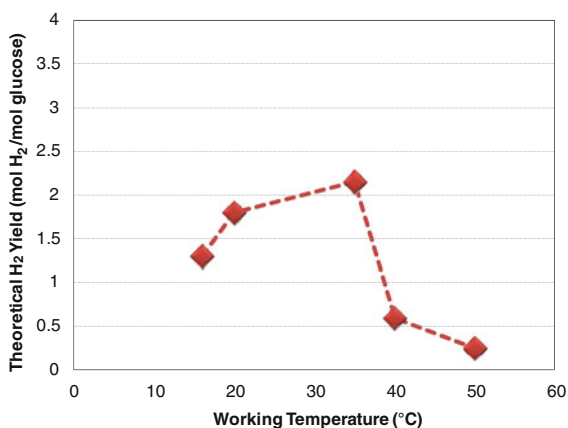
### 4.4.3 Yield of Tests According to Temperatures and Metabolic Products

As previously seen, the products of acetogenic fermentation (including  $H_2$  and liquid metabolites) vary according to the temperature (Table 4.2), which creates growth conditions better for some species which became dominant to the detriment of others.

The theoretical  $H_2$  yield ( $Y^*$ ) of the metabolites present in the broth for each working temperature can be calculated by applying Eq. (3.16); the results are shown in Fig. 4.13. The  $Y^*$  is far from the theoretical  $H_2$  yield if only acetic acid is present in the broth ( $4 \text{ mol}_{H_2}/\text{mol}_{Glu}$ ). In fact, among liquid metabolites, butyric acid is often the most abundant, and a butyrate fermentation yield of  $2 \text{ mol}_{H_2}/\text{mol}_{Glu}$  is the highest value. From Fig. 4.13 the yield is always less than 2, apart from the value at 35 °C that exceeds this threshold. This is also in agreement with several studies by other authors [17].

It is interesting to compare the experimentally evaluated yields of tests at different temperatures with the theoretical ones (Table 4.1); the results are shown in Fig. 4.13. This aspect has a strongly counterface from the energetic point of view. Assuming 2,882 and 240 kJ/mol of lower heating value (LHV) for glucose and

**Fig. 4.13** Theoretical  $H_2$  yield according to working temperature



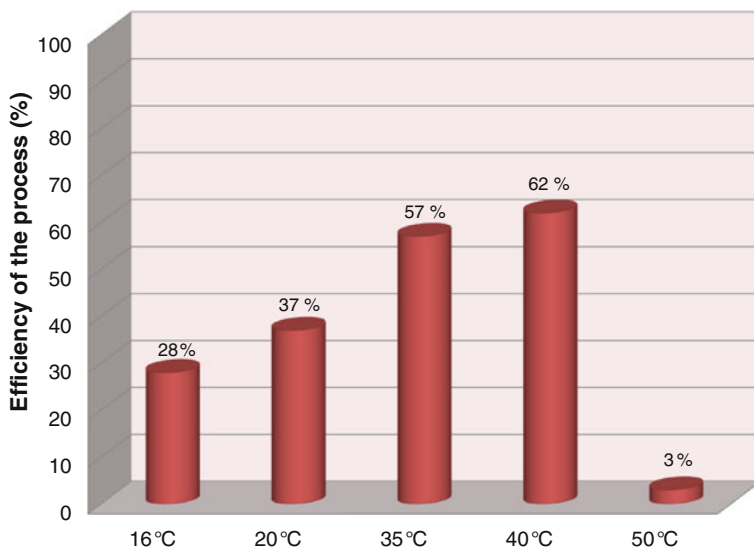


**Fig. 4.14** Efficiency of tests conducted at each working temperature

hydrogen, respectively, energy conversion efficiencies of about 33 and 17 % are calculated if acetate or butyrate fermentation pathways are assumed to occur (Eqs. 4.1 and 4.2). Considering the theoretical H<sub>2</sub> yield of Fig. 4.13, the energy conversion at 35 °C is equal to ~18 %, which drops to approximately 11 % taking into account the efficiency from Fig. 4.14.

## 4.5 Conclusion

In this Chapter the feasibility of converting glucose into hydrogen via dark fermentation in a bioreactor is shown, even at low temperatures such as 20 °C and at ambient temperatures exposed to natural fluctuations. However, the optimal temperature for fermentative H<sub>2</sub> production by mixed cultures is 35 °C. At extreme temperatures, i.e. 16 and 50 °C, the H<sub>2</sub> production is very low, although at 16 °C a residual HPB activity was seen. The variation of H<sub>2</sub> production at different temperatures could be linked to different metabolic pathways as a consequence of the activity of different bacteria species present in a mixed culture of HPB. Furthermore, the buffering of pH is very important for H<sub>2</sub> production, because it permits a more stable and longer-duration H<sub>2</sub> production, even though the cost of NaOH needs to be considered. These indications are very valuable for scale-up purposes.

## References

1. J. Wang, W. Wan, Effect of temperature on fermentative hydrogen production by mixed cultures. *Int. J. Hydrogen Energy* **33**, 5392–5397 (2008)
2. G. Evans, *Biowaste and Biological Waste treatment*, James and James Press, (2001)
3. D.H. Kim, J. Wu, K.W. Jeang, M.S. Kim, H.S. Shin, Natural inducement of hydrogen from food waste by temperature control. *Int. J. Hydrogen Energy* **36**, 10666–10673 (2011)
4. Y.W. Lee, J. Chung, Bioproduction of hydrogen from food waste by pilot-scale combined hydrogen/methane fermentation. *Int. J. Hydrogen Energy* **35**, 11746–11755 (2010)
5. Y. Mu, X.J. Zheng, H.Q. Yu, R.F. Zhu, Biological hydrogen production by anaerobic sludge at various temperatures. *Int. J. Hydrogen Energy* **31**, 780–785 (2006)
6. Y. Akutzu, Y.Y. Li, H. Harada, H.Q. Yu, Effect of temperature and substrate concentration on biological hydrogen production from starch. *Int. J. Hydrogen Energy* **34**, 2558–2566 (2009)
7. Y. Zhang, J. Shen, Effect of temperature and iron concentration on the growth and hydrogen production of mixed bacteria. *Int. J. Hydrogen Energy* **31**, 441–446 (2006)
8. W.M. Chen, Z.J. Tseng, K.S. Lee, J.S. Chang, Fermentative hydrogen production with *Clostridium butyricum* CGS5 isolated from anaerobic sewage sludge. *Int. J. Hydrogen Energy* **30**, 1063–1070 (2005)
9. H.H.P. Fang, H. Liu, Effect of pH on hydrogen production from glucose by a mixed culture. *Bioresour. Technol.* **82**, 87–93 (2002)
10. P.M. Vignais, B. Billond, J. Mayer, Classification and phylogeny of hydrogenase. *FEMS Microbiol. Rev.* **25**, 455–501 (2001)
11. I.K. Kapdan, F. Kargi, Review Bio-hydrogen production from waste materials. *Enzym. Microb. Technol.* **38**, 569–582 (2006)
12. M.W.W. Adams, L.E. Mortenson, The physical and catalytic properties of Hydrogenase II of *Clostridium pasteurianum*. *J. Biol. Chem.* **295**(11), 7045–7055 (1984)
13. N. Ren, J. Li, B. Li, Y. Wang, S. Liu, Biohydrogen production from molasses by anaerobic fermentation with a pilot-scale bioreactor system. *Int. J. Hydrogen Energy* **31**, 2147–2157 (2006)
14. T.D. Brock, M.D. Madigan, J.M. Martinko, J. Parker, *Biology of Microorganisms* (Prentice Hall Press, Englewood Cliffs, 1994)
15. M.H. Hwang, N.J. Jang, S.H. Hyun, I.S. Kim, Anaerobic bio-hydrogen production from ethanol fermentation: the role of pH. *J. Biotechnol.* **111**, 297–309 (2004)
16. P.A. Gibbs, Factors affecting the germination of spores of *Clostridium bifermentans*. *J. Gen. Microbiol.* **37**, 41–43 (1964)
17. K.S. Lee, P.J. Lin, J.S. Chang, Temperature effects on biohydrogen production in a granular sludge bed induced by activated carbon carriers. *Int. J. Hydrogen Energy* **31**, 465–472 (2006)

## Chapter 5

# Net Energy Production of H<sub>2</sub> in Anaerobic Digestion

In this chapter the analysis of net energy production by H<sub>2</sub> in anaerobic digestion (AD) is considered. The net energy production has previously been defined and evaluated by using the experimental data reported in Chap. 4, taking into account the effect of temperature on H<sub>2</sub> production. The net energy produced was evaluated by the difference between the energy produced in the form of H<sub>2</sub> and the total energy used to run the plant. We take into consideration the energy balance of a batch anaerobic bioreactor, following a geometrical scale-up procedure in order to take into account the thermal as well as the electrical energy necessary to run the bioreactor.

### 5.1 Introduction

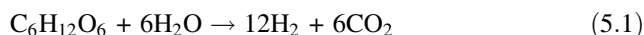
The important role of temperature and pH on fermentative hydrogen production was shown in Chap. 4. In particular, the increase in temperature could increase the ability of HPB to produce hydrogen during fermentation, but temperatures at higher levels (40–50 °C) cause a decrease in the hydrogen produced, shifting the biological pathways towards the production of other compounds, like lactic acid. While we have limited our considerations to improve the H<sub>2</sub> production by affecting the microorganisms, such as by altering temperature and pH, there is another important aspect that should be taken into consideration: the net energy production by the AD technology. The temperature is the most important parameter from an energetic point of view, because it influences not only the energy produced but also the energy necessary to run the bioreactor. Hence the temperature is the most important design parameter of a full-scale bioreactor producing energy by AD, due to its key role in the net energy balance of the technology [1]. Despite these facts, very few papers address the whole energy balance of hydrogen from AD [2]. Considering that the hydrogen bioreactor plant's purpose is to produce energy, a detailed analysis of the energy balance of the bioreactor is of the utmost important in the

selection of the operative working conditions, in order to find the most appropriate conditions needed to maximize the net energy production of the full-scale plant.

The present chapter aims to construct a scale-up methodology using the experimental bench-scale data of an anaerobic bioreactor operated in batch mode. The energy balance of full-scale dark AD will be determined in order to evaluate the quantity of net energy produced from a carbonaceous substrate as a function of two parameters: the working temperature and the diameter of the bioreactor. The net energy produced is evaluated as the difference between the energy produced and the total energy used to run the system at the working temperature. This latter term is composed of the heat used to keep the reactor at each working temperature, the heat lost from the bioreactor walls through natural convective phenomena [3] and the electrical energy used for mixing and pumping purposes. To define the optimal working temperature, the energy balance was calculated in relation to several operating parameters such as outdoor temperature and insulation materials, while considering the bioreactor diameter as the scale-up parameter.

## 5.2 Maximum Obtainable Energy

In order to evaluate the maximum obtainable energy, an important issue is how to appropriately evaluate and express the H<sub>2</sub> production yield and conveniently convert it into a parameter representing the conversion efficiency attained by the AD. The H<sub>2</sub> yield may, in turn, be expressed in terms of energy units. The concept of conversion efficiency derives from the existence of biological barriers to hydrogen production from organic substances that has been elucidated by considering the conversion of a simple carbohydrate, such as glucose, in the previous chapters. It is important to recall here (Eq. 5.1) that if complete glucose conversion is taken into account, 12 mol of H<sub>2</sub> can theoretically be produced from 1 mol of glucose:



This direct conversion of glucose into hydrogen, unfortunately, is not feasible at the moment in the sense that microorganisms are not able to carry it out. The real conversion potential, in fact, is lower than this theoretical value. At best, the conversion of glucose into hydrogen is limited to acetate production and is therefore 4 mol H<sub>2</sub>/mol glucose (Eq. 5.2); in practice only one third of the hydrogen production can be achieved, since part of the energy present in the original glucose remains embedded in the acetate.



Organic intermediate compounds act as electron acceptors, decreasing the  $H_2$  generation yield. In the case of the butyrate fermentation pathway, the conversion efficiency is reduced to 2 mol  $H_2$ /mol glucose:



The production of more reduced fermentation products, compared to acetate, is optimized in nature to sustain microbial growth and, conversely, not to produce  $H_2$ : it represents an energy waste from the point of view of microorganisms. This is primarily due to the fact that the electrons generated from the oxidation of substrate could be used in the metabolic pathways to produce many chemicals. Among them are propionate, butyrate, lactate, formate, ethanol, butanol, alcohols and ketones, with associated longer aliphatic acids which allow for NADH re-oxidation [4]. Taking into account the above considerations, the energy conversion efficiency may be calculated on a mass or energy basis. From an energetic perspective, the hydrogen production efficiency may be evaluated as expressed by Eq. 5.4, considering the fraction of the total energy content of the substrate recovered in the form of hydrogen:

$$\eta = \frac{\text{Energy content in produced } H_2}{\text{Energy content in the substrate}} \times 100 \quad (5.4)$$

Assuming 2,882 and 239.2 kJ/mol as lower heating values (LHVs) of glucose and hydrogen, respectively, energy conversion efficiencies of 33 and 17 % are calculated if the acetate (Eq. 5.2) or the butyrate (Eq. 5.3) fermentation pathways, respectively, are assumed to occur. These values represent the maximum energy obtainable from glucose; in practice, considering the experimentally evaluated  $H_2$  yield from glucose, it is possible to evaluate a mean value from different literature data [5]:

$$Y = 1.76 \pm 0.85 \text{ mol}_{H_2} / \text{mol}_{\text{glucose}} \quad (5.5)$$

with a relative uncertainty value of  $U = 48 \%$  considering different experimental results. Hence the energy efficiency is  $\eta = 15 \pm 9.8 \%$ : this means that butyrate fermentation is predominant and that acetate fermentation is present only in some cases, as experimentally confirmed by results reported in Chap. 4. It is important to emphasize the higher uncertainty present in the literature data. This explains why in practice energy efficiencies higher than 15 % of the original electrons present in the substrate towards  $H_2$  can rarely to be obtained, even under optimal process conditions. The above consideration concerns glucose, which is the most easily biodegradable substrate, but it is not suitable to be used as feedstock to produce energy in full plant applications. For this purpose, organic refuse, generally called biowaste, from the alimentary chain is usually the candidate: from farm producers, from consumers and from food production firms (Chap. 6). The evaluation of the amount

**Table 5.1** Units used to evaluate hydrogen production by anaerobic fermentation

mol H <sub>2</sub> /mol <sub>GI</sub>	mol H <sub>2</sub> /mol <sub>ESose</sub>	mmol H <sub>2</sub> /g <sub>Carbon</sub>
mol H <sub>2</sub> /mol <sub>ESose added</sub>	mmol H <sub>2</sub> /g <sub>COD</sub>	mL H <sub>2</sub> /g <sub>V<sub>S</sub>added</sub>
L H <sub>2</sub> /kg <sub>COD</sub>	L H <sub>2</sub> /L <sub>Reactor</sub>	L H <sub>2</sub> /g <sub>V<sub>S</sub>consumed</sub>

of energy converted into hydrogen becomes difficult in the case of biowaste, because different authors use different units at laboratory or pilot plant scales. Table 5.1 gives a brief list of the units present in the literature. Nevertheless, the evaluation of efficiency of biohydrogen production using organic wastes is of utmost importance, both from the research point of view and for technology scale-up purposes; the following section tries to answer this question.

### 5.3 Energy Conversion Parameters

For the purpose of comparing different results and in order to have a useful engineering parameter, the suggestion to evaluate the energy conversion by using two energy parameters is put forward. The first parameter, efficiency ( $\eta$ ), is used to take into account the quantity of energy produced as hydrogen that the bioreaction is able to extract, with reference to the available amount of energy embedded in the substrate. Equation 5.4 can be written in the following way:

$$\eta = E_p/E_0 \cdot 100 \quad (5.6)$$

where  $E_p$  is the total energy produced as H<sub>2</sub> and  $E_0$  is the energy embedded in the substrate.

$\eta$  can refer either to a mass or volume unit, but in the authors' opinion, in the present context, the use of a mass unit is preferred. The energy produced ( $E_p$ ) can be evaluated through the following expression:

$$E_p = \text{mol}_{\text{H}_2} * \text{LHV}_{\text{H}_2} / C_{\text{TSO}} \quad (5.7)$$

where mol<sub>H<sub>2</sub></sub> (mol/L) is the quantity of hydrogen produced per unit of fermenting broth, calculated using the experimentally evaluated volume and the ideal gas equation to take into account the working pressure and temperature; LHV<sub>H<sub>2</sub></sub> is the lower heating value of hydrogen per mol (239.2 kJ/mol); and  $C_{\text{TSO}}$  (g<sub>TSO</sub>/L) is the concentration of the fermenting broth expressed in total solids. The energy produced is thus relative to the total solids added. A good estimation of  $E_0$  can be obtained using the LHV in kJ/g<sub>TS</sub> of each substrate. Some comments on this aspect are necessary. The question of what is the “available” energy arises, and the answer is that it is the total edible energy, i.e. the energy which can be utilized by a living cell. This means that not all the C–C or C–H bonds are of the same quality; only some are utilizable by the cell machinery. As an example one can consider crude oil: it contains a large quantity of energy (with a very high LHV), but only a small



proportion of it is edible. Considering on the other hand glucose as a carbon source, all the chemical energy embedded in the glucose is edible, as generally accepted by biologists. In numerical terms the available energy of the glucose is 2,882 kJ/mol, which is the LHV of glucose. Considering organic refuse in term of chemical bonds which are able to store the chemical energy, a combination of different edible and inedible chemical energy present in the refuse can be envisaged. For instance sugar, cellulose, lignine and other combinations of C–C or C–H bonds present different degrees of edibility in terms of a macro-approach. Unfortunately, we do not at the moment have a probe able to measure the edible energy compared with the inedible, except in the case of biological tests. In other words we can evaluate the edible energy after a fermentation test, thus including in this the efficiency of the fermentation itself. Moreover, one can measure the total energy present in a refuse or a mixture of different ones by experimental determination of LHV. Hence the efficiency  $\eta$ , i.e. the energy produced as hydrogen from the available energy embedded in the refuse (LHV), is a parameter that can give us information relating to the ability of the biological process (microorganisms in such conditions as working parameters, bioreactor design etc.) to use the edible energy present in the organic refuse.  $\eta$  is global information on the technology used. Considering crude oil as a substrate, for example, the efficiency is very low using AD technology, contrary to what occurs with other technologies such as gasification or combustion. LHV is easily measured by means of a bomb calorimeter; some values for different suitable substrates are shown in Table 5.2.

The second parameter that one can use is the efficacy  $\zeta$ , which takes into account the efficiency of the actual test and that obtained with glucose under the same conditions. In this way, it is possible to easily evaluate the effectiveness of the applied (or candidate) technology: the more  $\zeta$  approaches glucose efficiency, the more the technology of anaerobic digestion (including microorganism consortium, working condition, type of bioreactor used etc.) is effective in the recovery of the energy embedded in the substrate. In addition, the parameter  $\zeta$  permits the scoring of different working conditions for the technology and permits a fruitful comparison

**Table 5.2** Experimentally evaluated LHV of several substances suitable for H<sub>2</sub> production

Substrate	LHV (kJ/kg <sub>TS</sub> )
Glucose	16,540 ± 80
Organic market waste	16,376 ± 150
Coffee seed skin	17,730 ± 45
Coffee grounds refuse	21,226 ± 150
Cooking refuse	18,350 ± 70
Rice stalk	13,710 ± 120
Sorghum	17,861 ± 65
Industrial honey refuse	11,123 ± 95
Sawdust	16,302 ± 85

for scale-up decisions. Therefore, the higher the efficacy value, the greater the effect of recovering energy in the form of hydrogen.

Lastly, considering the glucose efficiency value of Eq. 5.5 that has been experimentally evaluated, a considerable portion of carbon-reducing equivalents, and consequently the energy content of the original substrate, remains embedded in the chemicals present in the effluent from the hydrogen phase. In order to maximize the overall conversion yield and to ensure adequate substrate degradation, the biohydrogen production process should thus be thought of as part of a combined process where additional energy production and enhanced substrate conversion are attained in different process stages. These aspects will be discussed in detail in Chaps. 7 and 8.

## 5.4 Net Energy Balance

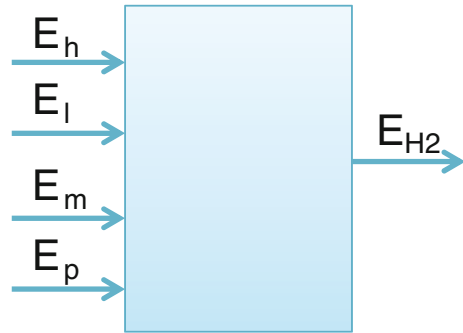
The net energy produced in an AD bioreactor producing H<sub>2</sub> corresponds to the difference between the energy contained in the gas produced per unit of bioreactor volume in a single batch run, or per unit time in the case of continuous running, under certain conditions, and the energy used to obtain and maintain the reaction conditions. To calculate the net energy balance, all the energy quantities were evaluated in energy units per unit volume of bioreactor (MJ/m<sup>3</sup>; MJ/(m<sup>3</sup> day)), and thus a reference volume and a reference time period in which each term must be calculated need to be considered. In addition, as a consequence of the fact that many data are available only at laboratory scale because dark anaerobic hydrogen production has not yet reached full industrial maturity, a scale-up criterion is necessary. A geometric scale-up criterion of the bench bioreactor in order to evaluate the influence of the scale has been used. The diameter  $D$  of the bioreactor was selected as a scale-up parameter in order to evaluate the net energy, using a cylindrical digester geometry with a constant ratio of 4 between the height ( $L$ ) and diameter ( $D$ ) and a constant ratio of 2 between the reactor diameter and that of the mixer one ( $d$ ), as in the bench-scale bioreactor used. The net energy production  $E_{\text{net}}$  may be calculated in the case of batch and continuous reactor operation modes as:

$$E_{\text{net}} = E_{\text{H}_2} - (E_h + E_l + E_m + E_p) \quad (5.8)$$

where

- $E_{\text{H}_2}$  Energy produced [MJ/m<sup>3</sup>]; [MJ/(m<sup>3</sup> day)]
- $E_h$  Heating heat [MJ/m<sup>3</sup>]; [MJ/(m<sup>3</sup> day)]
- $E_l$  Energy loss [MJ/m<sup>3</sup>]; [MJ/(m<sup>3</sup> day)]
- $E_m$  Energy for mixing [MJ/m<sup>3</sup>]; [MJ/(m<sup>3</sup> day)]
- $E_p$  Energy for pumping [MJ/m<sup>3</sup>]; [MJ/(m<sup>3</sup> day)].

**Fig. 5.1** Global view of the energies involved in the net energy balance of H<sub>2</sub> AD bioreactor



The evaluation of the net energy produced was performed by considering the hydrogen produced as a function of the working temperature, as well studied and recognized in the literature [6]. The calculation of the net energy production requires the evaluation of the heat demand necessary to keep the system at the working temperature. The heat required to keep the fermenting biomass at  $T_w$  is the sum of the heat used to warm the feeding biomass from the ambient outdoor temperature  $T_a$  to  $T_w$ , the heat lost from the digester walls, depending on the geography of the plant location, the seasonal variation and, obviously, the night/day oscillation, and the heat withdrawn from the out-stream in the case of continuous operation run.

Figure 5.1 is a global view of the energies involved in the energy balance of the H<sub>2</sub> reactor. Each energy term of Eq. (5.8) will be elucidated in the following sections, using as evidence the equations used in the scale-up procedure as a function of  $D$ .

In Table 5.3 several literature cases are reported: they show the best working temperature which maximizes the hydrogen production per unit of working volume along time necessary to reach this production in batch tests. This information is of utmost important in order to calculate the energy balance, because the time affects the energy used for agitation and that lost by natural convection across the bioreactor walls.

### 5.4.1 Energy Production

The energy produced per unit volume of reactor is the total energy contained in the gas produced relative to the reactor volume, i.e. the energy contained in the amount of hydrogen retrieved from a single batch run (or per unit time in the case of continuous mode); it can be calculated as:

**Table 5.3** Maximum specific hydrogen production per unit of volume and working temperature for batch bioreactors

References	Substrate	Microorganisms	Initial pH	$T_{w, \max}$ (°C)	Running time (h)	Productivity (mmol H <sub>2</sub> /L)
Wang and Wan [7]	Glucose	Mixed culture	7.0, no control	40	25	123
Zhang and Shen [8]	Sucrose	Mixed culture	8.0, no control	35	25	207
Mu et al. [9]	Glucose	Mixed culture	Control at 5.5	41	24	91
Tommasi et al. [10]	Glucose	Mixed culture	7.5, no control	25–26	50	60
Ruggeri et al. [11]	Glucose	Mixed culture	Control at 5.2	35	340	442
Gadhamshetty et al. [12]	Sucrose	Mixed culture	8.5, no control	22	466	120
		Mixed culture	8.5, no control	37	90	50
Tang et al. [13]	Cattle wastewater	Mixed culture	Control at 5.5	45	30	8
Karadag et al. [14]	Glucose	Sediments from geothermal hot spring	6.5, no control	51.7	16	625

$$E_{H_2} = F \cdot P_{H_2}(T_w) \cdot LHV_{H_2} \quad (5.9)$$

where  $P_{H_2}(T_w)$  is the specific production of H<sub>2</sub> and represents the amount of H<sub>2</sub> produced in a single batch run expressed as Nm<sup>3</sup>/m<sup>3</sup> (or per day for a continuous bioreactor, Nm<sup>3</sup>/(m<sup>3</sup> day)), which depends on the working temperature.  $LHV_{H_2}$  is the lower heating value of hydrogen (10.8 MJ/Nm<sup>3</sup>) and  $F$  is the liquid contained in the reactor, i.e., the fraction of reactor volume filled by liquid, usually assumed to be  $F = 0.9$ .

### 5.4.2 Heating Heat

The energy required to warm up the fermenting broth mainly depends on its specific heat ( $c_p$ ), the difference between ambient outdoor  $T_a$  and working temperature  $T_w$ , and the efficiency of the heating system  $\eta_C$ . The necessary heating energy per unit volume (kJ/m<sup>3</sup>) of the bioreactor may be calculated either as:

$$E_h = \frac{(\rho \cdot c_p \cdot \Delta T \cdot F)}{\eta_c} \quad (5.10)$$

in the case of a batch bioreactor, or as:

$$E_h = \frac{(\rho \cdot c_p \cdot \Delta T \cdot F)}{\eta_c \cdot \text{HRT}} \quad (5.11)$$

in the case of a continuous bioreactor,

where:

$\rho$	is the biomass density [kg/m <sup>3</sup> ]
$c_p$	is the biomass specific heat [kJ/(kg °C)]
$\Delta T = (T_w - T_a)$	according to the season [°C]
$\eta_c$	is the global efficiency of the system to furnish the heat taking into account $\eta_{\text{comb}}$ and $\eta_{\text{exc}}$
HRT	is the hydraulic retention time of the liquid in the bioreactor [day].

As sufficient assumptions, the  $\rho$  and  $c_p$  of water were used for the fermenting broth. The warming device was considered to be composed of a combustion boiler ( $\eta_{\text{comb}} \approx 0.8$ ) and a heat exchanger ( $\eta_{\text{exc}} \approx 0.6$ ); the global efficiency of the warming system was calculated as the product ( $\eta_c \approx 0.48$ ). The outdoor ambient temperature needs to be considered for different seasonal conditions, e.g., summer and winter conditions.  $T_a$  needs to be calculated on the basis of historical data; mean night and day values over the season could be considered in order to avoid an increase in computational complexity. A heat recovery of 50 % seems a good assumption, i.e. 50 % of the heat of the broth is recovered by adequate heat exchange at the end of the batch run or of the out-flow rate. The warming of the reactor wall and insulator and that of the NaOH solution necessary to maintain the pH at low value were neglected.

### 5.4.3 Heat Loss

The difference between the working temperature of the broth  $T_w$  and the ambient temperature  $T_a$  outside the reactor is responsible for the heat loss from the bioreactor. The lost energy must be supplied from the heating device of the temperature control system and it depends on the insulation of the fermenting broth from the external environment and the exposed surface. The necessary energy used to replace the heat loss per unit volume of reactor may be calculated as:

$$E_l = \frac{(4.5 \cdot \frac{k}{s} \cdot \Delta t(T_w) \cdot \frac{\Delta T}{D})}{\eta_c} \quad (5.12)$$

in the case of a batch run; while the following equation allows its evaluation in the case of a continuous reactor:

$$E = \frac{(4.5 \cdot k/s \cdot 24 \cdot \Delta T/D) + (\rho \cdot C_p \cdot F \cdot T_w/HRT)}{\eta_c} \quad (5.13)$$

where:

- $k$  is the thermal conductivity of the digester walls [kJ h<sup>-1</sup> m<sup>-1</sup> °C<sup>-1</sup>]
- $s$  is the thickness of the reactor/insulator walls [m]
- $\Delta t(T_w)$  is the total duration of fermentation [h]
- $D$  is the reactor diameter [m]
- 4.5 is a factor according to the geometrical scale-up criterion that has been adopted.

The other terms have been introduced previously. Regarding the construction material of the bioreactor, we consider as examples two cases:

- the bioreactor walls comprise a  $2.5 \times 10^{-3}$  m thick steel wall as structural material and  $30 \times 10^{-3}$  m thick polystyrene foam as insulating material, in which also the bottom and the top of the bioreactor walls are insulated with the same thickness of insulating material;
- the bioreactor walls are completely built with  $30 \times 10^{-3}$  m thickness of concrete material.

As shown in Chap. 4, the total duration of fermentation  $\Delta t$  depends on the working temperature and is related to the bioH<sub>2</sub> production shut-down. The duration of fermentation and H<sub>2</sub> production obtained experimentally according to the working temperature are reported in Table 5.4. The total resistance, i.e. the reciprocal of the overall heat transfer coefficient  $U$ , accounts for the total insulation of the broth from the outside environment, and can be calculated as the sum of the single resistances, i.e. internal broth, steel plus insulator and the external air resistances.

**Table 5.4** Total H<sub>2</sub> produced per unit of volume, duration of fermentation and energy production obtained by bench-scale bioreactor running at different temperatures

$T_w$ (°C)	H <sub>2</sub> produced (mmol H <sub>2</sub> /L)	$\Delta t$ (days)	Energy production (kJ/L)
16	15.4	6.6	3.32
20	215.3	23.9	47.36
35	442.0	13.8	95.15
40	96.0	8.4	20.67
50	1.1	12.5	0.10

The heat flux from the bioreactor comes across the three heat resistances in series, and therefore the global thermal resistance  $U^{-1}$  is:

$$U^{-1} = h_i^{-1} + \frac{s}{k} + h_e^{-1} \quad (5.14)$$

where  $h_i$  and  $h_e$  are the internal and external convective heat transfer coefficients, respectively. A large thickness of insulator creates a higher resistance because the phenomena of heat transfer in different materials are in series [15], hence both the convective coefficients,  $h_i$  and  $h_e$ , can be disregarded. Very thick polystyrene foam (or generally higher thickness of insulator) makes the foam resistance the only relevant contribution to the total resistance. The resistance to heat transport is here only considered in the insulating material; this assumption leads to overestimating the insulator thickness for the same energy loss.

#### 5.4.3.1 Focus on Thermal Insulator

Insulating materials are of great importance for minimizing the amount of heat exchanged between system and environment. The insulating materials are solid and usually inhomogeneous materials, characterized by a very low value of thermal conductivity  $\lambda$ , resulting mainly from the air enclosed in the pores of the material itself. The value of the conductivity coefficient  $\lambda$  (W/m K) indicates the ease with which the material transports energy via collisions at the molecular level, depending on the chemistry of the material, the phase considered (solid, liquid or gas), the crystalline structure, the temperature and the homogeneity of the materials [15]. Table 5.5 shows the thermophysical properties of some materials.

**Table 5.5** Thermophysical properties of some materials

Material	$T$ (°C)	$\lambda$ (W/m K)	$\rho$ (kg/m <sup>3</sup> )	$c_p$ [kJ/(kg K)]
Steel	20	52	7,800	0.44
Aluminium	20	220	2,700	0.93
Cotton	30	0.04	80	1.52
Glass wool	0	0.035	100	0.65
Expanded polystyrene	0	0.032	35	0.8
Expanded polyurethane	0	0.021	40	–
Cork sheet	0	0.04	130	–
Sheep wool	10	0.04	28	–
Straw	20	0.058	175	–
Recycled paper	20	0.07	400	–
Raw clay	20	0.132	700	–
Concrete	15	0.4–0.7	2,400	0.92

### 5.4.4 Electrical Energy

The electrical energy consumed to run the bioreactor is for mixing, filling up and emptying the bioreactor using a pump. In batch fermentation, the raw material and the inoculum are pumped in at the beginning of the run and the broth is pumped out at the end. The reactor is mixed throughout the run. The energy for pumping in the case of a batch reactor may be calculated as the energy necessary to lift the broth to the top of the reactor by using the following equation:

$$E_p = (q \cdot \rho \cdot W_p \cdot t_r \cdot 9.81 \times 10^{-3}) / V_R \quad (5.15)$$

where  $q$  is the volumetric flow rate (m<sup>3</sup>/h),  $t_r$  is the filling time (h),  $9.81 \times 10^{-3}$  is the conversion factor from kg<sub>f</sub>.m to kJ,  $V_R$  is the reactor volume and  $W_p$  is the energy to be supplied to the fluid per unit of broth mass, in kg<sub>f</sub>.m/kg, to transport it from the feed tank to the reactor. It can be evaluated by Eq. (5.16) under the hypothesis that the pressure in the tank is equal to that of the reactor and the fluid motion occurs in the turbulent flow regime [16]:

$$W_p = (g/g_c \cdot L + v^2/2g_c + f_f) / \eta_m \quad (5.16)$$

where  $g$  is the acceleration due to gravity,  $g_c$  is the Newton's-law proportionality factor  $g_c = 1.2 \times 10^8$  (kg m h<sup>-2</sup> kg<sub>f</sub><sup>-1</sup>),  $L$  is the height of reactor,  $v^2$  is the velocity of the fluid in the pipe,  $f_f$  represents the energy dispersed as heat generated to overcome the friction force per unit of mass of fluid occurring in the fluid along pipe between the feed tank and the reactor; finally,  $\eta_m$  accounts for the overall efficiency of the pump to convert mechanical energy in energy of motion. Considering a batch run of the bioreactor, it is possible to assume  $E_p \sim 0$  compared with the electrical energy used for the agitation during the fermentation. This hypothesis always seems valid, because the time  $t_r$  is of the order of hours compared to the duration of a batch process, which is of the order of weeks or months. In the case of continuous operation the energy used for pumping is:

$$E_p = \rho \cdot W_p \cdot 9.81 \times 10^{-3} \cdot F / \text{HRT} \quad (5.17)$$

where the terms have the same meaning as previously defined. It cannot be disregarded.

The evaluation of the energy required to mix the fermenting broth versus diameter was made by applying a turbulence scale-up criterion. The power number and the rotational Reynolds number were considered to evaluate the mixing performances of the bioreactor [17]. The rotational Reynolds number was considered to be independent of the reactor diameter, according to the turbulence scale-up criterion:  $\text{Re} \approx N_1 D_1^2 = N_D D_D^2$ , i.e., the power number is independent of the reactor diameter [17, 18]. A geometrical similarity was assumed for the vessel and impeller scale-up, i.e., an impeller-to-reactor diameter ratio equal to 0.5 was assumed,



similar to the bench-scale bioreactor. With the above assumptions, the following equation allows the estimation of the electrical power necessary to mix the broth:

$$P_w = \left(\frac{P_n \cdot \rho}{8g\pi}\right) \cdot N_1^3 \cdot D_1^6 \cdot D_D^{-4} \cdot F \cdot 10^{-3} \quad (5.18)$$

where  $l$  and  $D$  refer to the bench scale and to the actual bioreactor, respectively,  $N$  is the rotational number (rpm) and  $P_n$  is the power number. The procedure reported in Bailey and Ollis [18] was used to calculate the power number  $P_n$  for the bench-scale bioreactor. In Eq. (5.18)  $P_w$  is the power per unit volume ( $\text{kJ/m}^3$ ) of the reactor required to reach the target mixing performance, i.e. the value of the Reynolds number equal to that of the bench reactor. To evaluate the energy used for mixing it is necessary to take into account, in the case of batch mode, the running time given in Table 5.4 for each working temperature:

$$E_m = \frac{P_w \cdot \Delta t(T_w)}{\eta_{el}} \quad (5.19)$$

An efficiency of electrical energy conversion ( $\eta_{el}$ ) into mixing energy of 0.75 was considered. In the case of continuous mode the energy can be evaluated by using 24 h/day instead of the duration of the batch  $\Delta t$  in Eq. (5.19). All the above Equations were implemented in an Excel sheet to perform the net energy balance for each situation; only the case of a batch reactor was considered here because the data available on hydrogen production in this case are well recognized in the literature.

## 5.5 Results and Comments

### 5.5.1 Energy Production

The energy production as  $\text{H}_2$  achieved by the bench-scale bioreactor at each temperature investigated is reported in Table 5.4, in order to evaluate the net energy produced using the approach described in Sect. 5.4. In the present context, i.e., the net energy balance of the bioreactor, the diameter of the reactor  $D$  as scale-up parameter is able to link together all the energy terms including the energy production per unit of volume, because the energy production is linked to the third power of the diameter and the energy dispersed as heat and the energy for mixing depend on the square of the diameter. The energy production at different temperatures (from 16 to 50 °C) is shown in Fig. 5.2, the highest quantity of  $\text{H}_2$  was obtained at 35 °C. At this temperature a peak of energy produced occurs, in accordance with several other researchers, as the optimum point in the mesophilic range for biohydrogen production, as underlined in Table 5.3.

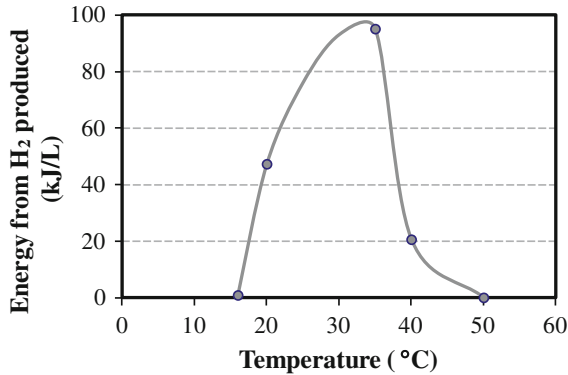


Fig. 5.2 Specific energy production as H<sub>2</sub> produced versus temperature

### 5.5.2 Net Energy Production

The net energy balance was evaluated in the following situations: winter and summer times with a mean ambient temperature of 5 and 15 °C, respectively, and for two bioreactor construction materials: concrete, and steel plus an insulator of polystyrene foam. In any case, for evaluating the effect of construction materials on net energy production, it is possible to find the thickness of insulator that maximizes the net energy, using the approach described in Sect. 5.4. In accordance with Eq. (5.8), the calculation of the net energy balance of a bioreactor producing H<sub>2</sub> is shown in Fig. 5.3 for concrete ( $30 \times 10^{-2}$  m thick) and in Fig. 5.4 for steel plus polystyrene foam ( $2.5 \times 10^{-3}$  m as structural material plus  $30 \times 10^{-2}$  m of insulator) versus the diameter of the bioreactor. In all the situations considered in Figs. 5.3 and 5.4, the net energy balance is never in the positive range. Figure 5.3a, b show the results of scale-up procedure evaluation for a bioreactor built with concrete walls (and without insulator) operated in winter time (a) and in summer time (b), respectively, with 50 % heat recovery as quoted in the assumptions. The results show that the net energy balance is always negative or equal to zero, except for some negligible cases for the evaluation conducted in summertime conditions with  $T_w = 35$  °C and for  $D > 4$  m.

Figure 5.4a, b report the evaluations of the net energy production for a H<sub>2</sub> bioreactor comprising steel covered with  $30 \times 10^{-2}$  m thick polystyrene foam as insulator in winter and summer time, with the assumption of 50 % heat recovery. Contrary to expectations, the best situation is reached by running the bioreactor not at 35 °C, which gives the maximum H<sub>2</sub> production, but at  $T_w = 20$  °C, in which the energy production is only about 50 % of the maximum value (see Fig. 5.2). This occurs because the energy produced by working at higher temperatures is consumed to heat the reactor to higher temperatures. During winter time, the net energy is never in the positive range for all the temperatures considered. This means that

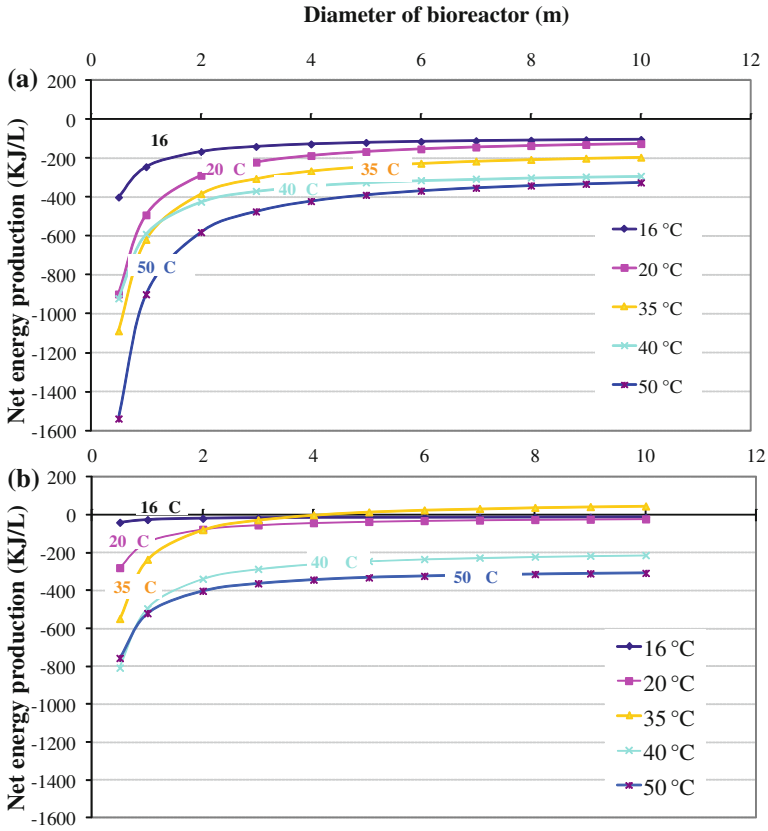
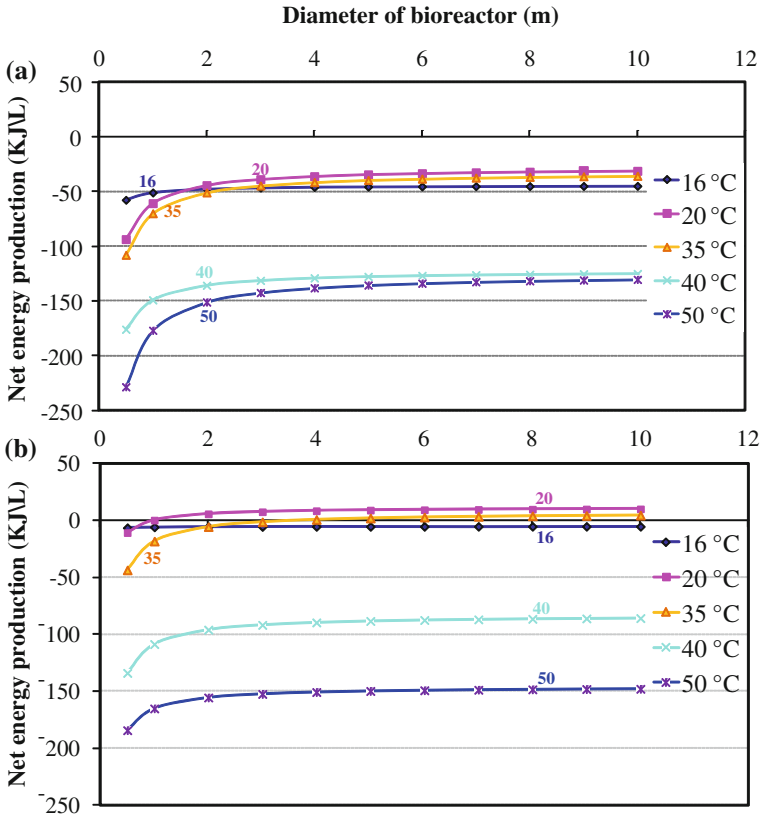


Fig. 5.3 Net energy productions versus bioreactor diameter for a concrete bioreactor with the assumption of 50 % heat recovery: **a** winter time and **b** summer time

during this period the energy produced is never able to compensate for the energy used to run the bioreactor. In addition in the summertime the net energy works out negative for diameters less than 1 m and becomes positive only for a few energy units per bioreactor volume at larger diameters, despite assuming a recovery of 50 % of the energy used to heat the fermenting broth.

On a deeper analysis of Figs. 5.3 and 5.4, the net energy production increases with the bioreactor diameter but this effect vanishes for diameters of over approximately 3 m. This fact suggests a scale-up criterion for larger diameters, which means that, for a larger quantity of feedstock to be treated in unit time, it is better to work with more than one bioreactor with smaller diameters (~3–4 m) instead of only one with a bigger diameter, for constructive reasons. Therefore, regarding the bioreactor diameter, for low diameters it is better to work at a lower temperature even if this means a lower biological activity of the microorganisms. Furthermore, without insulation it seems markedly better to choose a low reactor



**Fig. 5.4** Net energy production versus diameter for a bioreactor of steel and  $30 \times 10^{-2}$  m polystyrene foam insulation with the assumption of 50 % heat recovery: **a** winter time and **b** summer time

temperature as a strategy to maximize the recovery of energy. The 50 % of heat recovery results in an essential operational requirement to increase the net energy balance. Figure 5.5, where calculations are provided without taking into account the heat recovery, shows that net energy production is never in the positive range, even in the case of a reactor made of steel plus insulator.

Similar results (Fig. 5.6) are obtained using the specific hydrogen production data of other researchers, as reported in Table 5.3: in all the situations the net energy production is never in the positive range.

Figure 5.7 compares the different net energy productions under concrete and polystyrene foam in the same conditions: winter time and  $T_w = 35 \text{ }^\circ\text{C}$ . The reactor with insulation demonstrates a lower dependence on bioreactor diameter and at the

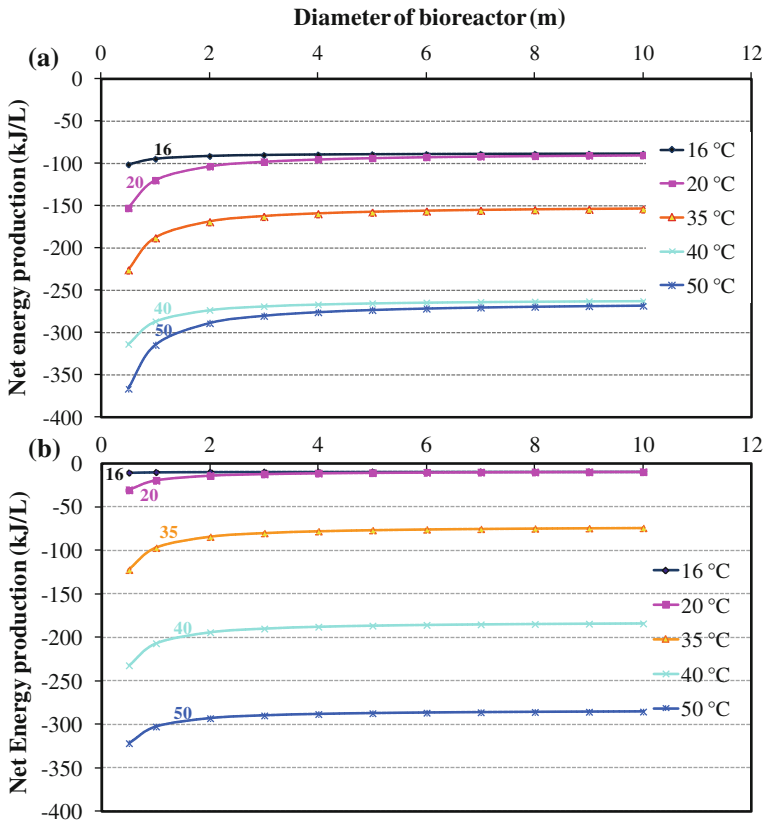


**Fig. 5.5** Net energy productions versus diameter for a bioreactor of steel and  $30 \times 10^{-2}$  m of polystyrene foam insulation without the assumption of 50 % of heat recovery: **a** winter time and **b** summer time

same time a smaller amount of negative net energy production. Furthermore, the thermal insulation of the reactor and in general the construction material play an important role in the total energy balance because it is necessary to take into consideration the energy used to produce the materials.

The above results show the necessity, for AD hydrogen production, to obtain energy from the volatile fatty acids (VFA) and other compounds in the residue present at the end of the acidogenic fermentation step. Several approaches are candidates for this purpose [19], ranging from photobiohydrogen production [20] to the use of microbial fuel cells [21] and the methanation of the liquid residue by AD. Chapters 7 and 8 are dedicated to raising the energy value of VFA to make the net energy balance of the whole system positive.

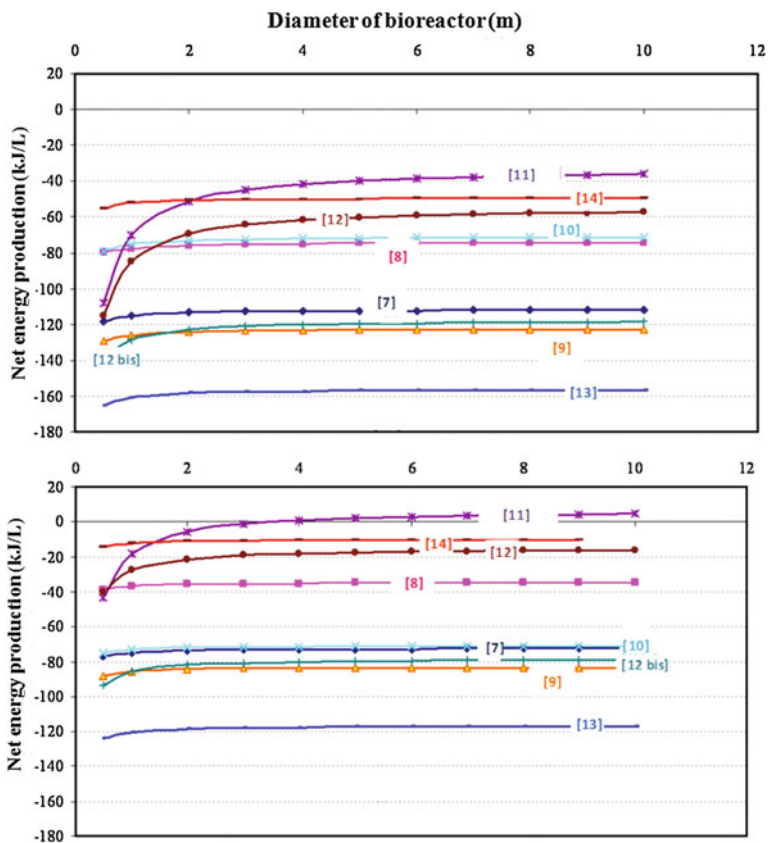


**Fig. 5.6** Net energy productions versus diameter for a bioreactor of steel and  $30 \times 10^{-2}$  m of polystyrene foam insulation with the assumption of 50 % of heat recovery using the specific H<sub>2</sub> production from different authors: **a** winter time and **b** summer time

### 5.6 Uncertainty Evaluation

The estimation of the uncertainty is a fundamental task to be performed in the present situation. The uncertainties of net energy were evaluated accordingly to the rules given in [22]. Considering that the *Guide to Uncertainty Measurement* (GUM) defines uncertainty as a quantifiable parameter associated with the results of a measurement procedure, the suggested approach has been utilized either to evaluate the uncertainty or to estimate the parameters with the most effect. This latter approach was obtained by using the expression given in [23], known as the *law of the propagation of uncertainty*. It is based on the evaluation of the partial derivatives of the parameters in the estimation of the net energy, called *sensitivity coefficients*, which describe how the output estimate varies with changes in the value of the input estimates. Applying this procedure to Eq. 5.8, the following results were

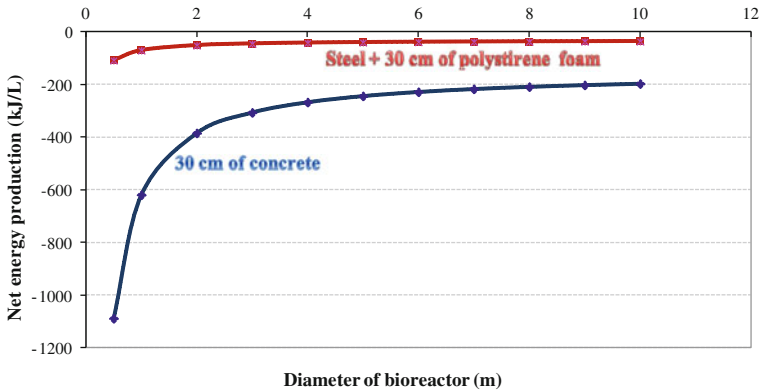


**Fig. 5.7** Comparison between the net energy production versus diameter of a steel plus polystyrene foam bioreactor and a concrete one

obtained. As concerns the main parameters affecting the net energy estimation, the warming energy has the highest predominance compared to other energy terms. It reaches almost the same numerical value in both winter time and summer time: 85 and 70 %, respectively. The variability either of ambient temperature  $T_a$  or of the global thermal efficiency  $\eta_C$  are the main sources of the uncertainty. With a  $T_a$  variability of around 5 °C and a relative variability of  $\eta_C$  of around 10 % in the values used for the calculation, the uncertainty of the net energy is around 50 kJ/L; uncertainty evaluations of  $T_a$  and  $\eta_C$  are constant, i.e. considering only the uncertainty due to the experimental data results in a range of 5–15 kJ/L; this confirms that  $T_a$  is the main parameter affecting anaerobic digestion.

According to the value of the net energy estimation reported in Figs. 5.3 and 5.4, it is possible to consider the suggested energy balance sufficiently acceptable in the estimation of the net energy of biohydrogen production. In any case, for a specific design of a detailed plant, the uncertainty could be reduced by taking into consideration the actual variation of ambient temperature for a specific geographical situation.

## 5.7 Conclusion

In this chapter a scale-up procedure to evaluate the net energy production of a bioreactor producing  $H_2$  is analyzed and applied. The main conclusions are:

- bioreactors which produce only  $H_2$  are not energetically sustainable, apart from a few energy units per unit of volume for a bioreactor running in summer time (at least for the considered temperature) and with the hypothesis of recovering 50 % of the energy used to heat the mass to a working temperature of 35 °C;
- the net energy produced depends mainly on the seasonal temperature variations;

- other parameters with an effect are the thickness of the insulation material, the thermal conductivity and the bioreactor diameter.

Different strategies of plant running are necessary to maximize the net energy production. For example, the recovery of the heat used to warm the fermenting broth is a fundamental aspect: without recovery the net energy balance is never in the positive range. The best working temperature to maximize the net energy produced by the plant is 20 °C, whereas 35 °C is the optimal temperature for maximizing biomass activity for hydrogen production. The uncertainty analysis of the procedure shows that the main influencing parameters are the ambient temperature, because this determines the quantity of energy to be used to heat the bioreactor, and the efficiency of the heating system. Therefore, this suggests that for a full-scale application a careful estimation of  $T_a$  variation is of utmost importance. Concerning the effect of diameter, it is possible to conclude that it is better to work at a low temperature (20 °C) for diameters less than 1 m, even if the energy produced is lower, because this increases the net energy, while for values over 3 m the effect is negligible. Consequently, in order to maximize the net energy of such a process, the strategy of managing the operative conditions requires much care, without disregarding the construction material to be used.

Lastly, in order to have a net positive energy balance to sustain the biohydrogen technology, it is necessary to increase the energy production by looking to valorize the chemicals remaining in the fermenting broth at the end of acidogenesis; a great quantity of energy (>80 % of that present in the feed) is still locked up in the reaction products, which can be converted into further energy in the shape of hydrogen, methane or electricity.

## References

1. B. Ruggeri, Thermal analysis of anaerobic digesters. *La Chimica e l'Industria* **66**(7–8), 477–483 (1984)
2. H. Bonallagui, O. Haonari, Y. Tauhami, R. Ben Chekh, L. Maronani, M. Hamdi, Effect of temperature on the performance of an anaerobic tubular reactor treating fruit and vegetable waste. *Process Biochem.* **39**, 2143–2148 (2004)
3. B. Ruggeri, Thermal and kinetic aspects of biogas production. *Agric. Wastes* **16**, 183–191 (1986)
4. P.C. Hallenbeck, Fermentative hydrogen production: principles, progress and prognosis. *Int. J. Hydrogen Energy* **34**, 7379–7389 (2009)
5. Z. Liu, C. Zhang, Y. Lu, X. Wu, L. Wang, B. Han, X.H. Xing, States and challenges for high-value biohyten production from waste biomass by dark fermentation technology. *Bioresour. Technol.* **135**, 292–303 (2013)
6. J.L. Wang, W. Wan, Factor influencing fermentative hydrogen production: a review. *Int. J. Hydrogen Energy* **34**, 799–811 (2009)
7. J.L. Wang, W. Wan, Effect of temperature on fermentative hydrogen production by mixed cultures. *Int. J. Hydrogen Energy* **33**, 5392–5397 (2008)
8. Y. Zhang, J. Shen, Effect of temperature and iron concentration on the growth and hydrogen production of mixed bacteria. *Int. J. Hydrogen Energy* **31**, 441–446 (2006)



9. Y. Mu, X.J. Zhung, H.Q. Yu, R.F. Zhu, Biological hydrogen production by anaerobic sludge at various temperatures. *Int. J. Hydrogen Energy* **31**, 780–785 (2006)
10. T. Tommasi, B. Ruggeri, G. Sassi, Preliminary Investigation on the Effect of pH on BioH<sub>2</sub> Production Under Ambient Temperature Variations, in Proceedings Second International Symposium on Energy from Biomass and Waste, Venice, Italy, Nov 2008
11. B. Ruggeri, T. Tommasi, G. Sassi, Energy balance of dark anaerobic fermentation as a tool for sustainability analysis. *Int. J. Hydrogen Energy* **35**, 10202–10211 (2010)
12. V. Gadhamshetty, D.C. Johnson, N. Nirmalakhandan, G.B. Smith, S. Deng, Feasibility of biohydrogen production at low temperatures in unbuffered reactor. *Int. J. Hydrogen Energy* **34**, 1233–1243 (2009)
13. G.L. Tang, J. Huang, Z.J. Sun, Q.Q. Tang, C.H. Yan, G.Q. Liu, Biohydrogen production from cattle wastewater by enriched anaerobic mixed consortia: influence of fermentation temperature and pH. *J. Biosci. Bioeng.* **106**(1), 80–87 (2008)
14. D. Karadag, A.E. Makinen, E. Efimova, J.A. Puhakka, Thermophilic biohydrogen production by an anaerobic heat treated-hot spring culture. *Bioresour. Technol.* **100**, 5790–5795 (2009)
15. W.M. Rohsenaw, J.P. Hartnett, *Handbook of Heat Transfer* (Mcgraw Hill Press, New York, 1973)
16. W.L. Mc Cabe, J.C. Smith, P. Harriot, *Unit Operations of Chemical Engineering*, 5th edn. (McGraw-Hill, New York, 1993)
17. S. Nagata, *Mixing Principles and Applications* (Wiley, New-Park, 1975)
18. J.E. Bailey, D.F. Ollis, *Biochemical engineering fundamentals*, 2nd edn. (McGraw-Hill Education Singapore Int. Editions, Singapore, 1986)
19. J.H. Reith, R.H. Wijffels, H. Barten, *Status and Perspectives of Biological Methane and Hydrogen Production* (Dutch Biological Fondation, Netherlands, 2003)
20. I.K. Kapdan, F. Kargi, R. Oztekin, H. Argun, Bio-hydrogen production from acid hydrolyzed wheat starch by photo-fermentation using different *Rhodobacter* sp. *Int. J. Hydrogen Energy* **34**, 2201–2207 (2009)
21. T.H. Pham, K. Rabaey, P. Aelterman, P. Clauwaert, L. De Shampelaire, N. Boon, W. Verstraete, microbial fuel cells in relation to conventional anaerobic digestion technology. *Eng Life Sci.* **6**(3), 285–292 (2006)
22. ISO TAG4, *Guide to the Expression of the Uncertainty in Measurements (GUM)*, Geneva (1994)
23. B. Ruggeri, Chemicals exposure: scoring procedure and uncertainty propagation in scenario selection for risk analysis. *Chemosphere* **77**, 330–338 (2009)

## Chapter 6

# Hydrogen Production from Biowaste

In this Chapter the feasibility of hydrogen production from organic waste (OW) is highlighted. Possible sources are the residue of municipal solid waste (MSW) sorting by mechanical/physical treatment, the OW separately collected from households and the waste produced along the entire food production chain. A brief review introduces the different kind of utilizable biomass and pretreatment processes necessary to make complex organic substrates easy to be metabolized by HPB. Some experimental tests are then presented with the aim of investigating the feasibility of using OW for H<sub>2</sub> production, selecting an easy and efficacious pretreatment method; tests with fruit and vegetable market wastes were conducted emphasizing the problems in scaling up the technology.

### 6.1 Biomass as Food for Microorganisms

Biomass in its traditional sense can be defined as “recent organic matter originally derived from plants as a result of the photosynthetic conversion process, or from animals, and which is destined to be utilized as a store of chemical energy to provide heat, electricity, or transport fuels” [1]. The chemical energy contained in the biomass is derived from solar energy by photosynthesis, the process by which plants take carbon dioxide and water from their surroundings and, using energy from sunlight, convert them into sugars, starches, cellulose, lignin etc. Biomass resources include wood from sustainable plantation forests or forest maintenance, residues from agricultural and breeding for food production as well as residues along the alimentary chain, including the production and the distribution, as well as at the points of utilization such as markets. In general, *biowaste* belongs to one of the three following groups [2]:

- animal waste (feces/manures)
- plant materials (grass clippings and vegetable peelings)
- processed materials (food industry and abattoir wastes)

OW is a major component in daily MSW and it can comprise more than 50 % if the “paper and card” plus “biowaste” categories are taken into account, as shown in Table 6.1.

Biowaste derived from plant material is principally composed of cellulose, though with different amounts of other plant structural compounds, including hemicelluloses and lignin [3].

Bearing in mind that MSW is composed largely of organic materials, the fermentation process seems to be adequate for both the organic part of MSW and the residues of the agro-industrial sector. Among the organic materials, sugars can be easily fermented into fuels such as ethanol, methane or hydrogen, but most organic materials are polymers with five or six carbon sugar units such as cellulose, hemicellulose and lignin, with different degrees of oxidation. Most of these carbohydrates can be converted into fuels, i.e. ethanol, hydrogen or methane, via biotechnology processes. In order to transform large quantities of organic waste materials into energy vectors, it is necessary to convert the carbohydrate polymers into low-molecular-weight monomer sugars. Sugars, starches, lipids and proteins present in organic waste are those most easily degradable by microorganisms, while

**Table 6.1** Typical composition of municipal solid waste in industrialized countries

Category	% (w/w) <sup>a</sup>	% (w/w) <sup>b</sup>	% (w/w) <sup>c</sup>	% (w/w) <sup>d</sup>	Inclusions
Paper and card	33.2	30.7	21.5	32.7	Newspapers, magazines, other papers, liquid containers, packaging card and other card
Biowaste	27	33.7	34.3	25.3	Garden waste, kitchen waste, other putrescibles and fine waste (<10 mm)
Glass	9.3	7.9	10.6	5.3	Brown, green, clear and other glass
Miscellaneous combustibles	8.1	5.2	6.7	5.6	Disposable nappies and other combustibles
Dense plastics	5.9	3.4	6.9	12.1	Clear and colored beverage bottles, other bottles, food packaging and other dense plastics
Ferrous metal	5.7	7.5	3.8	8.2	Beverage cans, food cans, other cans, batteries and other ferrous metals
Plastic film	5.3	4.6	n.a.	7.6	Refuse sacks and other plastic film
Textiles	2.1	3.3	2.6	n.a.	Textiles
Miscellaneous non-combustibles	1.8	2.5	12.6	n.a.	Miscellaneous non-combustibles
Non-ferrous metals	1.6	1.2	1.0	3.2	Non-ferrous beverage cans and other non-ferrous metals

*n.a.* not available, *w/w* weight/weight

<sup>a</sup> Warren Spring Laboratory data, presented to 1994 Harwell Waste Management Symposium

<sup>b</sup> An introduction to Household Waste Management, ETSU for the DTI, March 1998

<sup>c</sup> Burnley et al. 2007

<sup>d</sup> Centre for Sustainable System, University of Michigan, 2009; <http://css.snre.umich.edu>

some other fractions, such as lignocelluloses and keratin, are more difficult to degrade. Several enzymes, such as amylase, cellulase, protease, keratinase and lipase, carry out the biological degradation of these polymers, before further fermentation or digestion to produce ethanol or biogas.

Cellulose itself is a structural carbohydrate made up of a complex chain of hexose units. While hemicelluloses superficially resemble cellulose, they are more readily hydrolyzed; lignin however, found in woody tissue, is the most complex of all plant structural carbohydrates and, though originally derived from the conversion of cellulose, it is much less readily decomposed. OW routinely has high water content, often 80–90 % w/w [2], hence biomass has a heat value that can be partly “captured” in other, more immediately useful forms of energy [3], but the high water content makes it a good substrate for biological processes, e.g. anaerobic hydrogen production as well as biogas or bioethanol production. The estimated annual biosynthesis production of biomass is about  $170 \times 10^9$  t; 75 % is carbohydrate, mainly in the form of cellulose, starch and saccharose, 20 % is lignin and only 5 % is made up of other natural compounds, such as fats (oils), proteins and various substances [4]. It is evident that the main scientific attention towards searching for new organic feedstock should first be focused on efficient use and after-use recovery of carbohydrates. In fact, taking into account that each person produces on average more than 450 kg of MSW per year with about 60 % organic nature, and additional organic waste comes from food chain production and manufacturing, the great necessity of using these materials as feed to produce fuels is evident.

To make most complex and under-utilized organic sources quickly available to microorganisms, pretreatments are necessary. The pretreatment process, by either physical, chemical or biological means, is a well investigated process for ethanol production using lignocellulosic materials. Furthermore, some efforts have been made to treat waste materials in order to increase biogas production. A pretreatment process can enhance the bio-digestibility of the wastes for ethanol and biogas production and the accessibility of the enzymes to the materials, improving the yield of the bioreaction. From the process management point of view, this means that pretreatments are useful to accelerate the rate-limiting step of anaerobic digestion, since bacterial action proceeds more slowly in the hydrolysis stage than in either of the following acidogenic or methanation steps. During hydrolysis, complex insoluble organic polymers, such as carbohydrates, cellulose, proteins and fats, are broken down and liquefied by the extracellular enzymes produced by hydrolytic bacteria. This makes them more easily available for use by acidogenic bacteria.

## 6.2 Lignocelluloses in Organic Waste Materials

The main structural component of organic waste is cellulose, a biopolymer that consists of thousands of glucose units. Due to the compositional variability of OW, different types of cellulose are present, each of which has its own degree of biodegradability. The cellulose units are linked by  $\beta$ -1, 4-glucoside bonds, and the

resulting biopolymers are connected by means of hydrogen bonds of different strengths, which generate different types of cellulose. For this reason, cellulose exhibits different structural features, such as crystalline and amorphous parts. In addition, hemicellulose, a xylose-based biopolymer, offers structural support to these organic materials. Lignin can be found in the woody tissue of plants and provides structural support to the cell wall, as well as impermeability and resistance against oxidative stress and attacks by microorganisms [5]. The structure of hemicellulose looks like that of cellulose and it is easily hydrolysable. Conversely, lignin, although it is derived from the oxidation of cellulose, is an insoluble polymer difficult to degrade because it is composed of a longer chain of complex carbohydrates of high molecular weight than other plant structures. For this reason, in a bioprocess, lignin should be separated from the remaining components by means of an appropriate pretreatment in order to facilitate the transformation of the other structures. Lignocellulosic materials have varying proportions of these three components, usually 40–60 % cellulose, 20–40 % hemicellulose and 10–25 % lignin (see Table 6.2), while the salts are generally less than 10 % of the dry weight of the biomass.

Cellulose has already been described as the most abundant source of food, fuel, and chemicals and its usefulness is due to its ability to be hydrolyzed to glucose. The degradation of cellulose to glucose, also referred to as saccharification, can be accomplished by a chemical reaction (hydrolysis) that involves the addition of a water molecule. Two main methods, enzyme hydrolysis and acid hydrolysis, can affect the degradation of cellulose. Many fungi and bacteria secrete a multicomponent enzyme system called cellulase that has the ability to saccharify cellulose.

**Table 6.2** Contents of cellulose, hemicellulose and lignin in common organic waste

Lignocellulosic materials	Cellulose (%)	Hemicellulose (%)	Lignin (%)
Hardwood stems	40–55	24–40	18–25
Softwood stems	45–50	25–35	35–35
Nut shells	25–30	25–30	30–40
Corn cobs	45	35	15
Grasses	25–40	35–40	10–30
Paper	85–99	0	0–15
Wheat straw	30	50	15
Sorted refuse	60	20	20
Leaves	15–20	80–85	0
Cotton seed hairs	80–95	5–20	0
Newspaper	40–55	25–40	18–30
Waste paper from chemical pulps	60–70	10–20	5–10
Primary wastewater solids	5–15	n.a.	24–29
Swine waste	6.0	28	n.a.
Solid cattle manure	1.6–4.7	1.4–3.3	2.7–5.7
Coastal Bermuda grass	25	35.7	6.4
Switch grass	45	31.4	12.0

*n.a.* not available

Cellulase is composed a pool of four enzymes [5], such as *endoglucanase*, *cel-lulodextrinases*, *cellubiohydrolases*, and  $\beta$ -*glycosidase*, which act, through a series of reactions, by attacking the accessible cellulose sites till the simplest sugar, glucose, is produced.

The purpose of a pretreatment is to change the intrinsic properties of cellulose in order to prepare the materials for enzymatic degradation, a process which converts the carbohydrate polymers into fermentable sugars. The goal is to break the lignin seal and to disrupt the crystalline structure of cellulose. The best method and operative pretreatment conditions depend to a great extent on the type of lignocel-lulosic material. The crystallinity of cellulose, its accessible surface area, the degree of cellulose polymerization and the degree of acetylation of hemicelluloses are recognized to be the main factors that are able to affect the rate of biological deg-radation of lignocelluloses by enzymes. These factors are discussed briefly below. Native cellulose takes on an enzyme-resistant crystalline structure. Fan et al. [6] estimated that the crystalline portion is 50–90 % of the total cellulose, with the remainder being amorphous. It has been shown that cellulase hydrolyzes the accessible portion of amorphous cellulose more easily, while the enzyme is not effective in degrading the less accessible crystalline form. It is therefore widely accepted that reducing the crystallinity increases the digestibility of lignocelluloses. On the other hand, there are some studies [7] that have shown an increased digestibility of most crystalline lignocellulose types. This contrast may appear if the effects of other factors are ignored, for example the role of the pore size, which affects the surface available for the enzyme attack. Fan et al. [6], studying the effect of ball milling, observed an increase in crystallinity with a reduced size of cellulose due to milling. It is believed that re-crystallization during water swelling may increase the crystallinity of highly ball-milled cellulose and consequently the crys-tallinity might increase the available surface area, probably due to the decrease in pore size. Crystallinity is an important factor for biodegradation of lignocelluloses. However, it is not the only factor that affects enzymatic hydrolysis, because of the heterogeneous nature of celluloses and the contribution of other components, such as lignin. Another important aspect is the accessible surface area. The enzymatic hydrolysis of cellulose is a heterogeneous catalytic reaction, in a chemical reaction sense, and direct contact of cellulolytic enzyme molecules and cellulose is a pre-requisite for the reaction. It consists of the adsorption of enzymes from the liquid phases on the surface, the biodegradation of cellulose to simple sugars (mainly cellobiose and oligomers) and desorption of enzymes to the liquid phase. The pore volume of the material determines the contact surface between the cellulose and the enzymes. An increase in the former increases the mass transfer rate, which in turns increases the enzymatic reaction, as several studies have shown [8].

Lignocellulosic materials have two different types of surface area: external and internal. The former is related to the size and shape of the particles, while the latter depends on the pore structure of the cellulosic fibres. Dry cellulosic fibres are small, about 15–40  $\mu\text{m}$ , and they therefore have a considerable external specific surface area, e.g. 0.6–1.6  $\text{m}^2/\text{g}$ . The internal surface area of dried cellulosic fibres is smaller than the external one. This is due to the hydrogen bond and electrostatic interaction

that stabilizes the structures, which tend to reduce the available surface. One operation able to increase the available internal surface consists of lowering the strength of the interactions, by swelling the lignocellulose material with water and/or polar solvents in order to create a larger internal surface area. Drying the fibres could instead produce an irreversible collapse with a reduction in the accessible surface area due to the shrinking of the capillary pores.

In addition, the presence of lignin hemicelluloses and their relative abundance are other important parameters which can affect the pretreatment efficacy. Lignin is the most recognized factor in the recalcitrance of lignocellulosic materials to enzymatic degradation, since cellulose and hemicellulose are cemented together by lignin and this limits the enzyme accessibility (Fig. 6.1).

Several researchers [9] have reported a positive correlation between digestibility/fermentability and the extent of delignification. A correlation level of 40–50 % of delignification is able to increase the digestibility to 90 %, even though some contrasting results have been reported in the literature. Nowadays, it is generally accepted that delignification processes can improve the rate and extent of enzymatic hydrolysis, even though it is difficult to quantify this effect. However, part of the hemicellulose is also hydrolyzed during delignification methods, and so the delignification does not show only one effect. In other cases, it is important to note that the dissolution of the lignin is also an inhibitor of cellulase activity, while less inhibitory effects have been reported concerning xylanase and glucosidase activities [9]. The type of lignin is also significant. It is well known that softwood is more recalcitrant than hardwood and this effect is probably related to the type of lignin, since softwood mainly has guaiacyl lignin while hardwood has a mix of guaiacyl and syringyl lignin. Similarly to lignin, hemicellulose constitutes a physical barrier that surrounds the cellulose fibres and protects them from enzymatic attack. Many pretreatment methods have been shown to be able to remove hemicelluloses, for example the use of dilute sulfuric acid to improve the enzymatic hydrolysis. However, most of these processes act by also removing a part of the lignin, and therefore the improvement is not only due to the removal of hemicellulose.

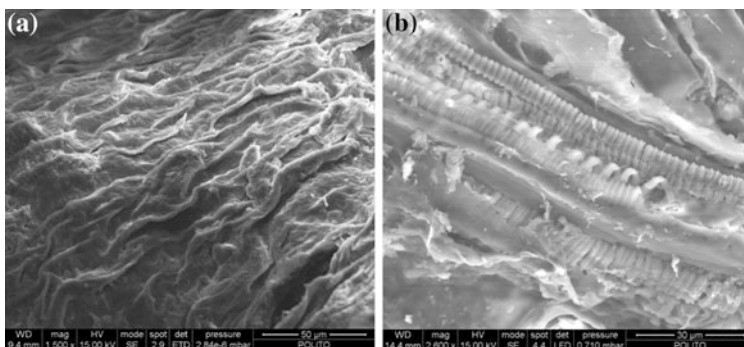


**Fig. 6.1** Scanning electron micrography: lignocellulose structure **a** before pretreatment and **b** after pretreatment

## 6.3 Biomass Pretreatments

Various pretreatment methods are candidates to favor hydrolysis, like milling, irradiation, microwave, steam explosion, ammonia fiber explosion (AFEX), supercritical CO<sub>2</sub> extraction and its explosion, alkaline hydrolysis, liquid hot-water pretreatment, organosolv processes, wet oxidation, ozonolysis, dilute and concentrated acid hydrolysis, and biological pretreatments [10]. The pretreatment can enhance the biodigestibility of the wastes for biogas and bioH<sub>2</sub> production, increasing the accessibility of the enzymes to the biowaste, but the choice of method depends greatly on the type of biowaste. For instance, lignin is the most recalcitrant component of the plant cell wall due to its high resistance to chemical and enzymatic attack [10], and it is a very complex molecule constructed of phenylpropane units linked in a three-dimensional structure which is particularly difficult to biodegrade. Technological factors such as energy demand should be carefully considered when selecting the pretreatment process according to the biomass, bearing in mind that some methods are efficacious for some biomasses but not for some others. A good criterion for feed selection in order to have profitable bioH<sub>2</sub> production is the right balance of the following points:

- biomass availability near the plant, to avoid excessive energy transport costs;
- easy biodegradability of biomass, in order to avoid high costs for the pretreatments;
- biomass from disposal problems is preferable to dedicated plantations;
- fruit and vegetable biomass refuse is preferable in order to overcome food–fuel conflict;
- complicated and high-energy-demand pretreatment methods that are rarely applied at full scales, like microwave, electron-beam and gamma-ray irradiation, vibro-energy milling and ozonolysis, should be avoided.

On the other hand, an effective and economical pretreatment should meet the following requirements:

- minimize the energy demand by reducing the cost of construction materials for pretreatment devices;
- avoid formation of possible inhibitors of hydrolytic enzymes and fermenting microorganisms.

Thus, after the above considerations, it is possible to conclude that in the OW feedstock material there is a large fraction of biomass of difficult digestibility, hence it is important to focus precisely on the effect of the pretreatment; only some pretreatments, among the interesting ones for full-scale application, will be considered here, but additional details can be found in [11]. It is important to remark that some of them are successfully applied to different waste streams originating from various agro-industries, agriculture and municipalities, but to date they remain in the infancy stage from a technological point of view.

Pretreatment methods are classified into *physical*, *physical–chemical*, *chemical* and *biological*; the following sections provide a brief description of each of them.



### 6.3.1 Physical and Physical–Chemical Pretreatments

Physical pretreatment normally involves a mechanical size reduction step which increases the accessible surface area to hydrolytic bacteria, and reduces the crystallinity and the degrees of polymerization of complex substrates prior to further pretreatments. Different types of physical processes such as *mechanical comminution* (e.g. ball milling, two-roll milling, compression milling and vibro-energy milling), *irradiation* (e.g. by gamma rays, electron beam, ultrasound and microwaves), *steam explosion* and *hydrothermolysis* can be used to improve the enzymatic hydrolysis and biodegradability of biowaste. These mechanical pretreatment techniques are time-consuming, energy-consuming and expensive for the process. Compression milling and steam explosion are apparently the only processes that have been tested at production scale. On the other hand, the irradiation techniques and hydrothermolysis have difficulties in industrial application and the processes' economy is still unclear [10, 11]. Therefore, in this context, we will exclude their description and will present only mechanical comminution and steam explosion pretreatments.

#### 6.3.1.1 Mechanical Comminution

Milling is a necessary first step in pretreatment in order to make the subsequent operations more efficacious. Among milling processes, the triturator, colloid mill, fibrillator, ball mill and dissolver are suitable for wet materials. A reduction in the size of organic waste is obtained through a mechanical pretreatment that increases the amount of soluble organic material. Shredding, pulping, crushing, or otherwise reducing the size of the waste gives bacteria access to a greater surface area. For example, a hydropulper produces two fractions, heavy and light, from incoming OW, but it also creates mixed organic slurry. The pretreatment technologies are different as far as the distribution of the chemical components in the waste between the fermentable fraction and rejected material is concerned, especially for dry matter such as ash, plastic or paper. When the source-separated organic waste is pressed through narrow slits, the screw presses the organic matter to form an organic fraction, while items such as plastic, paper, wooden substances, animal bones and metal are routed through the chamber into the reject fraction. Before treatment in the screw press, disk screen or extruder, the collected waste is treated with a “bag-opener”, which consists of large slowly rotating coils that cut open any bags and mix the waste. A pretreatment with a shredder (size reduction) and magnet separator to remove the metals requires a waste fraction without any impurities, for example plastic. This means that it is necessary to pretreat the MSW before the pretreatment process that is specifically dedicated to rupturing the lignocellulose structure. Waste materials can be comminuted by a combination of chipping, grinding and milling to reduce crystalline cellulose, and the size of the materials is usually 10–30 mm after

**Table 6.3** Energy requirement for mechanical comminution of agricultural lignocellulosic materials with different size reduction

Lignocellulosic materials	Final size (mm)	Energy consumption (kWh/tonne)	
		Knife mill	Hammer mill
Hardwood	1.60	130	130
	2.54	80	120
	3.2	50	115
	6.35	25	95
Straw	1.60	7.5	42
	2.54	6.4	29
Corn stover	1.60	NA	14
	3.20	20	9.6
	6.35	15	NA <sup>b</sup>
	9.5	3.2	NA <sup>b</sup>

chipping and 0.2–2 mm after milling or grinding [12]. The power requirement for mechanical comminution of agricultural materials depends on the final particle size and the waste biomass characteristics [5]. A comparison is shown in Table 6.3.

### 6.3.1.2 Steam Explosion

The steam explosion pretreatment method for lignocellulosic materials is conducted in the presence or absence of acid or basic chemicals in wet or dry conditions. In this method, a mechanically treated biomass is processed with high-pressure saturated steam for a certain time and then the pressure is swiftly reduced, which makes the materials undergo an explosive decompression. Steam explosion is usually conducted at a temperature of 160–260 °C, with a corresponding pressure of 0.69–4.83 MPa, for a period of time that ranges from several seconds to a few minutes, before the material is exposed to atmospheric pressure. The process causes hemicellulose degradation and lignin transformation due to the high temperature, and thus increases the potential of cellulose hydrolysis. Ninety percent efficiency of enzymatic hydrolysis has been achieved in 24 h for poplar chips pretreated by means of steam explosion, compared to only 15 % hydrolysis of untreated chips [13]. The residence time, temperature, size and moisture content affect steam explosion efficiency. The size determines the contact area between the steam and the material of the enhancing mass transfer phenomena, while the moisture affects so-called auto-hydrolysis. The latter phenomenon is of particular importance in processes conducted without acid or base addition, in which the hydrolysis is catalyzed by acids liberated from functional groups such as acetyl. Optimal conditions are defined as those in which the best substrate for hydrolysis is produced with the minimum amount of material being lost due to side reactions, such as

dehydration, and in which adequate carbohydrate linkages are disrupted by releasing most of the hemicelluloses into solution while leaving the cellulose fraction intact. Steam explosion is one of a very limited number of pretreatment techniques that have been made available through pilot-scale demonstrations [12], and commercial equipment is currently available, even though its use for OW of MSW is limited. The temperature and the duration determine the chemical changes in the three main constituents of lignocellulosic materials. The hemicelluloses are hydrolyzed to soluble sugars by the organic acids, mainly acetic acid derived from the acetylated hemicelluloses in straw. The pH during steam explosion is kept low (3–4) to degrade a higher quantity of hemicelluloses. However, under more drastic conditions involving higher temperatures or longer exposure times, the solubilized hemicelluloses undergo a series of secondary reactions and form furfural and hydroxymethyl furfural. The addition of  $\text{H}_2\text{SO}_4$  (or  $\text{SO}_2$ ) or  $\text{CO}_2$  can effectively improve enzymatic hydrolysis, decrease the production of inhibitory compounds and lead to a more complete removal of hemicelluloses. One of the advantages of steam explosion pretreatment is the low amount of energy that is required compared to mechanical comminution. Conventional mechanical methods require 70 % more energy than steam explosion to achieve the same size reduction. Steam explosion is recognized as one of the most cost-effective pretreatment processes for hardwood and agricultural residues, but it is less effective for softwood [14]. The limitations of steam explosion include destruction of a portion of the xylan fraction, incomplete disruption of the lignin–carbohydrate matrix and generation of compounds that may be inhibitory to the microorganisms used in downstream processes. Because of the formation of degradation products that are inhibitory to microbial growth, a pretreated biomass needs to be washed with water to remove the inhibitory materials along with water-soluble hemicellulose. A water wash decreases the overall saccharification yields, due to the removal of soluble sugars, such as those generated by hydrolysis of hemicelluloses. Usually, 20–25 % of the initial dry matter is removed by a water wash. Steam explosion and thermal pretreatments are being widely investigated for improving biogas production from different dedicated materials such as forest residuals and wastes such as cattle manure or municipal solid wastes [15]. However, there are several investigations combining thermal pretreatment with addition of bases such as NaOH, which usually gives a better result than individual thermal or chemical ones [16].

### ***6.3.2 Chemical Pretreatment***

Chemical pretreatment techniques have received by far the most attention among all categories of pretreatment methods. Typical examples include dilute acid, alkali, solvent, ammonia,  $\text{SO}_2$ ,  $\text{CO}_2$ , other chemicals (e.g.  $\text{H}_2\text{O}_2 + \text{Mn}^{2+}$ , ozone, EDTA,  $\text{KMnO}_4$ , urea and dioxane) and pH-controlled hydrothermolysis. Of these pretreatments, the alkaline and acid ones have been successfully tested on a pilot scale.

On the other hand, the use of organic solvents (the *organosolv* process) is expensive and their use is complex, requiring high-pressure equipment; ammonia pretreatment [e.g. ammonia fiber/freeze explosion (AFEX) and supercritical ammonia pretreatment] have not been tested on a pilot scale; SO<sub>2</sub> steam explosion seems appealing because it can effectively render softwoods digestible but SO<sub>2</sub> is highly toxic and may pose safety and health challenges [11]; explosion pretreatment in the presence of CO<sub>2</sub>, with or without steaming, seems an effective technique [17] although it has not been tested on a pilot scale; other chemicals tested as pretreatment agents are generally ineffective or too expensive and only bench-scale tests have been reported; pH-controlled hydrothermolysis can enhance enzyme digestibility by controlling the pH during pretreatment but has not been fully investigated for process characteristics and process economy [11].

After this short overview, acid and alkaline pretreatments will be considered, since they are the most inexpensive and effective techniques.

### 6.3.2.1 Acid Pretreatment

Concentrated acids, such as H<sub>2</sub>SO<sub>4</sub> and HCl, have been used to treat lignocellulosic materials. Although they are powerful agents for cellulose hydrolysis, concentrated acids are not extensively used due to problems of toxicity and hazard. Acid treatment can operate either under high temperature and low acid concentration (dilute acid treatment) or under low temperature and high acid concentration (concentrated acid treatment) [10]. The lower operating temperature in concentrated acid pretreatment (e.g. 40 °C) is a clear advantage compared to dilute acid processes from an energy point of view. However, high acid concentrations (e.g. 30–70 %) in the concentrated acid process makes it extremely corrosive and dangerous. Therefore, this process requires either specialized non-metallic constructions or expensive alloys. Pretreatments with acids such as acetic, nitric and sulfuric have also been used to remove lignin and cellulose from waste newsprint [18] and active sludge for biogas production. Of all the acid-based pretreatment techniques, sulfuric acid has been the most extensively studied, apparently because it is inexpensive and effective. The potential difficulties of the need for corrosion-resistant construction materials for reactors and gypsum generation, however, plague sulfuric acid's prospects as a long-term pretreatment chemical [11]. Direct saccharification results in low yields at moderate temperatures of around 40 °C with high acid concentration, because of sugar decomposition. High temperatures in dilute acid treatments favor cellulose hydrolysis. A neutralization of pH is necessary for downstream enzymatic hydrolysis or fermentation processes. Most of the arabinan, galactan and xylan in the biomass is hydrolyzed during the acid pretreatment. The cellulose remaining in the pretreated feedstock is highly digestible by cellulases from *Trichoderma reesei* [19]. This pretreatment produced a significant increase in the bioavailability of cellulose to hydrolysis enzymes. A wide range of feedstock materials, including agricultural residues and wastepaper, has been treated with acid.

### 6.3.2.2 Alkaline Pretreatment

Alkaline pretreatment involves the use of alkaline solutions such as sodium hydroxide (NaOH), lime  $[\text{Ca}(\text{OH})_2]$  or ammonia to remove lignin and a part of the hemicellulose structures to efficiently increase the accessibility of enzymes to cellulose [12]. The effect of an alkaline pretreatment depends on the lignin content of the materials, which would seem to suggest that bases mainly remove lignin. The mechanism of alkaline hydrolysis is the saponification of intermolecular ester bonds cross-linking xylan hemicelluloses and other components, for example lignin and other hemicelluloses. The mechanism of action seems to be due to the increase in porosity of the lignocellulosic materials as a consequence of the saponification reactions. Dilute NaOH treatment of lignocellulosic materials causes swelling and provokes different effects: an increase in the internal surface area, a decrease in the degree of polymerization, a decrease in crystallinity, separation of the structural links between the lignin and the carbohydrates, and disruption of the lignin structure [20]. Pretreatments can be performed at low temperatures but with a relatively long time and a high concentration of the base until pH 12 is reached. Alkaline pretreatment was shown to be more effective on agricultural residues than on wood materials. The digestibility of NaOH-treated hardwood increased from 14 to 55 % with a decrease in the lignin content from 20 to 55 %. In contrast, no effect of dilute NaOH pretreatment was observed for softwood with a lignin content greater than 26 %. The highest yield was obtained under the most severe conditions (alkaline peroxide, 120 °C and 120 min). Furthermore, bases such as  $\text{Ca}(\text{OH})_2$  could be a good solution when high loads of, e.g., lipids and phenolic compounds are subjected to anaerobic digestion [11]. Olive mill effluent is an example of seasonal waste with low pH (about 4.3) and high concentrations of lipids (about 13 g/L) and phenolic compounds (about 8 g/L). Addition of lime and bentonite greatly improves the digestion of olive mill effluents, with more than 91 % removal of COD [21]. Pretreatment with NaOH at a ratio of 5 g of base/kg of MSW increased biogas production under anaerobic fermentation by 35 % compared with untreated MSW [22].

### 6.3.3 Biological Pretreatment

This category comprises pretreatment techniques of applying lignin-solubilizing microorganisms to render lignocellulosic materials amenable to enzyme digestion [11].

In biological pretreatment processes, microorganisms such as brown, white and soft-rot fungi are used to degrade lignin and hemicellulose in waste materials. Brown rot fungi mainly attack cellulose, while white and soft rot fungi attack both cellulose and lignin. White rot fungi are the most effective basidiomycetes for biological pretreatment of lignocellulosic materials [20]. The advantages of biological pretreatment include low energy input, no chemical requirement and mild environmental conditions. However, the rate of hydrolysis in most biological

pretreatment processes is very low; therefore, biological pretreatments face major techno-economic challenges. Thus far, only bench-scale studies are known to have been conducted.

## 6.4 Biomass Feedstock for bioH<sub>2</sub> Production: An Overview

Food waste is the major component in MSW, and it accounts for the majority of the research on bioH<sub>2</sub> production [23]. It is composed of raw and cooked food discarded before or during food preparation; it includes high volatile solids, moisture content and salinity, and thus it is the main source of odor, decay, vermin attraction, groundwater contamination and greenhouse gas emission. Food waste has therefore gained interest as a potential feedstock for bioenergy. In the literature, the food wastes employed for bioH<sub>2</sub> studies are obtained mainly from dining-hall or restaurant waste. Food processing wastes such as tomato residue, cheese whey, rice slurry and apple pomace have also been tested for bioH<sub>2</sub> production [23]. In addition, solid wastes such as wheat, starch, the organic fraction of MSW containing fruit and vegetable waste, jackfruit peel etc. can be considered for hydrogen production [24].

BioH<sub>2</sub> production from food waste containing carbohydrates, fats, cellulose and hemicelluloses involves different metabolic pathways, which have not yet been studied in detail [25]. In general, bioH<sub>2</sub> production results from carbohydrate degradation through the acidogenesis and acetogenesis routes and is highly sensitive to certain environmental conditions such as pH, volatile fatty acids, temperature, hydrogen partial pressure, inoculum sources and food waste concentration, as reported in Chap. 2. With increasing energy demand worldwide, utilizing renewable resources such as food wastes and food processing wastes for bioH<sub>2</sub> production can be a novel and promising approach to substituting fossil fuels while at the same time solving disposal problems. A variety of alternative organic biowastes have been effectively used for H<sub>2</sub> production by anaerobic digestion, as listed in Table 6.4.

In particular, Table 6.5 shows literature data on values of H<sub>2</sub> productivity from different biowaste by AD processes, using mixed microbial cultures.

However, in the literature, the different pretreatment methods have shown different degrees of success, and in many cases the best pretreatment in one study is the worst in another one. This discrepancy could be due to the different uses of the substrate and/or the different types of inoculum. To overcome the above difficulties, we suggest scoring the pretreatment methods using two energy parameters, efficiency and efficacy, introduced previously. In the following Sect. 6.5 the results of a study aimed at establishing the proper pretreatment for each type of substrate present in the OW are reported. Different refuses were tested with low, medium or high concentrations of lignocellulosic material to obtain a representative picture of the entire palette of OW. The pretreatment option was evaluated on some food

**Table 6.4** Examples of feasible biomass for bioH<sub>2</sub> production

Manufacturing wastes	Food waste	Agro-waste	Other organic waste
Paper sludge	Cafeteria waste	Molasses	Waster activates sludge
Bean curd	Sugar beet juice	Sugary wastewater	Sewage sludge
Cheese whey	Mixed food waste from Restaurant	Vegetable mixed waste	Municipal wastewater
Rice slurry	Fruit juice	Starch wastewater	Municipal solid waste
Apple processing	Citrus peelings	Rice straw	Liquid swine manure
Palm and olive oil mill effluent		Sugar cane bagasse	
Olive mill		Fruit mixed waste	
Rice winery			
Beer lees			

**Table 6.5** Yield of bioH<sub>2</sub> production from biowaste by mixed microorganisms

Biowaste	Mode of operation	Mineral or vitamin supplements	pH/Temp	Yield	References
Apple processing wastewater	Batch	With	6.0	0.9 L H <sub>2</sub> /L <sub>medium</sub>	[26]
				(0.1 L H <sub>2</sub> /g <sub>COD</sub> )	
Food waste	Continuous	Without	6.5/35 °C	0.39 L H <sub>2</sub> /g <sub>COD</sub>	[27]
Molasses	Continuous	Without	7.0/35 °C	5.57 m <sup>3</sup> H <sub>2</sub> /m <sup>3</sup> <sub>reactor</sub> /day	[28]
Rice slurry	Batch	With	4.5/37 °C	0.35 L H <sub>2</sub> /g <sub>carbohydrate</sub>	[29]
Glycerol	Batch	With	6.5/35 °C	0.025 L H <sub>2</sub> /g <sub>COD</sub>	[30]
Beer lees	Batch	With	35 °C	0.053 L H <sub>2</sub> /g <sub>dry beer lees</sub>	[31]
Cheese whey	Continuous (UASB)	Without	5.0/30 °C	0.05 L H <sub>2</sub> /g <sub>SSV</sub> /day	[32]
Kitchen waste	Continuous (Inclined plug flow reactor)	Without	5.5	0.07 L H <sub>2</sub> /g <sub>SSV</sub>	[33]
Liquid swine manure	Feed–batch (anaerobic sequencing batch reactor)	With	5.0/37 °C	1.4 mol H <sub>2</sub> /mol glucose	[34]
Palm oil mill effluent	Continuous (HRT = 5 d)	Without	5.0	0.42 L H <sub>2</sub> /g <sub>COD</sub>	[35]
Fruit and vegetable waste	Batch	Without	5–6/35 °C	3.0 L H <sub>2</sub> /L <sub>medium</sub>	[36]

industrial wastes, using the AD process for bioH<sub>2</sub> production as a probe test to compare the efficiency of different pretreatment options. This analysis aims to provide additional knowledge on the mechanisms of action and to provide useful

information at an industrial scale. Three types of refuse were selected: sweet product residue (SPR), organic waste market (OWM), and coffee seed skin (CSS) waste. The SPR, OWM and CSS refuses contain various levels of lignocellulosic material (low, medium and high, respectively) and different amounts of sugar (high, medium and low, respectively). These residues were chosen to understand the feasibility of using refuse from the entire food chain as raw material for hydrogen production. The types of waste from the food industry tested were: SPR, i.e. confectionary residues removed from the market after the expiration date and manually separated from packaging; SPR<sub>ex</sub>, similar to SPR but the packaging was separated by extrusion at 200 atm; OWM residue taken from a local fruit and vegetable market; and CSS residue of a firm producing coffee. Table 6.6 shows the composition of the different types of refuse. The composition of SPR and OWM was defined using the information reported on the packaging and in the INRAN database [37]. The composition of the CCS refuse, which is also reported in Table 6.6, was provided by an independent laboratory.

## 6.5 Experimental Tests from Renewable Agro-Waste

The following sections present experimental tests aiming to produce hydrogen from different OW with different degree of lignocellulose material pretreated by different methods. After preliminary tests conducted in flasks to understand the best pretreatment to hydrolyze the biomass, we performed a test using an anaerobic stirred reactor, controlling physical parameters such as temperature and pH, in order to confirm the efficiency of H<sub>2</sub> production.

### 6.5.1 Investigation on Pretreatments and H<sub>2</sub> Production

#### 6.5.1.1 Pretreatments of Feedstock

Different pretreatment processes were tested: chemical (acid or basic), thermal (high temperatures for different times), ultrasonic, and a combination of the aforementioned treatments: acid/thermal and basic/thermal. All three refuses were initially mechanically treated with a kitchen blade mixer, which was used to liquidize the material to simulate an industrial milling treatment. A combination of different pretreatments may be optimal to increase the bioreaction yield in many situations. All the pretreatments used are briefly described below and the abbreviations are summarized in Table 6.7. Owing to the large variation in the composition of OWM over time, for this waste, several pretreatment options were tested to identify which one was the most adequate.



Table 6.6 Composition of the residues used

SPR	Parameters	Proteins	Carbohydrates	Sugars	Fat	Saturated fat	Dietary fiber	Sodium
	(g/mL)	0.04	0.29	0.11	0.12	0.06	0.01	$3 \times 10^{-4}$
	(% w/w)	5.99 %	46.08 %	17.52 %	20.08 %	8.94 %	1.34 %	0.05 %
OWM	Constituents	g	% (w/w)	Water	Soluble sugars	Starch	Proteins	Lipids
	Tomato	186	6.7	174.84	6.51	0.00	1.86	0.37
	Apple	268	9.7	228.34	26.80	0.00	0.54	0.00
	Orange	280	10.2	244.16	21.84	0.00	1.96	0.56
	Eggplant	215	7.8	199.31	5.59	0.00	2.37	0.86
	Lettuce	158	5.7	148.99	3.48	0.00	2.84	0.63
	Lemon	150	5.4	134.25	3.45	0.00	0.90	0.00
	Pepper	148	5.4	136.60	6.22	0.00	1.33	0.44
	Cabbage	161	5.8	148.44	4.03	0.00	3.38	0.16
	Celery	137	5.0	120.97	3.01	0.27	3.15	0.27
	Strawberry	156	5.7	141.18	8.27	0.00	1.40	0.62
	Grape	130	4.7	104.39	20.28	0.00	0.65	0.13
	Cucumber	156	5.7	150.54	2.81	0.00	1.09	0.78
	Fennel	180	6.5	167.76	1.80	0.00	2.16	0.00
	Pumpkin	167	6.1	157.98	5.85	1.50	1.84	0.17
	Kiwi	205	7.4	173.43	18.45	0.00	2.46	1.23
	Green bean	60	2.2	54.30	1.44	0.00	1.26	0.06
	Composition of OWM	2757	100.0	2485.48	139.83	1.77	29.19	6.28
				90.15 %	5.07 %	0.06 %	1.06 %	0.23 %
CSS	Hemicellulose	Cellulose	Lignin	Humidity	Ethanol-soluble substances	Ethanol-soluble substances	Water-soluble substances	
	(% w/w)	(% w/w)	(% w/w)	(% w/w)	(% w/w)	(% w/w)	(% w/w)	
	11.20	31.30	37.30	5.31	5.80		14.07	

**Table 6.7** Pretreatments tested, energy produced as H<sub>2</sub> and evaluation of efficiency ( $\eta$ ) and efficacy ( $\xi$ )

	Biowaste	Nomenclature	Embedded energy (kJ/L)	Produced energy (kJ/L)	$\eta$	$\xi$
SPR	No pretreatment	NP	5320.77	0.99	0.0186	1.0
	Acid pretreatment	AP	5320.77	0.35	0.0066	0.4
	Basic pretreatment	BP	5320.77	6.28	0.1181	6.4
	Thermal acid pretreatment	TAP	5320.77	0.02	0.0005	0.0
	Thermal basic pretreatment	TBP	5320.77	1.39	0.0261	1.4
SPR <sub>ex</sub>	No pretreatment	NP	1503.70	2.13	0.1408	1.0
	Basic pretreatment	BP	1503.70	24.10	1.6023	11.4
	Thermal basic pretreatment	TBP	1503.70	35.93	2.3897	17.0
OWM	No pretreatment	NP	755.08	2.53	0.3344	1.0
	Acid pretreatment	AP	755.08	17.00	2.2499	6.7
	Basic pretreatment	BP	755.08	4.39	0.5814	1.7
	Thermal pretreatment (10 min)	TP <sub>10min</sub>	755.08	10.53	1.3941	4.2
	Thermal pretreatment (90 min)	TP <sub>90min</sub>	755.08	10.97	1.4530	4.3
	Thermal acid pretreatment (15 min)	TAP <sub>15min</sub>	755.08	23.42	3.1008	9.3
	Thermal basic pretreatment (5 min)	TBP <sub>5min</sub>	755.08	18.22	2.4134	7.2
	Thermal basic pretreatment (15 min)	TBP <sub>15min</sub>	755.08	16.08	2.1291	6.4
	Thermal basic pretreatment (30 min)	TBP <sub>30min</sub>	755.08	25.08	3.3224	9.9
CSS	No pretreatment	NP	755.08	2.27	0.0891	1.0
	Thermal basic pretreatment <sup>a</sup>	TBP <sub>a</sub>	2553.13	11.23	0.4399	5.0
	Thermal basic pretreatment <sup>b</sup>	TBP <sub>b</sub>	2553.13	10.93	0.4286	4.8
	Ultrasonic pretreatment	UP	2553.13	11.83	0.4640	5.2

<sup>a</sup> Thermal basic pretreatment at 30 °C<sup>b</sup> Thermal basic pretreatment at 90 °C

*Acid pretreatment (AP)*: AP was carried out in a thermostatic chamber at 30 °C. The feedstock was treated for 24 h at pH 3, obtained with the addition of 2 N HCl. This pretreatment, which is also referred to as dilute acid hydrolysis, is one of the most commonly used methods. *Basic pretreatment (BP)*: BP was carried out in a thermostatic chamber at 30 °C at pH 12 for 24 h using 2 N NaOH. The effect of

basic pretreatment appears to suggest that the base mainly removes lignin. *Thermal pretreatment (TP)*: TP was carried out in a 20 L bench reactor equipped with a controlled mixer and a heating jacket at 90 °C and 2 atm for different time periods ranging from 5 to 90 min; approximately 60 min were necessary to reach the working temperature. Hemicellulose, heated to 150 °C, would already be partially solubilized into constituents, i.e. xylan and glucomannan, the former being less stable, depending on the nature of the substrate. During a thermal process, part of the hemicellulose is hydrolyzed into acids, which are produced together with other chemicals that are able to enhance the hydrolysis of hemicelluloses. *Thermal acid pretreatment (TAP)*: this pretreatment was carried out in the bench reactor at pH 3 with the addition of 2 N HCl to the broth at 90 °C and 2 atm for 30 min for SPR and 15 min for OWM. The purpose of combining the two processes was to increase the efficiency of the hydrolysis of the lignocellulosic components and to catalyze the solubilization of the hydrolysis products to prevent any inhibition phenomenon. *Thermal basic pretreatment (TBP)*: TBP was conducted under different conditions for each type of refuse. The pretreatment was carried out at pH 12 for SPR and SPRex, using 2 N NaOH at 90 °C and 2 atm for 30 min. The OWM pretreatment was carried out under the same conditions as SPR, but for different lengths of time: 5, 15 and 30 min. Two different conditions were considered for CSS. The first condition was at pH 12 with 2 N NaOH under gentle heating from 20 to 96 °C at atmospheric pressure. When the temperature reached this value, the heating was stopped, and the broth was left to return to 20 °C; the process lasted approximately 180 min. The second condition for the TBP was pH 12, 90 °C and 2 atm, with the temperature maintained at this value for 30 min. As for the TAP, the aim was to increase the amount of low-molecular-weight compounds and to improve their solubilization. *Ultrasonic pretreatment (UP)*: UP was carried out in an ultrasonic machine (Ultrasonic Cleaner model CP823) at 30 °C and atmospheric pressure with a power of 1.8 kW for 20 min. In this case, the aim was to verify the capacity of this innovative pretreatment to break down large molecules and to convert them into smaller ones, which are more easily digested by microorganisms.

### 6.5.1.2 Experimental Tests of H<sub>2</sub> Production

The anaerobic microflora used in these tests were obtained following the procedure reported in Chap. 2, in order to have as much as possible the same quality of inoculum using bovine manure. Tests were carried out in triplicate using 500 mL Erlenmeyer flasks continuously agitated on a shaker at 200 rpm for the entire duration of the test. The mixing rate was selected for two reasons: primarily to favor the evolution of dissolved H<sub>2</sub> in the broth and to prevent inhibition of the bioreaction and secondly to increase the shear-stress on HCB to decrease their vital activity. The working volume of each test was approximately 333 mL, comprising 300 mL of broth and 33 mL of inoculum. The initial pH of the broth was in the range 7–7.5 and was adjusted by 2 N NaOH. The flasks were initially flushed with nitrogen gas for 5 min to obtain anaerobic conditions. The treated sludge was used as inoculum in a

ratio of 10 % v/v. All the experiments were conducted at  $30 \pm 1$  °C in a thermostatic chamber without control. Gas composition was evaluated at the end of each test as average composition. The measures were performed by a gas chromatograph (Varian CP, 4900) equipped with a thermal conductivity detector (TCD) and two columns of 10 m, and argon gas was used as a carrier. The gas evolution during the fermentation tests was monitored by using the water-replacement method.

### 6.5.1.3 Energy Conversion Parameter

In order to score and select the most appropriate pretreatment, the two energy parameters already introduced in Chap. 5 were used. The following expression was applied to evaluate the energy contained in the feedstock ( $E_{OW}$ ):

$$E_{OW} = LHV_{OW} \cdot TSS_{OW} \quad (6.1)$$

where  $LHV_{OW}$  is the Lower Heating Value of the OW (kJ/kg) and  $TSS_{OW}$  is the concentration of the substrate evaluated as total suspended solids of the OW in the fermenting broth used (g/L). The initial energy contained in the SPR, SPRex, OWM and CSS was also calculated by applying Eq. 6.1.  $LHV_{SPR} = 19,591 \pm 50$ ,  $LHV_{SPRex} = 18,473 \pm 70$ ,  $LHV_{OWM} = 17,721 \pm 65$ , and  $LHV_{CSS} = 17,730 \pm 40$  in kJ/kg were measured by means of a bomb calorimeter.

The second parameter used was *efficacy* ( $\zeta$ ), differently than done in Chap. 5, it takes into account the efficiency of the actual test with pretreatment compared with that obtained without pretreatment.  $\zeta$  was calculated as follows:

$$\zeta = \eta_P / \eta_{NP} \quad (6.2)$$

where  $\eta_P$  is the efficiency obtained from the pretreated broth and  $\eta_{NP}$  is the efficiency obtained from the broth without any pretreatment. This parameter permits easily evaluation of the effectiveness of the applied pretreatment: if  $\zeta$  is less than 1, the pretreatment has lowered the efficiency and has likely produced some inhibitory substances, whereas if  $\zeta$  is approximately 1, the pretreatment has no effect on the bioreaction, and, lastly, if  $\zeta$  is greater than 1, the pretreatment is able to increase the energy produced as hydrogen compared with the untreated substrate. Therefore, the higher the efficacy value, the greater the effects of the pretreatment on increasing the energy produced in the form of hydrogen, and thus the efficacy is a means of scoring the pretreatment processes.

### 6.5.1.4 Results and Discussion

Figure 6.2 shows, as an example, the biogas evolution for SPRex, i.e. the OW after extrusion; the biogas starts to produce after 1 day, indicating that a physical pretreatment such as extrusion was useful to remove the packaging and to favor

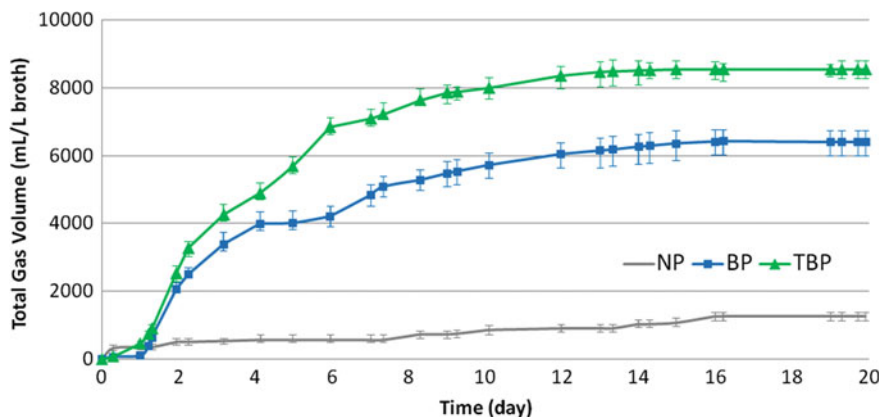


**Fig. 6.2** Cumulative gas production ( $H_2 + CO_2$ ) from SPRex with different chemical treatments: none (NP), alkaline (BP) and thermal alkaline (TBP)

hydrolysis. In Table 6.7 the results for all the tests are given (additional results are present in [38]) together with the value of the efficiency and the efficacy.

The shape of the saturation curves with SPRex of biogas production are similar for all the tests. Referring to Table 6.7 of energy produced, in the case of SPR it was noted that AP generates larger amounts of biogas than all the other pretreatments that show values below the NP test. This result is in agreement with the results of [39], which demonstrated that an acid pretreatment significantly increased the bioavailability of cellulose to enzymatic hydrolysis for fresh and processed vegetable refuses from agro-food industry wastes used as feedstock. However, to determine the effectiveness of the pretreatments, it is necessary to evaluate the energy produced through an estimate of the percentage of hydrogen in the biogas and not only the quantity of biogas produced. As a result, BP produces a greater percentage of hydrogen, 32.15 %, which is quite high compared with the values obtained with other pretreatments. In contrast, the results achieved with SPRex show that the pretreatments were able to significantly increase the amount of biogas produced from 1,000 mL of biogas per liter of broth to 8,000 mL/L of broth, with a hydrogen percentage of approximately 40 % v/v (Fig. 6.2), higher than the yields obtained with non-extruded SPR. This result suggests that the extrusion process at 200 atm had a significant impact on the macromolecules, breaking and changing them into smaller molecules that were able to be digested by the microorganisms, and thus greatly increasing the energy efficiency of the system.

The results obtained with OWM refuse show that all the pretreatments induced higher levels of biogas production: from 3,000 to 5,000 mL of biogas was produced per liter of broth. The hydrogen percentages achieved in the biogas are quite different and range between 34 and 51 % for all the situations tested, which means that OWM is suitable for biohydrogen production through anaerobic digestion. If the results are examined in more detail, it is possible to observe that all the pretreatments were able to improve the efficiency and that the highest percentages of

hydrogen were obtained when a combined pretreatment (chemical–thermal) was adopted, with TBP<sub>30min</sub> offering the highest value of 51.6 % v/v of hydrogen in the biogas.

Lastly, as far as CSS is concerned, which is the waste with the highest content of lignocellulosic structures (Table 6.6), two types of pretreatment were used: thermal-basic with different conditions and an ultrasonic pretreatment. It can be seen in Table 6.7 that all the pretreatments considerably increased the production of energy compared with the non-pretreated broth. While higher quantities of gas were obtained for TBP<sup>a)</sup> and TBP<sup>b)</sup>, UP produced less biogas. Although the ultrasonic pretreatment produced the best results, those obtained with thermal-basic for both the type (a) and type (b) pretreatments, which yielded similar results to those obtained through UP, should not be disregarded. As far as the value of SPR efficacy is concerned, BP shows the best results; the efficacy increased more than six-fold ( $\zeta = 6.4$ ), whereas TBP gave an increase of only 1.4 ( $\zeta = 1.4$ ). In our opinion, the reason for this large decrease in efficacy is driven by the thermal aspect, which constitutes the essential difference between these two pretreatments. The high temperatures caused a type of caramelization of the free sugars, which are present in significant amounts in SPR (more than 17 %; Table 6.6), and this in turn led to a decrease in the available substrate for the microorganisms. Another explanation could be that sugars react to the presence of proteins (6 %; Table 6.6) or amino acids at elevated temperatures, according to the so-called Maillard reaction. This involves a reaction between the aldehyde group of the sugar and the amino group present in the protein, which causes the formation of polymers of higher molecular weight and with dark colors. It is noticeable that in the case of SPR (Table 6.7), AP decreases the efficacy ( $\zeta = 0.4$ ), and this is amplified by temperature ( $\zeta = 0$ ), most likely because the acid is able to liberate some substances that are toxic to the microorganisms. In the case of SPRex, the best efficiency and efficacy were obtained through TBP, with  $\eta = 2.4$  % and  $\zeta = 17.0$ . However, the results with BP were also quite high,  $\eta = 1.6$  % and  $\zeta = 11.4$ ; these results were the highest values obtained when all the tested wastes were compared, which means that physical pretreatment performed through extrusion provides excellent results thanks to its capacity to break down the larger molecules and to allow them to dissolve in water, increasing the possibility of being digested by microorganisms. This fact can be corroborated by comparing the results obtained from the broths without pretreatment (NP) of SPR and SPRex, which clearly shows that the efficiency of SPRex is more than 10 times that of SPR:  $\eta = 0.019$  and  $\eta = 0.14$ , respectively. Regarding the OWM, it can be seen in Table 6.7 that the most appropriate pretreatment for greater efficacy was TBP at 30 min, with  $\zeta = 9.9$ , which shows that the energy produced increases nearly 10-fold with reference to the efficiency obtained with NP. Obviously, in the case of TBP<sub>30min</sub>, which required more time, more energy was consumed. However, it is also worth noting that the basic pretreatment presents certain other advantages, e.g., during the operation of a plant, as is well known, hydrogen production is accomplished with a concurrent production of liquid metabolites composed of large amounts of VFA, which tend to reduce the pH of the system at the risk of stopping the reaction due to solventogenesis. For this reason, it is

necessary to control the pH and to add a base. The basic feed, in the case of continuous operation, therefore leads to savings in the quantity of the base necessary for pH control. Examining Table 6.7, it is possible to state that for refuses with an average content of lignocellulosic material, such as OWM refuse, the best pretreatment is TBP<sub>30min</sub>. Lastly, for the CSS refuses, once again the results suggest an energy sustainability analysis (Chap. 9) to assess the most energetically sustainable pretreatment between UP, TBP<sup>a)</sup> and TBP<sup>b)</sup>, which present very similar levels of efficacy. It is important to note that the chemical analysis of biogas in all the tests has shown that the biogas was free of methane, indicating a lack of methanogenic activities. This can be considered an indirect confirmation of the fact that after the acid treatment of anaerobic sewage sludge, the mixed consortium is free of methanogens. As a final consideration, it is important to remark that all the three types of refuse were able to produce hydrogen without the addition of micronutrient or protein supplements to keep the microorganisms alive and that the substrate has a significant influence on the overall hydrogen production.

### ***6.5.2 H<sub>2</sub> Production from Vegetable Wastes in a Laboratory-Scale Bioreactor***

The objective of this test with a laboratory-scale bioreactor was to verify the feasibility and reproducibility of the production of H<sub>2</sub>. Organic waste market (OWM) was used in the test because of its variation according to the seasons, and its great daily abundance; therefore a different vegetable waste, relative to those used in the previous section, was collected. According to the results obtained previously, alkaline pretreatment was used. A test with glucose was carried out as a comparison.

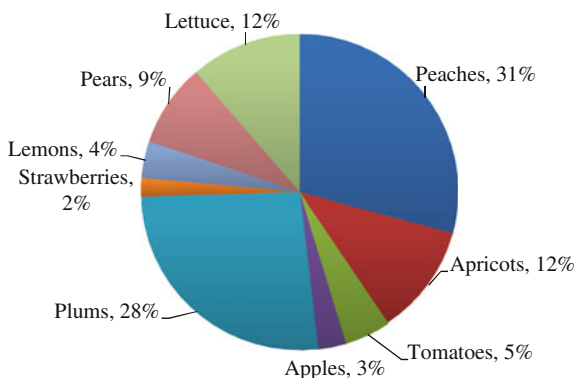
#### **6.5.2.1 Pretreatments of Substrate**

The anaerobic microflora used in this test were the same as that reported in the previous section. The OWM material used was taken from the local fruit and vegetable market. First of all, it was weighed and cut in small pieces, then the materials were finely chopped by a kitchen blade mixer; Fig. 6.3 shows the composition of the biowaste utilized. Initial pH and density were 4.0 and 0.9 g/mL, respectively. The chopped OWM was diluted with tap water (1:1), treated by adding 2 N NaOH to reach pH 12.5 and kept at this level for 24 h at 30 °C.

#### **6.5.2.2 Experimental Test of H<sub>2</sub> Production**

The pretreated 1.8 L of broth was inoculated in a ratio of 10 % v/v in a stirred-batch reactor STR (Minifors, Switzerland) as previously described in detail (Chap. 3); anaerobic conditions were obtained by sparging with nitrogen gas at the beginning

**Fig. 6.3** Composition (% w/w) of vegetable and fruit waste used in bioreactor test



of the fermentation. A different stirring power (300 rpm instead of 200) was necessary because of strong, apparently non-Newtonian behavior of the fermenting broth. The initial pH of the media was set to 7 and manually adjusted during fermentation, because of strong viscosity that did not permit good pH measurement. The experiment was conducted at 35 °C.

### 6.5.2.3 Analyses

Temperature, pH and redox potential were monitored online every minute using Iris NT Software (Infors AG, Switzerland). Liquid samples were taken out of the reactor at different times during the fermentation for the rough determination of sucrose by manual refractometry due to the impossibility of using the enzymatic test for glucose determination. The gas produced during the fermentation was constantly measured by a volumetric gas counter (Milligascounter, Ritter), and then collected in a Tedlar bag (SKC, 231-05 series) and analyzed with a gas chromatograph (Varian, CP 4900).

### 6.5.2.4 Results and Discussion

As a result of dark anaerobic fermentation over 1 L of vegetable waste diluted in tap water (1:1) produced approximately 10 L of gas containing hydrogen, whose proportion ranged on average from 18 to 42 % (v/v). Table 6.8 gives a comparison of results obtained with OWM and with glucose, both carried out in the same experimental conditions.

The H<sub>2</sub> content in the biogas was lower than that obtained using glucose; these results are in accordance with other studies [31, 34]. The two graphs (a and b) of Fig. 6.4 provide an overview of the parameters monitored during fermentation time. From the first graph (a), one can see on the left y-axis the cumulative gas produced (H<sub>2</sub> and CO<sub>2</sub>) developed after a few hours, and on the right y-axis the flow rate of



**Table 6.8** Comparison of bioreactor test with OWM and with glucose

Experimental results	Glucose	OWM
Lag phase (h)	13 ± 2	8 ± 3
Duration of test (days)	14 ± 0.5	6 ± 0.5
Maximum biogas production (L <sub>H<sub>2</sub></sub> /L)	21.3 ± 2	10 ± 0.3
Mean H <sub>2</sub> concentration (% v/v)	47.8 ± 2	30.0 ± 1.5
Maximum H <sub>2</sub> production (L <sub>H<sub>2</sub></sub> /L)	10.2 ± 1.4	3.0 ± 0.2
TS initial (g/L)	58 ± 1.5	31 ± 1.5
TS final (g/L)	0	1.5 ± 0.5
Δ <sub>TS</sub>	60	31
Y <sub>R</sub> = H <sub>2</sub> /Δ <sub>RS</sub> (mL/g)	170	97
Efficacy <i>versus</i> glucose (ζ <sub>Gluc</sub> )	100	57

the gas as an experimental derivative of the cumulative gas produced. At first glance, from Fig. 6.4b, one observes a strict relation between biogas evolution, pH and redox developments similar to that found in the glucose test, but the discontinuity of the pH and consequently the redox evolution is also evident. The strong non-Newtonian behavior of the broth impeded automatic control of the pH, and hence it was necessary to control it manually. Due to the consistency of the broth, some problems occurred during the fermentation time course; it caused poor agitation with the formation of lumps of material and these stuck to the pH electrode probe, thus making it impossible to measure the pH and blocking the control loop. On these occasions, manual controls were necessary.

Comparing this test with the one described in Chap. 4, conducted at the same temperature (35 °C) with glucose as carbon source (Table 6.8), one can make the following observations. Despite the presence of more complex substrates, mainly composed of carbohydrates with complex structure and a small percentage of proteins, fats and fibres, the microorganisms show a good ability to utilize vegetable biomass. This is confirmed from a very short lag phase of about 8 h, very similar to that of 13 h in the test with glucose. The short lag phase is certainly facilitated by the alkaline pretreatment that breaks down complex polymers in hydrolyzed monomers. Furthermore, the alkaline pretreatment has other advantages: it might be well adapted to a full-scale plant in which the waste tank of the anaerobic plant could be filled with alkaline solution at the beginning; it does not need direct energy consumption as it occurs with other treatments; and, finally, it also seems very efficacious with different vegetable streams. This probably occurs because the NaOH base is able to destructure the crystallinity of the hemicelluloses and increase the amorphous hemicelluloses, which are more easily attacked by the microorganisms' enzymes. However, because of the heterogeneous and complex nature of celluloses and the contribution of other components, such as lignin and other organic components, it is not the only factor affecting the enzymatic attack. The process is very complicated, because it involves several reactive and non-reactive phenomena, e.g. the dissolution of non-degraded polysaccharides, peeling-off reactions, such as the

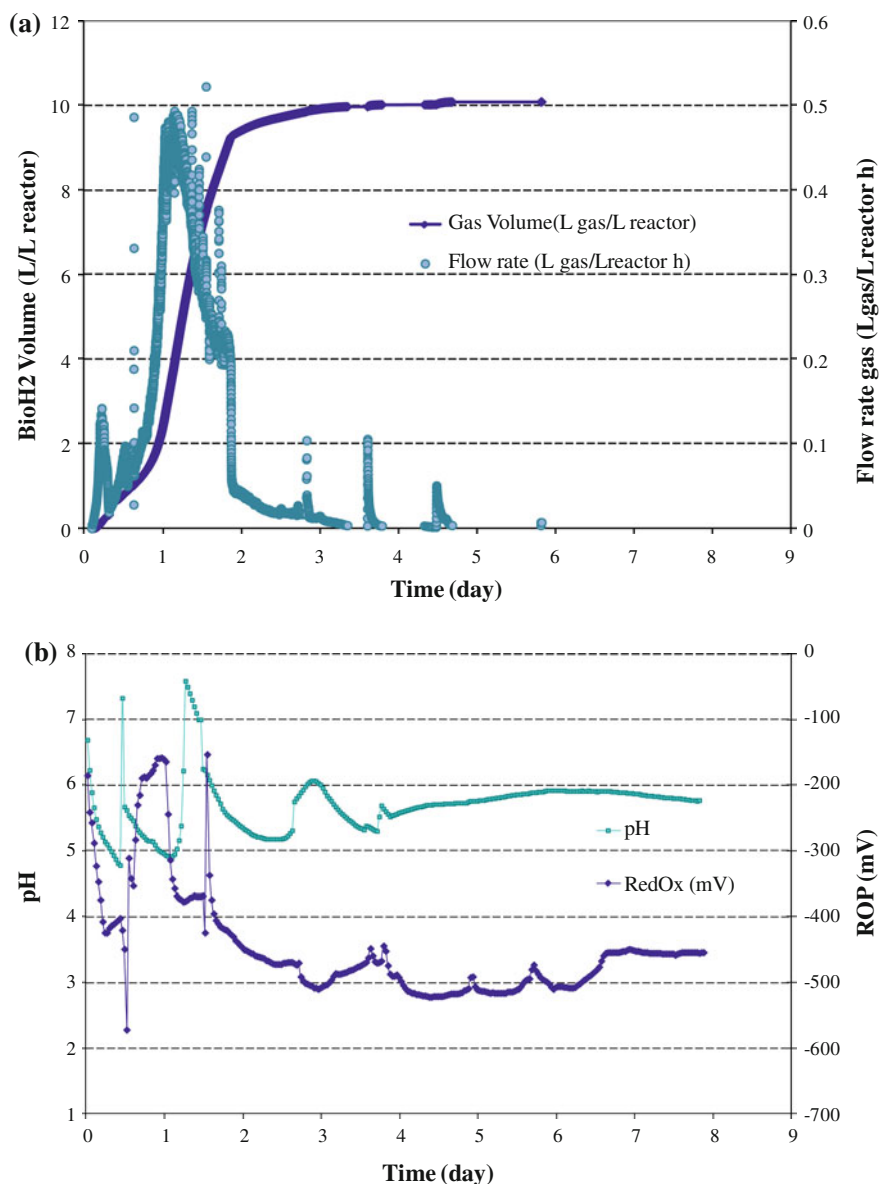


**Fig. 6.4** Test of OWM with alkaline chemical treatments at pH 12.5 with 2 N NaOH: **a** cumulative gas production ( $H_2 + CO_2$ ) and flow rate of the gas; **b** pH and redox time course

formation of alkali-stable end groups, the hydrolysis of acetyl groups and glycosidic bonds and the decomposition of dissolved polysaccharides. Another possible explanation for the lower lag phase could be the presence of sugars, together with the

large quantity of suspended solids, which creates a support for the microorganisms, increasing the contact surface between the enzymes and the sugars with beneficial effects on the mass transfer phenomena, a problem that is always present in such types of multiphase system, even in the presence of glucose only. As far as  $H_2$  productivity and  $H_2$  production are concerned (Table 6.8), the former is higher than glucose and the latter lower. The available sugars are lower than the glucose equivalent ( $\sim 60$  g/L), but those present in OWM refuse are more easily converted, shown by the shorter duration of the test. This aspect could also be explained by the mass transfer phenomena previously mentioned.

The rheological behavior of the broth deserves special mention. As experimentally verified (see Fig. 6.4), this behavior is not acceptable in a full-scale bioreactor, and this is one of the most important problems that need to be solved for the scaled-up procedure of such a full-plant application when using organic refuse as substrate to produce energy. As for the energy production, the energy efficacy seems to be a very good parameter to account for this aspect; from Table 6.8, the efficacy is  $\zeta = 57\%$  of that of glucose evaluated as a ratio of  $Y_R$ , but it is more than 11 times the efficiency obtained with Erlenmeyer flasks, indicating that the control of pH and the agitation are able to increase the overall efficiency of the process, even if the problem of mixing remains an open question regarding scale-up. The value of the efficiency of 57% vs. glucose, seems to indicate that there is still a great opportunity to increase the efficacy of the whole process. This result, in the authors' opinion, is a good proof of concept regarding the feasibility of using pretreated vegetable and fruit waste as feedstock for hydrogen production.

## 6.6 Conclusion

Residual biowastes are suitable substrates for  $H_2$  production. In general, extrusion of SPR provided the best results. The best values of efficiency and efficacy were achieved for TBP, which improved the performance obtained with the broth without pretreatment 17-fold. It is important to note that this type of refuse was extruded at 200 atm to remove packaging. OWM, despite providing one of the best results, is the substrate that produced the highest quantity of energy without any type of pretreatment. This means that among the substrates used, OWM is the most easily digested one; however, the best pretreatment, which improved the energy production 10-fold, was a combination of chemical and thermal processes. As far as SPR is concerned, exposure to high temperatures for a long period appears to be unsuitable for increasing energy production in such substrates, most likely because the caramelization reactions of the sugars hinder digestion by microorganisms. However, it was observed that the BP significantly increased the efficiency with respect to the substrate, with an efficacy value of 6.4. The use of UP, on the other hand, completely destroyed the lignocellulose structures and increased the substrate

surface area to a significant extent. The suggestion is that a basic pretreatment, in combination with a thermal one, is able to increase the hydrogen obtainable through the anaerobic fermentation process without the addition of micronutrients or other additives. The choice between a basic pretreatment, a basic/thermal pretreatment, and an ultrasonic one needs to be evaluated through a detailed life cycle assessment of the three options, in which it would be necessary not only to consider the energy consumed directly but also the energy necessary to obtain this energy and the energy necessary to obtain the chemicals. Lastly, a test of OWM with the bioreactor confirms the good opportunity to use OW for hydrogen production even though the problem of mixing the fermenting broth needs to be carefully addressed in the scale-up procedure.

## References

1. R.E.H. Sims, *The Brilliance of Bioenergy, in Business and in Practise* (James and James Press, London, 2002)
2. G. Evans, *Biowaste and Biological Waste Treatment* (James and James Press, London, 2001)
3. D.M. Mousdale, *Biofuels-Biotechnology, Chemistry and Sustainable Development* (CRC Press, Boca Raton, FL, 2008)
4. H. Röper, Perspektiven der industriellen Nutzung nachwachsender Rohstoffe, insbesondere von Stärke und Zucker. Mitt Fachgruppe Umweltchem Ökotoxikol Ges Dtsch Chemie **7**(2), 6–12 (2001)
5. N. Mosier, C. Wyman, B. Dale, R. Elander, Y.Y. Lee, M. Holtzapple, M. Ladisch, Features of promising technologies for pretreatment of lignocellulosic biomass. *Bioresour. Technol.* **96**(6), 673–686 (2005)
6. L.T. Fan, Y. Lee, D.H. Beardmore, Mechanism of the enzymatic hydrolysis of cellulose: effects of major structural features of cellulose on enzymatic hydrolysis. *Biotechnol. Bioeng.* **22**(1), 177–199 (1980)
7. C.E. Wyman, *Handbook on Bioethanol: Production and Utilization, Applied Energy Technology Series* (CRC Press, Taylor and Francis, Washington DC, 1996)
8. L. Zhu, J.P. O'Dwyer, V.S. Chang, C.B. Granda, M.T. Holtzapple, Structural features affecting biomass enzymatic digestibility. *Bioresour. Technol.* **99**(19), 3817–3828 (2008)
9. A. Berlin, M. Balakshin, N. Gilkes, J. Kadla, V. Maximenko, S. Kubo, J. Saddler, Inhibition of cellulase, xylanase and beta-glucosidase activities by softwood lignin preparations. *J. Biotechnol.* **125**(2), 198–209 (2006)
10. B. Ruggeri, M. Bernardi, T. Tommasi, On the pretreatment of municipal organic waste towards fuel production: a review. *Int. J. Environ. Pollut.* **49**, 226–250 (2012)
11. C.E. Wyman, *Handbook on Bioethanol: Production and Utilization* (CRC Press, Boca Raton, FL, 1996)
12. Y. Sun, J. Cheng, Hydrolysis of lignocellulosic materials for ethanol production. *Bioresour. Technol.* **83**, 1–11 (2002)
13. W.R. Grous, A.O. Converse, H.E. Grethlein, Effect of steam explosion pretreatment on pore size and enzymatic hydrolysis of poplar. *Enzym. Microb. Technol.* **8**(5), 274–280 (1986)
14. T.A. Clark, K.L. Mackie, Steam Explosion of the Softwood *Pinus Radiata* with sulphur dioxide addition. I. Process optimization. *J. Wood Chem. Technol.* **7**(3), 373–403 (1987)
15. O.E. Solheim, Method of and arrangement for continuous hydrolysis of organic material. US Patent 0,168,990 (2004)

16. J. Kim, C. Park, T.H. Kim, M. Lee, S. Kim, S.W. Kim, J. Lee, Effects of various pretreatments for enhanced anaerobic digestion with waste activated sludge. *J. Biosci. Bioeng.* **95**, 271–275 (2003)
17. V.P. Puri, H. Mamers, Explosive pretreatment of lignocellulosic residues with High-pressure Carbon dioxide for the production of fermentation substrates. *Biotechnol. Bioeng.* **25**, 3149–3161 (1983)
18. W.P. Xiao, W.W. Clarkson, Acid solubilization of lignin and bioconversion of treated newsprint to methane. *Biodegradation* **8**, 61–66 (1997)
19. T. Jeoh, C.I. Ishizawa, M.F. Davis, M.E. Himmel, W.S. Adney, D.K. Johnson, Cellulase digestibility of pretreated biomass is limited by cellulose accessibility. *Biotechnol. Bioeng.* **98** (1), 112–122 (2007)
20. L.T. Fan, M.M. Gharpuray, Y.H. Lee, *Cellulose Hydrolysis Biotechnology* (Monographs Springer, Berlin, 1987)
21. M. Beccari, M. Majone, M.P. Papini, L. Torrisi, Enhancement of anaerobic treatability of olive oil mill effluents by addition of  $\text{Ca}(\text{OH})_2$  and bentonite without intermediate solid/liquid separation. *Water Sci. Technol.* **43**, 275–282 (2001)
22. S. Ghosh, M.P. Henry, A. Sajjad, M.C. Mensiger, J.L. Arora, Pilot-scale gasification of municipal solid wastes by high-rate and two-phase anaerobic digestion (TPAD). *Water Sci. Technol.* **41**(3), 101–110 (2000)
23. N.H.M. Yasin, T. Mumtaz, M.A. Hassan, N.A.A. Rahman, Food waste and food processing waste for biohydrogen production: a review. *J. Environ. Manage.* **130**, 375–385 (2013)
24. G. De Gioannis, A. Muntoni, A. Poletti, R. Pomi, A review of dark fermentative hydrogen production from biodegradable municipal waste fractions. *Waste Manag.* **33**, 1345–1361 (2013)
25. K. Vijayaraghavan, D. Ahmad, M.K. Ibrahim, Biohydrogen generation from jackfruit peel using anaerobic contact filter. *Int. J. Hydrogen Energy* **31**, 569–579 (2006)
26. S.W. Van Ginkel, S.E. Oha, B.E. Logan, Biohydrogen gas production from food processing and domestic wastewaters. *Int. J. Hydrogen Energy* **30**, 1535–1542 (2005)
27. S.K. Han, H.S. Shin, Biohydrogen production by anaerobic fermentation of food waste. *Int. J. Hydrogen Energy* **29**, 569–577 (2004)
28. N.Q. Ren, J.Z. Li, B.K. Li, Y. Wang, S.R. Liu, Biohydrogen production from molasses by anaerobic fermentation with a pilot scale bioreactor system. *Int. J. Hydrogen Energy* **31**, 2147–2157 (2006)
29. H.H.P. Fang, C.L. Li, T. Zhang, Acidophilic biohydrogen production from rice slurry. *Int. J. Hydrogen Energy* **31**, 683–692 (2006)
30. Y. Akutsu, D.Y. Lee, Y.Y. Li, T. Noike, Hydrogen production potential and fermentative characteristics of various substrates with different heat-pretreated natural microflora. *Int. J. Hydrogen Energy* **34**, 5365–5372 (2009)
31. M. Cui, Z. Yuan, X. Zhi, J. Shen, Optimization of biohydrogen production from beer lees using anaerobic mixed bacteria. *Int. J. Hydrogen Energy* **34**, 7971–7978 (2009)
32. E. Castello, C. Garcia y Santos, T. Iglesias, G. Paolino, J. Wenzel, L. Borzacconi, C. Etchebehere, Feasibility of biohydrogen production from cheese whey using a UASB: links between microbial community and reactor performance. *Int. J. Hydrogen Energy* **34**, 5674–5682 (2009)
33. S. Jayalakshmi, K. Joseph, V. Sukumaran, Biohydrogen generation from kitchen waste in an inclined plug flow reactor. *Int. J. Hydrogen Energy* **34**, 8854–8858 (2009)
34. X. Wu, J. Zhu, C. Dong, C. Miller, Y. Li, L. Wang, W. Yao, Continuous biohydrogen production from liquid swine manure supplemented with glucose using an anaerobic sequencing batch reactor. *Int. J. Hydrogen Energy* **34**, 6636–6645 (2009)
35. K. Vijayaraghavan, D. Ahmad, Biohydrogen generation from palm oil effluent using anaerobic contact filter. *Int. J. Hydrogen Energy* **31**, 1284–1291 (2006)
36. B. Ruggeri, T. Tommasi, Efficiency and efficacy of pretreatment and bioreaction for bio-H<sub>2</sub> energy production from organic waste. *Int. J. Hydrogen Energy* **37**, 6491–6502 (2012)

37. INRAN, Istituto Nazionale di Ricerca per gli Alimenti e la Nutrizione. [http://nut.entecra.it/646/tabelle\\_di\\_composizione\\_degli\\_alimenti.html](http://nut.entecra.it/646/tabelle_di_composizione_degli_alimenti.html). Accessed 15 Oct 2014
38. B. Ruggeri, A.C. Luongo Malave, M. Bernardi, D. Fino, Energy efficacy used to score organic refuse pretreatment processes for hydrogen anaerobic production. *Waste Manage.* **33**, 2225–2233 (2013)
39. I. Del Campo, I. Alegría, M. Zazpe, M. Echeverría, I. Echeverría, Diluted acid hydrolysis pretreatment of agri-food wastes for bioethanol production. *Ind. Crops Prod.* **24**(3), 214–221 (2005)

## Chapter 7

# Valorization of Liquid End-Residues of H<sub>2</sub> Production by Microbial Fuel Cell

Microbial fuel cell (MFC) technology can be employed in order to add value to the metabolic products of acetogenesis fermentation after H<sub>2</sub> production. Considering the total conversion of glucose into acetic acid as the only bioproduct, only 1/3 of the energy available is converted in H<sub>2</sub> from a thermodynamic point of view (Chap. 5). Furthermore, in practical terms, the energy necessary to carry out the pretreatments must be considered as energy used to perform the energy balance, in order to render the organic contents accessible to microorganisms (Chap. 9). Nevertheless, the aim of this book is to focus on anaerobic technology and its energy sustainability; the conversion of H<sub>2</sub> production residues, such as VFA, into additional H<sub>2</sub> or CH<sub>4</sub> or electricity needs to be investigated. Even if the MFC technology is in its infancy, it deserves a very close attention for the possibility of generating electrical energy or additional H<sub>2</sub>. The present chapter is devoted to explore the potential of MFC technology.

### 7.1 Overview of Bioroutes for Recovery of Additional Energy

The way to increase the overall energy production of an H<sub>2</sub> process is to extract the residual bioenergy embedded in the liquid metabolites at the end of acidogenesis. This bioenergy can be recovered as methane, or directly as electrical energy, or as additional H<sub>2</sub>. Table 7.1 gives a list of biotechnologies that are under research studies for extracting the remaining potential bioenergy from liquid end-products, while in Fig. 7.1 the same information is reported in a more synthetic way.

#### 7.1.1 Photofermentation

The combination of *photosynthetic bacteria* with hydrogen-producing bacteria (HPB) can provide a system for additional hydrogen production from residual

**Table 7.1** Alternative strategies for additional recovery of energy, after a first stage of H<sub>2</sub> anaerobic production

Second stage after H <sub>2</sub> production by AD	Principle and kind of produced energy	Advantages	Disadvantages
Photofermentation	N <sub>2</sub> ase and captured solar energy used to convert organic acids to <b>H<sub>2</sub></b>	Solar light exploitation	<ul style="list-style-type: none"> <li>• Little knowledge about potential pathways</li> <li>• Light-dependent</li> </ul>
Biogas production by AD	Standard anaerobic digestion used to convert organic acids to <b>biogas (methane)</b>	Well-known technology widely used	<ul style="list-style-type: none"> <li>• Low production rate</li> <li>• Large reactor volume required due to HRT greater with respect to H<sub>2</sub> production</li> </ul>
Microbial fuel cells (MFCs)	Electrons realised from organic acid oxidation are used to produce <b>electricity</b>	<ul style="list-style-type: none"> <li>• Directly conversion of VFA into electricity</li> <li>• Production of a gas without energy value (only CO<sub>2</sub>) which does not require treatment</li> <li>• Long lifetime (up to 3–5 years)</li> </ul>	<ul style="list-style-type: none"> <li>• Large surface area electrodes required</li> <li>• Ohmic losses</li> <li>• Low power density (0.001–0.1 mW/cm<sup>2</sup>)</li> </ul>
Enzymatic fuel cells (EFCs)	Employ enzymes to catalyze the oxidation of fuel at the electrode surface, releasing <b>electrons</b>	Higher power density (1.6–4 mW/cm <sup>2</sup> )	<ul style="list-style-type: none"> <li>• Incomplete oxidation of fuel</li> <li>• Low lifetimes</li> <li>High costs</li> </ul>
Organelle-based biofuel cells	Immobilized mitochondria on conductive electrode that convert chemical energy into <b>electricity</b>	<ul style="list-style-type: none"> <li>• Power density between MFCs and enzymatic FCs</li> <li>• Complete oxidation of the fuel at high rate</li> </ul>	<ul style="list-style-type: none"> <li>• High costs</li> <li>• Necessity to immobilize mitochondria on electrode; difficult at large scale</li> </ul>
Microbial electrolysis cells (MECs)	Electrical energy added to drive conversion of organic acids to <b>H<sub>2</sub></b>	Theoretical production of pure H <sub>2</sub>	<ul style="list-style-type: none"> <li>• Added energy required</li> <li>• Low current density</li> <li>• Large surface area electrodes required</li> </ul>
Metabolic engineering	Genetic modification, gene addition to create novel <b>hydrogen-producing pathways</b>		<ul style="list-style-type: none"> <li>• Unproven</li> <li>• Little knowledge about potential pathways</li> </ul>

chemicals such as VFA at the end of anaerobic digestion (AD). In such a coupled system, the low-molecular-weight organic acids are converted in a second step to hydrogen by photosynthetic bacteria at the expense of light energy. Non-sulfur purple photosynthetic bacteria are able to capture light and to convert organic acids



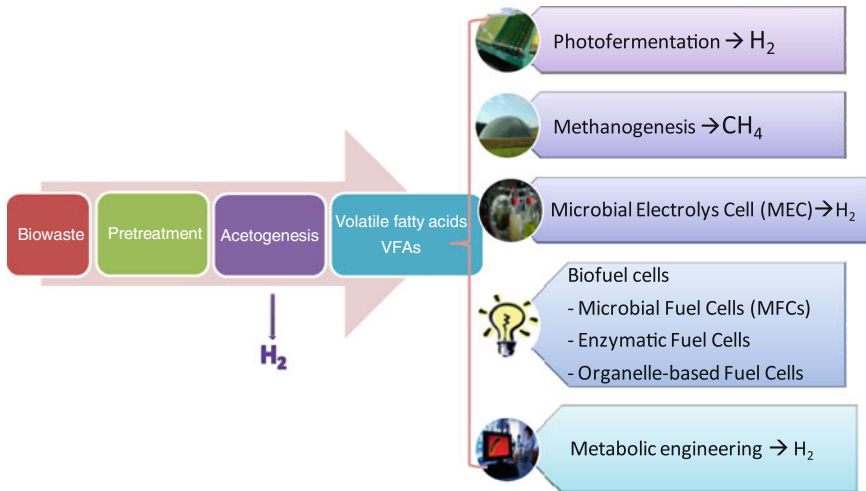


**Fig. 7.1** Schematic view of alternative biological routes to harvest additional bioenergy from organic waste refuses

to hydrogen by a photofermentation reaction, where H<sub>2</sub> is driven by nitrogenase; the required ATP is formed via the photosynthetic capture of light energy [1]. Even though the overall yield in such a two-stage fermentation process was found to be higher compared to a single one [2], many factors restrict the practical application of this process. In fact, nitrogenase-driven hydrogen production is potentially sensitive to the nitrogen content of the medium/substrate since it represses nitrogenase synthesis and moreover inhibits the enzyme activity [1]. The most severe constraint is the fact that photosynthetic efficiencies, with either solar radiation or tungsten lamps, are very low: the majority of captured light is dissipated as heat (>80 %), even at moderate light intensities [3]. The combinations of many technical parameters present very significant hurdles for the development of a full-scale process, with high costs, e.g. for transparent impermeable photobioreactors with enhanced surface area.

### 7.1.2 Biogas Production

Biogas production by AD in a second stage, here called two-step anaerobic digestion (TSAD), is the process that appears to be the most suitable for reaching the maturity of a full plant application in a short time. It consists of the separation into two stages of the natural metabolism of an anaerobic bacteria consortium

present in a digester. This approach will be treated in detail in Chap. 8, along with the results obtained by a pilot plant at laboratory scale using fruit and vegetable refuses as feed.

### **7.1.3 Microbial Fuel Cells**

MFC technology represents the newest approach to bioelectricity generation from biomass using bacteria. In an MFC, microorganisms mediate direct conversion of chemical energy stored in organic matter into electrical energy: the oxidation of various fermentable substrates (e.g. glucose and sucrose), complex substrates (e.g. domestic wastewater and paper wastewater) and organic matter present in aquatic sediments produces electrons under microbiological activities at the anode; these electrons are recovered on the electrode surface and they travel through an external circuit to reach the cathode, where a reduction reaction occurs.

### **7.1.4 Microbial Electrolysis Cells**

*A bio-electrochemically assisted microbial reactor (BEAMR), or more simply a microbial electrolysis cell (MEC), permits the generation of hydrogen gas and other reduced products at the cathode using organic electron donors. The terms “electrochemically” and “assisted” are used in this process because additional voltage is required by the circuit compared with MFC [4]. An external power supply can support the process and therefore circumvent thermodynamic constraints that, in its absence, render the generation of hydrogen impossible [5]. Examples of electron donors might be acetate and wastewater. The anodic oxidation of acetate is the same reaction occurring in the anode of a MFC that harvests electrical energy through an external resistance. In the case of MECs, hydrogen is produced at the cathode with platinum as a catalyst. The separation between the anode and cathode chambers of a MEC is accomplished with an ion-selective membrane (cation exchange membrane, CEM). CEMs are used to obtain cathodic hydrogen gas that is as pure as possible. However, CEMs give rise to higher ohmic voltage loss in the cell and a pH gradient over the membrane, resulting in a lower current production for a given applied voltage. Removing a part of the membrane helped to minimize the pH gradient between anode and cathode: Clauwaert and Verstraete [6] conducted operations of MECs without an ion exchange membrane and found that this could help to lower the construction costs, to lower the ohmic cell resistance and to improve MEC conversion efficiency by minimizing the pH gradient between anode and cathode. They demonstrated that membrane-less MECs with plain graphite can be operated for methane production without pH adjustments and that the ohmic cell resistance*

was reduced by approximately 50 %; as a result, the current production increased from 66 to 156 A m<sup>-3</sup> MEC with an applied voltage of -0.8 V. In this condition, methane was the main product.

### ***7.1.5 Metabolic Engineering***

Another possible path towards increasing hydrogen yields is to alter the metabolism of microorganism species through *metabolic engineering* by genetic manipulation in order to overcome the thermodynamic/metabolic barriers. These tools are not yet well developed and there is a lack of studies. Several avenues can be pursued in the future in attempts to introduce NAD(P)H-dependent hydrogenase/pathways. In a recent study [7], a ferredoxin-dependent NAD(P)H:H<sub>2</sub> pathway was introduced into an *E. coli* strain expressing a [Fe-Fe] hydrogenase, the maturation enzymes and ferredoxin. Some increase over basal activity was noted, and variations in hydrogen production led the authors to conclude that the system was thermodynamically severely limited, and thus impractical. However, levels of expressed hydrogenase activity are quite low in this strain, making it difficult to draw definitive conclusions. Another suggested approach is to use reverse electron flow to generate reduced ferredoxin with enough reducing power to drive hydrogen evolution by hydrogenase [1]. Of course, this requires energy input and it was suggested that a small amount of electrons from the respiratory chain could be used to generate an electrochemical gradient that would drive ferredoxin reduction. This approach has not yet been tested and it is not known how to construct the appropriate pathways. Thus, metabolic engineering pathway deserves some criticism, but with further investigations the metabolic system could be adapted to drive higher biohydrogen production by AD.

### ***7.1.6 Mitochondria-Based Fuel Cells***

Mitochondria are present in the cytoplasm of living cells of animals, plants and fungi, and are responsible for energy conversion. This organelle, called “the powerhouse of the cell” contains the enzyme and coenzymes of the Krebs’ cycle and the electron transfer chain, but unlike a cell it has no need to transport fuel across the cell wall and therefore mitochondria can completely oxidize fuel at a faster rate, ensuring that no toxic byproducts are produced as waste. This organelle-based fuel cell theoretically can provide power densities between those of enzyme-based fuel cells (EFCs) and MFCs, with a lifetime and efficiency similar to that of MFC. A proof of the concept was made for the first time by Arechederra and Minteer [8], who immobilized mitochondria within tetrabutylammonium bromide-modified Nafion membrane, obtaining a power density of 0.2 mW/cm<sup>2</sup>, lower than

those obtainable in both MFCs and EFCs. Moreover, they obtained a complete oxidation of pyruvate into carbon dioxide without an external mediator with stability of up to 60 days. However, this pathway seems to be difficult to apply to full-scale plants that valorize waste, at least at present.

### ***7.1.7 Enzyme-Based Fuel Cells***

EFCs utilize isolated enzymes as catalysts for fuel oxidation at the anode and reduction at the cathode. Appropriate choice of enzymes permits such reactions to occur under relatively mild conditions: neutral pH and ambient temperature. In addition, immobilization of specific enzymes for reaction on electrodes, such as carbon, can eliminate the separation into compartments of components required in conventional MFCs [9]. EFCs have the advantage of higher power density (1.65–4.1 mW/cm<sup>2</sup>) [10] but they are limited by incomplete oxidation of fuel at the electrode surface. Due to the exclusion of such components, EFC have the capacity to be miniaturized and, consequently, micrometer-dimension membrane-less EFCs have been developed [9, 11]. However, due to the short lifetime of enzymes and their specificity, they are not indicated as a second step for H<sub>2</sub> production.

## **7.2 MFCs: Principles and Applications**

The MFC is a promising green technology that permits the conversion of biodegradable materials present in wastewater directly into electricity. In the anode chamber, the decomposition of organic substrates by microorganisms, via the respiratory chain, generates electrons (e<sup>-</sup>), which are transferred to the cathode through an external electric circuit, and protons (H<sup>+</sup>), which travel via CEM to the cathode [12]. A schematic view of a MFC is shown in Fig. 7.2.

The anode and cathode chambers are separated by a CEM. On the anode side a bio-electrochemical reaction occurs between microorganisms and a fuel/substrate which is oxidized, releasing CO<sub>2</sub>, electrons and protons to the solution. The CO<sub>2</sub> produced moves toward the top of the anode, protons are transported to the cathode chamber through the membrane and electrons are harvested on the electrode surface and go through an external electric wire; the bacteria grow on the anode, colonizing it. The cathode chamber is sparged with air to provide dissolved oxygen at the electrode surface for the reduction reaction; a resistor completes the circuit, utilizing the electrical energy.

The following equations illustrate the redox reactions occurring in a MFC in the case of glucose as fuel:

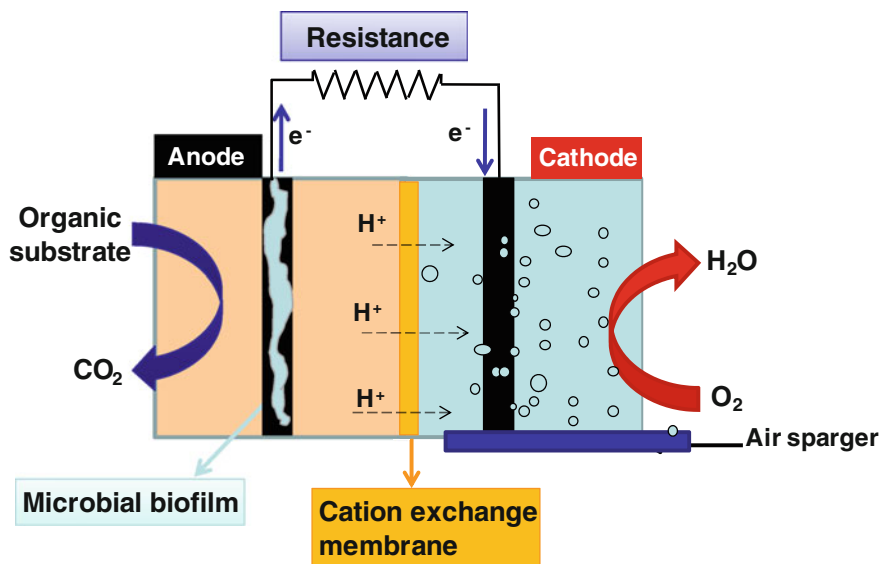
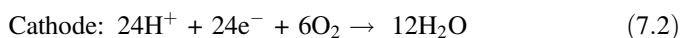


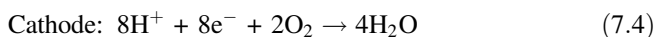
Fig. 7.2 Schematic views of components of a microbial fuel cell



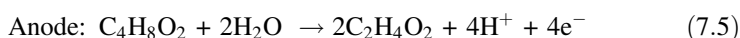
(Theoretically  $\Delta G_0 = -2,840 \text{ kJ/mol}$ )



In the case of the use of VFA formed in the first acidogenic step for H<sub>2</sub> production, the following theoretical reactions should be taken into account in the case of the use of acetate, where 8e<sup>-</sup> per mol are produced:



similarly, butyrate produces 4e<sup>-</sup> per mol:



Among various energy technologies (e.g. incineration, gasification, bioethanol-based fermentation, AD for bioH<sub>2</sub> and biogas production), the MFC presents a number of attractive features, such as direct electricity generation, high conversion efficiency and a reduced amount of sludge production [13]. Although the functionality of a MFC is similar to that of a chemical fuel cell, as they both include

reactants, two electrodes (anode and cathode), the MFC has the following substantial advantages:

- working at ambient temperature and pressure;
- using neutral electrolytes and avoiding expensive catalysts (e.g. platinum);
- not using a traditional fuel supply but organic wastes;
- not needing to be recharged/replaced after exhaustion, as happens for lithium ion batteries.

Conversely, there are still several problems associated with a low yield of power generation, such as biofouling, adequate and lower cost of the electrode material, cation transport rather than protons, and high costs of the system causing a decrease in the global energy efficiency.

However, the use of MFCs has great potential for a broad range of applications, e.g. electronic power sources for space shuttles, self-feeding robots and also as an additional sustainable step in wastewater treatment plants, especially in remote situations, where difficulties in electrical energy supply can arise. In fact, MFCs can potentially be installed in environments that are not easily reachable, where bacteria flow in the MFC compartments can be self-sustained by the surrounding environment. Even if not suitable for high energy demands, the MFCs can generate enough power to permit microelectronics and sensor systems to run at acceptable specifications. The main challenge for MFC technology is to replace the energy-expensive aerobic wastewater treatment, alone or in association with AD plant. Virtually any biodegradable organic material can be used in a MFC, including VFA, carbohydrates, proteins, alcohols and even recalcitrant materials like cellulose [4]. Furthermore, large amounts of excess sludge are produced, requiring an appropriate treatment and disposal. MFCs are therefore a valid option for extracting the energy still embedded in liquid residues of acidogenic fermentation thanks to VFA-oxidizing microorganisms. The bacterial reaction can be carried out over several different temperatures ranges, depending on the tolerance of the bacteria, ranging from mesophilic (15–35 °C) to thermophilic (50–60 °C) and psychrophilic temperatures (<15 °C). The current that can be generated by an anodic biofilm typically increases with the amount of active biomass attached to the electrode. MFCs exhibit low coulombic efficiencies (the ratio of the electrical charges harvested to the input charges produced by the oxidation reaction) determined by the internal resistance of the device, mainly due to inefficient electron transfer between the microbial cells and the anode. This inefficiency results in incomplete oxidation of the fuel, the production of liquid metabolites and the adsorption of organic substrates used as fuel on the biomass; all these problems could be addressed by future research programs.

### ***7.2.1 Anode Microbiology***

In a bioanode, electrochemically active microorganisms, generally bacteria, oxidize a substrate (electron donors) and transfer these electrons to the electrode (Fig. 7.3).

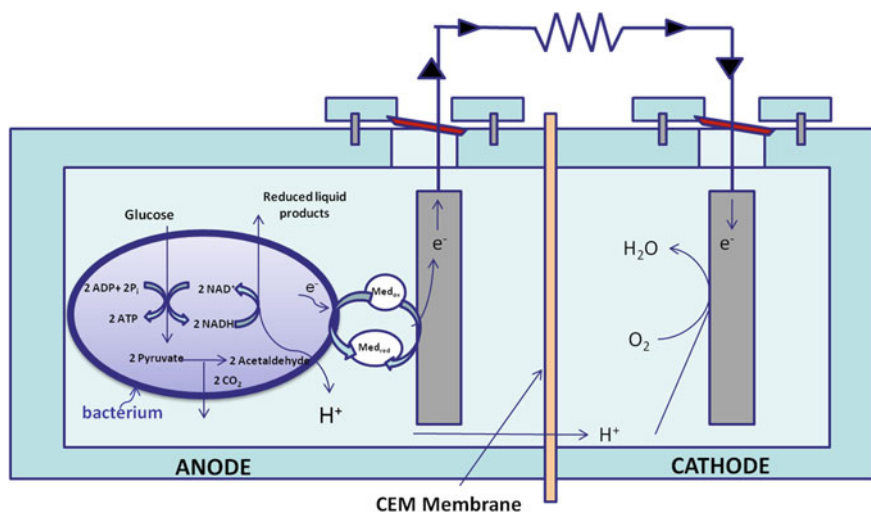


**Fig. 7.3** Working principle of an MFC

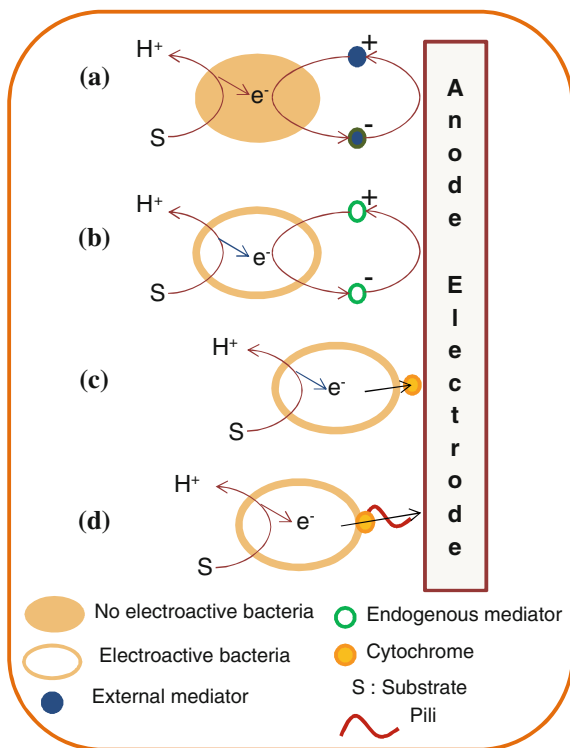
In anaerobic conditions, reducing equivalents generated during fermentation move through a series of redox components towards an available terminal electron acceptor. In this way, a proton motive force is generated, helping to produce energy-rich phosphate bonds in ATP, which is useful for microbial growth and subsequent metabolic activities. MFCs are mainly based on harvesting available electrons using non-biological materials (electrodes) as intermediate electron acceptors [14].

Electron transfer to the electrode can occur by different mechanisms grouped into two different modes, *direct electron transfer* (DET) and *mediated electron transfer* (MET), based on the carrier involved (Fig. 7.4). DET occurs due to a physical contact between bacterial cells (e.g. cytochromes and nanowires) and anode, without the involvement of any redox species or mediator. *Geobacter*, *Rhodospirillum rubrum* and *Shewanella* are the most-studied bacterial genera that use DET through membrane bounds for electron transfer. MET indicates the involvement of mediators for extracellular electron transfer from the biocatalyst to the anode. The mediators may be added artificially or may be shuttles naturally excreted by bacterial activity as primary and/or secondary metabolites [15].

In *bio-electrochemical systems* (BES), depending on the configuration as well as the intended application, the microbial catalysts can be an axenic culture or a mixed culture. MFCs that use mixed bacterial cultures have some important advantages: a lower sensitivity to process disturbances, larger substrate versatility and higher power generation [16].

While in axenic culture the bio-electrocatalysis is attributed to the activity of only one bacterial culture, in a BES operating with a mixed culture the interactions within members of the entire microbial community determine the so-called electrochemically active consortium. These electrochemically active consortia could be

**Fig. 7.4** Schematic illustration of electron transfer: **a** addition of artificial mediator; **b** “natural” redox mediator; **c** direct surface contact; **d** direct electron transfer



obtained by either sediment (both marine and lake sediment) or activated sludge from wastewater treatment plants by subsequent enrichment techniques. By means of molecular analysis, electrochemically active species of *Geobacter* spp., *Desulfuromonas* spp., *Alcaligenes faecalis*, *Enterococcus faecium*, *Pseudomonas aeruginosa*, *Clostridium* spp., *Bacteroides* spp., *Aeromonas* spp. and *Brevibacillus* spp. have been detected in mixed consortia. The microbial community established on the bioanode may vary in a mixed culture depending on the inoculum, type of substrate, operational conditions and reactor design. It is evident that a change in the community composition will influence the efficiency of the corresponding anode performance [17] but, to date, no typical composition for the anode community has been found [18]. However bacteria belonging to the taxonomic class of *Proteobacteria* usually comprise the majority of the bioanode community [19, 20] on different electrode materials. In addition many bacteria which have been isolated from the mixed culture communities can be characterized as metal reducers or as other types of anaerobic respirers [21, 22].

The study of the electron transfer mechanisms within microbial biofilms is one of the most challenging aspects of MFC research. Many microorganisms possess the ability to transfer the electrons derived from the metabolism of organic matters to the anode. Microbes transport electrons to the electrode through an electron transfer system which consists of many components in the bacterial extracellular matrix,



together with electron shuttles dissolved in the bulk solution. *Geobacter* belongs to the metal-reducing microorganisms which produce biologically useful energy in the form of ATP during the reduction of metal oxides under anaerobic conditions in soils and sediments. The electrons are transferred to the final electron acceptor, such as  $\text{Fe}_2\text{O}_3$ , mainly by direct contact of mineral oxides and metal-reducing microorganisms. The anodic reaction in MFCs without external mediators belongs primarily to the families of *Shewanella*, *Rhodospirillum rubrum* and *Geobacter*, where the anode acts as the final electron acceptor just like the solid mineral oxides. *S. putrefaciens*, *G. sulfurreducens*, *G. metallireducens* and *R. ferrireducens* transfer electrons to the solid electrode (anode) using this system. Mediators play an important role in electron transport for those microbes that are unable to transfer the electrons to the anode; they take electrons from microbes and discharge them at the anode surface. *Actinobacillus succinogenes*, *Desulfovibrio desulfuricans*, *Escherichia coli*, *Proteus mirabilis*, *Proteus vulgaris*, and *Pseudomonas fluorescens* need external mediators, while some microbes can provide their own. For example, some dominant Gram-negative bacteria such as *Pseudomonas* spp. can produce metabolites, such as pyocyanin and/or phenazine-1-carboxamide, which can act as electron shuttles (mediators), not only for *Pseudomonas* but also for other species. When an MFC is inoculated with anaerobic sludge, mixed-culture microbes are in the anode chamber and interact with themselves, enhancing the overall performance and allowing different substrate utilization.

A diversity of mechanisms by which microorganisms may transfer electrons to the anode of a MFC has been proposed, as shown schematically in Fig. 7.4. Currently, artificial mediators are employed only in specific cases, for example using *Saccaromyces cerevisiae*, which is not able to produce endogenous redox mediators. Today, much attention is directed to the study of natural shuttling of electrons via soluble compounds (Fig. 7.4b) and direct contact (Fig. 7.4c, d).

### 7.2.2 Electrical Parameters

The difference between positive cathodic and negative anodic potentials is considered to be the cell voltage which drives the electron flow from anode to cathode, called the electromotive force (*emf*). According to standard electrical principles, due to the positive potential difference ( $\Delta V$ ) between cathode and anode of a MFC, the flow of electrons ( $I$ ) generates a useful power ( $P$ ):

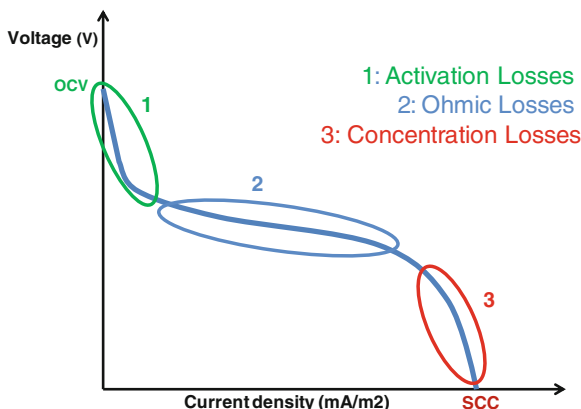
$$P = I \cdot \Delta V \quad (7.6)$$

The ratio between the voltage and the current is determined by the external resistance ( $R_{\text{ext}}$ ) according to Ohm's law:

$$\Delta V = I \cdot R_{\text{ext}} \quad (7.7)$$

When the external resistance is infinite (open circuit conditions), no current flows and the open circuit voltage (*OCV*) is obtained. Conversely, when the  $R_{\text{ext}}$  is

**Fig. 7.5** Voltage–current polarization curve; the circles 1, 2, 3 represent losses occurring



zero (short circuit conditions,  $\Delta V = 0$ ), the short circuit current ( $I_{sc}$ ) is generated. Alternatively, the relationship between the cell voltage and the current (density) can be calculated by a polarization curve (Fig. 7.5). Despite the microbial nature of the process, it is affected by electrochemical laws and principles which generally result in lowering the attainable voltage [23] and, consequently, in limiting the power generation of MFCs. In order to improve performance, a wide range of techniques have been utilized, to understand either scientific fundamentals or the role of materials, as well as to investigate MFC performance bottlenecks [24].

The power performance curve can be calculated by considering the experimental evaluation of the polarization curve (Fig. 7.6). The power delivered by a fuel cell is maximized when the external load matches the internal resistance of the fuel cell

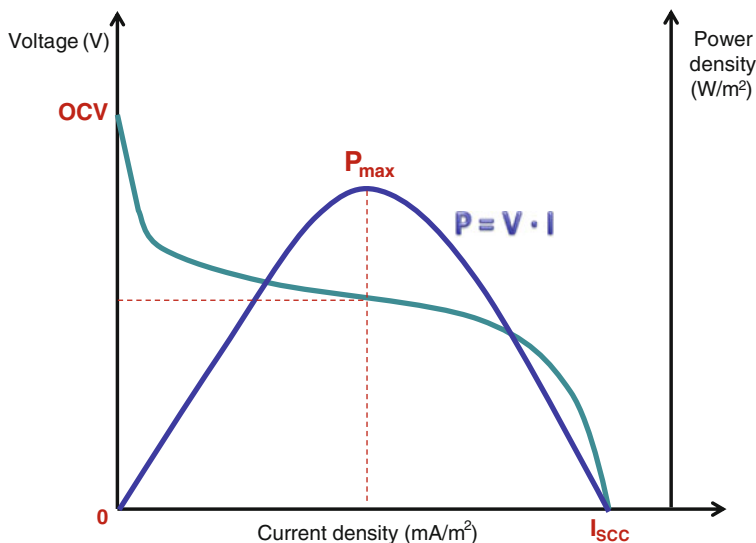


**Fig. 7.6** Cell voltage and power density as a function of the current density

system [25]. The microbial system that leads to electrical production is dependent on the total electron transfer chain, i.e. from bacteria to anode and from cathode to final electron acceptor. While the overall thermodynamics are quite favorable for anaerobes, there are numerous internal resistance mechanisms that diminish the potential use of the electrons at the cathode via the anode [26]. The bacteria involved in electricity production are able to overcome the resistance posed by the system. One way to minimize losses is to operate the MFC under optimal conditions for power generation using an optimal external resistance [27], which is usually correlated with the internal resistance of the MFC [28], following electrochemical theory supported by biological investigations.

The following equation is used for monitoring the energy production under an external resistance as electrical load during MFC usage.

$$\text{Energy (J)} = \int_{t_0}^{t_{final}} V \cdot I \cdot dt \quad (7.8)$$

### 7.3 Application of MFCs

The MFC is able to deliver power outputs at the desired voltage or current by connecting the electrical polarities of several MFC devices in series or in parallel. Therefore, the system could permit linkage of the advantage of wastewater treatment to the recovery of electricity.

MFC principles have been demonstrated at laboratory-scale devices even though real full-scale applications are currently limited by power yield and long-term performance. One of the first applications could be the development of pilot-scale reactors using the digester effluents of a bioreactor producing  $H_2$  using food processing wastewater as feed. In the long term, more dilute substrates, such as domestic sewage, could be treated with MFCs, decreasing the need for substantial amounts of electrical energy for the treatment. Furthermore, the conductive materials used to manufacture electrodes play an important role in MFC performance (e.g. power generation), costs and energy sustainability.

Many alternative applications could also emerge, ranging from biosensor development and energy generation from the seafloor, to MFCs operating on various biodegradable fuels. A simple monitoring system has been reported [29], comprising an ultra-lowpower impulse-radio ultra-wide-band transmitter (TX) and a nanostructured piezoresistive pressure sensor connected to a digital read-out circuit requiring 40  $\mu\text{W}$  powered by two MFCs connected in series. Tests conducted with a laboratory prototype with a total volume of 0.34 L, continuously fed with sea water and a synthetic substrate, has given  $0.7 \pm 0.1$  V as open circuit voltage and  $3 \pm 1$  A  $\text{m}^{-2}$  as short circuit current; the maximal power density was  $0.6 \pm 0.2$  W  $\text{m}^{-2}$  (Fig. 7.7).



**Fig. 7.7** MFC design used to conduct tests for continuous generation of electricity

The success of specific MFC applications in wastewater treatment will depend on the concentration and degree of biodegradability of the organic matter in the influent, the temperature, and the absence of toxic chemicals. The growing pressure on the environment and the call for renewable energy sources will further stimulate development of this technology, soon leading to its successful implementations. MFCs undoubtedly have potential in terms of energy recovery during wastewater treatment: they may occupy a niche market in terms of a stand-alone power source and also in the direct treatment of wastewater.

## 7.4 Integrated Bioenergy Production System

An environmental and sustainable alternative to the traditional wastewater treatment plant is represented by an integrated biological system which produces hydrogen using organic waste; it comprises two promising and innovative technologies, TSAD (H<sub>2</sub> + CH<sub>4</sub>) and MFC (Fig. 7.8).

The incoming biomass is first hydrolyzed (mechanical/chemical or enzymatic treatment), then fermented by TSAD and finally used in a MFC. These biological processes permit purification and transformation of waste by microorganisms into energetic products: either H<sub>2</sub> or CH<sub>4</sub>, and electricity. Biogases rich in H<sub>2</sub> and CH<sub>4</sub>, after an upgrade for CO<sub>2</sub> removal, are subsequently converted in a *combined heat and power* module (CHP). The heat obtained from the CHP is usually returned to the digester to ensure the working temperature, which could be in the mesophilic or thermophilic range. The electrical power (direct from MFC and indirect from AD) can be used for running reactors, and the overflow is used to furnish an energy

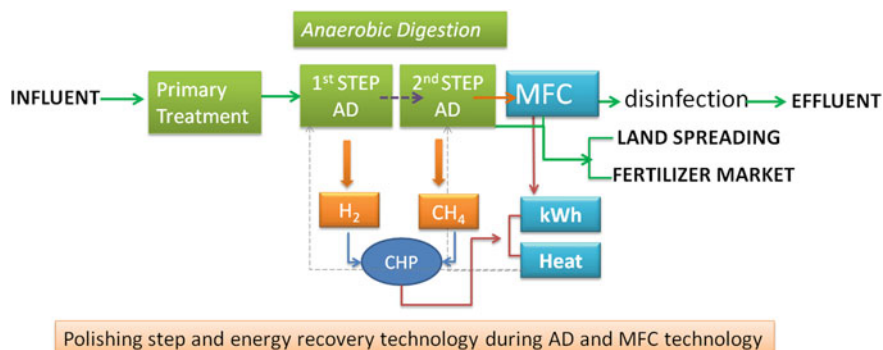


**Fig. 7.8** Conceptual suggestions for alternative processes for wastewater treatment and energy recovery

service to society. The MFC step, unlike AD, needs to be fuelled by more hydrolyzed biomass, such as VFA. In fact, suspended and particulate organic matter is difficult to process because it can cause clogging of the system, which poses a serious threat to technical operations. In contrast, the AD system is able of dealing with either suspended or particulate waste streams.

Direct benefits of using the suggested integrated system as an alternative to the usual aerobic treatment could be the lack of need for aeration and the recovery of electrical energy useful for the wastewater plant, saving in this manner the energy cost. In fact, aerobic treatments cost about  $0.4 \text{ € kg}^{-1} \text{ COD removed}$ . In contrast, AD permits a slight positive balance thanks to the energy recovery, saving  $0.06 \text{ € kg}^{-1} \text{ COD removed}$ . MFC technology is in the middle at the moment, costing about  $0.29 \text{ € kg}^{-1} \text{ COD removed}$  [23].

The production of hydrogen and biogas at mesophilic temperatures, combined with no need for external electrical energy input, permits the energy sustainability of the production process. An MFC completes the  $\text{H}_2 + \text{CH}_4$  gas production system, contributing to lowering the energy costs of AD technology, even if the power density generation is low ( $\sim 10 \text{ mW/L anode}$ ). This integration could be a promising challenge for organic waste residues because its implementation can give a positive energy contribution, after, however, ensuring an adequate disposal system. The TSAD process integrated with MFC technology could increase the efficiency of harvesting the energy embedded in the substrate as chemical bonds into  $\text{H}_2$  and  $\text{CH}_4$ , compared with the standard anaerobic process for biogas production.

## 7.5 Experimental Study

Here, two case studies are reported:  $\text{H}_2$  and electricity production by MFC using sodium acetate as fuel; this choice is aimed, in the first instance, to simulate the treatment of metabolite residues obtained at the end of  $\text{H}_2$  production by dark fermentation.

### 7.5.1 Production of H<sub>2</sub> from Acetate by MEC

A MEC prototype made of two Plexiglas frames (8 cm × 8 cm × 2 cm per frame) was used; the total reactor volume of 0.256 L is the sum of the total anodic and cathodic compartments both connected with a recirculation vessel, as showed in Fig. 7.9. The anode and cathode frames were completely filled with granular graphite and connected to the external electric circuit with a graphite rod (5 mm diameter, Morgan, Belgium). A CEM (Ultrex CMI7000, Membranes International Inc.) was used to separate the anode and the cathode chambers. The medium contained 6 g L<sup>-1</sup> Na<sub>2</sub>HPO<sub>4</sub> · 2H<sub>2</sub>O, 3 g L<sup>-1</sup> KH<sub>2</sub>PO<sub>4</sub>, 0.2 g L<sup>-1</sup> MgSO<sub>4</sub> · 7H<sub>2</sub>O, 0.1 g NH<sub>4</sub>Cl, 0.0146 g L<sup>-1</sup> CaCl<sub>2</sub> and trace elements; 1 g of sodium acetate (C<sub>2</sub>H<sub>3</sub>O<sub>2</sub>Na) was fed in discontinuous mode to the anodic frame upon depletion. Peristaltic pumps (Watson Marlow) were used to circulate the anodic and cathodic liquid at 6 L day<sup>-1</sup>. The external vessel of the anodic compartment was inoculated with 10 mL anaerobic sludge, taken from the anode of running MFCs in order to have a conversion of acetate into H<sub>2</sub>; tests were performed at room temperature (22 ± 2 °C). A power supply was used to obtain an applied voltage of 800 ± 2 mV. The current was measured by placing a 1.07 Ω resistor in the electrical circuit. A data acquisition unit (HP 34970A, Agilent, USA) was used to record voltage and current every minute. The coulombic H<sub>2</sub> recovery was calculated as the ratio of the actual current produced and the theoretical one obtainable from the substrate. The gas volume was measured with a water replacement method, while the composition of the gas produced, methane and carbon dioxide, was analyzed with an Intersmat IGC 120MB gas chromatograph; the qualitative hydrogen presence was determined by a H<sub>2</sub> sensor (OPUS, Zellweger Analytics, UK). Polarization curves were obtained with a potentiostat at a scan rate of 0.2 mV s<sup>-1</sup> after an open circuit stabilization of 15 min.

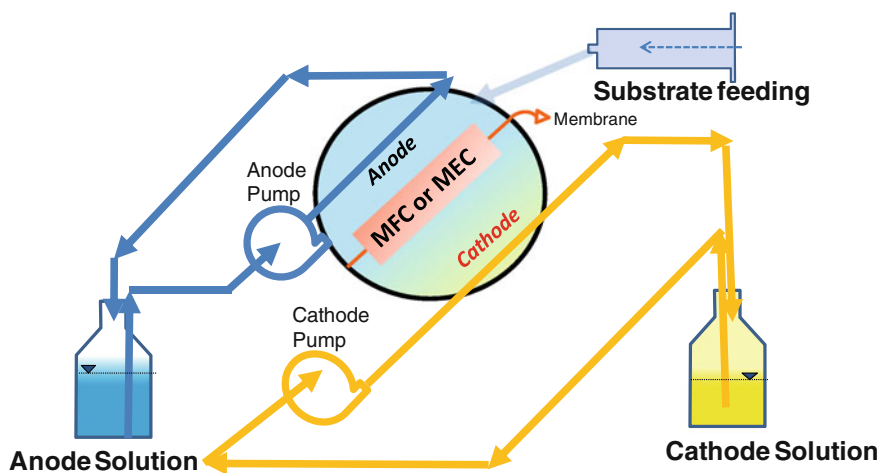


**Fig. 7.9** Schematic overview of an MFC or MEC with anode and cathode chamber connected with a recirculation pump and separated by CEM membrane

### 7.5.1.1 Experimental Results

Figure 7.10 shows that after 2 days of lag phase the number of moles of electrons (Coulombs) sharply increases, and the cumulative H<sub>2</sub> production follows the same curve. This is due to the direct proportionality between Coulombs (mol e<sup>-</sup>) and hydrogen. The coulombic H<sub>2</sub> recovery expresses the recovery of electrons as current generated over the amount of electrons dosed as sodium acetate, which is 84.4 %. The generated current recorded  $I(t)$  was used to calculate the amount of electron recovery versus time. Sodium acetate was oxidized in the bioanode by microorganisms while H<sub>2</sub> was electrochemically produced in the cathode. The following half reactions describe the reactions occurring:

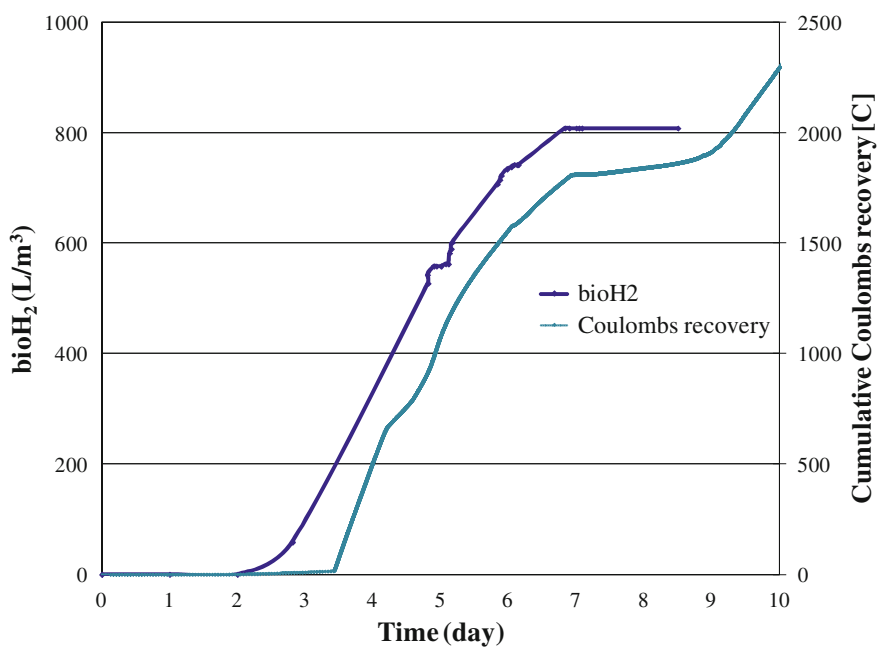
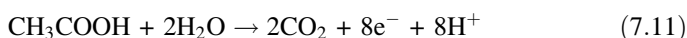
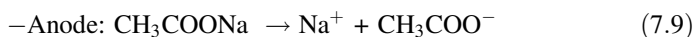


**Fig. 7.10** Cumulative chemical H<sub>2</sub> and Coulomb production in MEC test batch-fed with sodium acetate

**Table 7.2** Experimental yield and efficiency of MEC tested

Efficiencies of the MEC	
$Y_{H_2}$	2.4 mol <sub>H<sub>2</sub></sub> /mol <sub>Sodium acetate</sub> or 5.31 g <sub>H<sub>2</sub></sub> /g <sub>Sodium acetate</sub>
$\eta_{H_2} = Y_{H_2}/Y_{\text{theoretical}}$	60 %
Theoretical $V_{H_2}$	0.29 L
$V_{H_2}$ obtained	0.21 L
$\eta_{\text{vol } H_2} = V_{H_2, \text{obtained}}/V_{H_2, \text{theoretical}}$	70.69 %

Other process efficiencies are indicated in Table 7.2: the high coulombic H<sub>2</sub> recovery, based on the amount of substrate consumed, demonstrates that sodium acetate is a good substrate as electron donor at ambient temperature also.

The CEM proved to be very useful into achieve a high flux of H<sup>+</sup> protons from anode to cathode. The CEM used in a MEC produces relative pure hydrogen gas at the cathode [30]. The CEM, however, causes a higher ohmic cell resistance and a build-up of a pH gradient across the membrane, causing a lower current production for a given applied cell voltage [6, 31] with such an alkalization effect, more dominant in poorly buffered solution. When the CEM is omitted in the MEC, methanogenesis can easily become dominant and gas composed of carbon dioxide, hydrogen and methane is produced. Other tests conducted with the same configuration of Fig. 7.9 but without the separation with an ion-selective membrane (CEM) confirm the production of a high value H<sub>2</sub> + CH<sub>4</sub> gas; methane production in a MEC may also be more robust than hydrogen production.

Hence, an MEC (either with or without CEM membrane) installed after a conventional anaerobic digester to remove the residual organics present in the effluent of the digester could be a practical finishing step at ambient temperatures.

### 7.5.2 Production of Electricity from Acetate by MFCs

The MFC device used (Fig. 7.7) consists of two circular frames, anode and cathode; both compartments were made in polymethyl methacrylate (PMMA) with an internal diameter of 12 cm and thickness of 1.5 cm (internal volume for each chamber ~170 ml) separated by a robust cation exchange membrane (CEM, CMI 7000, Membranes International Inc., Glen Rock, NJ, USA). Carbon felts (soft felt SIGRATHERM GFA5, SGL Carbon, Germany) were used in both chambers as a planar anode electrode and assembled with a graphite rod (diameter 5 mm, SGL Carbon, Germany) to ensure an effective electron recovery capability. The experiments were conducted at room temperature (24 ± 2 °C). MFCs were inoculated in the anode chamber by sea water, previously enriched with subsequent culture inoculum in anaerobic conditions. The first 5 days of tests were conducted in batch mode, in order to permit the adaptation of bacteria to the new conditions inside the MFC. After the start-up period, MFCs were operated in semi-continuous mode (fed-batch)



using a syringe pump (NE-1600 Programmable Syringe Pump, USA) with HRT of 3 days and organic loading rate of  $1 \text{ g L}^{-1} \text{ day}^{-1}$ . The medium contained other nutrients such as  $\text{Na}_2\text{HPO}_4$ ,  $\text{NaH}_2\text{PO}_4$ ,  $\text{CH}_3\text{CO}_2\text{Na}$  and peptone, dissolved in a solvent comprising 30 % of distilled water and 70 % of filtered fresh sea water, in order to guarantee a good support of oligoelements and vitamins. The cathode compartment was filled with potassium ferricyanide ( $6.58 \text{ g L}^{-1}$ ), used as an oxidant compound, and a buffer solution of mineral salts  $\text{Na}_2\text{HPO}_4$  ( $8.2 \text{ g L}^{-1}$ ) and  $\text{NaH}_2\text{PO}_4$  ( $5.2 \text{ g L}^{-1}$ ). The mixing of the solutions at both anode and cathode chambers was obtained by the recirculation of anolyte and catholyte with a 500 mL reservoir, at a high flow rate ( $30 \text{ mL min}^{-1}$ ) by multichannel peristaltic pumps at both anode and cathode chambers (Peri-Star Pro 4 and 8 channel, USA, respectively).

Electrochemical experiments were run on a multi-channel potentiostat (BioLogic) in a two-electrode set-up configuration: a working and counter electrodes, inserted in anode and cathode positions, respectively. Measurements were recorded using EC-Lab<sup>®</sup> software version 10.1x (BioLogic) for data acquisition. Experiments were performed to measure cell open circuit voltage (OCV), current density and linear sweep voltammetry behavior, in order to gain information on the dynamics of electron transfer and, hence, on power generation. Polarization curves were measured at a scan rate of  $1 \text{ mV s}^{-1}$ . The power density was calculated from the  $I$ - $V$  curves by  $P = IV/v$ , where  $I$ ,  $V$  and  $v$  represent current, voltage output and medium anode volume, respectively. Furthermore, both anode potential (referred to Ag/AgCl electrode) and total MFC potential were continuously monitored for 1 month in open circuit voltage conditions and under resistances (1000, 820, 330, 220  $\Omega$ ), by using a Data Acquisition Unit (Agilent, 34972A). The current interrupt (CI) technique was used in order to obtain information on the internal resistance of the MFC and its dependence on electrode materials and operating conditions. The CI method was carried out using a perturbation to the system with a very short duration (50 ms); when the MFC produced a stable current output ( $I$ ) at fixed potential (0.30 V), the circuit was opened, and thus an initial steep potential ( $V_R$ ) was followed by a further slow increase in the potential ( $V_A$ ). The steep increase is related to the ohmic losses caused by the internal resistance ( $R_{\text{int}}$ ), which can be calculated as  $R_{\text{int}} = V_R/I$ . Carbon felt was used as the anode electrode because it exhibits high mechanical strength and good conductivity; furthermore, its plane structure reduces the distance between the two electrodes, improving MFC performance.

### 7.5.2.1 Experimental Results

The evolution of open circuit voltage and maximal power density ( $P_{\text{max}}$ ) over time was observed through polarization tests (Fig. 7.11). At the start, the uncolonized anodes were initially inactive and hence, during the first 5 days of operation, only the cell potential at OCV conditions was monitored, in order to avoid perturbation of the system, considering that in the first period only the acclimatization of bacteria to the new conditions inside MFCs occurs. After 5 days of operation, the operating voltage was increased to values greater than 0.3 V, indicating a successful start-up,

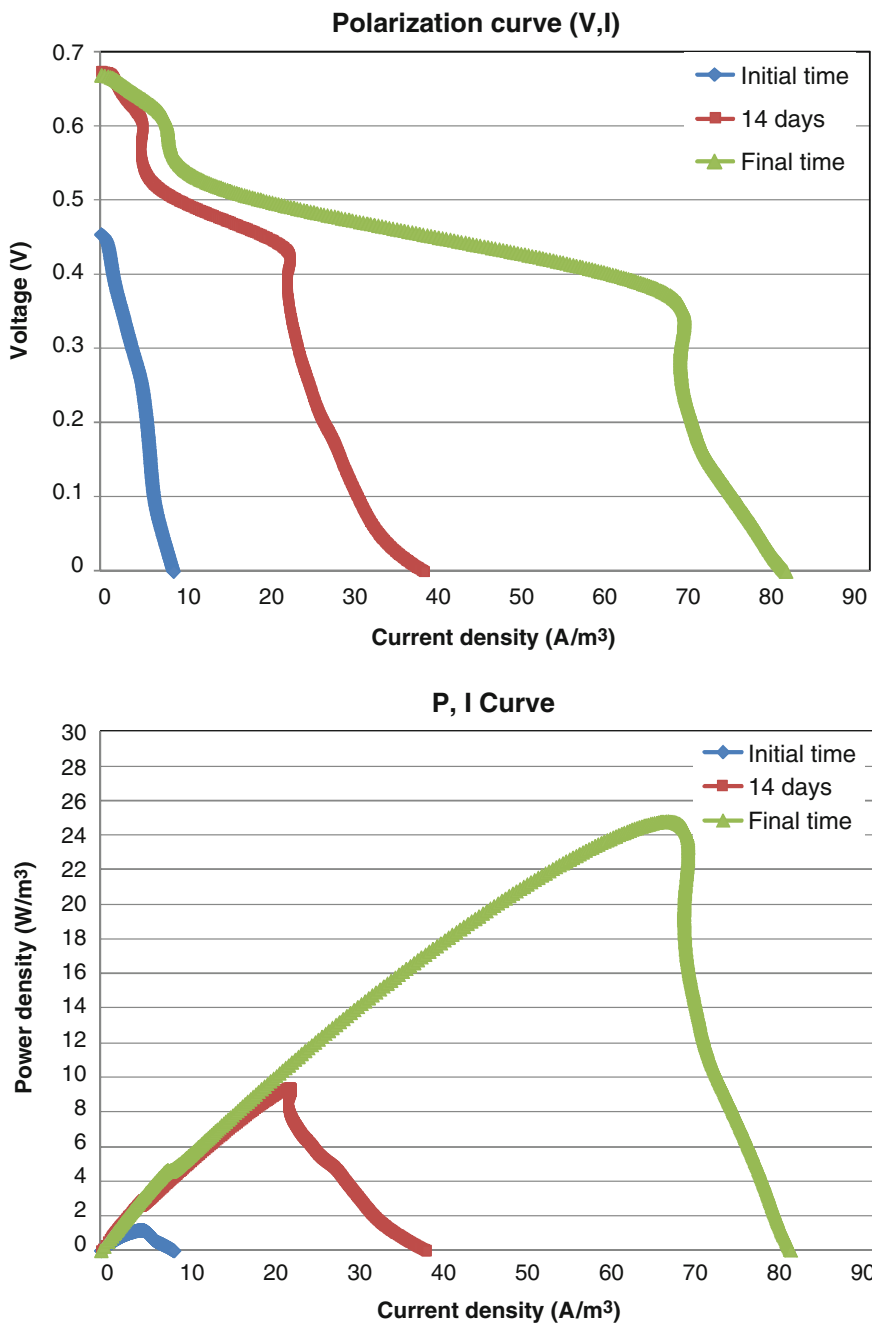


Fig. 7.11 *V-I* and *P-I* curves for the MFC with carbon felt as anode at the start time, after 14 days and final time of test running

**Table 7.3** Electrical parameters during time course of MFC test

Time (days)	OCV	$P_{\max}$ (mW)	$P_{\max}$ ( $\text{mW m}^{-2}$ )	$P_{\max}$ ( $\text{W m}^{-3}$ )	$I_{\text{SCC}}$ ( $\text{mA m}^{-2}$ )	$R_{\text{int}}$ ( $\Omega$ )
0	0.45	0.2	18	1.2	127.0	37.4
3	0.68	1.4	134.6	8.3	603.7	7.4
14	0.67	4.2	373.0	24.8	1204.3	7.4
27	0.71	3.3	290.0	19.3	920.5	6.5

confirmed also by the turbidity of the anode compartments. The internal resistance was determined using the CI method; accordingly to the  $I$ - $V$  curves, the internal resistances decreased by about 14 % between the start time and the 10th day. This reduction can be explained by the growth of reducing microorganisms at the anode, which colonize the electrode material creating a biofilm on the carbon felt surface.

Colonization improves the electron transport mechanisms between cell membrane and anode and hence reduces the internal resistance, which limits the current output. Carbon felt gives the best performance in terms of maximal power output ( $P_{\max}$ ), reaching a value of about  $25 \text{ W m}^{-3}$  after 14 days (Table 7.3). The results are in accordance with other results obtained using mixed populations [32]; moreover, stable operating conditions were successfully achieved after 10 days and for more than 3 months of test running. As a consequence, the internal resistances decreased about fivefold ( $\sim 83$  %) compared with the initial values, with a positive effect on the current and power densities (Table 7.3). This is a well-known issue with the CI method, since MFCs are bio-electrochemical systems in which the polarization resistance associated with the microbial activity is not negligible compared to the ohmic resistance.

Linear sweep voltammetry measurements were carried out 1 h after the replacement of fresh acetate medium at the anode and reducing cathode solution, when the power generation returned to a steady value. Moreover, good maintenance of fresh reagents in both chambers proved to be extremely important; some effects were revealed even if anolyte and catholyte recirculation was continuously applied to guarantee reduction of the influence of environmental factors, maintaining constant operating conditions (such as substrate concentration and pH) and facilitating mass transfer. For example, short circuit current ( $I_{\text{SCC}}$ ) increased about six-fold after refilling, reaching  $173 \text{ A m}_{\text{anode}}^{-3}$  ( $2.6 \text{ A m}^{-2}$ ), and OCV changed from 0.54 to 0.61 V. The huge increase of current is due to the reactivation of bacteria metabolisms after famine conditions due to depletion of the fuel, which is mainly glucose, with the consequent release of electrons to the anode. Consequently, the power output also tripled, reaching  $31 \text{ W m}_{\text{anode}}^{-3}$  ( $\sim 0.5 \text{ W m}^{-2}$ ).

One of the most important parameter in evaluating MFC performance is the energy. Energy is expressed either in joules (J) or kilowatt-hours (kWh), and it can be calculated by multiplying power by time. Over a period of 1 month, changing the resistances step by step from 1,000 to 220  $\Omega$ , an energy value of 600 J ( $3.5 \text{ kJ/L}_{\text{anode}}$  or  $3.5 \text{ MJ/m}_{\text{anode}}^3$ ) was recovered in the present test.

Bearing in mind that 1 kWh = 3.6 MJ, a MFC in 1 month can produce 0.17 Wh with an energy density of  $\sim 1 \text{ Wh/L}_{\text{anode}}$  and  $1 \text{ kWh/m}_{\text{anode}}^3$ .

This analysis shows the distance towards achieving positive energy performances using MFC technology.

## 7.6 Conclusion

Different biological routes to further increase the overall balance of bioenergy production are briefly presented in this chapter; routes that vary from conventional AD to novel biofuel cells, underlining the role of MFCs and microbial electrolysis cells in an integrated system.

Considering that the net energy balance of biological H<sub>2</sub> production via dark fermentation cannot be positive, an integrated system producing H<sub>2</sub>, CH<sub>4</sub> and electrical energy via MFCs could be a promising challenger in the use of organic waste as an energy-positive waste treatment system. The two-step AD process, integrated with MFC technology, can increase the global energy efficiency of using organic wastes relative to the standard anaerobic process for biogas production.

## References

1. P.C. Hallenbeck, Fermentative hydrogen production: principles, progress and prognosis. *Int. J. Hydrogen Energy* **34**, 7379–7389 (2009)
2. K. Nath, M. Muthukumar, A. Kumar, D. Das, Kinetics of two-stage fermentation process for the production of hydrogen. *Int. J. Hydrogen Energy* **33**, 1195–1203 (2008)
3. S. Hoekema, R.D. Douma, M. Janssen, J. Tramper, R.H. Wijffels, Controlling light-use by *Rhodobacter capsulatus* continuous cultures in a flat-panel photobioreactor. *Biotechnol. Bioeng.* **95**(4), 613–626 (2006)
4. B. Logan, *Microbial Fuel Cells* (Wiley, Hoboken, 2008)
5. P. Clauwaert, Electrodes as electron donors for microbial reduction processes. Ph.D. thesis, Ghent University, Belgium (2009)
6. P. Clauwaert, W. Verstraete, Methanogenesis in membraneless microbial electrolysis cells. *Appl. Microbiol. Biotechnol.* **82**, 829–836 (2008)
7. A. Veit, M. Kalim Akhtar, T. Mizutani, P.R. Jones, Constructing and testing the thermodynamic limits of synthetic NAD[P]H: H<sub>2</sub> pathways. *Microb. Biotechnol.* **1**(5), 382–394 (2008)
8. R. Arechederra, S.D. Minter, Organelle-based biofuel cells: immobilized mitochondria on carbon paper electrodes. *Electrochim. Acta* **53**, 6698–6703 (2008)
9. A. Heller, Miniature biofuel cells. *Phys. Chem. Chem. Phys.* **6**, 209–216 (2004)
10. J. Kim, H. Jia, P. Wang, Challenges in biocatalysts for enzyme-based biofuel cells. *Biotechnol. Adv.* **24**, 296–308 (2006)
11. N. Mano, F. Mao, A. Heller, Characteristics of a miniature compartment-less glucose-O<sub>2</sub> biofuel cell and its operation in a living plant. *J. Am. Chem. Soc.* **125**, 6588–6595 (2003)
12. B.E. Logan, B. Homelers, R. Rozendal, U. Schröder, J. Keller, S. Freguia, P. Aeterman, W. Verstraete, K. Rabaey, Microbial fuel cells: methodology and technology. *Environ. Sci. Technol.* **40**(17), 5181–5192 (2006)

13. T. Tommasi, B. Ruggeri, S. Sanfilippo, Energy valorization of residues of dark anaerobic production of hydrogen. *J. Clean. Prod.* **34**, 91–97 (2012)
14. P. Aelterman, K. Rabaey, P. Clauwaert, W. Verstraete, Microbial fuel cell for wastewater treatment. *Water Sci. Technol.* **54**, 9–15 (2006)
15. S. Venkata Mohan, S. Srikanth, G. Velvizhi, M. Lenin Babu, in *Chapter 14: Microbial Fuel Cells for Sustainable Bioenergy Generation: Principles and Perspective Applications*, ed. by V.K. Gupta, M.G. Tuohy. *Biofuel Technologies* (Springer, Heidelberg, 2013), pp. 335–368
16. U. Schröder, Anodic electron transfer mechanisms in microbial fuel cells and their energy efficiency. *Phys. Chem. Chem. Phys.* **9**, 2619–2629 (2007)
17. P. Aelterman, K. Rabaey, H.T. Pham, N. Boon, W. Verstraete, Continuous electricity generation at high voltages and currents using stacked microbial fuel cells. *Environ. Sci. Technol.* **40**, 3388–3394 (2006)
18. P. Aelterman, K. Rabaey, L. De Schampelaire, P. Clauwaert, N. Boon, W. Verstraete, in *Microbial Fuel Cell as an Engineered Ecosystem*, ed. by J. Wall, C.S. Harwood, A.L. Demain. *Bioenergy* (ASM, Washington DC, 2008), pp. 307–320
19. B.E. Logan, J.M. Regan, Microbial challenges and applications. *Environ. Sci. Technol.* **40**, 5172–5180 (2006)
20. D.R. Lovley, Bug juice: harvesting electricity with microorganisms. *Nat. Rev. Microbiol.* **4**, 497–508 (2006)
21. K. Rabaey, N. Boon, S.D. Siciliano, M. Verhaege, W. Verstraete, Biofuel cells select for microbial consortia that self-mediate electron transfer. *Appl. Environ. Microbiol.* **70**, 5373–5382 (2004)
22. G.T. Kim, M.S. Hyun, I.S. Chang, H.J. Kim, H.S. Park, B.H. Kim, S.D. Kim, J.W.T. Wimpenny, A.J. Weightman, Dissimilatory Fe(III) reduction by an electrochemically active lactic acid bacterium phylogenetically related to *Enterococcus gallinarum* isolated from submerged soil. *J. Appl. Microbiol.* **99**, 978–987 (2005)
23. P. Aelterman, Microbial fuel cells for the treatment of waste streams with energy recovery. Ph. D. thesis, Gent University Belgium (2009)
24. D. Hidalgo, T. Tommasi, V. Cauda, S. Porro, A. Chiodoni, K. Bejtka, B. Ruggeri, Streamlining of commercial Berl saddles: a new material to improve the performance of microbial fuel cells. *Energy* **71**, 615–623 (2014)
25. J.B. Benziger, M.B. Satterfield, W.H.J. Hogarth, J.P. Nehlsen, I.G. Kevrekidis, The power performance curve for engineering analysis of fuel cells. *J. Power Sources* **155**, 272–285 (2006)
26. P. Liang, X. Huang, M.Z. Fan, X.X. Cao, C. Wang, Composition and distribution of internal resistance in three types of microbial fuel cells. *Appl. Microbiol. Biotechnol.* **77**, 551–558 (2007)
27. P. Clauwaert, P. Aelterman, T.H. Pham, L. De Schampelaire, M. Carballa, K. Rabaey, W. Verstraete, Minimizing losses in bio-electrochemical systems: the road to applications. *Appl. Microbiol. Biotechnol.* **79**, 901–913 (2008)
28. P. Aelterman, M. Versichele, M. Marzorati, N. Boon, W. Verstraete, Loading rate and external resistance control the electricity generation of microbial fuel cells with different three-dimensional anodes. *Bioresour. Technol.* **99**, 8895–8902 (2008)
29. T. Tommasi, A. Chiolerio, M. Crepaldi, D. Demarchi, A microbial fuel cell powering an all-digital piezoresistive wireless sensor system. *Microsyst. Technol.* **20**, 1023–1033 (2014)
30. R.A. Rozendal, H.V.M. Vamalers, C.J.N. Buisman, Effects of membrane cation transport on pH and microbial fuel cell performance. *Environ. Sci. Technol.* **40**, 5206–5211 (2006)
31. D. Call, B.E. Logan, Hydrogen production in a single chamber microbial electrolysis cell (MEC) lacking a membrane. *Environ. Sci. Technol.* **42**, 3401–3406 (2008)
32. P. Aelterman, K. Rabaey, P. Clauwaert, W. Verstraete, Microbial fuel cells for wastewater treatment, *Water Sci. Technol.* **54**(8), 9–15 (2006)

# Chapter 8

## Two-Step Anaerobic Digestion Process

In this chapter the valorization of the liquid end-products of  $H_2$  production under anaerobic digestion (AD) will be considered in order to increase the quantity of energy produced via methane dark fermentation, which is a well-established technology with several full-plant applications around the world. After an introduction to the fundamentals of so-called two-step anaerobic digestion (TSAD), some experimental results will be provided in order to demonstrate the feasibility of TSAD. The effect of the main engineering parameters in the process will be elucidated as well as the experimental results in batch and continuous modes. TSAD is an attractive technology in the panorama of renewable energy production using organic wastes. A final consideration of the scale-up procedure will be explained and discussed.

### 8.1 Introduction

Anaerobic digestion (AD) is one of the most promising technologies able to synchronize human activities with natural cycles; in fact, it is able to digest organic matter to produce energy and an organic byproduct with possible use in agriculture. AD is quite widespread in Europe and today it is able to produce 8.3 Mtoe (megatonnes of oil equivalent) of energy [1], which represents approximately 0.4 % of the 1,703 Mtoe of primary energy consumption of the 27 countries of the European Union in 2009 [2]. In order to widen and effectively display the potentiality of this technology, many problems had to be solved. Considering that approximately 120–140 million tonnes of biowaste are produced every year in the EU [3] and a tonne of refuse is able to produce 0.5–0.7  $N\ m^3$  of biogas, with a mean value of 60 % of methane, it is possible to obtain approximately 40 Mtoe of primary energy. In addition, by using the biogas produced by treatment of the refuse of pig and cattle breeding farms and meat manufacturing, an additional 12.5 Mtoe can be obtained [4], which means a potential of 52.5 Mtoe, six times the actual value. Despite appearances, many different bottlenecks need to be solved to implement the use of AD. For example, several technical problems such as mixing, foam formation,

pumping the inlet and the outlet streams, and the dimensions and the typology (liquid, solid, semi-solid) of the bioreactor for such types of refuse. Moreover, at the territorial scale, the options of decentralized versus centralized treatment plants poses many social and logistic problems in the diffusion of the technology. The main obstacle to the penetration of the technology is in regard to investment and running costs. The question is how a new generation of AD technology can be devised in order to move towards the solution of such problems.

AD, from a biological point of view, is a complex multistep process that involves the action of multiple microbes and several gaseous and liquid products, and thus strict process control and product purification are required; nevertheless, it is a classical anaerobic bioconversion process that has been practiced for over a century and used in full-scale facilities worldwide [5].

The introduction of multi-stage AD processes was intended to improve digestion by having separate reactors for the different stages of AD, i.e. providing flexibility to optimize each reaction in order to increase the process performances, primarily the energy produced. Today a system comprising two reactors is suggested: the first one is for hydrolysis/liquefaction–acetogenesis, and the second for methanogenesis. This approach, in the authors' opinion, is not adequate because it does not consider the optimization of all the AD biochemical stages, particularly the synergic actions of acetogenic and methanogenic microbes.

Generally, such a process contains a particular step, the so-called rate-limiting step, which is the slowest and thus limits the rate of the overall process. However, the rate-limiting step is not always the same over a wide range of operating conditions; in the case of AD it depends mainly on the waste characteristics. It is generally accepted that the content of lignocellulose structures determines the extension of AD. In principle, the multi-step process can overcome the problem of the rate-limiting step due to the possibility of working under different conditions in each step, optimizing each single stage involved in the AD. AD comprises three main biological steps, hydrolysis, acidogenesis and methanogenesis, and it is necessary to optimize all of them. Since most refuse is limited by the rate of cellulose hydrolysis, a greater attention to this step is required. Several pretreatment processes of different natures were reported and analyzed in Chap. 6. The new approach in AD, in addition to the pretreatments, consists of separating the biological chain of acetogenesis and methanogenesis in two different bioreactors. TSAD consists of the separation of the natural ecology and metabolism of an anaerobic bacteria consortium into two distinct classes: hydrogen-producing bacteria (HPB), mainly *Clostridium*, and hydrogen-consuming bacteria (HCB), methanogens.

The idea of the coproduction of hydrogen and methane from biomass was first proposed in the late 1990s. The advance of research progress in TSAD, in which biohydrogen and biomethane are produced by fermentation in different reactors, has increased during recent years. Several researchers have directed their interest to the TSAD process [6–9] and this topic is increasing in importance in the scientific literature. Research is based on different feeding substrates, classified as sugar-rich biomass, cellulose and lignocellulose-based biomasses.

To the authors' knowledge, there have been almost 50 publications in total to date. A TSAD process enables a more flexible operation and a higher energy yield than a one-step AD, through a separation of acidogenesis with  $H_2$  production from methanogenesis with  $CH_4$  production. TSAD is obtainable by the enrichment of specific microorganisms in each stage, HPB in the first stage and HCB in the second [10]. This generally increases the process stability and in continuous mode a short hydraulic retention time (HRT) is necessary. In the first stage a low HRT is necessary to wash out the methanogens, while a relatively long HRT is maintained for the second stage to ensure sufficient time for the slow-growing methanogens [11] and to prevent overloading and accumulation of toxic substances. Generally the HRT of the second stage of TSAD is lower than that of a one-stage AD. Other attractive attributes of such TSADs include better decomposition of lignocellulose contents in organic refuses and more effective pathogen destruction in the hydrolysis/acidification stage. Despite the high performance and great potential of TSAD, however, there are several hurdles remaining [12]. For the hydrolysis/acidification as a hybrid first stage, the necessity to strengthen the competitiveness of HPB over hydrolyzing ones to improve VFA production remains an open issue.

On the other hand, the literature has seldom given general and exhaustive explanations supporting TSAD, often limiting efforts to particular case studies, with particular substrate types and operational conditions. In particular, few studies take into account the overall potential energy recovery of TSAD compared to one-stage AD, focusing on the reasons and the conditions for actual enhancement of energy recovery by metabolic phase separation. The reasons for the success of a TSAD system were associated, generally, with process advantages, such as higher efficiency in converting VFA into methane in the second stage and significantly higher hydrolysis efficiency after the hydrogen production step, with the increase in soluble organic matter allowing higher productivity in the second stage [13]. Other beneficial effects of TSAD lie in higher degradation kinetics and in the minimization of loss of reactant, as for example the feed-out issue, which often occurs in single-stage AD as the consequence of not ideally mixed bioreactors due to a bypass of feeding substrate. In other words, the reactor cascade approach is more similar to the ideal continuous stirred tank reactor (CSTR).

In addition, a mixture of hydrogen and methane has recently received extensive attention as a vehicle fuel, although *hythane* was recently trademarked [14]. Methane is considered to be a clean fuel for vehicle use compared to gasoline or diesel, even if its limitation is its narrow flammability range with poor combustion efficiency and an intensive energy requirement for ignition of  $CH_4$ -powered vehicles. It is, however, a slow burning-speed fuel with a high ignition temperature. Hydrogen perfectly complements the weak points of methane because it increases the H/C ratio, decreasing the  $CO_2$  emission per unit of energy produced, so it improves the fuel efficiency, extending the narrow range of flammability, reducing combustion duration and improving heat efficiency; the engine is easy to ignite with less input energy. Thus hythane, which has been developed as a high-value gas fuel for vehicles, combines the advantages of hydrogen and methane. Studies on mixtures of hydrogen and methane have been carried out [15] focusing on combustion



properties as means for optimizing the fuel efficiency of hythane. However, the independent production of hydrogen and methane from fossil-based material is unsustainable; the bioprocess is an alternative to fossil-based process. Biological hydrogen and methane production from renewable biomass such as organic refuses via fermentation possesses, instead, the advantage of sustainability over fossil-based processes, even though a down-stream approach is necessary for the purification of the biogas containing hydrogen and methane to form the optimal fuel blend of hythane. However, hydrogen is not freely available as a fuel and it must be generated from hydrogen-rich sources. Over 97 % of the world's hydrogen demand is now being derived from fossil fuels, with a net negative energy gain negating some of hydrogen's advantages. In order to consider hydrogen as a sustainable alternative fuel to replace fossil fuels, it is necessary to produce it from cheap and readily available renewable feedstock, via processes that can yield as high a net energy gain as possible. TSAD has the potential to generate hydrogen and methane from renewable feedstocks. In the previous chapters, the feasibility of biohydrogen production from organic waste streams has been demonstrated. The use of organic waste streams to produce biohydrogen and biomethane as a fuel could be a sustainable approach, because energy production and waste stabilization could be accomplished simultaneously. A modified form of the AD process (TSAD) plus a pretreatment step is here given as a candidate process with the greatest potential, due to its higher rate and its unique ability to utilize organic wastes as feedstock.

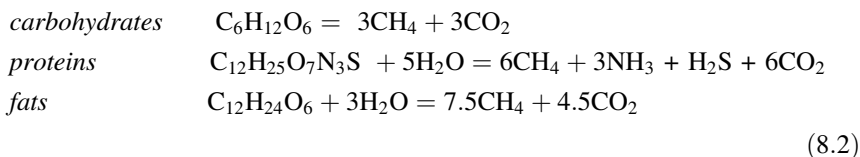
Even though promising features of TSAD technology already exist, a deeper knowledge of the fundamentals of biochemical and chemical principles and on the technological barriers of TSAD is necessary to overcome obstacles to the full-scale application of the process.

## 8.2 Scientific Rationale of TSAD

AD presents several advantages as a means for disposing of organic refuses, mainly due to the possibility of working at low-temperature ranges, to its stable operation under continuous mode [16], and to its ability to produce a suitable quantity of energy independently from light, assuring in this manner biogas production throughout the whole 24 h. In addition, AD technology has gained great experience thanks to full-scale applications around the world. The stoichiometry of the formation of methane from biomass follows the following general equation:



where  $\alpha = 1/4(4c - h - 2o + 3n + 2s)$  and  $\beta = 1/8(4c + h - 2o - 3n - 2s)$ ; considering the main organic constituents of an organic refuse, three stoichiometry equations can be written:



If one considers glucose as the most easily fermentable substance, the maximum allowable energy is 2,401 kJ/mol of utilized glucose, taking into account a LHV of methane of 800.32 kJ/mol; this represents a theoretical efficiency of 84 % with a LHV of glucose of 2,872 kJ/mol.

In the case of TSAD, the stoichiometric reactions (8.3) and (8.4) can be written with yields of 4 and 2 mol<sub>H<sub>2</sub></sub>/mol<sub>Glu</sub>, respectively, from a stoichiometric point of view, assuming that either the acetic or the butyric pathways are followed to produce H<sub>2</sub>, with acetate or butyrate as the only main sub-product and considering the stoichiometry conversion of both acetate and butyrate into methane and carbon dioxide:



This means a recovery of 89 and 86.3 % of the energy embedded in glucose in the case of only the acetic or only the butyric route, respectively. In both cases the recovered energy is higher than in the case of one-stage AD with only methanation: values 5 and 2.3 % higher are reached, respectively.

AD is a complex process and the above equations represent only a mass balance. AD fermentation can be divided into several phases, as is generally accepted. In each phase one metabolic group of microorganisms is more active than the others, driving the sequential action: hydrolytic-fermentative bacteria, acidogenic bacteria, aceticlastic methanogens, and hydrogenotrophic methanogens. Proton-reducing acidogenic bacteria produce hydrogen, acetic and butyric acids, as well as many other organic compounds (see previous chapters). Some acetogens utilize hydrogen to produce acetate in so-called *homoacetogenesis*. In the last step, methane is produced by methanogens, which are members of the Archaea: *Methanobacteriales*, *Methanococcales*, *Methanomicrobiales*, *Methanosarcinales*, and *Methanopyrales* [17]. They can be separated into three main categories, which use different substrates to produce methane: (i) the hydrogenotrophs, which use hydrogen and carbon dioxide; (ii) the methylotrophs, which use methylamines, dimethylsulfide and methanol; and (iii) the acetotrophs, which utilize acetate to produce methane. However, some species share different nutrient requirements and cannot be placed in a single category, e.g. *Methanosarcina* spp. are the most metabolically diversified and *Methanosaeta* spp. can only use acetate. The ecological diversity of methanogens is detailed in [18]. The syntrophic association of hydrogenotrophic methanogens with hydrogen-producing acetogens, for hydrogen transfer, is energetically favorable in metabolic conversion for the production of methane; it is possible only if the microorganisms are closely attached. The AD research

community largely accepts that about 30 % of the methane produced is due to the interspecies hydrogen transfer [19] mechanism, while the remaining methane is produced using other substrates. The optimum pH for methane-forming bacteria is 6.7–7.5; only *Methanosarcina* spp. are able to be active at a pH below 6.5, while the metabolisms of different methanogens are substantially suppressed at low pH [19]. The interactions of microorganisms in anaerobic systems sketched above are reviewed and superbly detailed in [20], which describes the use of different molecular techniques available nowadays. Examples are quantitative real-time polymerase chain reaction (rt-PCR) assays to analyze anaerobic microbial consortia, which in the authors' opinion, could be of great help to engineers in designing and controlling AD processes. As stated above, hydrogen is the key intermediate in anaerobic consortium activity. In the last decade much research attention has been directed to hydrogen production and its use, especially on dark fermentation for biological hydrogen production; this has produced a large contribution to the knowledge of acid fermentation. The key point for acidogenic fermentation to produce hydrogen is the separation of the HPB from the HCB in the anaerobic microorganism consortium: this can be achieved using several approaches, as reviewed in [21], but in TSAD the problem is how to maintain the different species for sufficient time in a batch process or for a long time in a continuous one. As reported in Chap. 2, the main affecting parameter is the pH, either in the selection of the HPB or for the activity of the consortium. The microorganism species present in large proportion in the HPB consortium (responsible for H<sub>2</sub> production) are predominantly *Clostridium* spp., with Enterobacteriaceae and *Streptococcus bovis*, together with 7–10 % of unidentified affiliated species. The metabolites most commonly formed during H<sub>2</sub> fermentation are acetate, propionate, butyrate, ethanol, butanol and others at lower concentrations, indicating that acidogenic as well as acetogenic phases are present.

The use of mixed microflora of HPB is an imperative in the case of complex waste material, because it may provide a useful combination of metabolic pathways supporting the more efficient decomposition and hydrogenation of the biomass, compared with pure bacterial species. Also in this case, the use of real-time PCR is an efficient tool in the evaluation of the HPB community and helps in controlling an industrial reaction of a fermentative system. The study of the bacterial evolution in consortia is in its infancy, but some suggestions on the dynamics of interspecies bacteria are available [22]. As reported in Chap. 3, the pH variation during time is the main parameter affecting hydrogen production because the HPB do not adapt well to rapid changes in the environmental conditions. This might induce some metabolic alteration and subsequently an inhibition of H<sub>2</sub> production. In addition, a low pH is crucial for inhibition of methanogenesis and possibly of other H<sub>2</sub>-consuming microorganisms, such as acetogens. Conversely, it is well known that at pH < 4.5 hydrogen production shuts down due to the shift in metabolic pathways towards solventogenesis [23] with the production of acid at higher carbon content such as caproate and higher alcohols, and, most importantly, at low pH, the activity of hydrogenase, which is coupled with the electron shuttle Fd, stops. In general, hydrogenase activity uptake and turnover are low in cells maintained at pH < 5.2.

From a full-scale point of view, this emphasizes the necessity of pH control by an external control loop, in order to ensure that hydrogenogenesis proceeds. In conclusion, the influence of pH has been recognized as a key factor in the regulation of anaerobic consortium activity thanks to its multiple roles: regulation of hydrogenase activity, suppression of methanogen growth and switching towards solventogenesis. For all of these reasons, pH is the key parameter to be utilized in TSAD to separate HPB from HCB. Another important aspect in the case of continuous processes is the *kinetic selection* of microorganisms of high importance. As reported in Chap. 2, the maximum specific growth rate of the HPB consortium is approximately 4–5 times higher than that of HCB:  $\mu_{\max\text{HPB}} = 0.215 \text{ h}^{-1}$  and  $\mu_{\max\text{HCB}} = 0.055 \text{ h}^{-1}$ , although these are mean values due to the presence of different species in both consortia. The HCB need 4–5 times longer than the HPB to reproduce themselves. In order to clarify the use of kinetic selection we consider, for simplicity, a continuous stirred tank reactor (CSTR) containing only one bacterium species and only one organic substrate S. The mass balances for the substrate and the bacterium are:

$$dS/dt = -Y_{X/S}^{-1} \cdot \delta X/\delta t + Q/V \cdot (S_0 - S) \quad (8.5)$$

$$dX/dt = \delta X/\delta t - Q/V \cdot X \quad (8.6)$$

where the parameters are:

- $Y_{X/S}$  the yield of bacteria on the substrate [#]
- $S$  the concentration of the substrate in volume V [g/L]
- $S_0$  the concentration of the substrate in the feed [g/L]
- $X$  the concentration of the bacteria in volume V [g/L]
- $Q$  the feed flow rate [L/h]
- $V$  the volume of the reactor [L]
- $t$  the time [h].

Considering that bacterial growth follows Monod kinetics, Eqs. (8.5) and (8.6) in the steady-state condition become:

$$S_{SS} = K_S D / (\mu_{\max} - D); \quad X_{SS} = Y_{X/S} \cdot (S_0 - S_{SS}) \quad (8.7)$$

where  $\mu_{\max}$  is the maximum specific growth rate of the microorganisms and  $D$  is the dilution  $D = Q/V \text{ [h}^{-1}\text{]}$ , i.e. the inverse of the HRT, which under ideal mixing conditions coincides with the permanence time of the microorganisms in the reactor. From the first equation of (8.7), the more  $D$  approaches  $\mu_{\max}$ , the more  $S_{SS}$  approaches  $S_0$ , and hence  $X_{SS}$  approaches zero; this means that the bioreactor is moving to so-called *wash-out* conditions, where the microorganisms are no longer present in the bioreactor vessel and the bioreaction stops. The relationship between dilution  $D$  or *HRT* ( $\text{HRT} = D^{-1}$ ) and the microorganism concentration in a steady-state condition is shown in Fig. 8.1.

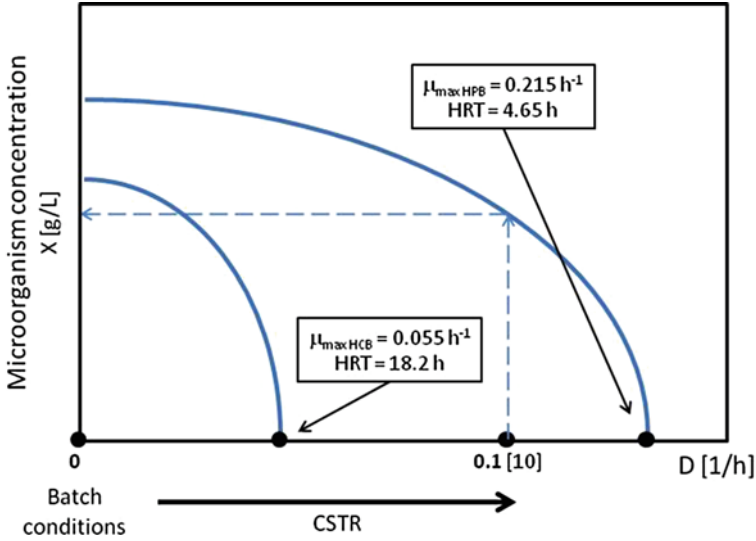


**Fig. 8.1** Visualization of kinetic selection between HPB and HCB

Consider now a situation similar to that shown in Fig. 8.1, where two microorganism species having different maximum specific growth rates are present. It is possible to produce two curves showing the steady-state conditions with different wash-out conditions. The wash-out occurs at HRT = 4.65 and 18.2 h for HPB and HCB, respectively; working with HRT = 10 h (Fig. 8.1), it is possible to have the HCB concentration equal to zero in the reactor, while the HPB concentration is non-zero, albeit lower than the concentration occurring in a batch reactor. Under these operational conditions, it is possible to separate the HPB population from the HCB one. It is important to remark that the above situation represents an ideal one, because both HPB and HCB are composed of a consortium of microorganisms which have different  $\mu_{\max}$ , therefore the HRT causing the wash-out is not a single value but has a more or less wide range, depending on the abundance of relative bacterial species in the consortium. If the outlet flow rate of a first reactor, working at HRT = 10 h, is used as the feed flow rate of a second larger reactor, with HRT = 18.2 h or higher, in the first reactor only a HPB consortium is present and produces biogas with a high hydrogen concentration, while the second reactor contains HCB and biogas rich in methane is produced. In this manner, the goal of separating different microorganism consortia of anaerobic bacteria could be reached. Although the above approach is valid, it is possible to evaluate the efficacy in the selection of HPB over HCB only by experiments, working under such HRT values. Some HRT values are given in Table 8.1 for an acidogenic reactor for different type of refuses producing a hydrogen-rich biogas. Experimental values are quite different from 4.65 h, ranging from 4 h to 4 days, for several reasons: firstly because HPB comprise several bacterial species having different growth rates, and mainly because the bacterial growth rate depends strongly on the nature of the

**Table 8.1** Hydraulic retention time (HRT) from several continuous reactors producing hydrogen

Material	HRT	References
Fruit and vegetable waste + swine manure	2 days	Schievano et al. [9]
Maize silage + swine manure	2.5 days	Schievano et al. [9]
Olive pomace + swine manure	2.5 days	Schievano et al. [9]
Waste rice flow + swine manure	2.5 days	Schievano et al. [9]
Molasses	3.9–10.5 h	Ren et al. [24]
Sucrose	12 h	Lin et al. [25]
Vegetable kitchen waste	4 days	Lee et al. [26]
Dairy waste water	4–6 h	Fang et al. [27]
Food waste leachate	3 days	Kim et al. [28]
Food waste	3 days	Chinellato et al. [29]
Garbage and waste paper	2.5–6 days	Kataoka et al. [30]
Food waste	1.3 days	Chu et al. [31]
Food waste	1.9 days	Lee and Chung [32]

substrate, hence some species could be favored and others could suffer some detrimental effects in the presence of a substrate having different components.

In fact, Lee and Chung [32] demonstrated the appearance of different bands under different HRTs for different substrates, by a bacterial community analysis in both hydrogen and methane reactors at steady-state conditions using genomic DNA extraction and polymerase chain reaction (PCR) sequencing. This demonstrates that the HRT and the substrate nature are important parameters able to determine the relative composition of the microbial communities in the reactor; in addition, in [33], *Thermoanaerobacterium thermosaccharolyticum* was identified as the dominant species, even with different substrates and HRTs, and so this microorganism is robust and can grow in different environmental conditions. Moreover in the same study the phylogenetic affiliation of the bacterial community was evaluated for methane reactors. The bacterial consortium converged into three phyla, *Firmicutes*, *Proteobacteria* and *Actinobacteria*, which are completely different from the communities present in hydrogen reactors; in addition the methane bacterial communities were different in the methane reactors of TSAD compared with one-stage processes. This could explain the different performances of the two processes. Evaluations for methane reactors of TSAD pointed out that the Archaeal bacterial distribution was similar for all conditions, indicating that Archaeal community structures were not affected by changes in substrates and HRT. Although the relative dominance of microorganisms did not change, the concentration of microorganisms and their activities might have been altered. The methanogen-dominant band analysis could be attributed to *Methanosarcina acetivorans* str, which belongs to the acetoclastic methanogens. *Methanosarcina* spp. was reported to be dominant at high acetate concentration [34], and the results were consistent with high acetate concentrations in the methane reactors of a TSAD. In this reactor, hydrogenotrophic methanogenesis activity was present, as the presence of *Methanoculleus* spp. demonstrated, being responsible for the methane pathway [35].

**Table 8.2** Hydraulic retention time (*HRT*) for methanation step in a TSAD process

Material	HRT (days)	References
Food waste	12	Chinellato et al. [29]
Garbage and waste paper	18–30	Kataoka et al. [30]
Food waste	5	Chu et al. [31]
Food waste	7.7	Lee and Chung [32]
Organic waste	12	Luo et al. [13]
Vegetable waste	8	Zuo et al. [36]
Food waste leachate	27	Kim et al. [28]

Table 8.2 reports some HRT values for the methanation phase of a TSAD from literature data. All the data given in Tables 8.1 and 8.2 refer to laboratory studies conducted by different researchers. To the authors' knowledge there are no full-plant applications of TSAD in service. Table 8.1 has more copious data than Table 8.2 thanks to the great interest in hydrogen production via dark AD in recent decades. A comparison between HRT mean values of 2.5 and 13.5 days for the first, acidogenic, and the second, methanogenic phases, respectively, shows that the volume of the first reactor is lower than the second one by 5.4 times or more. This is an important aspect, because the difference in volumes (and hence HRT) of reactors seems to influence the total energy produced [13]. The volume reduction of the methanogenic reactor reduces either the investment or the running costs of the whole plant. In this respect, it is interesting to compare the HRT of one-step AD with that of TSAD. The HRT of AD depends on many parameters such as the type of substrate, the concentration of organic matter in the feed, the type of reactor, the applied organic loading rate and the working temperature. The HRT of one-step AD ranges from 15 to 35 days or more, as reported in [19] and in Table 8.3.

Considering a HRT of 13.5 days, the mean value of the data reported in Table 8.2, the volume of the reactor might be three times lower, with a strong reduction of capital investment, energy and economic costs to run the plant.

Another important aspect concerns energy recovery in TSAD compared with one-stage AD. To date, only a few studies have focused on the reasons and the conditions to apply in order to enhance energy recovery by biological phase

**Table 8.3** HRT used for one-step AD (\*)

Substrate	Working temperature	HRT (days)
Slaughter waste	Thermophilic	40
Organic fraction of MSW	Thermophilic	40
Vegetable waste	Mesophilic	30–35
Silage	Mesophilic	32–35

(\*) Private communication by AUSTEP, a company specialized in designing and managing AD plants (<http://www.austep.com>)

separation. The most important contributions to these aspects came from [33, 37, 38]: the energy produced by TSAD was in the range of 20–30 % higher than the one-step AD, either in mesophilic or thermophilic conditions. The success of the TSAD system was associated, in general, with the advantages of higher efficiency in converting VFA into methane in the methanogenic reactor. Pakarinen et al. [38] suggest a significantly higher hydrolysis efficiency after the hydrogen production step, with the increase in soluble organic matter and VFA production through fermentation, allowing higher productivity of the methanogenic phase. More precisely, the higher energy production lies in higher degradation kinetics of VFA. More recently, [9] compared TSAD with one-stage AD using different refuses and found that energy recovery was in the range of 9–19 MJ/kg VS<sub>added</sub>; the overall energy was significantly higher (8–43 %) for the TSAD than one-step AD in the large majority of the laboratory experimental conditions tested. These preliminary results should drive further research to better understand the conditions for achieving higher performances using TSAD.

### 8.3 Energy Efficiency

Two energy parameters were used for evaluation of TSAD energy efficiency, considering both the energy produced as hydrogen in the first reactor and that produced as methane in the second reactor. The energy parameters used, already introduced in Chap. 5, are *energy conversion efficiency*  $\eta$ , the ratio of the quantity of energy that the bioreaction is able to extract as hydrogen plus methane to the amount of energy available embedded in the substrate, and the *efficacy*  $\zeta$ , comparing the energy conversion efficiency of TSAD to that obtained in a one-step AD process. The *efficacy* allows comparison of different processes aimed at increasing the value of the refuses in energy terms; in this case, it is sufficient for comparing TSAD against the one-step AD process. The *efficiency* can be evaluated as:

$$\eta = \text{Produced energy (H}_2 + \text{CH}_4) / \text{Initial energy embedded in the substrate} \times 100. \quad (8.8)$$

$\eta$  is a measure of the potential of the whole process, including the pretreatment, if present, and the bioreaction, to harvest the energy; while the *efficacy* in mathematical terms is:

$$\zeta = \frac{\eta_{TSAD}}{\eta_{one-step AD}} \quad (8.9)$$

The use of the efficacy parameter allows evaluation of the effectiveness of TSAD in comparison with different processes, such as one-step AD, in a simple and effective way.



## 8.4 Modeling of TSAD

A regression curve was built to characterize the experimental total gas production data, due to the great difficulties in the setting up of a real kinetic in the two-step process because of the presence of different bacterial species and the very complex chemical composition of the substrate. A cumulative gas production model per volume unit of fermentative broth was used. The regression model of Gompertz, suitable for description of the saturation phenomena, was suggested to this end. The cumulative total gas production was described with the following modified Gompertz model, with the boundary condition  $G = G_1 + G_2$ :

$$G = G_{1,\max} \exp \left\{ - \exp \left[ \frac{R_{1,\max} * e}{G_{1,\max}} (\lambda - t) + 1 \right] \right\} + G_{2,\max} \exp \left\{ - \exp \left[ \frac{R_{2,\max} * e}{G_{2,\max}} (\lambda - t) + 1 \right] \right\} \quad (8.10)$$

$G$  represents the cumulative volume of gas generated during time  $t$  as the sum of the hydrogen and methane contributions, and is evaluated at standard conditions (NL/L);  $R_{\max}$  (NL/Lh) is the gas production rate;  $G_{\max}$  (NL/L) is the total quantity of gas produced; subscripts 1 and 2 refer to methane and hydrogen, respectively;  $\lambda$  (h) is the lag phase duration. Equation 8.10 represents gas evolution over time as the contribution of the two gases; it is not able to give any significant insight into the biological evolution of methane and hydrogen, due to the empirical nature of the Gompertz model. Equation 8.10 can be used to estimate the five parameters  $G_{1,\max}$ ,  $R_{1,\max}$ ,  $G_{2,\max}$ ,  $R_{2,\max}$  and  $\lambda$  from experimental data points, using the means of the best-fit procedure of minimizing the squared sum of errors between the experimental data and the model.

## 8.5 Experimental Tests for H<sub>2</sub> and CH<sub>4</sub> Production

In the present section, the experimental tests are reported, one in batch mode and a second one in continuous mode, aimed at evaluating the feasibility of TSAD. The present experimental tests concern the production of hydrogen and methane by separation of the AD biological pathway conducted using two substrates: organic waste market (OWM) and coffee seed skin (CSS). Coffee production waste is, in fact, rich in lignocellulose material as representative of hard biodegradable substances. In both cases a pretreatment step was applied in order to favor the breakdown of the lignocellulose structures and to increase the biogas production.

### 8.5.1 Preparation and Pretreatment of the Feedstock

The OWM was obtained from a local fruit and vegetable market at the end of the day, and the CCS was provided by a coffee-producing firm as pellets of approximately 0.5 cm diameter and 1–2 cm length. Firstly, both OWM and CSS were crushed into semi-liquid paste and powder, respectively, by a kitchen blade mixer, then dispersed in tap water, with a dilution ratio of 1:2 and 1:15, respectively.

Table 8.4 reports the structural analysis of the CCS refuse together with some physical proprieties; the OWM composition was similar to the one reported in Table 6.6 and its LHV of  $17,680 \pm 80$  kJ/kg<sub>TS</sub> was experimentally determined by a calorimeter bomb. A necessary pretreatment was applied in order to generate C5 and C6 sugars as much as possible to increase the biodegradation rate, considering the high percentage of lignocellulose structures in the CSS and the difficulty in biodegrading such structures (as described in Chap. 6). Out of many candidate pretreatment options, basic pretreatment (BP) was select as the most appropriate one. In the case of CCS the BP was conducted in the following manner: the dispersion was achieved with 2 N NaOH to pH = 12 and it was continuously mixed at 1,000 rpm, in a pretreatment reactor of 20 L equipped with a control heating system in order to keep the system at 30 °C for 24 h. In the case of OWM, the BP was conducted at pH = 12 at 30 °C in a thermostatic room for 24 h with an agitation rate of 200 rpm. At the end of pretreatment, samples were withdrawn and the evaluation of total solids (TS) was performed. The initial pH, before the addition of inoculum, was 7.3, obtained using 2 N HCl. CCS samples were observed with a scanning electron microscope (SEM) before and after the pretreatment and at the end of the fermentation tests, in order to evaluate the effect of the pretreatment and the bioreaction.

### 8.5.2 Seed Microflora for H<sub>2</sub> and CH<sub>4</sub> Production

The seed microorganism consortium for H<sub>2</sub> production was obtained by treating a bovine waste sludge with 2 N HCl at pH = 3 for 24 h at  $30 \pm 1$  °C in a thermostatic room on a rotating shaker at 200 rpm in order to kill all the methanogens; in this manner the HPB, able to form spores, are preserved for the test (Chap. 2). The

**Table 8.4** Structural composition and physical properties of coffee seed skin (CSS)

Hemicellulose (% w/w)	Cellulose (% w/w)	Lignin (% w/w)	Humidity (% w/w)	Density (% w/w)	Lower heating value (kJ/kg)
11.2 <sup>a</sup>	31.3	23.4	4.4	0.729	17.730
12.5 <sup>b</sup>	22.1	51.2	6.2	0.702	18.996
11.9 ± 0.6 <sup>c</sup>	26.7 ± 4.6	37.3 ± 13.9	5.3 ± 0.9	0.716 ± 0.014	18.363 ± 0.633

<sup>a</sup> Raw data furnished by firm; <sup>b</sup> Raw data from authors' independent analysis; <sup>c</sup> Mean values between <sup>a</sup> and <sup>b</sup>

initial conditions of the sludge before the acid treatment were: pH = 7.5, density = 1,014 kg/m<sup>3</sup> and total solid concentration (TS) = 17,930 mg/L, with 80.82 % of volatile solid (VS). The treated sludge was used as inoculum, with a ratio of 10 % v/v of fermenting broth.

Bovine waste sludge (HCB) was used with no treatment as the seed microorganism consortium for CH<sub>4</sub> production; the sludge was stored at 4 °C for 2 weeks before being used, after having been taken from dairy cow breeding; a ratio of 10 % v/v of fermenting broth was used as inocula also in the case of methane fermentation. The choice of bovine manure was made because it is one of the best sources of methanogenic bacteria.

### 8.5.3 Experimental Procedure

#### 8.5.3.1 Batch Tests

All the tests were conducted by using a 14 L bench bioreactor (Chemap-Fermenter, Switzerland) in a batch mode (Fig. 8.2) equipped with pH and temperature control loops and two Ruston turbines, one at the bottom of the reactor and the other one at the liquid/gas interphase, in order to prevent the formation of a pastry shell. All the tests were conducted at 35 ± 1 °C using a working volume of 11 L, comprising 10 L of carbon sources plus 1 L of inoculum. The anaerobic condition was obtained by sparging nitrogen gas at the beginning of the fermentation for 15 min.

The two tests, one with OWM and the other with CCS, pretreated as reported above, were repeated three times. In the case of CCS, a one-step AD test in batch mode was also conducted, while in the case of OWM the one-step AD test was not conducted owing to the abundant data present in the literature; the operative conditions of both experiments are given in Table 8.5.

The one-step AD test was conducted using HCB, while the TSAD was conducted using both HPB and HCB, in order to evaluate H<sub>2</sub> and CH<sub>4</sub> production. The methanation of the one-step fermentation was conducted in the following manner: the pH was adjusted at 7.3 and the set-point of the pH control loop was fixed at 7.3 before inoculation with untreated bovine waste sludge; this condition was maintained till the biogas production shut down.

The TSAD fermentation was conducted differently: the HPB was used at the start of the test, and in this case the initial pH was also set to 7.3; after the natural pH decline towards the acid range, the pH set-point was fixed at 5.2. When the production of biogas containing hydrogen shut down, the pH was gradually changed from acid values to neutral ones by 2 N NaOH and the set-point was fixed at pH = 7.3. At this point HCB was inoculated in the fermenting broth, after changing the mixing rate from 300 to 50 rpm. Thereafter, when necessary, the pH was brought back into the basic range by the control loop in order to prevent HPB

**Fig. 8.2** Chemap-Fermenter of 14 L used for the batch tests



activity; the pH naturally remained at around 7.2, after a lag phase of the methanogenesis step of approximately 20 days, throughout the duration of test without control.

The TSAD tests, both for OWM and CCS, were conducted using the same procedure. In all the tests of hydrogen production, after the natural decrease to 5.2 the pH was maintained at this value via a control system device. This value was selected to prevent high accumulation of organic acids, which could induce a shift of microorganism activity to the solventogenic phase and a decline in H<sub>2</sub>

**Table 8.5** Experimental conditions of batch tests

Test	Start-up conditions			End of acidogenic phase			End of methanogenic phase		
	Conc. (g <sub>TS</sub> /L)	pH	Temp. (°C)	Conc. (g/L)	pH	rpm	Conc. (g/L)	pH	rpm
CSS one-step	41.8 ± 8.3	7.4 ± 0.5	35 ± 1	–	–	–	34.6 ± 7.2	7.4 ± 0.5	50
CSS two-step	41.8 ± 8.3	7.4 ± 0.5	35 ± 1	37.5 ± 13.3	5.2 ± 0.4	300	30.3 ± 5.1	7.3 ± 0.5	50
OWM	42.1 ± 5.2	7.3 ± 0.4	35 ± 1	35.1 ± 11	5.2 ± 0.4	300	29.1 ± 6.3	7.4 ± 0.5	50

production. Different mixing intensity values were adopted in TSAD, bearing in mind the high sensitivity of methanogens to shear stress [19] and the inhibition caused by high levels of dissolved hydrogen on HPB; 300 and 50 rpm for hydrogen and methane production stages, respectively, were used. Both the CCS and the OWM tests were carried out with the use of tap water only, without any other added nutrients or chemicals.

### 8.5.3.2 Continuous Tests

The continuous tests were conducted only with OWM, due to the difficulty of obtaining a sufficient quantity of CCS residues for a long period at a laboratory scale; in contrast, OWM is easily to acquire daily from the local fruit and vegetable market. The continuous tests were conducted by placing in series the Minifor Fermenter as acidogenic reactor and the Chemap Fermenter as methanogenic reactor (Fig. 8.3). The working volumes were 1.3 and 13 L for the Minifor and Chemap, respectively, and the HRT ratio was 1:10 between acidogenic and methanogenic phases. The fermenting broth was transferred from the acidogenic reactor to the methanogenic one by gravity, the feed was introduced only into the acidogenic reactor, and both reactors worked under a pressure of about 30 mBar, in order to prevent any air infiltration which over a longer period could break down the anaerobic conditions.

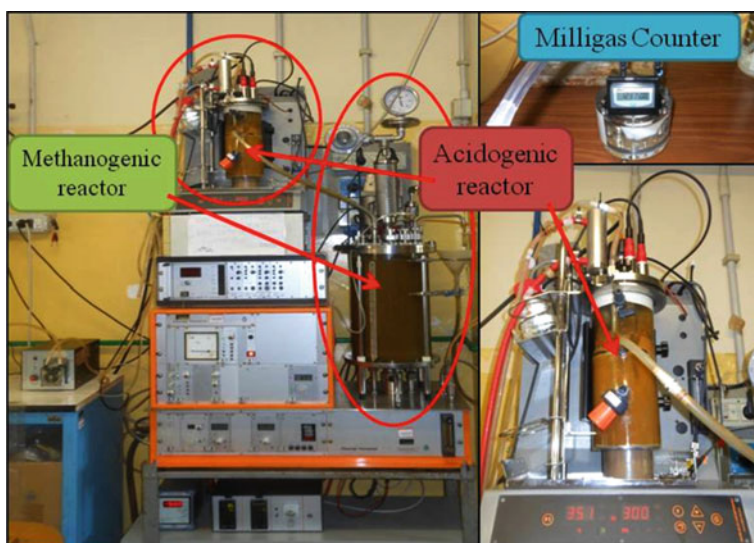


**Fig. 8.3** Experimental apparatus: acidogenic and methanogenic reactors in series operated in continuous mode

Both reactors were thermostated at  $35 \pm 1$  °C and automatically controlled by an electrical resistance.

One of the most important aspects in the case of a TSAD continuous reactor is the start-up of the fermentation, which in many situations needs a long time, of the order of months. After several tests, the following procedure was found to be the most adequate one: at the beginning, the pH of both reactors was set to 7.2, and hence the different inocula, prepared as described in Sect. 8.5.2, were used as seeds in the ratio of approximately 10 % v/v. The reactors operated in batch conditions until the biogas production reached approximately the exponential phase, i.e. the highest production rate, previously evaluated by batch tests. At this point, both reactors were shifted into continuous mode. The first HRT tested was the longer one, in order to prevent microorganism wash-out, in either the H<sub>2</sub> or CH<sub>4</sub>-producing reactors, due to the imperfect mixing which provokes liquid feed by-pass in the vessels. A lower HRT was achieved by increasing the feed flow rate incrementally up to the working conditions.

Because the methanation step requires more time from the biological point of view, it is important to start the methanation reactor first and then the hydrogen one in order to match the two reactors in continuous mode at the maximum production rate of the two reactors in the same time. Obviously the start time needs to be evaluated experimentally by batch tests for specific substrates. Different conditions were applied in order to maintain the different microbial consortia over time in both reactors. Specifically, in the first reactor (H<sub>2</sub>) the pH was maintained at 5.2, and in the second one (CH<sub>4</sub>) at 7.2, through two different control loop systems. In addition, as occurred in the case of batch tests, the mixing intensities were different: 300 rpm for the H<sub>2</sub>-producing reactor, to degas the hydrogen from the fermenting broth and to increase the shear-stress on methanogens eventually present in the reactor, and 50 rpm for the CH<sub>4</sub>-producing reactor, to decrease the shear-stress on methanogens and to favor the agglomeration/flocculation of the microorganisms. In these conditions, three HRT were tested: 15, 10 and 2.5 days for the methanation reactor, corresponding to 1.5, 1 and 0.25 days for the hydrogen-producing reactor, respectively. For each tested HRT, the pseudo-steady-state condition was considered to be reached after at least three times the HRT for the methane-producing reactor, which is longer; hence for the hydrogen-producing reactor the pseudo-steady-state condition was considered after 30 times the applied HRT (Table 8.6).

**Table 8.6** Experimental parameters tested in continuous mode

Operational conditions for the continuous tests						
	H <sub>2</sub> reactor			CH <sub>4</sub> reactor		
Hydraulic retention time (HRT) (days)	0.25	1	1.5	2.5	10	15
Feed flow rate (L/day)	5.2	1.3	0.87	–	–	–
Organic feed flow rate (g <sub>TS</sub> /day)	208	52	34.8	–	–	–
Energy feed flow rate (kJ/day)	3,677	919.4	615.3	–	–	–
Solid load rate in H <sub>2</sub> reactor (SLR) (g L <sup>-1</sup> day <sup>-1</sup> )	160	40	26.8			

### 8.5.3.3 Analytical Measurements

pH (HA405-DXK-S8, Mettler Toledo), redox potential (ROP, Pt4805-DXK-S8, Mettler Toledo), temperature (Iris, Infors HT), and cumulative biogas volume produced (Milligas Counter, Ritter) were monitored and registered over a period of time, during batch tests as well as continuous ones. The total solids (TS) were evaluated at the beginning and at the end of the hydrogen and methane steps; the gas was collected in plastic bags (SCK Quality Samples Bag, <http://www.skinc.com>) which were changed on a time and gas quantity basis. The average concentrations of H<sub>2</sub>, O<sub>2</sub>, CH<sub>4</sub>, CO<sub>2</sub>, CO and N<sub>2</sub> were measured in each bag by means of an off-line gas chromatographic analysis device (Varian, CP 4900) equipped with columns as described in the previous chapters. The LHV was determined using a bomb calorimeter PARR 1261 (Parr Instrument Co., USA). For the structural analysis of CSS, it is necessary to consider that carbohydrates and lignin make up a large portion of the biomass samples. Carbohydrates can be of a structural or non-structural nature; structural carbohydrates are bounded in the biomass matrix, while non-structural carbohydrates can be removed using extraction or washing steps. Lignin is a complex phenolic polymer. The methodology adopted for CSS characterization is the following: the non-structural carbohydrates were extracted by rinsing twice for 10 min with water at 65 °C, at a solid:liquid ratio of 10 %. The extracted fraction was analyzed to determine the carbohydrate monomers. The total oligomer content was determined from the sum of the total sugars, after hydrolysis with 4 % H<sub>2</sub>SO<sub>4</sub> at 120 °C for 1 h, and the content extracted with water. The solid residue was delignified twice in 1.5 % NaOH at 90 °C for 15 min at a solid:liquid ratio of 8 %. Lignin was recovered from the alkaline phase by means of precipitation at pH = 2 with H<sub>2</sub>SO<sub>4</sub>, and spectrophotometrically determined by ultraviolet (UV) spectrophotometry at 205 nm. The hemicellulose content was calculated as the difference between the extracted acid and the extracted water. CSS samples were observed before and after pretreatment, as well as at the end of fermentation tests, by means of a scanning electron microscope (SEM), Quanta FEI Inspect 200LV; samples were fixed on a carbon base and covered with a 50 nm stratum of silver, before observations with SEM.

## 8.6 Results

### 8.6.1 Batch Tests

#### 8.6.1.1 Two-Step H<sub>2</sub> + CH<sub>4</sub> Production from Organic Waste Market

The time course of cumulative gas production and pH for one of the three replicate tests are shown as an examples for simplicity in Fig. 8.4. Table 8.7, instead, reports the quantitative aspects evaluated as mean values of the triplicate tests in order to take into account the experimental uncertainty in these kinds of experiments. It is possible to see that the pH control is efficacious for governing the growth of



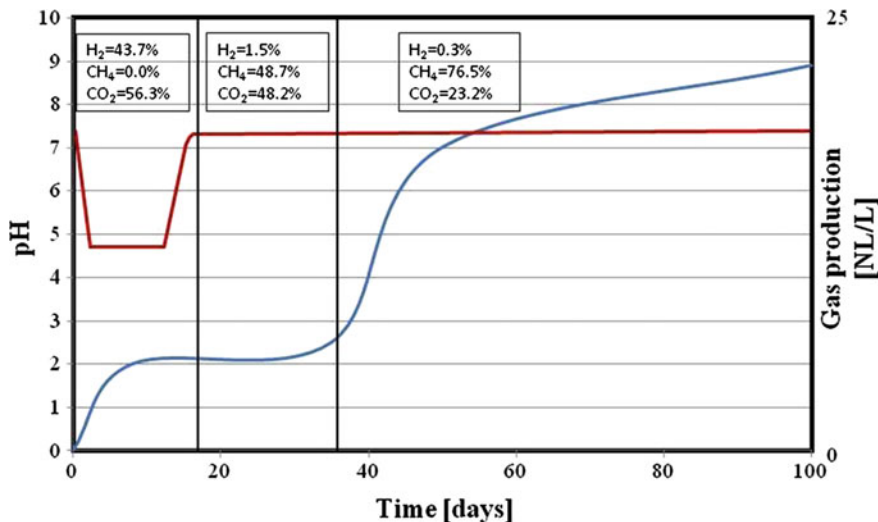


**Fig. 8.4** Cumulative gas production and pH versus time for one of batch tests carried out with OWM

different microorganism species; HPB and HCB clearly show different activities under different pH conditions. This aspect is very important, because the pH is the only parameter that is easily controllable at an industrial scale to increase biogas production [39].

Referring to Fig. 8.4, the test began with pH = 7.3, according to [40], as a result of mixing the pretreated substrate (pH 12) with the inoculum pretreated at pH 3 and adjusted with 2 N NaOH. In all the experiments the pH decreased naturally and progressively as VFA production occurred. The pH decrease was stopped at 5.2 by a control loop, in order to prevent solventogenesis with decrease of H<sub>2</sub> production. The first step ended on approximately the 11th day, when biogas production shut down; at this time, the pH was set to 7.3 and after 3 days without biogas production inoculation with the methanogenic consortium was performed. The cumulative gas production in the first step was about 2.5 L/L of biogas with 43.7 % of H<sub>2</sub>. The lag phase of the methanation stage lasted about 15 days, during which methanogenic microorganisms were adapting to the environmental conditions and competing with acetogenic bacteria (mainly *Clostridium*) for survival.

The presence of both groups of microorganisms was proved by the biogas composition reported in Fig. 8.4: in fact the more the time evolves, the higher the biogas composition moves towards higher CH<sub>4</sub> concentrations. This is an indication of HCB predominance in the microbiological consortium. Upon completion of the lag phase, during which the predominance of methanogens occurred thanks to pH control, the biogas production started to rise exponentially for almost 15 days, then the biogas production rate decreased over time, approaching zero at the culmination of the experiments. The second step finished at about 100 days for all the tests, reaching a cumulative biogas production of about 21 L/L with a contribution of the

**Table 8.7** Quantitative aspects of experimental results of batch tests

Test	Biogas production (L/L)		Mean gas composition (% v/v)		Recovered energy (kJ/L)		Total energy (kJ/L)
	H <sub>2</sub> phase	CH <sub>4</sub> phase	H <sub>2</sub>	CH <sub>4</sub>	H <sub>2</sub> phase	CH <sub>4</sub> phase	
CSS one-step	–	2.86 ± 0.38	–	62.0 ± 3	–	56.54 ± 10.18	56.54 ± 10.18
CSS two-step	0.49 ± 0.1	8.05 ± 0.66	0.8 ± 0.3	77.5 ± 8.1	0.03 ± 0.014	199.4 ± 36.87	199.4 ± 36.87
OWM	2.42 ± 0.51	21.1 ± 1.22	42.1 ± 4.2	74.5 ± 6.2	10.62 ± 2.16	590.5 ± 248.3	600.87 ± 167.14

LHV<sub>G1</sub> = 2.872 kJ/mol; LHV<sub>H2</sub> = 239.2 kJ/mol; LHV<sub>CH4</sub> = 800.32 kJ/mol

**Table 8.8** Experimental efficiency evaluation of batch tests

Test	Specific energy (kJ/g <sub>TS</sub> )	Available energy (kJ/g <sub>TS</sub> )	Efficiency (%)
CSS one-step	1.87 ± 0.57	18.36	10.4
CSS two-step	5.15 ± 1.9	18.36	28.4
OWM	14.27 ± 5.99	17.70	80.6

second step of about 18 L/L; after this time the biogas production rate remained positive but with very low values. The H<sub>2</sub>, CH<sub>4</sub> and CO<sub>2</sub> average composition is shown in Fig. 8.4 for each time interval.

Table 8.8 shows the values of efficiency, which was evaluated by considering the cumulative H<sub>2</sub> and CH<sub>4</sub> production for each step and taking into account the quantity of produced gas in each time interval, multiplied by the H<sub>2</sub> and CH<sub>4</sub> concentrations present in the bag for the same time intervals.

The H<sub>2</sub> contribution to the total energy harvested by TSAD is of the order of 2 % for OWM: this confirms that the energy contribution of the H<sub>2</sub> produced in the first stage is low compared with the total energy recovered. Nevertheless, in the authors' opinion, the hydrogen phase represents a pretreatment step of the biological nature of the organic compounds, able to make them more accessible to the second stage, and it allows a large increase in the amount of methane produced, despite its low energetic contribution. This can be explained by the fact that the acidogenic stage converts sugars (glucose, xylose and mannose) into organic acids, alcohols and organic compounds, which have a more linear structure which is more biodegradable than the cyclic ones. This aspect is numerically expressed by the value of the efficiency  $\eta = 80.6$  as the mean value of the three tests.

### 8.6.1.2 Two-Step H<sub>2</sub> + CH<sub>4</sub> Production from Coffee Seed Skin

Coffee seed skin was selected as being representative of a large family of refuse containing lignocellulose materials which are difficult to digest. In consideration of this fact a basic pretreatment, as described in Sect. 8.5.1, was utilized. As it is difficult to evaluate the effects of the pretreatment through the chemical structural analysis described in Sect. 8.5.3.3, due to the necessary manipulation of the sample which interferes with the pretreatment itself, a qualitative estimation was made through a SEM analysis shown in Fig. 8.5.

The comparison between Fig. 8.5a, b shows the pretreatment effects. The main aspect concerns the increase in the specific surface of the lignocellulose structure; from the first and second pictures of the material before and after the pretreatment, respectively, it is evident that the fibers comprising the external stratum of lignin, which blocks the internal spirals of the hemicellulose containing the cellulose, are completely destroyed. This favors the release of C5 and C6 monomers directly into the liquid; moreover it increases the contact surface area between microorganisms and enzymes (cellulase-like) for the depolarization process and the subsequent digestion process. Figure 8.5c, in comparison with (a) and (b), clearly shows the

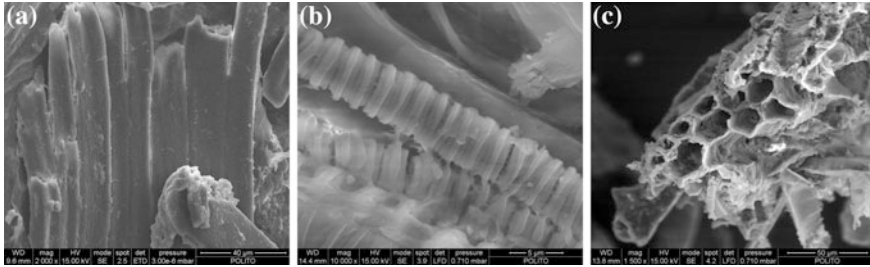


**Fig. 8.5** SEM micrographs of the lignocellulose structure of CSS: **a** before the basic pretreatment, 2000 $\times$ ; **b** after the pretreatment, 2600 $\times$ ; **c** at the end of TSAD, 3000 $\times$  (for comments see text)

effect of the bioreaction: the cellulose, inside the spirals of the hemicellulose structure, was removed and utilized by the microorganisms.

Figure 8.6 depicts the time course for one of the TSAD tests of CSS refuse. The strategy of pH variation adopted was similar to the TSAD tests with OWM. The pH, starting from the initial value of 7.3, naturally decreased until point A; during this period, a small quantity of gas was produced (less than 0.2 NL/L) with a low hydrogen concentration (1.5 %). The pH remained at around 5.2 from point A to point B (vertical bars), and the control loop intervened few times; the gas quantity in this period increased to 0.5 NL/L and the hydrogen percentage decreased. In the time interval from point B to point C, the pH was manually increased several times up to 7.2.

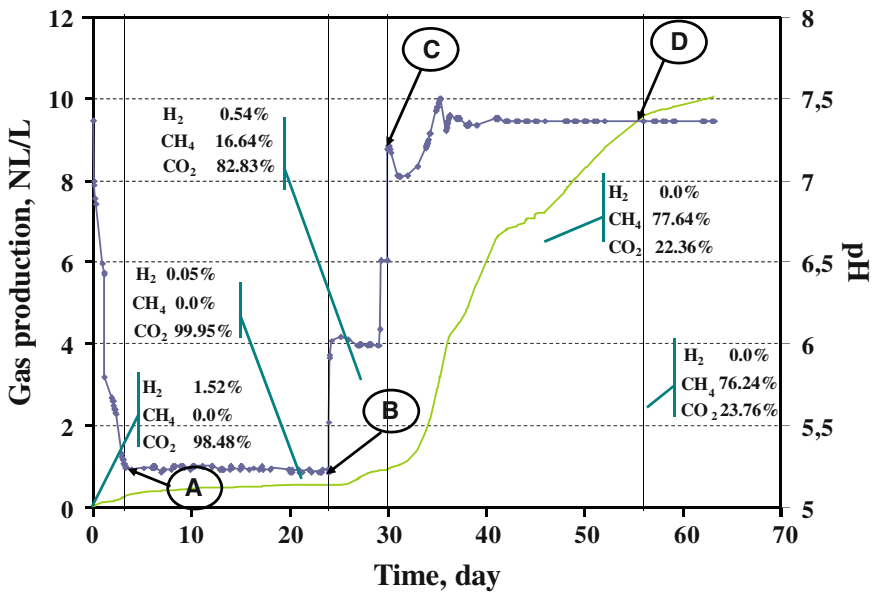


**Fig. 8.6** TSAD of CSS: time course of cumulative biogas production (—) and pH (◆)

During this time, the quantity of gas produced reached a value of approximately 1 NL/L, the  $\text{CH}_4$  concentration increased and the  $\text{H}_2$  concentration reached 0.54 % v/v. At point C, the inoculation with untreated cattle waste sludge as HCB seed occurred. After this point the pH was left free to change: it decreased in 1 day to approximately 7.0, and then it increased to 7.5 and remained at around 7.4 for the entire duration of the fermentation without any intervention of the control loop. The gas production reached 10 NL/L and the mean methane concentration was 77.6 % v/v.

After point D, the gas production rate decreased to a very low value (0.0013 NL/L · h), and the test was interrupted on the 64th day, even though the production rate was not zero.

Figure 8.6 shows that in some time intervals acetogenic and methanogenic microorganisms compete with each others for predominance. This is confirmed by the pH decrease shown at point C, when the pH control loop was voluntarily interrupted and the pH was free to change; it moved towards the acid range, indicating VFA production, which is a clear indication of HPB activity. The quantitative aspects of the energy produced are shown in Tables 8.7 and 8.8. The latter shows that the TSAD efficiency is equal to 28.4 %, while the one-step AD efficiency is 10.4 % for CSS. These results, which are lower than the OWM ones, can be considered acceptable considering the lignocellulose nature of the refuse, even though an improvement would be possible. A comparison between the one-step AD and the TSAD shows that the energy increase is largely due to the methane increase in the second step; in other words, the  $\text{H}_2$  contribution is unimportant, while the efficacy of the whole process, including the pretreatment step, is  $\zeta = 2.73$ , i.e. the energy produced by TSAD is almost three times that of the one-step AD. Observing the “recovered energy” column of Table 8.7, it is evident that the hydrogen contribution is very limited, as occurred in the case of OWM. Comparing the CSS experimental results with the OWM ones (Table 8.9), it is possible to argue that the effect of the first acidogenic step as a biological pretreatment seems to have more biochemical effect in the case of a substrate containing higher amounts of lignocellulose structure. This is probably because biodegradation of lignocellulose materials benefit from the presence of *Clostridium* spp. in HPB thanks to their ability to produce cellulase [41], which causes hydrolysis of the cellulose.

The CSS experimental data were analyzed, as shown in Sect. 8.4. Figure 8.7 shows the cumulative gas production predicted by the modified Gompertz model compared with experimental data. The estimated parameters of the model are:  $R_{1,\max} = 0.061$  NL/L,  $R_{2,\max} = 0.500$  NL/L and  $\lambda = 30.8$  days. It is interesting to note that  $G_{\max} = G_{1,\max} + G_{2,\max}$  is equal to 19 NL/L, which is more than twice the experimentally determined value. This is due to the fact that the test was stopped at the 64th day but gas production had not completely stopped, although the production rate was very low (Fig. 8.6). Another characteristic is that the methanation lag phase lasted 30 days, overlapping with the acid phase fermentation. Recalling the empirical nature of the Gompertz model, the progress could be due to the fact that, at the beginning of test, only the monomers dissolved in the liquid during the acid phase were utilized as substrate by the microorganisms; at the same time, several enzymes attacked the cellulosic polymers. This hypothesis seems realistic, considering the short time necessary for methanogenesis to start (point C in

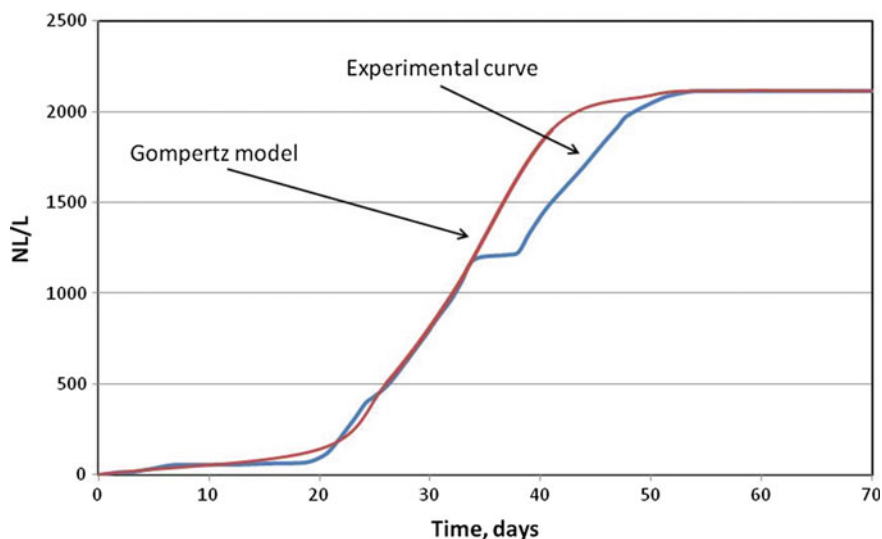


**Fig. 8.7** Comparison between the experimental data and the modified Gompertz model for the CSS test

Fig. 8.6) after the pH changed. The phase during which all the free sugars were consumed is the exponential one; the digestion then proceeded inside the hemicellulose structures, probably controlled either by mass transfer phenomena or by the very low depolymerization rate, as recorded by the variation in biogas production rate around the 45th day and supported by Fig. 8.5c.

### 8.6.1.3 Energy Recovery in Two-Step $H_2 + CH_4$ AD

The energy obtained was evaluated according to the method described in Sect. 8.3; the results are reported in Tables 8.7 and 8.8. The efficiency values were calculated by considering the experimental results of the three tests and the relative uncertainties ( $U$ ) have been computed as standard deviations of data. Evaluations of efficiency and relative uncertainty for the one-step AD with OWM were performed taking into account multiple literature data. In addition, Student's  $t$ -test evaluations comparing one-step AD and TSAD are given in Table 8.9.

**Table 8.9** Efficiency, efficacy, uncertainty and statistical comparison between one-step and two-step AD

	$\eta$	$\zeta$	$U$ (%)	Student's $t$ -test
CSS <sub>one step</sub>	10.4		34.6	$t = 2.7386$
CSS <sub>two steps</sub>	28.4	2.73	38.0	$p < 0.052$
OWM <sup>a</sup> <sub>one step</sub>	56.0		32.1	$t = 1.4090$
OWM <sub>two steps</sub>	80.6	1.59	30.1	$p < 0.2316$

<sup>a</sup> Data taken from literature considering a mean production of  $300 \text{ NL}_{CH_4}/\text{kg}_{TS}$

The evaluations aimed at understanding whether the mean values of efficiency between one-step and two-step AD have sufficient statistical significance. It can be observed from Table 8.9 that TSAD efficacy in the case of CSS is very high: the harvested energy is about three times that of one-step AD, while the total recovered energy in the case of TSAD of OWM is 1.59 higher than that recovered in a one-step AD. The comparison of the two efficacies shows the higher effectiveness of TSAD in the case of materials which are more difficult to digest. This confirms the hypothesis that the first acidogenic stage operates as a biological pretreatment step, which is more effective in the case of lignocellulose material than with easily digestible sugars. The efficiency also takes into account the effect of the basic pretreatment, which is a necessary step for AD processes in the authors' opinion. The relative uncertainty (Table 8.9) of each test is very high (mean value 33.7 %), with higher value for CSS. This may be due to difficulties in repeating the same experimental conditions in different tests, even if the same refuses are used, because of the high chemical and biological complexity of the system (e.g. different chemical residues after the pretreatment and varying microorganism population balance growth in the consortium from test to test). AD, as well as other digestion processes, shows a large experimental uncertainty, even when the same operational protocol is used. Moreover, the necessary mathematical manipulation of the experimental data introduces a propagation of the experimental uncertainty. The experimental uncertainty for the present results was calculated based on the dispersion of three replicate tests. This could decrease the validity of the results from a statistical point of view, but it has a fundamental importance, in the authors' opinion, in comparing different results before designing the bioreactor for scale-up purposes. The last column of Table 8.9 shows the results of Student's *t*-test; the statistical reliability is higher for CSS than for OWM. In the latter case the probability that the difference in efficiency could be due to randomness is less than 23 %. In other words, the probability of obtain more energy using TSAD with OWM as substrate is 77 %, whereas in the case of CSS it is about 95 %. The experimentally evaluated efficiencies of TSAD with their relative uncertainties are in good agreement with the literature data.

### 8.6.2 Continuous Tests TSAD from OWM

The productivity [ $\text{NL L}^{-1} \text{ day}^{-1}$ ] of hydrogen and methane in different coupled sequential reactors versus time is shown in Fig. 8.8. Gas production rates are reported as a function of HRT versus time; the time axis starts when the feed flow rate in continuous mode begins. The behavior in the steady state has an oscillatory nature in all the situations tested; this is not surprising in view of the complexity of the system under study.

Observing the nature of the oscillations, it is possible to argue that their frequency is higher in the case of lower HRT; in other words, it seems that the system is able to absorb oscillations when the new substrate is introduced in the highest

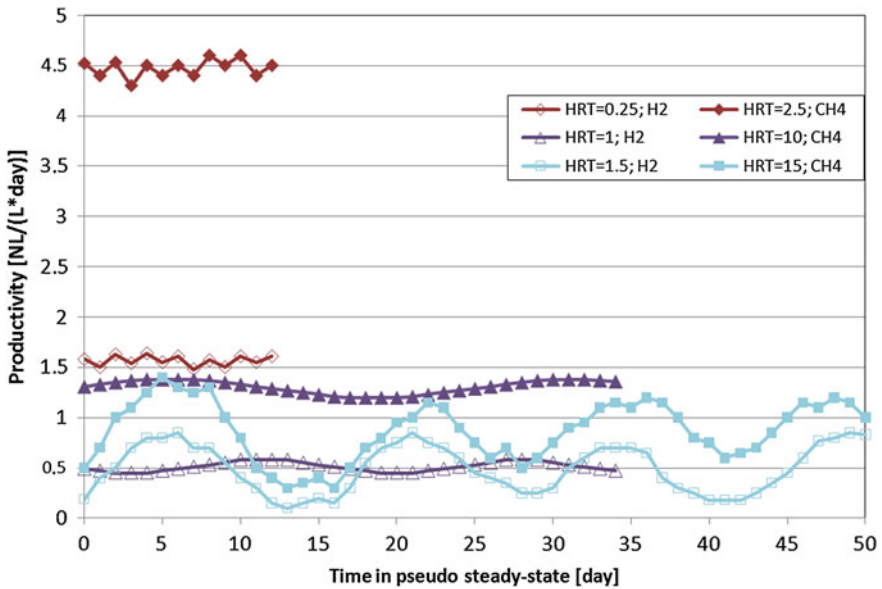


**Fig. 8.8** Experimental productivity of  $H_2$  and  $CH_4$  in steady-state conditions for OWM tests

quantity per unit of time. Increasing the HRT, the oscillations are more smoothed. These different frequencies of oscillation lead us to suppose that different phenomena at different HRT are responsible for the oscillatory behavior. The oscillation at low HRT could be induced by some macro-phenomenon, such as the variation in feed composition, or induced by non-ideal mixing conditions (i.e. a fraction of the fluid entering rapidly finds its way to the effluent stream, while another fraction remains in the vessel for a long time before entering the exit pipe).

These phenomena are obviously also present in the case of higher HRT. A high feed flow rate is able to replace the fluid leaving more rapidly; hence the effects caused by a different residence time on the microorganism consortium are attenuated by the replacement of fresh feed. At a low feed flow rate, however, the larger oscillation frequency could probably be due to phenomena linked to the behavior of the microorganisms. In other words, at higher HRT, in the authors' opinion, oscillations could be caused by phenomena of a biological nature. The question is whether the oscillations are stable or whether they move toward unstable behaviors. The answer can be given only through experimental tests prolonged for longer times. The oscillations revealed by the present tests at a time equal to three times the HRT for the methane-producing reactor and to 30 times the HRT for the hydrogen-producing reactor seem to be stable, but wash-out phenomena in the hydrogen reactor could occur at longer operational times, and a large modification in microorganism balance could be experienced in the consortia in the methane



**Table 8.10** Experimental conditions and results for the TSAD continuous tests

Hydraulic retention time for H <sub>2</sub> reactor (days)	0.25	1	1.5
Hydraulic retention time for CH <sub>4</sub> reactor (days)	2.5	10	15
Hydrogen production (NL L <sup>-1</sup> day <sup>-1</sup> )	1.67	0.49	0.19
Methane production (NL L <sup>-1</sup> day <sup>-1</sup> )	4.52	1.31	0.99
Total energy production (kJ/day)	1,799	521	389
Efficiency $\eta$ (%)	49	56	63

reactor; tests for longer times are necessary to answer these questions. In Table 8.10 are given the operative conditions for the continuous tests, the specific hydrogen and methane production (mean value), the total energy harvest by TSAD and the efficiency values. Generally the efficiency is lower than that for batch tests, but it is of the same order as the one-step AD (Table 8.9). Continuous TSAD has an approximately equal efficiency to one-step AD operated in continuous mode (HRT = 35 days or more) but with a half or a third of the reactor volume, and hence has low investment costs even though operating an additional H<sub>2</sub>-producing reactor with one tenth of the volume is necessary. The statistical significance analysis was not performed for continuous tests due to the low number of tests, although productivity variations were recorded.

In the authors' opinion, additional experimental tests are necessary on continuous TSAD to understand whether such oscillation behaviors depend on randomness or not, and their relative influence on performances.

## 8.7 Conclusion

In the present chapter, the scientific rationale of the two-step AD (TSAD) process is analyzed; the main aspects were confirmed with experimental tests, either in batch or in continuous mode, using two sources representative of organic refuses. Experimental results show that the energy produced as hydrogen and methane gases is higher than that harvested using a one-step AD; specifically it is in the range of 1.5–2.7 times higher, although an uncertainty of  $\pm 30\%$  was recorded experimentally. The energy efficiency for continuous bioreactors is lower than the batch test ones, but some oscillatory behaviors at steady state are present. It is of particular interest for scale-up purposes that the same efficiency was obtained with TSAD at low HRT, compared with traditional one-step AD, but with a methanation bioreactor dimension of a half or a third, hence lowering the investment costs, even though an additional hydrogen reactor of one tenth of the volume is necessary. Finally the hydrogen step appears to be a pretreatment process able to create better substrate utilization with additional methane production in the methanation step.

## References

1. Biogas Barometer Euroserve'er, Syst Solaires Le Journal des Energies Renouvelables **200**, 104–119 (2010). <http://www.euroserv-er.org/pdf/baro200b.pdf>. Accessed 26 Sept 2014
2. Eurostat European Commission, <http://www.euroserv-er.org/pdf/baro200b.pdf>. Accessed 26 Sept 2014
3. European Commission, Communication from the commission to the council and the European Parliament on future steps in bio-waste management in the European Union (2010), [http://ec.europa.eu/environment/waste/compost/pdf/com\\_biowaste.pdf](http://ec.europa.eu/environment/waste/compost/pdf/com_biowaste.pdf). Accessed 26 Sept 2014
4. N. Colonna, V. Alfano, M. Gaeta, La stima del potenziale di biogas da biomasse di scarto del settore zootecnico in Italia. ENEA report RSE/2009/201 (2009), [http://www.enea.it/it/Ricerca\\_sviluppo/documenti/ricerca-di-sistema-elettrico/censimento-biomasse/rse201.pdf](http://www.enea.it/it/Ricerca_sviluppo/documenti/ricerca-di-sistema-elettrico/censimento-biomasse/rse201.pdf). Accessed 26 Sept 2014
5. H. Bouallagui, Y. Touhami, R. Ben Cheikh, M. Hamdi, Bioreactor performance in anaerobic digestion of fruit and vegetable wastes. *Process Biochem.* **40**, 989–995 (2005)
6. X. Wang, Y.C. Zhao, A bench scale study of fermentative hydrogen and methane production from food waste in integrated two-stage process. *Int. J. Hydrogen Energy* **34**, 245–254 (2009)
7. A. Giordano, C. Cantù, A. Spagni, Monitoring the biochemical hydrogen and methane potential of the two-stage dark-fermentative process. *Bioresour. Technol.* **102**, 4474–4479 (2011)
8. A.M. Lakaniemi, P.E.P. Koskinen, L.M. Nevatalo, A.H. Kaksonen, J.A. Puhakka, Biogenic hydrogen and methane production from reed canary grass. *Biomass Bioenergy* **35**, 773–780 (2011)
9. A. Schievano, A. Tenca, S. Lonati, E. Manzini, F. Adani, Can two-stage instead of one-stage anaerobic digestion really increase energy recovery from biomass? *Appl. Energy* **124**, 335–342 (2014)
10. M.A.D.L. Rubia, F. Raposo, B. Rincón, R. Borja, Evaluation of the hydrolytic–acidogenic step of a two-stage mesophilic anaerobic digestion process of sunflower oil cake. *Bioresour. Technol.* **100**, 4133–4138 (2009)
11. S. Ponsá, I. Ferrer, F. Vázquez, X. Font, Optimization of the hydrolytic–acidogenic anaerobic digestion stage (55 °C) of sewage sludge: influence of pH and solid content. *Water Resour.* **42**, 3972–3980 (2008)
12. Z.K. Lee, S.L. Li, P.C. Kuo, I.C. Chen, Y.M. Tien, Y.J. Huang, C.P. Chuang, S.C. Wong, S.S. Chen, Thermophilic bio-energy process study on hydrogen fermentation with vegetable kitchen waste. *Int. J. Hydrogen Energy* **35**(24), 13458–13466 (2010)
13. G. Luo, L. Xie, Q. Zhou, I. Angelidaki, Enhancement of bioenergy production from organic wastes by two-stage anaerobic hydrogen and methane production process. *Bioresour. Technol.* **102**, 8700–8706 (2011)
14. Eden Energy, Annual report for the year ended 30 June 2010, <http://www.edenenergy.com.au/pdfs/2010%20Eden%20Annual%20Report.pdf>. Accessed 26 Sept 2014
15. F. Ma, Effects of hydrogen addition on cycle-by-cycle variations in a lean burn natural gas spark-ignition engine. *Int. J. Hydrogen Energy* **33**, 823–831 (2008)
16. J. Bartacek, J. Zabranska, P.N.L. Lens, Developments and constraints in fermentative hydrogen production. *Biofuels Bioprod Biorefining* **1**, 201–214 (2007)
17. D.R. Boone, W.B. Whitman, P. Rouviere, Diversity and taxonomy of methanogen, in *Methanogenesis* ed. by J.G. Ferry (Chapman and Hall Co., New York, 1993), pp. 35–80
18. J.L. Garcia, B.K.C. Patel, B. Ollivier, Taxonomic, phylogenetic, and ecological diversity of methanogenic Archaea. *Anaerobe* **6**(4), 205–226 (2000)
19. D. Deublein, A. Steinhauser, *Biogas from Waste and Renewable Resources*, 2nd edn. (Wiley-CCH, Weinheim, 2010)

20. G. Talbot, E. Topp, M.F. Palin, D.I. Massé, Evaluation of molecular methods used for establishing the interactions and functions of microorganisms in anaerobic bioreactors. *Water Res.* **42**, 513–537 (2008)
21. I. Valdez-Vazques, H.M. Poggi-Varaldo, Hydrogen production by fermentative consortia. *Renew. Sustain. Energy Rev.* **13**, 1000–1013 (2009)
22. C.H. Chin-Hung Cheng, S.C. Hsu, C.H. Wu, P.W. Chang, C.Y. Chiu-Yue Lin, C.H. Hung, Quantitative analysis of microorganism composition in a pilot-scale fermentative biohydrogen production system. *Int. J. Hydrogen Energy* **36**, 14153–14161 (2011)
23. H.B. Ding, G.Y.A. Tan, J.Y. Wang, Caproate formation in mixed-culture fermentative hydrogen production. *Bioresour. Technol.* **101**, 9550–9559 (2010)
24. N. Ren, J. Li, B. Li, Y. Wang, S. Liu, Biohydrogen production from molasses by anaerobic fermentation with pilot-scale bioreactor system. *Int. J. Hydrogen Energy* **31**, 2147–2157 (2006)
25. C.Y. Lin, S.Y. Wu, P.J. Lin, J.S. Chang, H.C. Hung, K.S. Lee, F.Y. Chang, C.Y. Chu, C.H. Chen, C.H. Lay, A.C. Chang, Pilot-scale hydrogen fermentation system start-up performance. *Int. J. Hydrogen Energy* **35**(24), 13452–13457 (2010)
26. H.S. Lee, W.F.J. Vermaas, B.E. Rittmann, Biological hydrogen production: perspectives and challenges. *Trends Biotechnol.* **28**, 262–271 (2010)
27. H.H.P. Fang, H.Q. Yu, Effect of HRT on mesophilic acidogenesis of dairy wastewater. *J. Environ. Eng.* **12**, 1145–1148 (2000)
28. S. Kim, J. Bae, O. Choi, D. Ju, J. Lee, H. Sung, S. Park, B.I. Sang, Y. Um, A pilot scale two-stage anaerobic digester treating food waste leachate (FWL): performance and microbial structure analysis using pyrosequencing. *Process Biochem.* **49**, 301–308 (2014)
29. G. Chinellato, C. Cavinato, D. Bolzonella, S. Heaven, C.J. Banks, Biohydrogen production from food waste in batch and semi-continuous conditions: evaluation of a two-phase approach with digestate recirculation for pH control. *Int. J. Hydrogen Energy* **38**, 4351–4360 (2013)
30. N. Kataoka, S. Ayame, A. Miya, Y. Ueno, N. Oshita, K. Tsukahara, S. Sawayama, N. Yokota, Studies on hydrogenmethane fermentation process for treating garbage and waste paper, in *ADSW 2005 Conference Proceedings 2, Process Engineering* (2005)
31. C.F. Chu, Y.Y. Li, K.Q. Xu, Y. Ebie, Y. Inamori, H.N. Kong, A pH- and temperature-phased two-stage process for hydrogen and methane production from food waste. *Int. J. Hydrogen Energy* **33**, 4739–4746 (2008)
32. Y.W. Lee, J. Chung, Bioproduction of hydrogen from food waste by pilot-scale combined hydrogen/methane fermentation. *Int. J. Hydrogen Energy* **35**, 11746–11755 (2010)
33. G. Luo, L. Xie, Q. Zhou, I. Angelidaki, Enhancement of bioenergy production from organic wastes by two-stage anaerobic hydrogen and methane production process. *Bioresour. Technol.* **102**, 8700–8706 (2011)
34. C.F. Chu, Y. Ebie, K.Q. Xu, Y.Y. Li, Y. Inamori, Characterization of microbial community in the two-stage process for hydrogen and methane production from food waste. *Int. J. Hydrogen Energy* **35**, 8253–8261 (2010)
35. S.G. Shin, G. Han, J. Lim, C. Lee, S. Hwang, A comprehensive microbial insight into two-stage anaerobic digestion of food waste-recycling wastewater. *Water Resour.* **44**(17), 4838–4849 (2010)
36. Z. Zuo, S. Wub, W. Zhang, R. Dong, Performance of two-stage vegetable waste anaerobic digestion depending on varying recirculation rates. *Bioresour. Technol.* **162**, 266–272 (2014)
37. D. Liu, D. Liu, R.J. Zeng, I. Angelidaki, Hydrogen and methane production from household solid waste in the two-stage fermentation process. *Water Res.* **40**, 2230–2236 (2006)
38. O.M. Pakarinen, H.P. Tahti, J.A. Rintala, One-stage H<sub>2</sub> and CH<sub>4</sub> and two-stage H<sub>2</sub> + CH<sub>4</sub> production from grass silage and from solid and liquid fractions of NaOH pre-treated grass silage. *Biomass Bioenergy* **33**, 1419–1427 (2009)
39. B. Demirel, O. Yenigun, Two-phase anaerobic digestion processes: a review. *J. Chem. Technol. Biotechnol.* **77**, 743–755 (2002)

40. P.Y. Lin, L.M. Whang, Y.R. Wu, W.J. Ren, C.J. Hsiao, S.L. Li, J.S. Ghang, Biological hydrogen production of the genus *Clostridium*: metabolic study and mathematic model simulation. *Int. J. Hydrogen Energy* **32**, 1728–1735 (2007)
41. R. Koukiekolo, H.Y. Cho, A. Kosugi, M. Inui, H. Yukawa, R.H. Doi, Degradation of corn fiber by *Clostridium cellulovorans* cellulases and hemicellulases and contribution of scaffolding protein CbpA. *Appl. Environ. Microbiol.* **71**(7), 3504–3511 (2005)

# Chapter 9

## Energy Sustainability Evaluation of Anaerobic Digestion

In the present chapter, the energy sustainability of anaerobic digestion (AD) technology is discussed. A procedure in three steps is described and then applied to AD. The suggested procedure can help in local planning, in allocation financial resources for the exploitation of new energy processes as well as in selecting the most sustainable choice of several research programs from an energetic point of view. The sustainability scores permit, moreover, the comparison of many operating options for the same technology to identify the best operational conditions towards a sustainable energy perspective. The content of the present chapter is partially contained in [1].

### 9.1 Introduction to Energy Sustainability

A main requirement of society nowadays is energy supply: a good direction is the promotion of energy-producing technologies which have been recognized as sustainable from an energy perspective. Oil production, in fact, is destined to decrease rapidly and will no longer be able to satisfy the global requirements of society. Different renewable resources are now being exploited: solar energy, wind power, water power, energy crops and organic refuses offer possible solutions [2]. Organic waste market (OWM) refuses represent approximately 60 % of daily refuse production, and several technologies are realistic candidates for using it as an energy source [3]. They range from the use of microorganisms [4] to thermal methods, such as gasification, pyrolysis and incineration [5], to the direct conversion of organic matter into electrical energy through the use of microbial fuel cells, as discussed in Chap. 7 [6, 7]. New technologies have been developed in recent years, and others are now at the development stage. The real need is to establish which criteria should be used to select the most appropriate technology to valorize the resources [8]. In this context, economic criteria on their own appear to be inappropriate, because data can easily be manipulated according to the working hypothesis and the conclusions might not be completely reliable [9].

Currently, many technologies are presented as sustainable at the theoretical level. However, there are in reality insufficient tools to verify whether the technologies are truly sustainable, considering not only their energy service but their entire life cycle. Moreover, there are insufficient tools for ranking technologies on the basis of their sustainability; in this respect, we are in a stage of infancy and more robust tools are welcomed.

In this panorama, the present chapter aims to propose a new procedure for scoring the energy sustainability of an energy process, showing its application to AD processes.

## 9.2 Tools and Definition of Operative Conditions

The procedure is articulated in three steps for scoring the energy sustainability of an energy process. An energy process is defined as an aggregate of machineries able to convert one form of energy in another one to furnish an energy service (major details in [1]). Each step of the proposed procedure is characterized by using a different sustainability tool:

1. Energy sustainability index (ESI)
2. Analogical model (AM)
3. Energy returned on investment (EROI) and energy payback time (EPT).

This procedure can help in local planning, in allocating financial resources for the exploitation of new energy processes and in selecting the most sustainable choice, from an energetic point of view, of several research programs. In addition, the sustainability scores (step 3) allow the comparison of several technological options for the same resource in order to identify the best one and, for a specific technology, the best operational conditions from an energy sustainability perspective.

A first screening of many processes is performed using the ESI, which takes into account the total energy produced relative to the direct energy spent. Only an  $ESI > 1$  indicates that a process may be sustainable.

The processes that have passed the first selection are subsequently studied using the AM method, represented by the quantification of each material and energy flow in a flow-chart, which allows estimation of the amount of *useful energy* [1], adopting a life cycle assessment (LCA) approach: each energy contribution is included. Focusing on *indirect energy* is particularly important, because it is often not considered in the present literature. A theoretical as well as a practical error is introduced if the indirect energy is disregarded, because it has a great impact as a quantitative value. The term *useful energy* has been used here to indicate the energy delivered to society, making a distinction with the term *net energy*, which is the energy produced by the process (or plant) minus the direct energy necessary to run the process itself. Useful and net energy differ from each other by the indirect energy flow (Fig. 9.1). The selection of appropriate boundary conditions is a

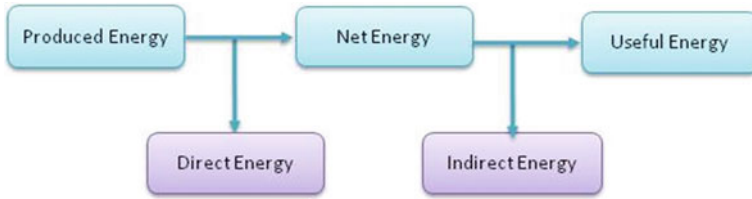


**Fig. 9.1** Main energy blocks in the balance of a energy-producing process

fundamental point in the sustainability analysis; the use of different boundary conditions, in fact, means that non-comparable or inconsistent results could be generated by using different inputs or outputs of the system under study.

The procedure is finally completed by using two parameters: EROI and EPT. They were primarily used in economic evaluations and subsequently have been introduced for energy analysis. Here they are described on the basis of the useful energy for a sustainability assessment.

The procedure is here applied to the AD technology considering different types of organic wastes in order to find the best choice for guaranteeing optimal energy sustainability. The two-step AD (TSAD) technology has been studied in depth at a laboratory scale in order to estimate the energy produced ( $E_{\text{prod}}$ ), then a scale-up procedure considering as scale-up parameter the diameter  $D$  [10] was used in order to evaluate the energy sustainability for different reactor diameters, identifying the minimum diameter that guarantees a good sustainability performance for several biomass types.

The sustainability analysis is performed using the experimental results given in Chap. 8 for OWM, as well as additional ones, considering a TSAD detailed in [11, 12]. In addition, literature data are used for several organic refuses, considering a one-step AD, in order to show how the procedure may be used to find the most sustainable configuration of the AD plant. All the energy terms in the present case of AD, which occurs in a cylindrical reactor, have been evaluated per unit of volume of fermenting broth; in the case of the application of the procedure to different technologies an appropriate base unit needs to be definite ( $\text{m}^2$  in the case of photovoltaic panels, for example).

The bench reactor has a diameter of 0.25 m, while OWM was used without any addition of chemicals, merely diluted in water. Two types of pretreatment were conducted, a basic and a thermal–basic one, to analyze different technical options for the same technology. The basic pretreatment (BP) consists of adding 8 g of 2 N NaOH per liter of broth; the thermal–basic one consists of adding the same quantity of NaOH and moreover heating the broth from ambient temperature (5 and 15 °C in winter and summer time, respectively) to 120 °C using hot water through a heating jacket and maintaining the temperature for 30 min. The overall heating time was 1 h, then the broth was cooled to 35 °C, which is considered the operational reactor temperature (mesophilic range) through natural convection heat transfer.

### 9.3 Energy Sustainability Index (ESI)

#### 9.3.1 Theoretical Definition of ESI

The first step of the procedure allows preliminary selection among many processes, or among different operational conditions of the same process, using the same energy source of those that are candidates to be sustainable from an energy perspective, and to point out those that are certainly unsustainable. This first screening is performed by evaluation of the ESI, which takes into account the total energy produced by the process minus the *energy cost* to produce the *available energy* (Fig. 9.2), compared to the direct energy spent for running it (Eq. 9.1). *Direct energy* means the energy necessary to run the process, namely electricity and heat.

$$ESI = \frac{\text{Produced Energy} - \text{Energy Cost}}{\text{Direct Energy}} \tag{9.1}$$

Only an ESI > 1 indicates that a process may be sustainable, i.e. it merits a more detailed evaluation in order to take into account the indirect energy necessary to

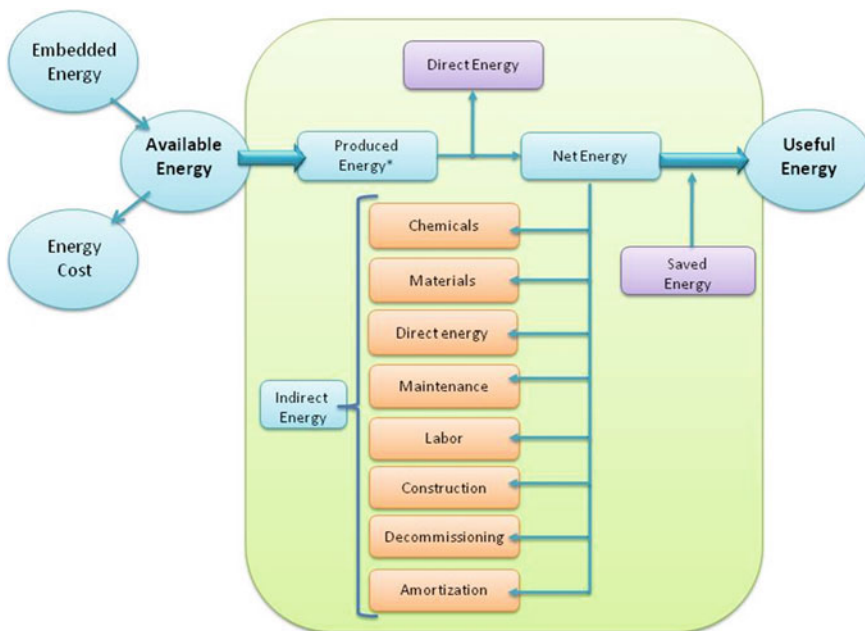


Fig. 9.2 Analogical model of a generic process



build and run the process. If a process has an  $ESI \leq 1$ , it must be rejected from an energy sustainability perspective, and spending further time in a deeper analysis of the energy balance is completely useless; moreover, the process and the operative conditions need to be revisited or abandoned.

Figure 9.1 shows a block diagram of the energy balance of a process: the produced energy is decreased by two terms: firstly direct energy, obtaining the net energy, and secondly indirect energy, in order to evaluate the useful energy. If a process has an  $ESI \leq 1$ , the net energy is zero or negative, i.e. additional energy needs to be produced from another process, so useful energy certainly has a negative value; no additional analysis is necessary.

In the evaluation of energy sustainability, the most important energy flow is the useful energy; it represents the real amount of energy generated by the process and available to sustain the requirements of society (welfare, health, education etc.). Useful energy must be positive in order to ensure that the process really produces energy for society's needs. If net energy is negative, it is evident that changes in the operational conditions are necessary; otherwise the abandonment of the process is inevitable and another process needs to be taken into consideration. If net energy is positive (and this is guaranteed by  $ESI > 1$ ), the process is a candidate to be energetically sustainable, but it is necessary to verify this by moving to the next step in sustainability analysis.

### 9.3.2 *ESI Application to AD Technology*

The ESI tool, described in Sect. 9.3.1, is here applied to the AD technology, considering the operative conditions defined in Sect. 9.2: OWM with BP and OWM with thermal–basic pretreatment (TBP). Tables 9.1 and 9.2 show the ESI results for diameters from 0.5 to 10 m considering the BP and the TBP tests, respectively.

From Table 9.2, the ESI results show that the TBP test is never sustainable from an energy point of view, as ESI is always lower than 1; this means that TBP is not suitable for AD.

In contrast to the data of Table 9.1, the BP test seems instead to be more interesting for diameters greater than 1 m; in this case energy sustainability may be guaranteed, but further studies should be done to verify this hypothesis.

Another application of the ESI concept can be found in [13], where sonication is reported as a suitable pretreatment able to increase biogas (energy) production, but it is not applicable because of its electrical energy expenditure. In the case of the presence of such an *energy cost* term (as for example the case of energy crops production), this value needs to be taken into account as a negative term to lower the produced energy, because it was already spent to produce the available energy (see Sect. 9.4.1).

**Table 9.1** ESI results for diameters from 0.5 to 10 m considering the basic pretreatment test (BP)

Diameter (m)	Produced energy (kJ/L)	Direct energy (kJ/L)	ESI (#)
0.5	469.23	563.8	0.83
1	469.23	311.5	<b>1.51</b>
2	469.23	185.4	<b>2.53</b>
3	469.23	143.4	<b>3.27</b>
4	469.23	122.4	<b>3.84</b>
5	469.23	109.7	<b>4.28</b>
6	469.23	101.3	<b>4.63</b>
7	469.23	95.3	<b>4.92</b>
8	469.23	90.8	<b>5.17</b>
9	469.23	87.3	<b>5.37</b>
10	469.23	84.5	<b>5.55</b>

**Table 9.2** ESI results for diameters from 0.5 to 10 m considering the thermal–basic pretreatment test (TBP)

Diameter (m)	Produced energy (kJ/L)	Direct energy (kJ/L)	ESI (#)
0.5	377.70	871.4	0.43
1	377.70	679.1	0.56
2	377.70	582.9	0.65
3	377.70	550.8	0.69
4	377.70	534.8	0.71
5	377.70	525.2	0.72
6	377.70	518.8	0.73
7	377.70	514.2	0.73
8	377.70	510.7	0.74
9	377.70	508.1	0.74
10	377.70	505.9	0.75

## 9.4 Analogical Model

### 9.4.1 Analogical Model Description

The second step permits detailed analysis of the energy balance of a process using the AM (Fig. 9.2), from *available energy* to *useful energy*.

The AM is a flow-chart in which each energy flow is considered; it is, obviously, more complete than the ordinary energy balance shown in Fig. 9.1, and represents the same energy balance of a process but with a greater level of accuracy.

The quantification of the AM starts with the available energy; this represents the energy available from the process input that could be converted into useful energy. The available energy is the real energy of the inlet flow able to supply the society,

taking into account all the required energy expenditures. It is evaluated as the balance of the energy embedded in the feed (generally its LHV) and the energy spent to make this feed ready. In the present context of AD processes, glucose has a LHV of 2,872 kJ/mol, while the energy cost for producing it from sugar beet is 916.2 kJ/mol [14], so the available energy is only 1,956 kJ/mol. Considering waste coming from a different process as feed, the energy cost is zero, following the LCA allocation criterion, so the available energy in this case coincides with the LHV of the refuses.

The *produced energy* is the total energy produced by the process; it is the gas produced in an AD process, the electricity produced in a photovoltaic panel, etc. This term is obviously lower than the available energy, since there is an efficiency factor due to the energy transition from the maximum theoretical amount to the effective real one. In other words, the ratio between produced energy and available energy gives the global efficiency of the technology under observation into harvesting energy, even if in a different form. It is important to point out that the produced energy term does not indicate the process power, but the energy as a product of such power over a time period (the process life); society, in fact, consumes energy and not power. Produced energy, minus energy cost to produce the feed if present, represents the true available energy potentially able to supply society: this is the value to be considered in the AM analysis.

The next step is the evaluation of the direct energy that is spent in order to operate the process: heating, heat energy loss, electricity for mixing, pumping, and whatever requires energy consumption.

*Net energy* is the difference between produced energy and direct energy. The production of renewable energy carriers, such as the bio-fuel ones, requires energy expenditure, like any other process. At this point of the procedure there is the certainty that net energy has a positive value, as it was verified previously that  $ESI > 1$ . This is the required qualification for further analysis to investigate the indirect energy contributions, as the direct ones have already been quantified.

Indirect energy permits a global view of the process under study, focusing the attention on a real energy balance and not allowing it to be distorted by false perceptions. It happens that many processes are indicated to be better than others because they allow the production of more net energy. However, this preference has no scientific evidence if not supported with more data. One indispensable requirement for selecting the more energy-sustainable process from many others is the evaluation of indirect energy; great care should be given to its definition, both from a theoretical and a practical point of view. The next section is entirely devoted to its detailed description.

The last energy term to be calculated in completing the AM is the *useful energy*. It represents the real amount of energy delivered to society to sustain it. If this value is positive, this means that the process is definitely sustainable from an energy perspective. Net energy and useful energy differ from each other due to the contribution of the indirect energy.

### 9.4.1.1 Indirect Energy

All the contributions of a process which involve energy expenditure in an indirect way are considered when evaluating the indirect energy ( $E_{ind}$ ), which is expressed in mathematical terms in the following equation:

$$E_{ind} = E_{chem} + E_{mat} + E_{dir\ en} + E_{main} + E_{lab} + E_{constr} + E_{decomm} + E_{amort} - E_{saved} \quad (9.2)$$

where

- $E_{chem}$  is the indirect energy spent to produce the *chemicals* used in the process
- $E_{mat}$  is the indirect energy spent to produce the *materials* to construct the plant
- $E_{dir\ en}$  is the indirect energy for producing the *direct energy* necessary to run the plant
- $E_{main}$  is the indirect energy for *maintenance*
- $E_{lab}$  is the indirect energy for *labor*
- $E_{constr}$  is the indirect energy for *construction*
- $E_{decomm}$  is the indirect energy for *decommissioning*
- $E_{amort}$  is the indirect energy for *amortization*
- $E_{saved}$  is the indirect energy for *saved energy*.

Indirect energy needs to be measured in a physical energy unit; hence it is necessary to convert all the material and energy flows into energy units comparable between them; i.e. they should be expressed in MJ per liter of broth in the case of AD. Here each term is explained.

*Indirect energy for chemicals* ( $E_{chem}$ ) evaluates the energy that is spent elsewhere in the world to produce the chemicals required by the process under study. The conversion from a material flow to an equivalent energy one is allowed by using the *global energy requirement* (GER) [15], as shown in Eq. 9.3:

$$E_{chem} = \sum_i (GER_{chem,i} \times m_{chem,i}) \quad (9.3)$$

where  $GER_{chem}$  [ $MJ_{eq}/kg$ ] is defined as the sum of all the contributions of the energy life cycle (direct, indirect, capital and feedstock energy) for producing chemicals and is evaluated in energy units per unit mass of material;  $m_{chem}$  is the quantity of chemicals required by the process and is expressed in kg per liter of broth for the AD technology. The  $i$  subscripts indicate each single type of chemical required by the process.

*Indirect energy for materials* ( $E_{mat}$ ) evaluates the energy that is spent elsewhere in the world to produce the materials required by the process for its construction. It is evaluated by using the *GER*, as shown in Eq. 9.4:

$$E_{\text{mat}} = \sum_i (\text{GER}_{\text{mat},i} \times m_{\text{mat},i}) \quad (9.4)$$

where  $\text{GER}_{\text{mat}}$ ,  $m_{\text{mat}}$  and  $i$  subscripts have the same meaning as the chemical ones in Eq. 9.3, but referring to the construction materials.

An analogous approach needs to be made about the *indirect energy necessary to produce the direct energy* ( $E_{\text{dir en}}$ ) as shown in Eq. 9.5:

$$E_{\text{dir en}} = \sum_i (\text{GER}_{\text{dir en},i} \times m_{\text{dir en},i}) \quad (9.5)$$

where  $\text{GER}_{\text{dir en}}$ ,  $m_{\text{dir en}}$  and  $i$  subscripts have the same meaning as before, but refer to the direct energy. Each type of direct energy spent in the process needs to be evaluated in its indirect contribution. Considering for example the electricity taken from the grid, it is necessary to evaluate the energy expenditure that occurs elsewhere for producing each unit of electricity (power plant construction, grid maintenance etc.). *GER* values are expressed in an appropriate unit,  $\text{MJ}_{\text{eq}}/\text{kWh}$  in the case of electricity,  $\text{MJ}_{\text{eq}}/\text{N m}^3$  in the case of using natural gas to produce electricity in loco, and so on.

The *indirect energy for maintenance* ( $E_{\text{main}}$ ) estimates the energy consumed in maintenance operations, and its evaluation depends strongly on indirect energy for materials. During the working life of a process, in fact, many parts of the constructed plant may have to be replaced (pumps, pipes, etc.) because of wear-and-tear or damage.  $E_{\text{main}}$  is calculated by applying Eq. 9.6:

$$E_{\text{main}} = E_{\text{mat}} \times \gamma \quad (9.6)$$

where  $\gamma$  is a percentage that correlates the indirect energy for maintenance with the indirect energy for materials, and its value should be carefully decided on the basis of the specific characteristics of the process under study.

The evaluation of the *indirect energy for labor* ( $E_{\text{lab}}$ ) is intrinsically difficult, so this parameter is often disregarded. Using Eq. 9.7, a theoretical approach for considering the labor contribution in all its aspects is proposed:

$$E_{\text{lab}} = (E_{\text{lab,food}} + E_{\text{lab,others}}) \quad (9.7)$$

Indirect energy for labor aims to evaluate the energy required to support the human labor in the process under study. It is composed of two main components:  $E_{\text{lab,food}}$  is the energy required for producing the meals necessary for the biological support of the workers;  $E_{\text{lab,others}}$  includes all the other direct and indirect forms of energy consumption linked to the workers' daily activities (clothing, appliances, fuel for transportation from house to factory etc.).

Equation 9.7 presents a theoretical approach that is very difficult to apply in a practical evaluation, especially when considering  $E_{\text{lab,others}}$  due to the strong interrelationship among many different aspects of human life. Regarding the energy

consumption linked to the workers' daily activities, it is hard to evaluate which portion of it should be assigned to the process under study, rather than to another one that is involved in the workers' lives. For this reason, the decision to neglect  $E_{\text{lab, others}}$  and to consider only  $E_{\text{lab, food}}$  using Eq. 9.8 has been taken:

$$E_{\text{lab}} \sim E_{\text{lab, food}} = (\text{GER}_{\text{meal}} \times n_{\text{meal}} \times n_{\text{workers}} \times t_{\text{workers}}) / V_{\text{broth}} \quad (9.8)$$

where  $\text{GER}_{\text{meal}}$  refers to the energy required by a single meal, considering the direct plus indirect energy consumption necessary to produce, transport, conserve and prepare food;  $n_{\text{meal}}$  is the total number of meals per day of a single worker;  $n_{\text{workers}}$  is the number of workers necessary to run the process under examination;  $t_{\text{workers}}$  is the working time of each worker of the process considering the number of work-days per year of the plant life;  $V_{\text{broth}}$  is the volume of fermenting broth necessary to make  $E_{\text{lab}}$  consistent with other energy terms;  $\text{GER}_{\text{meal}}$  evaluation is a complex study, about which research has been recently reported in [16].

*Indirect energy for construction* ( $E_{\text{constr}}$ ) and for *decommissioning* ( $E_{\text{decomm}}$ ) may be discussed together, as they represent the energy consumed for building and for dismantling the plant, respectively. Their evaluation may be achieved using Eqs. 9.9 and 9.10:

$$E_{\text{constr}} = E_{\text{chem},c} + E_{\text{mat},c} + E_{\text{dir en},c} + E_{\text{lab},c} \quad (9.9)$$

$$E_{\text{decomm}} = E_{\text{chem},d} + E_{\text{mat},d} + E_{\text{dir en},d} + E_{\text{lab},d} \quad (9.10)$$

Indirect energy both for construction and decommissioning is evaluated considering the amount of chemicals, materials, direct energy and human labor required for the construction operations ( $c$  subscripts) and for the decommissioning ones ( $d$  subscripts). Each term may be evaluated using Eqs. 9.3–9.5 and 9.7, taking into consideration the complexity of the plant and making an estimation of the time necessary for building and dismantling; an analysis of the plants already in service was performed in the present examples.

*Indirect energy for amortization* ( $E_{\text{amort}}$ ) is the energy necessary to reconstruct the plant after its decommissioning. The aims of an energy-producing process are in fact two-fold: firstly producing energy, and secondly storing an amount of energy that allows to rebuild the process in order to ensure the energy supply to society. This last target guarantees that the energy production needed by society does not have to be stopped for technological reasons at the end of the plant's life (approximately 10–25 years), but continues by a new similar process or an improved one. The amount of energy that needs to be stored somewhere is equal to the sum of indirect energy for chemicals and for materials, as shown in Eq. 9.11:

$$E_{\text{amort}} = E_{\text{chem}} + E_{\text{mat}} \quad (9.11)$$

*Indirect energy for saved energy* ( $E_{\text{saved}}$ ) quantifies the energy saving that the process allows. If one or more inputs of the process are refused produced by another

process, their energy revaluation allows the saving of energy. In fact final disposal, to which the refuse was directed before (e.g. landfill or incineration), is no longer required, so there is an energy saving. The formula for  $E_{\text{saved}}$  is given in Eq. 9.12:

$$E_{\text{saved}} = \sum_i (\text{GER}_{\text{input},i} \times m_{\text{input},i}) \quad (9.12)$$

where  $\text{GER}_{\text{input}}$  is the GER of the final disposal avoided and is expressed in  $\text{MJ}_{\text{eq}}$  per kg of the pertinent input;  $m_{\text{input}}$  is the amount of input [kg/L]; and the  $i$  subscripts indicate the single type of input of the process. In the case of OWM, it is the energy saved for incineration and/or landfill.

Looking at the AM in Fig. 9.2,  $E_{\text{saved}}$  is the only positive term; for this reason only it is represented separately from indirect energy, although it has an indirect nature. This choice underlines its peculiarity, i.e. it represents an energy profit instead of an energy expenditure.

### 9.4.2 Analogical Model Application to AD Technology

The AM is here applied to the AD technology, in order to clarify each step from both theoretical and practical points of view.

#### 9.4.2.1 Available Energy

The calculation of the *available energy* ( $E_{\text{available}}$ ) is based on the lower heating value (LHV) of the wastes, considering how much energy is obtaining by burning it completely, as given in Eq. 9.13:

$$E_{\text{available}} = m_{\text{biomass}} \times \text{LHV}_{\text{biomass}} \quad (9.13)$$

where  $m_{\text{biomass}}$  is the quantity of biomass and is expressed in kg of total solids per liter of broth, and  $\text{LHV}_{\text{biomass}}$  is the LHV of the biomass in MJ/kg. This is true only in the case of organic wastes as inputs. If energy crops are considered as inputs, as occurs in many full-plant applications, the energy cost term needs to be evaluated too: i.e. it is necessary to calculate the energy expenditure to produce the crops.

#### 9.4.2.2 Produced Energy

The *produced energy* ( $E_{\text{prod}}$ ) is the total energy embedded in the produced gas, i.e. the energy contained in the amount of hydrogen and methane retrieved from the reactors in the case of TSAD, during its lifetime. Equation 9.14 indicates how it can be calculated:

$$E_{\text{prod}} = P_{\text{H}_2}(T_w) \times \text{LHV}_{\text{H}_2} + P_{\text{CH}_4}(T_w) \times \text{LHV}_{\text{CH}_4} \quad (9.14)$$

where  $P_{\text{H}_2}(T_w)$  and  $P_{\text{CH}_4}(T_w)$  are the specific productions of  $\text{H}_2$  and  $\text{CH}_4$ , respectively, at the working temperature  $T_w$ , and are expressed as  $\text{Nm}^3$  of  $\text{H}_2$  and  $\text{CH}_4$  per liter of broth;  $\text{LHV}_{\text{H}_2}$  and  $\text{LHV}_{\text{CH}_4}$  are the LHV's of hydrogen and methane (10.8 and 36.18  $\text{MJ}/\text{Nm}^3$ ), respectively.

### 9.4.2.3 Direct Energy

The next step is the evaluation of the direct energy ( $E_{\text{direct}}$ ) that is spent in order to operate the process:

$$E_{\text{direct}} = E_{\text{dpret}} + E_{\text{H}_2\text{react}} + E_{\text{CH}_4\text{react}} \quad (9.15)$$

$$E_{\text{dpret}} = E_{\text{hp}} + E_{\text{lp}} + E_{\text{mp}} + E_{\text{pp}} \quad (9.16)$$

$$E_{\text{H}_2\text{react}} = E_{\text{hw}} + E_{\text{lw}} + E_{\text{mw}} + E_{\text{pw}} \quad (9.17)$$

$$E_{\text{CH}_4\text{react}} = E'_{\text{hw}} + E'_{\text{lw}} + E'_{\text{mw}} + E'_{\text{pw}} \quad (9.18)$$

where  $E_{\text{hp}}$  and  $E_{\text{hw}}$  are the amounts of heat necessary to reach the pretreatment temperature (if present) and the working temperature, respectively;  $E_{\text{lp}}$  and  $E_{\text{lw}}$  are the thermal energy losses, which depend on the outdoor ambient temperature and the duration of the pretreatments and the fermentation, respectively;  $E_{\text{mp}}$  and  $E_{\text{mw}}$  are the electrical energies necessary to mix the fermenting broth during the pretreatments and the fermentation, respectively;  $E_{\text{pp}}$  and  $E_{\text{pw}}$  are the electrical energies necessary for the pumping during the pretreatments and the fermentation, respectively. The primes in Eq. 9.18 indicate that the terms are referred to the  $\text{CH}_4$ -producing bioreactor. Each of the previous terms is expressed in  $\text{MJ}/\text{L}$ .

Equation 9.15 shows that direct energy evaluated for AD technology is composed of three terms: one regarding the pretreatment ( $E_{\text{dpret}}$ ), one the  $\text{H}_2$ -producing reactor ( $E_{\text{H}_2\text{react}}$ ) and the last one the  $\text{CH}_4$ -producing reactor ( $E_{\text{CH}_4\text{react}}$ ). Each one is characterized by its specific direct energy consumption.

Each component of Eqs. 9.15–9.18 has been described in detail in Chap. 5 for the  $\text{H}_2$  reactor; the same equations are also valid in the case of pretreatments and of the  $\text{CH}_4$  reactor; in addition, the same construction materials as for the  $\text{H}_2$  reactor (Chap. 5) have been considered in the present calculations.

### 9.4.2.4 Net Energy

The next step is the evaluation of *net energy* ( $E_{\text{net}}$ ) as the difference between produced energy and direct energy, as shown in Eq. 9.19:



**Table 9.3** GER values of chemicals and materials

Steel	29,411 kJ/kg
Polystyrene	89,610 kJ/kg
NaOH	5.669 kJ/kg
Water	0.091 kJ/kg

$$E_{\text{net}} = E_{\text{prod}} - E_{\text{dir}} \quad (9.19)$$

It is expressed in MJ per liter of broth.

### 9.4.2.5 Indirect Energy

All the contributions of the AD process that involve an energy expenditure in an indirect way are considered when evaluating the indirect energy, which is expressed in mathematical terms in Eq. 9.2.

Indirect energy for chemicals ( $E_{\text{chem}}$ ) and for materials ( $E_{\text{mat}}$ ) is evaluated by applying Eqs. 9.3 and 9.4. The TSAD process requires NaOH and water as chemicals, and steel and polystyrene as materials.  $\text{GER}_{\text{chem}}$  and  $\text{GER}_{\text{mat}}$  have been evaluated by using SimaPro 7.2.4 software [17] and the Ecoinvent database [14], as shown in Table 9.3.

Indirect energy for direct energy ( $E_{\text{dir en}}$ ) may be evaluated by applying Eq. 9.5. A heat exchanger is used for heating the broth to the operational temperature and the electricity is produced using a part of the biogas produced as fuel, avoiding electricity expenditure from the grid. The direct energy required by the process is available thanks to combined heat & power (CHP) devices and to the heat exchanger, whose construction requires an energy expenditure that represents the indirect energy spent to produce and use the direct energy. It has been assumed to consider only the construction materials of the devices (steel), in order to simplify its estimation and to ensure at the same time reliability of the results.

Indirect energy for maintenance ( $E_{\text{main}}$ ) is evaluated by applying Eq. 9.6, assuming a  $\gamma$  equal to 15 %. The evaluation of the indirect energy for labor ( $E_{\text{lab}}$ ) is made using Eq. 9.8;  $n_{\text{meal}}$  has been assumed to be two per day, while  $n_{\text{workers}}$  is equal to one as AD is not a labor-intensive technology;  $t_{\text{worker}}$  was assumed to be 220 days/year for the life of the AD technology (15 years). Finally, all the above energy fluxes crossing the boundaries of the system are considered to be diameter-dependent and the diameter is considered to be a scale-up parameter.

Indirect energy for construction ( $E_{\text{constr}}$ ) and for decommissioning ( $E_{\text{decomm}}$ ) are evaluated using Eqs. 9.9 and 9.10. Considering the AD process, only human labor is required for construction, and it has been considered that a single workman works for 30 days to assemble the plant in the case of diameters up to 2 m, and for 90 days for higher diameters. The same assumptions have been made for indirect energy for decommissioning; the necessary fuel consumption for these operations were considered to be 5 % of the energy embedded in the construction materials.

Indirect energy for amortization ( $E_{\text{amort}}$ ) and for saved energy ( $E_{\text{saved}}$ ) are evaluated using Eqs. 9.11 and 9.12. Considering AD technology, the organic waste used as input would have required municipal incineration, which is no longer necessary as it is used for energy revaluation in the AD process; the saved energy in this case is 436.29 kJ/kg of municipal solid wastes [14].

#### 9.4.2.6 Useful Energy

In mathematical terms, useful energy can be evaluated from the difference between net energy and indirect energy, as shown in Eq. 9.20:

$$E_{\text{useful}} = E_{\text{net}} - E_{\text{ind}} \quad (9.20)$$

Useful energy is expressed in MJ<sub>eq</sub> per liter of fermenting broth.

#### 9.4.2.7 Analogical Model Results

Table 9.4 reports the evaluation of each term of the AM for a TSAD that produces hydrogen and methane using basic-pretreated OWM. It shows that the energy sustainability is guaranteed only for diameters higher than 4 m (useful energy values in bold). Results regarding the TBP tests are not reported, since energy sustainability is never reached, as has been verified applying the ESI criterion; this technology (TBP) has not been considered in the evaluation of either EROI or EPT.

The comparison between Tables 9.1 and 9.4 underlines the upgrade occurring in the energy sustainability assessment: at the end of the first step of the procedure

**Table 9.4** Energy flows (kJ/L) of the AD analogical model (BP test)

Diameter (m)	Produced energy (kJ/L)	Direct energy (kJ/L)	Net energy (kJ/L)	Indirect energy (kJ/L)	Useful energy (kJ/L)
0.5	469.23	563.8	-94.55	11,204.9	-11,299.46
1	469.23	311.5	157.70	1,831.5	-1,673.78
2	469.23	185.4	283.82	578.5	-294.67
3	469.23	143.4	325.86	414.2	-88.34
4	469.23	122.4	346.88	359.6	-12.76
5	469.23	109.7	359.49	333.4	<b>26.05</b>
6	469.23	101.3	367.90	318.1	<b>49.77</b>
7	469.23	95.3	373.90	308.1	<b>65.85</b>
8	469.23	90.8	378.41	300.9	<b>77.50</b>
9	469.23	87.3	381.91	295.6	<b>86.35</b>
10	469.23	84.5	384.72	291.4	<b>93.32</b>

only a bioreactor with a diameter greater than 1 m may be sustainable; at the end of the second step this result was refined: only processes with a diameter greater than 5 m are (not “may be”) sustainable from an energy point of view.

## 9.5 EROI and EPT

### 9.5.1 EROI and EPT Description

The second step has allowed verification of the effect of the scale-up, i.e. the diameter, on energy sustainability in AD technology. The last step of the procedure proposed here allows scoring of the processes and compiling a list considering their sustainability level. To this end, two parameters are introduced: EROI and EPT.

Revisiting the concept of EROI introduced in [18], here the EROI is intended to be the ratio between the total amount of net energy delivered to society by a technology during its working lifetime and the indirect energy spent over the same time period. It is a ratio between two energy quantities and is therefore dimensionless. In mathematical terms, EROI is expressed in Eq. 9.21:

$$\text{EROI} = \frac{E_{\text{net}}}{E_{\text{ind}}} \quad (9.21)$$

where  $E_{\text{net}}$  is the net energy and  $E_{\text{ind}}$  is the indirect energy.

Each process that remains under consideration at the third step is energy-sustainable, therefore  $\text{EROI} > 1$ . The process with the highest EROI has the best energy sustainability performance.

EROI should not be confused with energy efficiency conversion, which is well depicted by the First and Second Laws of classical thermodynamics. EROI is only loosely related, at least in the short term, to the concept of return of monetary investment, but this aspect lies outside the purpose of the present book.

EPT is a related concept to EROI. It is the time required by the plant to produce the energy necessary to rebuild the plant itself (materials and construction). The higher the EPT value, the lower the annual rate of useful energy and hence the lower the energy sustainability. In other words, EPT is the length of the operational plant lifetime necessary to produce the first amount of energy that really sustains society.

The mathematical expression for EPT is shown in Eq. 9.22, where  $t$  [years] is the plant lifetime:

$$\text{EPT} = \frac{E_{\text{ind}}}{\frac{E_{\text{net}}}{t}} \quad (9.22)$$

EROI and EPT together describe the energy sustainability level of each process, so they are fundamental tools for decision-making in the energy sector.

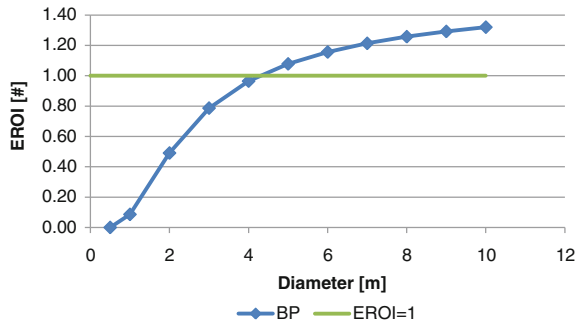


Fig. 9.3 EROI evaluation for AD technology: OWM as substrate with basic pretreatment

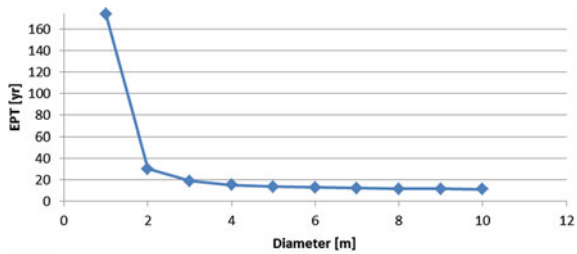


Fig. 9.4 EPT evaluation for AD technology: OWM as substrate with basic pretreatment

### 9.5.2 Use of EROI and EPT in TSAD

The BP test (OWM with basic pretreatment) is scored on the basis of its energy sustainability using EROI vs. reactor diameter; the calculation results are reported in Fig. 9.3. In Fig. 9.3 the horizontal line refers to the case for EROI = 1; it helps graphically to highlight when energy sustainability is guaranteed (above the line) or not (under the line). If EROI = 1 the technology is able to produce only the energy necessary to sustain itself. The application of the procedure proposed in Sect. 9.2 shows that energy sustainability is reached for diameters greater than 4 m; larger diameters increase the energy sustainability of the AD process.

The EPT evaluation for the BP test is shown in Fig. 9.4; the EPT results confirm the conclusion obtained by evaluation of EROI, adding a time consideration: energy sustainability is gained after a minimum of 15.5 years, referring to a diameter of 4 m; in fact sustainability is guaranteed for diameters higher than 4 m. The AM was evaluated considering a process life of 15 years; this means that the minimum reactor diameter should be at least 5 m, with an EPT of 14 years, because an EPT value equal to the working lifetime of the plant does not make sense. In addition the EPT evaluation gives a clear indication of the necessity to enhance the plant lifetime by making the right choices from the technology point of view (materials, maintenance, etc.) and to build plants with larger diameters.

**Table 9.5** Ranges of produced energy (kJ/L) using different substrates

Substrates	$E_{prod\ min}$ (kJ/L)	$E_{prod\ max}$ (kJ/L)
Pig slurry [19]	104.9	463.0
Pig manure [19]	397.9	526.9
Sorghum silage [19]	468.7	574.8
Residues from fruit juice processing [19]	454.4	594.9
Pig blood [19]	604.5	999.1

### 9.5.3 Use of EROI and EPT in AD

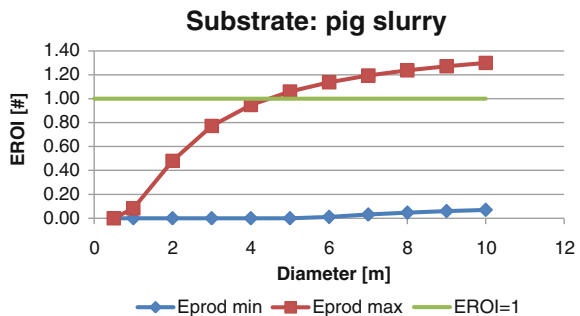
In this section the sustainability analysis procedure is applied to different types of organic wastes, using the range of energy productivity from literature data. In the AM, EROI and EPT have been evaluated using as input different types of biomass, with different characteristics in volatile solids having different ranges of biogas productivity. When changing the substrate, the amount of biogas produced also changes, and thus obviously its methane percentage. In performing the analysis, the same conditions (materials and operating parameters) used for the OWM pretreated with NaOH were considered as a part of the energy expenditure to run the process and considering only CH<sub>4</sub> production, hence only one reactor. Table 9.5 shows the produced energy for different substrates.

Results are shown in Figs. 9.5, 9.6, 9.7, 9.8 and 9.9. As EROI and EPT are strongly correlated, only EROI results are shown in order to avoid the presentation of too many data which may be confusing to the reader.

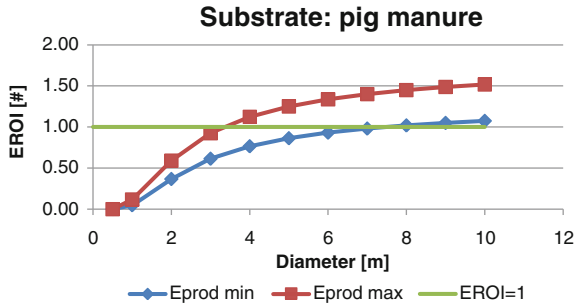
From Fig. 9.5 it is clear that pig slurry is not a very good substrate for AD technology, as a consequence of the large variation in biogas and energy productivity. EROI > 1 is reached for diameters greater than 4.5 m in the case of maximum productivity. If the choice to use pig slurry as feed for AD is taken, great attention should be paid in setting up the operational conditions in order to stay inside the EROI > 1 area.

Figure 9.6 shows the results of the EROI evaluation using pig manure as substrate. It is possible to see that pig manure is a good substrate for AD technology, as its EROI is positive for diameters greater than 8 m considering its minimum  $E_{prod}$ ,

**Fig. 9.5** EROI evaluation for AD technology using pig slurry as substrate



**Fig. 9.6** EROI evaluation for AD technology using pig manure as substrate



**Fig. 9.7** EROI evaluation for AD technology using sorghum silage as substrate

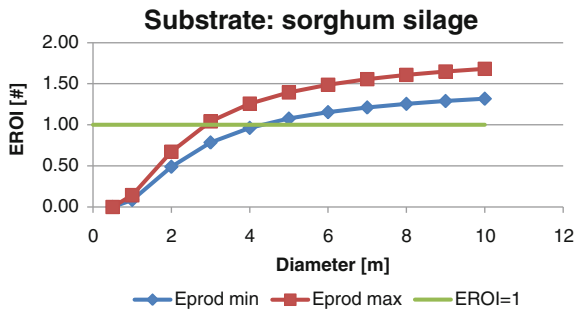
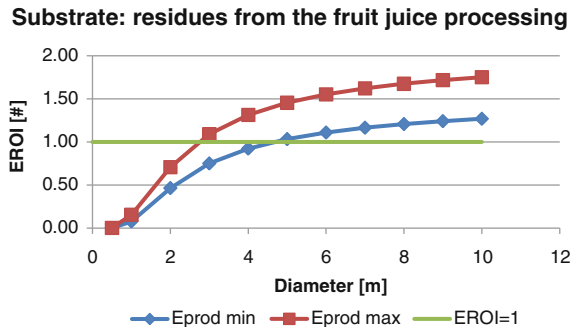


**Fig. 9.8** EROI evaluation for AD technology using residues from fruit juice processing as substrate

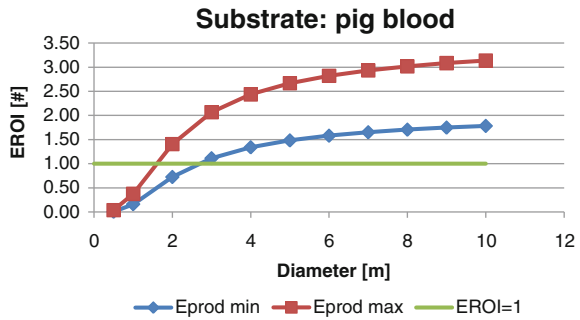


while it is positive for diameters greater than 3 m considering its maximum  $E_{prod}$ . If the reactor diameter is greater than 8 m, there is the certainty that there are energy-sustainable conditions; if it has a value between 3 and 8 m, care should be taken in setting the operating conditions to stay inside the  $EROI > 1$  area.

Figure 9.7 shows the EROI evaluation for sorghum silage. Sorghum silage is a good substrate for AD technology: the EROI is positive for diameters greater than 4 m considering its minimum  $E_{prod}$ , and for diameters greater than 3 m considering its maximum  $E_{prod}$ .

Figure 9.8 shows the results for fruit juice processing plant residues as feed for the AD process. In this case too, the fruit juice processing residues are a good

**Fig. 9.9** EROI evaluation for AD technology using pig blood as substrate



substrate for AD technology, as its EROI is positive for diameters greater than 5 m considering the minimum  $E_{prod}$ , and for diameters greater than 3 m considering the maximum  $E_{prod}$ .

Finally, in Fig. 9.9, the EROI of an AD process having the pig blood residue of meat manufacturing as feed is shown. Pig blood appears to be a good substrate for AD technology, as its EROI is positive for diameters greater than 3 m considering the minimum  $E_{prod}$ , and for diameters greater than 1.5 m considering the maximum  $E_{prod}$ .

Comparing the different substrates considered in this analysis, the most energy-sustainable AD process is the one using pig blood as feed, with a maximum EROI of 3.14, while the worst one is pig slurry with a maximum EROI of 1.30.

## 9.6 Conclusion

In the present chapter a procedure has been proposed for evaluating the energy sustainability of a process, and moreover for scoring different processes using the same energy sources on the basis of their energy sustainability level. The procedure comprises three steps: ESI evaluation, AM computation and finally determination of EROI and EPT.

Application of the procedure allows definition of the process steps and moreover establishment of the operative conditions necessary for increasing the energy sustainability of the entire technology.

The procedure was applied and results were shown for AD technology considering the reactor diameter as the scale-up parameter.

The first example regards the use of OWM as the substrate feed for AD technology comprising three steps: (i) pretreatment, where the substrate is treated with a base (pH 12), (ii)  $H_2$ -producing reactor, where hydrogen-rich gas is produced, and (iii)  $CH_4$ -producing reactor, where methane-rich gas is produced.

The second example regards the application of the proposed procedure to “classical” one-step AD, where only the  $CH_4$ -producing reactor is present, considering different substrates as feed. Generally larger bioreactor diameters for AD are preferred, albeit depending on the substrates used.

## References

1. B. Ruggeri, S. Sanfilippo, T. Tommasi, Sustainability of ( $H_2+CH_4$ ) by anaerobic digestion via EROI approach and LCA evaluations, in *Life Cycle Assessment of Renewable Energy Sources*, ed. by A. Singh, D. Pant, S.I. Olsen (Springer, New York, 2013), pp. 169–194
2. L.T. Angenent, K. Karim, M.H. Al-Dahhan, R. Domiguez-Espinosa, Production of bioenergy and biochemicals from industrial and agricultures waste water. *Trends Biotechnol.* **22**(9), 477–485 (2004)
3. G. Evans, *Biowaste and Biological Waste Treatment* (James and James Science Publishers, London, 2001)
4. J.T. Pfeffer, J.C. Liebman, Energy from refuse by bioconversion, fermentation and residue disposal processes. *Resour. Recovery Conserv.* **1**(3), 295–313 (1976)
5. G. Guéhenneux, P. Baussand, M. Brothier, C. Poletiko, G. Boissonnet, Energy production from biomass pyrolysis: a new coefficient of pyrolytic valorization. *Fuel* **84**(6), 733–739 (2005)
6. B.E. Logan, *Microbial Fuel Cells* (Wiley, Hoboken, 2008)
7. P. Aelterman, K. Rabaey, P. Clauwaert, W. Verstraete, Microbial fuel cell for wastewater treatment. *Water Sci. Technol.* **54**, 9–15 (2006)
8. E. Sentimenti, U. Biorgi, Energia ed economia. *Tpoint Eni Tecnologie* **8**(2), 22–26 (2006)
9. C.J. Cleveland, R. Costanza, C.A.S. Hall, R. Kaufmann, Comparing different energy processes from energy and the U.S. economy: a biophysical perspective. *Science* **225**, 890–897 (1984)
10. G.D. Najafpour, Bioprocess scale-up, in *Biochemical Engineering and Biotechnology* (Elsevier, Amsterdam, 2007), pp. 287–330
11. R.E. Mejias, in *Optimization of biogas production in two-stage anaerobic fermentation of organic waste market using alkaline pretreatment*. Master of science thesis, Politecnico di Torino, Turin, Italy (2013)
12. G. Rametta, in *Verifica sperimentale della valorizzazione energetic dei rifiuti mercatali mediante fermentazione anaerobica bistadio*. Master of science thesis, Politecnico di Torino, Turin, Italy (2013)
13. B. Ruggeri, F. Battista, M. Bernardi, D. Fino, G. Mancini, The selection of pretreatment options for anaerobic digestion (AD): a case study in olive oil waste production. *Chem. Eng. J.* **259**, 630–639 (2015)
14. The Ecoinvent Database, <http://www.ecoinvent.org/database>. Accessed 27 Feb 2014
15. P.P. Franzese, T. Rydberg, G.F. Russo, S. Ulgiati, Sustainable biomass production: a comparison between gross energy requirement and energy synthesis methods. *Ecol. Ind.* **9**, 959–970 (2009)
16. S. Sanfilippo, B. Ruggeri, LCA Alimentazione: stima del consumo energetico per la produzione, il trasporto e la preparazione del cibo in Italia. *La Rivista di Scienza dell'Alimentazione* **38**(4), 1–16 (2009)
17. Product ecology consultants, SimaPro 7.2.4 Software. Pré Consultants, Amersfoort, The Netherlands (2010)
18. D.J. Murphy, C.A.S. Hall, M. Dale, C. Cleveland, Order for chaos: a preliminary protocol for determining the EROI of fuels. *Sustainability* **3**, 1888–1907 (2011)
19. Agenzia Servizi Settore Agroalimentare delle Marche, La filiera del biogas, <http://www.laboratoribiomasse.it/media/docs/downloads/103-1.pdf>. Accessed 17 Oct 2014



# Conclusion

The purpose of this book aimed at the development of sustainable biological energy technology using organic waste. The authors followed a step-by-step experimental approach in order to gradually determine biological parameters and dynamics which influence the production of hydrogen and methane by anaerobic digestion, driven by the up-to-date theoretical findings on the subject. Attention was then focused on the integration of dark bioH<sub>2</sub> technology into a system which uses organic waste as substrate for hydrogen-producing bacteria (HPB) and where liquid residue metabolites (VFA) are used as the substrate for methane-producing bacteria. Moreover, this system increases the energy value of the liquid metabolites to achieve the energy sustainability of the whole process. The use of organic refuses and the further valorization of H<sub>2</sub> end-products might be a promising goal from the perspective of developing effective sustainable energy processes and hence of solving some disposal problems. Therefore, this book can be useful for understanding the fundamentals of the process from the perspective of design and scaling-up of the technology for a real-world full-scale application. In practical terms, the authors have taken into account conditions experimentally proven and easily realizable at the industrial scale, either for economical or for practical aspects. Examples are the use of mixed microorganism consortia, the chemical selection of HPB present in mixed anaerobic microorganisms, the selection of the pretreatment options for the substrate, and the relatively low working temperature of reactors. For these reasons, the authors have neglected particular tricky conditions, like the use of pure culture and heat pretreatment, even if they might achieve greater efficiency. The experimental investigation of the H<sub>2</sub> and the two-step AD (H<sub>2</sub> + CH<sub>4</sub> in sequence) production has been carried out over a period of more than 3 years, highlighting many important aspects of the technology that are briefly illustrated below.

The physiological characteristics of HPB, their metabolisms and the ecological factors which govern dark H<sub>2</sub> production have a key role in achieving the goal of increasing H<sub>2</sub> production. Experimental results, shown to select HPB, clearly reveal that acid pretreatment is an effective method of increasing HPB in an anaerobic microorganism consortium and is able to avoid methanogenesis during

fermentation. The high  $H_2$  gas concentration (50–70 %) and the absence of methane confirm the feasibility of acid pretreatment, which is highly selective for *Clostridium* spp., but also other bacteria, including facultative bacteria. Facultative anaerobic bacteria are less sensitive to oxygen than strict anaerobes, i.e. Clostridia, and they are sometimes able to recover hydrogen production activity after accidental oxygen introduction by rapidly depleting oxygen. Therefore, it could be feasible to run a full-scale plant in which in the first phase the bioreactor is filled with an acid solution; the mixed microorganisms are able to tolerate some variations in the inlet stream as well as some oxygen failure better than a single biological species. In addition, this approach does not need high energy expenditure, as occurs in the case of heat treatment. The aim of the study was to control the behaviour of the fermentation by macro-parameters such as pH and redox potential. For this reason, a detailed kinetic study was conducted to highlight the dynamics of glucose consumption as well as  $bioH_2$  evolution using an enriched HPB biomass. The kinetics were studied by applying an experimental approach such as the *modified initial rate method*, while the dynamics were studied by using the *relaxation time* approach. The glucose consumption was found to be of first-order kinetics, while for the biogas evolution an inhibited kinetics appeared above 60 g/L of glucose with a maximum production rate around 100 ml/L h. The  $H_2$  content ranged from 40 to 60 %; this suggests aiming for a carbohydrate concentration below 60 g/L in the stream of fermenting broth. The positive effect of mixing, which is able to degas the biogas dissolved in the medium, consequently increasing the  $H_2$  production, has been highlighted. This effect could be estimated at around 30 % in the case of glucose; in other words the suggestion for a full-scale plant is to have a high mixing rate in the range of 300–400 rpm to favor hydrogen evolution and to prevent any inhibition of the HPB microorganism activity. The dynamics of the biogas evolution was studied using a macro-approach and the relaxation time tools, to explain the experimentally detected behaviors of pH and redox potential. In particular, pH is the most important parameter in the regulation of the enzyme pool involved in  $H_2$  evolution, suggesting a robust pH control chain for the bioreactor. An experimental procedure was proposed and applied to evaluate a theoretical reference yield of  $H_2$  on glucose, taking into account the VFA as well as ethanol produced from the HPB microorganisms. The effect of temperature on  $H_2$  production has been investigated in detail, even at low temperature (20 °C) or at ambient temperature exposed to natural fluctuation; this because the temperature plays an important role both on the microorganism activity and on the net energy production of the process. The optimal temperature for fermentative  $H_2$  production by mixed cultures is found to be 35 °C. At extreme temperatures, i.e. 16 and 50 °C, the  $H_2$  production is very low, even though at 16 °C a residual HPB activity was recognized, while at 50 °C the  $H_2$  production was found to be very low. The variation in  $H_2$  production at different temperatures could be linked to different metabolic pathways as a consequence of

the activity of different bacterial species present in a mixed culture of HPB. Furthermore, the buffering of pH is very important for H<sub>2</sub> production, because it permits a more stable and a longer H<sub>2</sub> production, even though the cost of the NaOH needs to be considered. These indications are very valuable for scale-up purposes. The evaluation of net energy production has deserved particular attention as the first step toward the energy sustainability of the AD technology. A scale-up procedure was analyzed and applied in order to evaluate the net energy production of a bioreactor producing H<sub>2</sub>. The main conclusions are: (i) bioreactors which produce only H<sub>2</sub> are not energetically sustainable; (ii) the net energy produced mainly depends on the seasonal temperature variations; and (iii) other parameters having an effect are the thickness of the insulator material, its thermal conductivity and the bioreactor diameter. By means of the net energy analysis, different strategies of running full-scale plant must be considered in order to maximize the net energy production. In this context, recovering the heat used to warm up the fermenting broth is a fundamental aspect. One of the most important results of the net energy analysis is that the temperature needed to maximize the net energy produced by the plant is 20 °C, while 35 °C is the optimal temperature which corresponds to the maximum biomass activity for hydrogen production. This suggests warming a full plant to 20 °C instead of 35 °C. The uncertainty analysis of the net energy approach emphasizes that the main influencing parameter is the ambient temperature, because it determines both the quantity of energy to be used to heat the bioreactor, and the efficiency of the heating system; therefore a careful estimation of ambient temperature and its variation throughout the day and seasons is of utmost importance.

Another important parameter was the diameter ( $D$ ) of the reactor, linked to the working temperature; it is possible to conclude that it is better to work at low temperature (20 °C) for diameters less than 1 m, because this increases the net energy production, even though the produced energy is lower, while for  $D > 3$  m the effect is negligible.

A significant aspect is the need to increase the global energy harvesting from such organic waste, in order to have a net positive energy balance to sustain the biohydrogen technology, by looking to valorize the energy content of the chemicals remaining in the fermenting broth at the end of acidogenesis, which is approximately 80 % or more of that present in the feed.

A focus on residual biowastes as suitable substrates for H<sub>2</sub> production was presented. Several necessary pretreatments have been verified at experimental scales. General validity has been noticed for different organic waste streams: extrusion provided the best results for mechanical pretreatment, and basic pretreatment for chemical pretreatment. The energy production was improved 17-fold compared with the case without the pretreatment. This type of extrusion at 200 atm resulted to be very effective in removing the packaging occluding some food residues, such as

plastics and paper. Residues of fruit and vegetable markets, despite providing one of the best results, are the substrates that produced the highest quantity of energy without any type of pretreatment. This means that they are the most easily digested substrates among many candidate organic refuses as feed. Tests carried out with a bench bioreactor using organic waste market confirm the great opportunity of using organic waste for hydrogen production, although problems of mixing the fermenting broth need to be carefully addressed in the scale-up procedure. Considering that the net energy balance of biological  $H_2$  production via dark fermentation cannot be positive, the integration of  $H_2$ ,  $CH_4$  and microbial fuel cells (MFC) could be a promising avenue because their implementation can contribute to an energy-positive waste disposal system for organic waste. The two-step AD (TSAD) process, integrated with MFC technology, can increase the global energy efficiency of using organic wastes with respect to the standard anaerobic process for biogas production.

The scientific rationale of TSAD was analyzed; the main aspects have been confirmed with experimental tests, either in batch or in continuous modes, using two feeds representative of organic refuses. Experimental results show that the energy produced as hydrogen and methane gases is higher than the harvested energy using a one-step AD; specifically it is in the range of 1.5–2.7 times higher, although an uncertainty of  $\pm 30\%$  was recorded experimentally. The energy efficiency for continuous bioreactors is lower than batch test ones, but some oscillatory behaviors at steady state are present, although the energy produced per unit time is higher than the batch case. The result obtained with TSAD at low HRT, compared with traditional one-step AD, is of particular interest for scale-up purposes: the same efficiency was obtained but by using a methanation bioreactor with smaller dimensions (1/2 or 1/3), hence lowering the investment costs, even though an additional hydrogen reactor of 1/10 of the volume of the methane reactor is necessary. Finally, the hydrogen step appears to be a pretreatment process able to induce better substrate utilization with additional methane production in the methanation step. TSAD consists of the separation of the natural ecology and metabolism of the anaerobic bacteria consortium into two distinct classes, hydrogen-producing bacteria (HPB) and hydrogen-consuming bacteria (HCB). In the first stage, the acid pH and short hydraulic retention time (HRT) conditions are chosen to produce  $H_2$ , while in the second stage neutral pH and higher HRT conditions are adopted to favor methanogenesis with  $CH_4$  production.

A possible scheme is shown for scale-up purposes towards a full-scale application perspective, utilizing previously mechanically pretreated organic waste; the following Fig. 1 shows a flow diagram of a 400 L working volume pilot plant able to produce biohydrogen and biogas in a continuous mode, utilizing different residence times to separate the HPB from the HCB, and adopting the wash-out principle).

This scheme takes into account the pretreatment processes highlighted in the previous sections and uses two reactors in series, one for hydrogen production and a second one for methane production. Liquid residues can be utilized after sedimentation/filtration as feed for an MFC to produce electricity directly. The plant comprises the following parts: A: feed preparation tank; B: bio $H_2$  reactor;

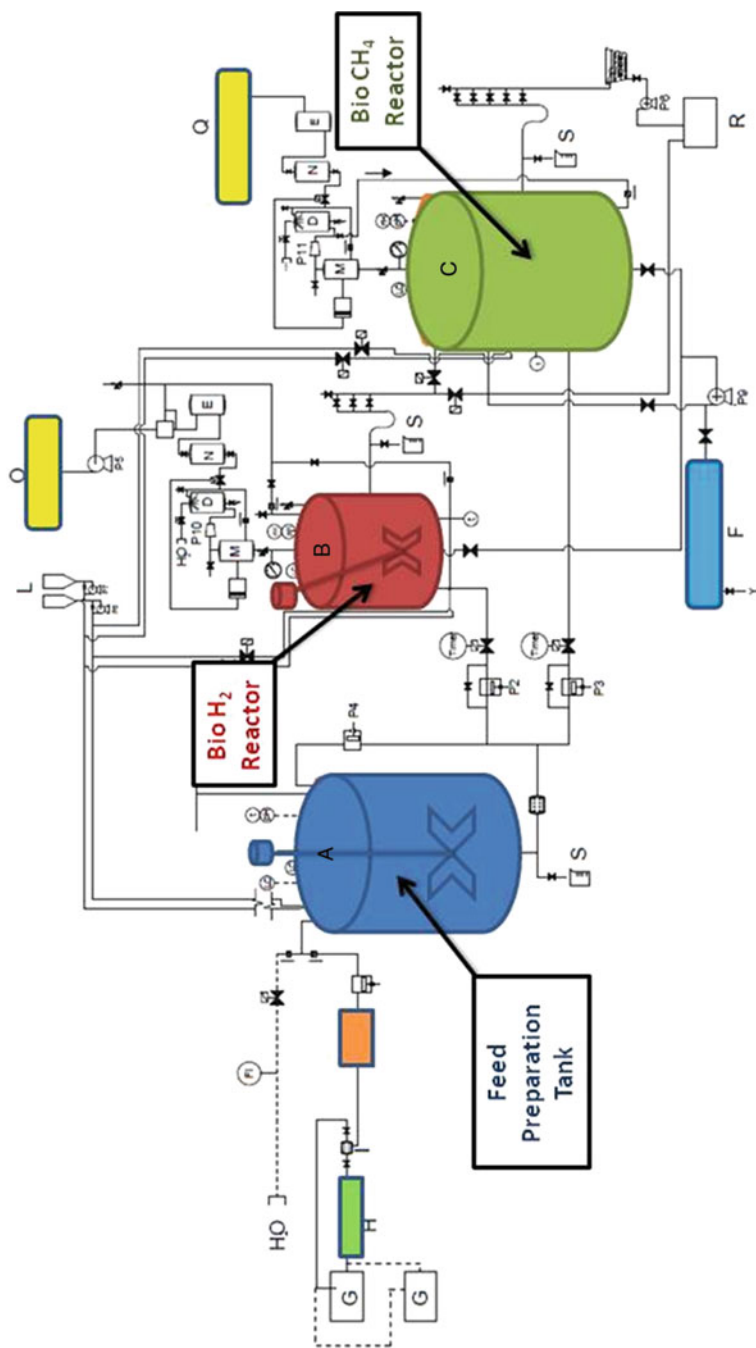


Fig. 1 Pilot plant for TSAD process (private communication Didacta Italia, didacta.it)

C: bioCH<sub>4</sub> reactor; D: absorption column; E: activated carbon adsorption column; F: heating system; G: feed tank (one running, one on stand-by); H: crush screw; I: online filter; L: pH control reservoirs; M: pressure control device; N: silica gel drying column; O: hydrogen-rich gas storage tank under pressure; Q: biogas storage system at 1 atm; R: digestate reservoir tank; S: liquid sampling device. The scheme outlined concerns two-step anaerobic fermentation in a continuous mode and highlights problems linked to the scale-up criteria towards full plant application, such as mixing and stability for long periods.

In the book a procedure was proposed for evaluating the energy sustainability of a process, and moreover for scoring different processes using the same energy sources on the basis of their energy sustainability level; the proposed procedure was applied to TSAD and one-step AD. The procedure comprises three steps: Energy Sustainability Index (ESI) evaluation, Analogical Model (AM) computation and, finally, evaluation of Energy Returned On Investment (EROI) and Energy Payback Time (EPT). It allows definition of the process steps and moreover the establishment of the operating conditions needed for increasing the energy sustainability of the entire technology; moreover it allows evaluation of the conditions under which AD is an effective technology able to supply society's needs; in this respect the large effect of the bioreactor diameter is emphasized.

On the other hand, further investigations should be made on the best mixing rate as a technological parameter to improve the H<sub>2</sub> yield. Significant improvements can be also expected through rapid gas removal and separation. Regarding the working conditions of the bioreactor, further study should be aimed at choosing an adequate hydraulic retention time in order to work in continuous mode, always in accordance with the specific growth rate of HPB. Fixed-bed bioreactors (not considered in the book) for liquid organic refuse containing a consortium of mesophilic bacteria could enhance the rate of hydrogen production to a greater extent than reported for other approaches in the case of a very diluted stream; experimental verifications are welcomed.

The literature cites a large number of studies on the biochemistry, enzymology and technology of biohydrogen and biomethane production processes. While each one has its merits and demerits in terms of technology and productivity, none of them has been rigorously evaluated in terms of cost for commercialization and energy sustainability. Only a limited number of economic analyses on dark fermentation processes are available, and in any case these calculations are made without taking into account the costs of pretreatments, biomass, personnel and construction; they could therefore be unreliable.

The authors used two parameters to overcome these difficulties, Energy Return On Investment (EROI) and Energy Payback Time (EPT), to evaluate the energy sustainability of the AD process, disregarding the attention to costs and computing only the energies. This approach poses a strict linkage between the physical significance of the energy and the process producing it, allowing evaluation of the effective energy able to sustain society, now and in the future.